



The University of
Nottingham

UNITED KINGDOM · CHINA · MALAYSIA

School of Life
Sciences

Effect of Mannose Receptor (MR)-binding polymers on human macrophages

**Thesis submitted to the University of Nottingham for the title of
Doctor of Philosophy (PhD)**

Diego de Medeiros Costa

January, 2019

Abstract

Mannose receptor (MR) is an endocytic lectin receptor with the capacity to bind sugars and collagen through its different domains. This receptor is mainly found in macrophages and dendritic cells and is important in pathogen recognition, cell activation, antigen presentation, control of homeostasis, and cell adhesion. It has been under study over the past decades and became a target in drug development. With the intention to modulate its function, our group had developed a library of glycopolymers, with different sugar moieties conjugated as pendant groups and with different lengths able to bind to different domains of MR. Our previous studies showed that glycopolymers with SO₄-3-Gal sugar moieties were able to bind to mouse macrophages through the CR domain of MR in a pH-independent manner leading to decreased MR expression on the cell surface and inhibiting the collagen uptake activity in these cells. Its mechanism of action is thought to be by trapping of MR in the form of a complex of glycopolymer-MR in the endosome. The hypotheses of this project are that SO₄-3-Gal glycopolymers could be recognised by human MR and modulate MR-function in human myeloid cells. Therefore, the aims of this project are: 1) Investigate the recognition of SO₄-3-Gal glycopolymers by the CR domain of human MR and by human myeloid cells; 2) Investigate the effect of glycopolymers on MR function in human myeloid cells; and 3) Investigate the effect of glycopolymers on MR distribution within human myeloid cells. The results showed that SO₄-3-Gal glycopolymers are recognized by human macrophages and its binding is dependent on polymer concentration and temperature of incubation. These polymers inhibited MR surface expression, as well as, decreased collagen uptake by human monocyte-derived macrophages. Macrophages were affected by these polymers and presented less MHCII molecules on its surface in response to IFN- γ and produced less kynurenine in response to IFN- γ and LPS. However, it was not possible to confirm trapping of MR in the endosome. It was also found that IFN- γ stimulation in human macrophages does not lead to decreased MR expression, as it is expected in mice. The results achieved in this thesis with the SO₄-3-Gal GPs are novel in relation to MR surface blocking, collagen uptake inhibition and IDO inhibition in human macrophages. It adds to the current targeting strategies of MR. It also opens the possibility to explore cellular activities that could be affected by carbohydrate-based targeting approaches like modulation of cell growth, cell migration or other effector functions such as cytokine release.

Acknowledgements

I owe this work to many people who helped me along in this journey of being a PhD student. First, I'm grateful for my family and friends back home for their understanding with my long absences and time away from home. This work would not be achieved without all the support necessary that my parents deposited over the years, doing whatever was necessary for me to be successful in this step of my life.

For my supervisors Luisa and Beppe who always had total attention and always gave 110% supervision support in all these years. I own this work a lot to them and to Francesca, who I can say was a co-supervisor and trained me in the work with polymers. They were all very generous with their knowledge and contributed a lot to my academic progress.

I am also thankful to all the lab members, Sirina, Farah, Sonali, Oli, Yasir, Mohammad, Philemon, Darryl. Each one of them had always been helpful and taught me important things in moments when I was stuck. To work alongside them made the journey less challenging.

I am also grateful for the company of my office colleagues, especially Alesandra and Matt, who were guiding lights.

I also would like to thank everyone who contributed with technical support, David Onion and Nicki with all the help with flow cytometry, Ian and Chris, who trained me in microscopy and in many times had to stay along when I needed to capture images.

Should not forget to thank Dr. Sally Wheatley for providing cells and to Dr. Clare Isacke for providing antibodies for my experiments.

Table of Contents

Abstract	i
Chapter 1 - Introduction	1
1. Glycan biology	1
1.2. C-type Lectins.....	3
1.3. The Mannose Receptor superfamily: Dec205, Endo180, mPLAR and MR.....	6
MR and Endo180.....	6
MR.....	7
MR; an historical perspective	11
Regulation of MR expression	15
MR contribution to disease pathogenesis	16
Targeting of lectin receptors.....	17
1.4. Macrophages in health and disease	19
Classically activated M1 macrophages	21
Alternatively activated M2 macrophages	24
Macrophages in disease.....	26
1.5. Results leading to this project.....	28
1.6 Hypothesis and aims	42
Table 2. List of polymers used in this present work.....	42
Chapter 2 - Materials and Methods.....	43
2.1. Analysis of polymer binding to human CR domain.....	43
2.2. Isolation and preparation of human monocytes	45
2.3. Analysis of polymer binding and uptake by human macrophages	47
2.4. Analysis of cell surface markers.....	49
2.5. Inhibition of gelatin uptake by human macrophages.....	52
2.6. Macrophage preparation for protein extraction	53
2.7. Culture of MRC5 cells.....	54
2.8. Cell lysate preparation	54
2.9. Western Blot analysis.....	56
2.10. Indoleamine 2, 3 dioxygenase (IDO) activity assay.....	59
2.11. Fluorescence microscopy.....	60
Chapter 3 – The interaction of MR-binding glycopolymers with human macrophages	63

3.1. Polymer S100-DP187 binds the cysteine-rich (CR) domain of human MR	64
3.2. Association of MR-binding polymers with human monocyte-derived this macrophages	67
3.3. Phenotypic characterisation of human macrophages	71
3.4. Effect of temperature on the association of MR-binding polymers to human macrophages.....	73
3.5. Polymer association to macrophages is dose-dependent.	77
3.6. Uptake of polymer S100-DP187 by human macrophages can be competed with polymer S100-DP240	78
3.7. Discussion.....	80
Chapter 4 - Effect of MR-binding glycopolymers in human macrophages	84
4.1. Effect of glycopolymers on gelatin binding/uptake by human macrophages.....	85
4.2. Endo180 is expressed in human macrophages.....	93
4.3. Cell surface markers expression after polymer incubation	95
4.4. IDO activity is affected by polymer S100-DP240	99
4.5. Total MR and Endo180 expression after incubation with polymer S100-DP187	106
4.6. MR and Endo180 expression in M2 and M1 macrophages	110
4.7. Discussion.....	113
Chapter 5 – MR co-localization	118
5.1. Detection of MR and Endo180 by Immunofluorescence.....	120
5.2. Antibody optimization for IF	123
5.2. MR colocalization to EEA1 and LAMP1	133
5.2.2. Analysis of colocalization of MR vs EEA1 and MR vs MR.....	139
5.3. Discussion.....	156
Chapter 6 - Final Discussion	159
Analysis of Polymer Uptake by Human Macrophages.....	164
Effect of S100 polymers on MR biology.....	165
7. References	176

List of Figures

Figure 1. Different forms for D-Glucose and D-Mannose..	8
Figure 2. Structure of MR	10
Figure 3. Overview of MR function	11
Figure 4. Expanded mechanism for the mannose-specific endocytosis receptor	13
Figure 5. The general mechanism of ATRP (Matyjaszewski, 1999).	30
Figure 6. Mannose receptor structure and polymers chemical identity.	32
Figure 7. General mechanism of RAFT polymerisation.	33
Figure 8. Internalisation of glycopolymers by CD206-presenting cells	35
Figure 9. Mechanism of modulation of MR endocytic activity <i>in vitro</i> , and MR activity inhibition <i>in vivo</i> .	37
Figure 10. GPs inhibit CD206 (MR) endocytic activity <i>in vitro</i>	40
Figure 11. Summary of polymer binding assay	44
Figure 12. Summary of isolation and preparation of human monocytes.	47
Figure 13. Analysis of MR Cysteine-rich (CR) domain sequence alignment between species <i>Mus musculus</i> and <i>Homo sapiens</i> .	65
Figure 14. Recognition of polymer S100-DP187 by the CR domain of human MR and of polymer M100-DP187 by the CTLD4-7 region of mouse MR.	66
Figure 15. Binding of polymers S100-DP187 and M100-DP187 to human macrophages generated in the presence of M-CSF, GM-CSF or M-CSF + IL-4	70
Figure 16. Mean fluorescence intensity for cell surface markers in M-CSF and M-CSF + IL-4 macrophage cultures	72
Figure 17. Temperature effect on polymer association to human macrophages	76
Figure 18. Effect of polymer dose on their association with human macrophages	77
Figure 19. Summary of the competition assay between S100-DP240 and S100-DP187.	78
Figure 20. RAFT synthesized polymer, S100-DP240, competes with ATRP synthesized polymer, S100-DP187	79
Figure 21. Effect of polymers (1 hour incubation) on gelatin uptake by human macrophages.	87
Figure 22. Effect of different polymer concentrations (1 hour incubation) on gelatin binding to human macrophages	91
Figure 23. Effect of polymers (6 hour incubation) on gelatin uptake by human macrophages.	92
Figure 24. Analysis of Endo180 expression in human macrophages	94
Figure 25. Cell surface markers expressions in macrophages are affected by polymer S100-DP187.	96

Figure 26. Cell surface markers expression in macrophages are affected by polymer S100-DP187.....	98
Figure 27. S100-DP240 reduces IDO activity in IFN- γ /LPS treated macrophages.....	100
Figure 28. S100-DP240 effect in kynurenine production was not due to a decrease in cell viability	103
Figure 29. Polymer S100-DP240 inhibit HLA-DR expression in M1 activated macrophages.	105
Figure 30. Analysis of total MR expression by human macrophages after treatment with polymers for 2 hours.....	106
Figure 31. MR and Endo180 possess opposite regulation in the presence of IL-4	108
Figure 32. IFN- γ alone does not promote downregulation of MR in human monocyte-derived macrophages after 24 hours treatment.....	111
Figure 33. Endo180 is downregulated by IL-4 and IFN- γ + LPS	112
Figure 34. Detection of Endo180 and MR in human macrophages by immunofluorescence. Coverslips were prepared with M-CSF and M-CSF+IL-4-treated macrophages.....	122
Figure 35. Detection of Endo180 and MR in human macrophages by immunofluorescence.	126
Figure 36. Optimization process for MR, Endo180 and EEA1 detection by immunofluorescence	131
Figure 37. Pearson's correlation coefficient formula.....	134
Figure 38. Colocalization of MR vs EEA1 and MR vs MR by confocal microscopy	138
Figure 39. MR and EEA1 localization in the cell nucleus.....	141
Figure 40. Image showing confocal layers from a cell stained with MR (green), EEA1 (red), DNA (blue)	142
Figure 41. Example 1: Colocalization analysis and line intensity profiles of MR (green) vs EEA1 (red) in human macrophages	143
Figure 42. Example 2: Colocalization analysis and line intensity profiles of MR (green) vs EEA1 (red) in human macrophages	144
Figure 43. Example 3: Colocalization analysis and line intensity profiles of MR (green) vs EEA1 (red) in human macrophages	145
Figure 44. Example 4: Colocalization analysis and line intensity profiles of MR (green) vs EEA1 (red) in human macrophages	146
Figure 45. Example 1: Colocalization analysis and line intensity profiles of MR (green) vs EEA1 (red) in human macrophages treated with S100-DP240 for 4 hours.....	147
Figure 46. Example 2: Colocalization analysis and line intensity profiles of MR (green) vs EEA1 (red) in human macrophages treated with S100-DP240 for 4 hours.....	148
Figure 47. Example 3: Colocalization analysis and line intensity profiles of MR (green) vs EEA1 (red) in human macrophages treated with S100-DP240 for 4 hours.....	149

Figure 48. Example 4: Colocalization analysis and line intensity profiles of MR (green) vs EEA1 (red) in human macrophages treated with S100-DP240 for 4 hours.....	150
Figure 49. PCC values for MR vs EEA1 in untreated and in polymer S100-DP240 treated macrophages	151
Figure 50. Example 1. Colocalization analysis and line intensity profiles of MR (green) vs MR (red) in human macrophages.....	152
Figure 51. Example 2. Colocalization analysis and line intensity profiles of MR (green) vs MR (red) in human macrophages	153
Figure 52. MR localization in the cell nucleus. Volocity software 3D image showing MR localization in the cell nucleus	154
Figure 53. Image showing confocal layers from a cell stained with MR (mouse-green), MR (rabbit-red), DNA (blue)	155

List of Tables

Table 1. C-type lectins groups' organization with its respective type of binding.	5
Table 2. List of polymers used in this present work.	42
Table 3. Polymer type, molecular weight and polymer concentration used in different assays. Table	48
Table 4. List of antibodies used for macrophage profile analysis by flow cytometry (no polymer).	50
Table 5. List of antibodies used for macrophage cell surface marker quantification after polymer treatment.	51
Table 6. SDS-PAGE gel (6%) preparation protocol.	57
Table 7. Stacking gel preparation protocol.	57

Declaration

I declare that this work has been achieved in the duration of my PhD studies at the University of Nottingham, and is my original effort unless otherwise stated. Information from other resources has been recognized.

No part of this thesis has been submitted for assessment leading to another degree.

Diego de Medeiros Costa

List of Abbreviations

APC – Antigen-presenting cell.
ARG1 – arginase-1
ATP – Adenosine triphosphate
BMDM – Bone marrow-derived macrophage
CHO – Chinese hamster ovary cell
CLR – C-type lectin receptors
CRD – Carbohydrate recognition domain
CTA – chain-transfer agent
CTLD – C-type lectin-like domain
CuAAC- copper(I)-catalyzed azide alkyne cycloaddition
DAMPs – Damage-associated molecular patterns molecules
DCs - Dendritic cells
DC-SIGN – Dendritic cell-specific intercellular adhesion molecule-3-grabbing non-integrin
D-Glc – D-glucose
D-Xyl – D-Xylose
ER – Endoplasmic reticulum
FACS – Fluorescence activated cell sorting
FNII – Fibronectin type II
GAINAc – N-acetylgalactosamine
GAS – Gamma interferon activation site
GlcNAc – N-acetylglucosamine
GM-CSF – Granulocyte-macrophage colony-stimulating factor
G100-DP187 – Glycopolymer with 100 % galactose sugar moieties and 187 repeating units
G100-DP240 - Glycopolymer with 100 % galactose sugar moieties and 216 repeating units
HEPES – (4-(2-hydroxyethyl)-1-piperazinethanesulfonic acid
IGF-1 insulin-like growth factor
IFN- γ – Interferon gamma
ILCs – Innate lymphoid cell
IL-1 β – Interleukin 1 beta
IL-4 – Interleukin 4
IL-4 – 4R α – Interleukin receptor 4 alpha chain
IL-13 – Interleukin 13
iNOS – Inducible nitric oxid synthase

ISGs – Interferon-stimulated genes
ITAM – Immunoreceptor tyrosine-based activation motifs
JAK – Janus kinase
LPS – Lipopolysaccharide
MAMPs – Microbial-associated molecular patterns
MBL – Mannose binding lectin
MCP1 – Monocyte chemoattractant protein-1
M-CSF – Macrophage colony-stimulating factor
MHC I - Major histocompatibility complex class I
MHCII- Major histocompatibility complex class II
MR – Mannose receptor
MUC1 – Mucin 1
M100-DP187 - Glycopolymer with 100 % mannose sugar moieties and 187 repeating units
NK – Natural Killer
NF κ B - nuclear factor kappa-light-chain-enhancer
PRRs – Pattern recognition receptors
RAFT – reversible addition-fragmentation chain transfer
SHP1 – Src homology region 2 domain-containing phosphatase-1
SHP2 - Src homology region 2 domain-containing phosphatase-1
STAT1 - Signal transducer and activator of transcription 1
STAT6 - Signal transducer and activator of transcription 6
S100-DP187 - Glycopolymer with 100 % SO₄-3-Gal sugar moieties and 187 repeating units
S100-DP240 - Glycopolymer with 100 % SO₄-3-Gal sugar moieties and 240 repeating units
TGF β – Tumour growth factor β
TLR – Toll-like receptor
TNF α – Tumor necrosis factor alpha
TR – Texas Red

Chapter 1 - Introduction

1. Glycan biology

Glycans (carbohydrates, sugars) cover the surfaces of mammalian cells as attachments to protein and lipid backbones and is produced through a process called glycosylation. During the glycosylation process molecules are transported from the endoplasmic reticulum to the Golgi and the cell membrane (van Kooyk and Rabinovich, 2008). Glycans are among the molecules with the most complex structures (Varki et al., 2015). They play a major role in the control of both the innate and adaptive immunity (Marth and Grewal, 2008, Rabinovich et al., 2012, van Kooyk and Rabinovich, 2008, Johnson et al., 2013), and is part of multiple biological processes, such as cell proliferation and differentiation which are key during development (Johannssen and Lepenies, 2017).

The glycosylation process is mediated by a number of enzymes including both glycosyltransferases – enzymes that catalyse the transfer of a sugar from a nucleotide sugar donor or a lipid sugar to a substrate , and glycosidases – enzymes that catalyse the hydrolysis of glycosidic bonds in glycan molecules (van Kooyk and Rabinovich, 2008). More than 100 genes encoding for glycosyltransferases and glycosidases have been characterized (Ohtsubo and Marth, 2006). Glycosylation provides structural variations to a given protein, leading to identical proteins linked to different glycan structures, which are known as glycoforms. This diversity gives the mammalian glycome - all the glycans in a particular cell tissue, or organism (Cummings and Pierce, 2014), an estimated variation of thousands of potential glycan structures (Cummings, 2009). The mammalian glycosylation inventory comprises N-linked glycosylation and O-linked glycosylation (van

Kooyk and Rabinovich, 2008). Glycans linked to lipids or proteins through a nitrogen atom is said to be N-linked, whilst glycans linked by an oxygen atom is said to be O-linked. Both types of glycans are found at the extracellular surface of the plasma membrane (Taylor and Drickamer, 2011). Glycans biosynthesis is dictated by metabolism, signal transduction, and cellular status (Hudak and Bertozzi, 2014). The enzymatic process of vertebrate glycosylation uses several monosaccharides (fucose, galactose, *N*-acetylgalactosamine, glucose, *N*-acetylglucosamine, glucuronic acid, mannose, sialic acid and xylose) which, in combination, provide a large variety of potential glycans due to the many different types of anomeric linkages that are possible between two monosaccharides and the formation of branches (Ohtsubo and Marth, 2006). This determines the three-dimensional orientation and shape of the glycan which is critical for recognition by carbohydrate-binding molecules. Glycan pattern recognition is highly specific, requiring precise spacing of multiple atomic-binding determinants in a distinct glycan structure.

Cells, whether eukaryotic or prokaryotic, present a sugar coat on its surface: the glycocalyx (Varki, 2011, Cohen and Varki, 2010). In vertebrates, the glycocalyx comprises glycoproteins, glycolipids and proteoglycans. This is the immediate source of interaction with the environment and mediates cell-cell and cell-pathogen contact. The cell-glycan interaction plays a role in activation, trafficking, and regulation of immune cells. Nearly all cell-surface and secreted proteins are glycoproteins (Schnaar, 2016).

1.2. C-type Lectins

Glycans interact with glycan binding proteins (lectins), through carbohydrate recognition domains (CRDs) that bind specific groupings of 2-7 sugars in precise configurations (Taylor and Drickamer, 2014). One exception are the singlets which bind sialic acids residues through immunoglobulin(Ig)-like domains (Bornhöfft et al., 2018). Thus, glycan recognition depends on the specific arrangement of sugars. There are more than 80 lectins in humans that serve in both self and pathogen recognition. Lectins initiate and regulate inflammation and recognize and destroy pathogens; however, pathogens may subvert the immune system by secreting enzymes that hydrolyse glycans on its cell wall, diminishing potential recognition (Garfoot et al., 2016). Another mechanism used by pathogens (e.g. meningococci, *Trypanosoma* and *Helicobacter*) to escape the immune system is to synthesize glycans that include terminal structures similar to those found in mammalian glycans, a mechanism known as molecular mimicry (van Kooyk and Rabinovich, 2008).

Among the known lectins, C-type lectin receptors (CLRs) are the largest and most diverse of the lectins found in animals. CLRs can be found as transmembrane or secreted proteins. A modular carbohydrate-recognition domain (CRD) that in most cases binds sugars in a Ca^{2+} -dependent manner is found in C-type lectins (Weis et al., 1998). C-type CRDs found in the immune system can contribute to cell adhesion, turnover of glycoproteins and pathogen recognition (Weis et al., 1998). Soluble C-type lectins can function as growth factors, opsonins (mannose binding lectin, ficulins), antimicrobial proteins and may also be found in the extracellular matrix (galectins) and they regulate processes such as development, respiration, coagulation, angiogenesis and

inflammation (Brown et al., 2018). Signalling pathways in C-type lectin receptors are diverse.

The expression of individual C-type lectins is often limited to cell lineages and such receptors can function as cell-type-specific markers (Brown et al., 2018).

Residues that are conserved among C-type CRDs form a hydrophobic core and disulphide bonds that define the overall fold of the domains (Weis et al., 1992). Sugar binding domains that do not necessarily bind sugars through a conserved Ca^{2+} -binding site are known as C-type lectin-like domains (CTLDs) (Weis et al., 1998). C-type lectins are a family of more than 1000 proteins that are defined by having one or more CTLDs (Brown et al., 2018). Proteins were divided in 16 groups on the basis of phylogeny and domain organization (Drickamer and Taylor, 2015). These molecules may bind to carbohydrates in a Ca^{2+} -dependent manner through conserved residues within the CTLD, for example, motifs like Glu-Pro-Asn (EPN) confers specificity for mannose residues while Gln-Pro-Asp (QPD) motifs confers specificity to galactose (Zelensky and Gready, 2005, Weis et al., 1998). Lectin groups 1, 2, 3, 4 and 6 (Mannose Receptor family) have domains that bind glycans at the conserved Ca^{2+} -binding site. Groups 5 and 8 possess domains that bind sugars through non-canonical sites. Other groups contain C-type lectin-like domains but lack Ca^{2+} -binding site residues and sugar-binding (Drickamer and Taylor, 2015).

C-type lectin groups	Type of binding
Group 1, Group 2, Group 3, Group 4 (Selectin family), Group 6 (Mannose receptor family)	Bind glycans at the conserved calcium-binding site
Group 5 (Dectin-1), Group 8 (Layilin)	Bind glycans through non-canonical sites
Group 7, Group 9, Group 10, Group 11, Group 12, Group 13, Group 14, Group 15, Group 16,	Lack sugar binding

Table 1. C-type lectins groups' organization with its respective type of binding.

Transmembrane CLRs can trigger signalling pathways that result in the activation or inhibition of cell functions. CLR engagement by pathogen-derived ligands or self-ligands may lead to endocytosis and/or elicit signalling pathways in CLR-expressing cells. The signalling cascade induced upon CLR activation is strongly affected by the intracellular motif present in the cytoplasmic domain of the CLR itself or associated CLR adaptor proteins. In some instances, signalling pathways are induced through immunoreceptor tyrosine-based activation motifs (ITAMs). ITAMs can either be an integral component of the CLR cytoplasmic tail or may require the use of adaptor signalling proteins. In myeloid cells, ITAMs facilitate recruitment of tyrosine-protein kinase ZAP70 (SYK kinase) in T cells, which induces a downstream signalling pathway (Geijtenbeek and Gringhuis, 2016) that primarily induces Nuclear factor κ B (NF- κ B)-dependent pro-inflammatory responses. In contrast, inhibitory receptors recruit tyrosine and inositol phosphatases, including SHP1 and SHP2, which negatively regulate the inflammatory signalling pathways induced by other receptors (Redelinguys and Brown, 2011). CLR-mediated signalling impacts important functions in

antigen presenting cells (APCs) such as cytokine production, the expression of costimulatory molecules, and subsequent T cell activation.

1.3. The Mannose Receptor superfamily: Dec205, Endo180, mPLAR and MR

MR superfamily in humans, includes MR, the urokinase-type plasminogen activator receptor-associated protein (Endo180), PLA2R and DEC 205 (Martinez-Pomares, 2012). Each of these receptors possess a Cysteine Rich (CR) domain, a fibronectin type II (FNII) domain and eight (MR, Endo180, PLA2R) or ten (DEC-205) C-type lectin-like domains (CTLDs).

MR and Endo180

MR and its other family member, Endo180, mediate collagen uptake by macrophages and fibroblasts. This process is necessary for tissue remodelling, as well as, facilitates the spread of tumors (Madsen et al., 2017). Collagen is a major component of extracellular matrix. Type I collagen is found in interstitial matrix and forms highly ordered suprastructures in the cornea, skin, tendons and bones. Perturbed collagen homeostasis is associated with a range of diseases, including organ fibrosis, scarring, and arthritis. Malignant tumor cells need to breach collagen-rich matrices to disseminate and form metastasis (Bonnans et al., 2014). Collagenolytic matrix metalloproteinases (MMPs) initially cleave fibrillary collagens at a single site (Fields, 2013). Collagen fragments are further degraded by extracellular proteinases or internalized by macrophages and fibroblasts for lysosomal degradation (Everts et al., 1996, Madsen et al., 2011). One important route for collagen clearance is through endocytosis by the mannose receptor (MR) and Endo180 (East et

al., 2003, Martinez-Pomares et al., 2006b). Cleaved or heat-denatured collagen (gelatin) is internalized with higher avidity than intact collagen (Madsen et al., 2007). FNII domains mediate gelatin binding in MR (Napper et al., 2006b) and Endo180 (Wienke et al., 2003). CR domain is not active in Endo180 (East and Isacke, 2002), therefore binding of sulfated sugars to this receptor is not expected. Endo180 binds mannose, fucose and N-acetylglucosamine in a Ca^{2+} -dependent way (East et al., 2002). In Endo180, the critical FNII domain is integrated into a rigid L-shaped structure that allows the adjacent CTL1 domain to participate in collagen binding. Carbohydrate binding to the CTL2 domain augments binding of glycosylated type IV collagen to Endo180 (Jürgensen et al., 2011). Endo180 possess multiple binding sites for type I collagen. The interaction between Endo180 and collagen is likely represented by a multivalent interaction of a single triple helix with several receptors (Jürgensen et al., 2011, Madsen et al., 2007). Collagen binding to MR and Endo180 is not Ca^{2+} -dependent (Jürgensen et al., 2011, Martinez-Pomares et al., 2006b).

MR

MR (or CD206) is an endocytic receptor, part of C-type lectins, present on the surface of selected populations of macrophages, dendritic cells (DCs) and nonvascular endothelium cells (Martinez-Pomares, 2012). MR has numerous roles including clearance of endogenous molecules, promotion of antigen presentation, and modulation of cellular activation and trafficking (Martinez-Pomares, 2012). In rabbit alveolar macrophages, MR was identified as a 175 kDa transmembrane receptor (Wileman et al., 1986).

MR has two independent lectin sites, the cysteine rich (CR) domain that recognises sulphated sugars presented in glycoprotein hormones such as lutropin and chondroitin sulfate A and B (Taylor

et al., 2005). The CR domain binds sulfated galactose and N-acetylgalactosamine (GalNAc) in positions 3 and 4 in a calcium-independent manner (East and Isacke, 2002, Taylor et al., 2005, Leteux et al., 2000, Liu et al., 2000). The domain folds into a threefold symmetrical β -trefoil shape (Liu et al., 2000). The other lectin site – the CTLD - recognizes mannose, fucose, N-acetylglucosamine (GlcNAc) in a calcium-dependent manner (Taylor et al., 2005, Taylor et al., 1992, Taylor and Drickamer, 1993). MR CTLDs binding affinity for sugars is as follows: L-Fucose = D-Mannose > D-GlcNAc \sim D-Glc > D-Xyl (Shepherd et al., 1981). The orientation of the hydroxyl at C-4 of mannose is crucial for the formation of a high affinity recognition site. C-6 appears to be less important, but still play partial role in receptor recognition. Orientation of hydroxyl in C-2 determines the different affinity between D-mannose and D-glucose for the receptor (Figure 1).

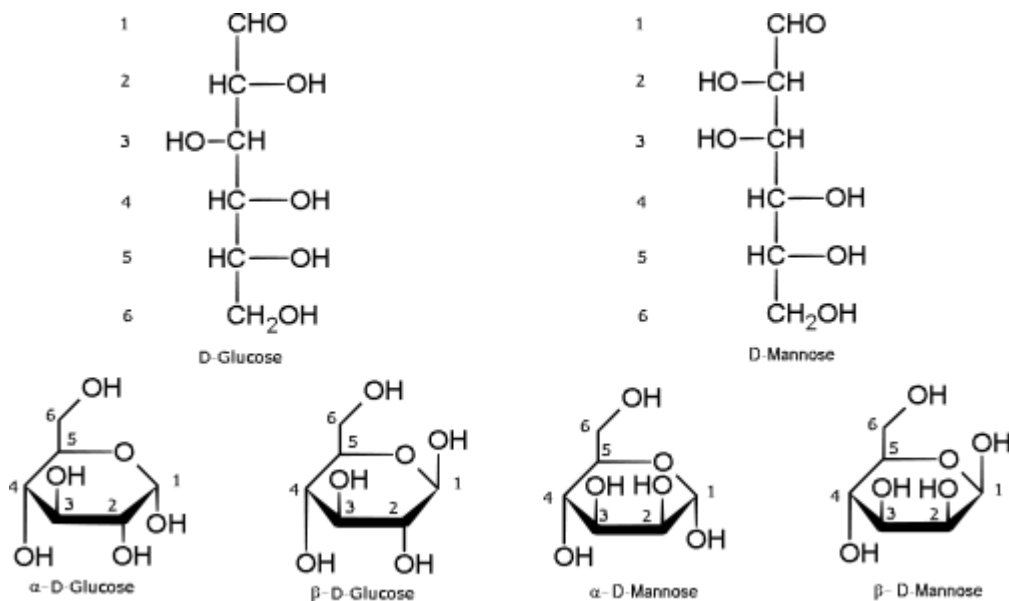


Figure 1. Different forms of D-Glucose and D-Mannose. The same carbons are numbered from 1 to 6 in the open-chain form and in the cyclic form of D-Glucose and D-Mannose. The Carbon 1 in the cyclic form is asymmetric, meaning that there are two forms for each D-Mannose and D-Glucose.

In contrast to Mannose receptor which is known to bind both sulfated and mannosylated glycans through distinct CRDs, the C-type lectin, Langerin, is present on the surface of Langerhans cells and is extremely unique among C-type lectins, recognizing both sulfated and mannosylated glycans via a single CTLD in a Calcium dependent manner (Tateno et al., 2010). In MR, the CR domain binds sulphated carbohydrates, particularly, galactose or GalNAc sulphated in Position 3 or 4 (Martinez-Pomares, 2012), Langerin binds to 6'-sulfo-LacNAc (N-acetyl-D-lactosamine) (van Gisbergen et al., 2005), whereas no binding was observed for either its position isomer, 6-sulfo-LacNAc (Terada et al., 2005), or unsulfated form. A weak, but significant signal was also observed for 6-sulfated GlcNAc (Tateno et al., 2010), suggesting that sulfate at the C-6 of the non-reducing end sugar might be important for Langerin recognition. This way, MR and langerin do not bind sulphated glycans in the same manner. Mannose receptor also has a key role in collagen internalization through the FNII domain (Figure 2). Glycosylation, proteolytic cleavage and changes in conformation are able to alter MR function (Martinez-Pomares, 2012). MR was also shown to recognize glycosylation sites of Hepatic Growth Factor B-chain (HGF- β) in a Ca^{2+} -dependent manner, mediated by CTLD (Ohnishi et al., 2012).

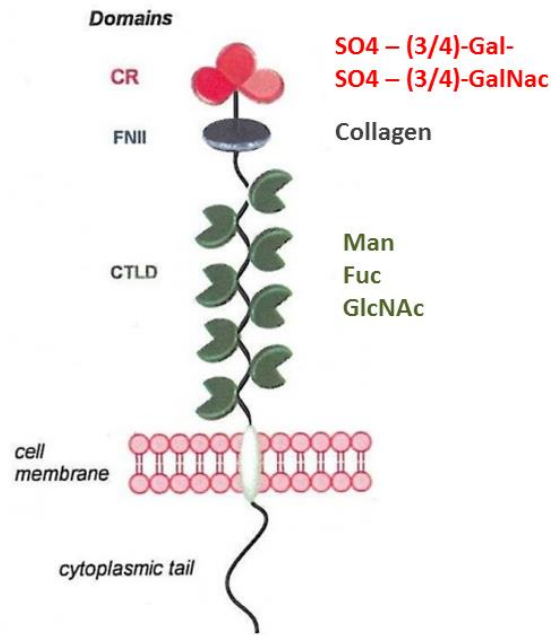


Figure 2. Structure of MR. Mannose receptor possesses three main regions – the Cysteine-Rich lectin domain (CR) which binds sulphated sugars (sulfated galactose and sulfated N-acetylgalactosamine), glycoprotein hormones such as lutropin and chondroitin sulfate A and B; the Fibronectin type II (FN II) domain which binds collagen and eight C-Type Lectin-like Domains (CTLD) which binds mannose, fucose and N-acetylglucosamine.

MR is a highly endocytic receptor which undergoes constant recycling between the plasma membrane and the early endosomal compartment (Gazi and Martinez-Pomares, 2009). Endosomal acidification is thought to induce ligand release from the receptor, with the empty receptor recycling back to the surface. The recycling process is dependent on actin polymerization (Figure 3).

In the cytoplasmic tail of Mannose Receptor (MR), a di-aromatic motif of Tyr¹⁸-Phe¹⁹ mediates receptor endosomal sorting (Schweizer et al., 2000). Signaling pathways mediated by other CLRs such as macrophage MR or DEC205 remains largely unknown.

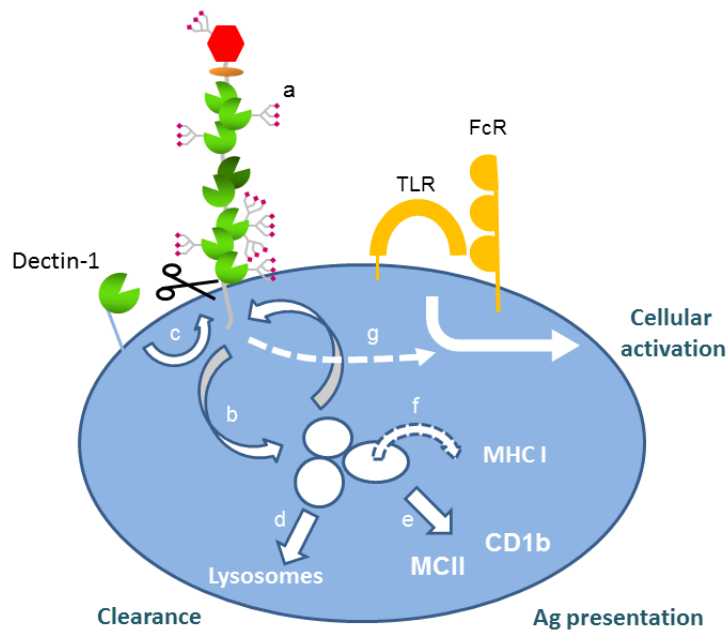


Figure 3. Overview of MR function. (a) Glycosylation of the mannose receptor regulates binding properties. (b) MR recycles constantly between the membrane and the early endosomal compartment with most of the receptor being found at the early endocytic compartment. (c) MR shedding is induced by dectin-1 engagement. MR ligands can undergo degradation in the lysosomes (d), be presented through the MHCII and CD1b pathways (e), or cross-presented (f) by MHCI. (g) MR modulates cell activation through TLR and FcR activation. Adapted from (Martinez-Pomares, 2012).

MR; an historical perspective

In 1978, the first study (Stahl et al., 1978) showing evidence of alveolar macrophages from rats being able to bind glycoproteins was published. In the definition of receptor-mediated binding it is necessary to observe ligand specificity and saturability. Saturability of binding to the receptor when increasing amounts of ligand are presented to the cells demonstrates a limited number of binding sites per cell, with the binding strength depending of the chemical structure of the ligand (Stahl et al., 1978). Glycoconjugates with galactose at the terminal position did not bind to alveolar

macrophages and did not function as an effective inhibitor. The recognition of glycoproteins by alveolar macrophages showed to be serum-independent; it was restricted to macrophages and was not present on polymorphonuclear leukocytes or lymphocytes (Stahl et al., 1978).

Receptor-mediated endocytosis is employed by many eukaryotic cells as a means of assimilating macromolecules with high selectivity from the environment (Tietze et al., 1980). Glycoconjugates uptake by macrophages involved binding of ligand to the receptor and subsequent internalization of the receptor-ligand association (Tietze et al., 1980). Uptake was observed to proceed linearly over time and this was explained by receptor recycling within the cell (Tietze et al., 1980). In other words, when the receptor-ligand complex is internalized, the ligand is dissociated from the receptor inside the cell, allowing the receptor to be recycled back to the membrane (Tietze et al., 1980). At 4 °C, it is believed that mannosylated macromolecules only bind to the cell surface (Stahl et al., 1980), for internalization of receptor-glycomolecule to occur, a higher temperature is necessary (37 °C). In alveolar macrophages, uptake inhibition was only seen after the bulk of receptors were internalized. It was also observed that a large fraction of receptors remained inside the cells at any given time.

The MR endocytic process was shown to involve binding of the molecule to a specific receptor and its association with coated pits on the membrane and internalization in coated vesicles (Tietze et al., 1982). After internalization, the ligand dissociates from the receptor and may be redirected for degradation in the lysosomes (Goldstein et al., 1979). Evidence of receptor recycling was initially indirect; (i) the ability of cells to internalize ligands far exceeded the number of receptors on the membrane and (ii) uptake proceeds in the absence of protein synthesis. Receptor-ligand (R-L) complex may follow the 'Cycling pool' path and be recycled back to the

membrane (Tietze et al., 1982). R-L complex may also follow the 'non-releasable pool' path, in this compartment, a drop in pH in the endosome causes dissociation of receptor-ligand (Figure 4).

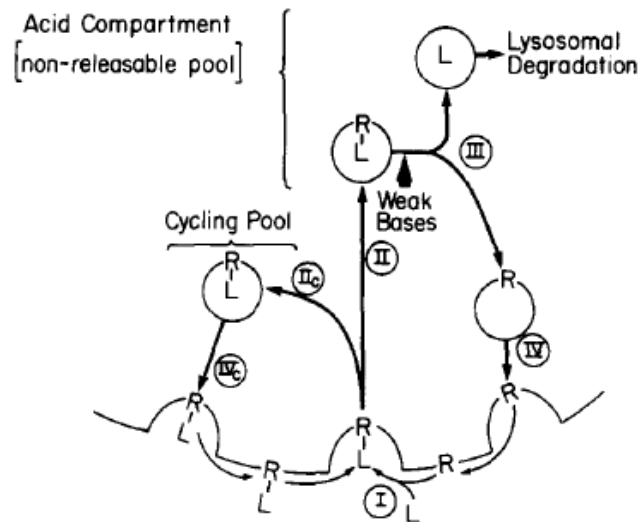


Figure 4. Expanded mechanism for the mannose-specific endocytosis receptor. Diagram showing the free receptor pool and the receptors that are part of the cycling pool. Dissociation of receptor-ligand is pH dependent. Intracellularly there is a pool of unoccupied receptors that move to the surface. The receptor-ligand may continuously cycle between the intracellular compartments and cell surface. Weak bases could cause a depletion of surface receptor pool by 50-80%. This depletion could result from the trapping of receptor ligand complexes in the non-releasable pool. The receptor cycling pool is not affected by weak bases (Tietze et al., 1982).

In rat alveolar macrophages, the intracellular MR pool was estimated as 4-fold larger than the cell-surface receptor pool (Stahl et al., 1980). The cell surface pool of active MR was calculated as around 75000; while the total cell pool could reach 375000. Glycomolecule uptake can reach 2×10^6 molecules/h per cell in these cells. This suggests that each receptor, on average, might take 11 minutes for each cycle, from cell surface to internalization and back to surface again. Acidification may also seem to be necessary for recycling of unoccupied receptors. Receptors in acid intracellular compartments moved to the surface, whether or not ligands were present. Neutralization of the acid compartments lead to trapping of receptors inside the cell (Wileman et al., 1984).

Receptor-ligand dissociation could occur in the presence of ATP or GTP (Wileman et al., 1985). The dissociation was shown to be dependent of acidification, suggesting that an ATP-dependent proton pump is responsible for acidification of the endosomes (Wileman et al., 1985). Mannose receptor is capable of both mediating phagocytosis of mannose-coated particles (Shepherd and Hoidal, 1990) and mediating pinocytosis of soluble mannosylated glycoproteins (Stahl, 1990). A signal for phagocytosis is present within the cytoplasmic tail (Ezekowitz et al., 1990).

MR is considered a marker of immature dendritic cells (DC) and participates in the immune response initiation against a wide array of microorganisms. DC maturation occurs after cellular activation and during migration of DCs to lymph nodes, resulting in down-regulation of endocytic capacity while the ability to present MHC II/peptide complexes to T cells are maximized (Steinman, 1991). Maturation can be achieved by bacterial products, such as LPS. In APCs MR efficiently transports antigens to intracellular compartments for processing and presentation. Mannosylated antigens could be internalized in high numbers and in a short period of time and resulted in a maximal T cell response activation (Engering et al., 1997). Mature dendritic cells present diminished capacity for glycosylated antigen presentation (Engering et al., 1997). Glycosylation has a major impact on the immunogenicity of proteins. The α -Gal epitope may cause anaphylactic reactions in humans and the nonhuman sialic acid Neu5Gc induces antibody responses upon dietary absorption (Lepenies and Seeberger, 2014). Glycosylation of the antibody fragment crystallisable domain (Fc domain) affects recognition by Fc γ receptors, leading to modulation of the immune response (Pincetic et al., 2014).

Mannosylation of antigens showed to be an effective strategy for macrophage and dendritic cells (DCs) targeting. This strategy not only promote vaccine-induced immune responses, antitumor

responses, but induce tolerance as well (Lepenies et al., 2013). Oxidized mannan coupled with the human tumor antigen, MUC1, binds to Mannose Receptor leading to efficient internalization and cross-presentation therefore mediating a potent antigen-specific CD8⁺ T cell response (Apostolopoulos et al., 2000). The presence of aldehydes in the oxidized mannan-MUC1 is responsible for the increased presentation by MHC I class molecules. After internalization there is a rapid access to the class I pathway via endosomes to the ER and the Golgi complexes for co-presentation by MHC class I molecules. Presence of mannose on an antigen leads to a 100-10000-fold increase in MHC class II presentation to T cells (Tan et al., 1997, Engering et al., 1997). In the presence of oxidized mannan there is a selective passage to the class I pathway. Early-stage breast cancer patients in a clinical study part of a tumor immunotherapy with oxidized mannan-MUC1 showed that mannan-MUC1 based vaccines had therapeutic potential (Apostolopoulos et al., 2006). Mannan-based protein delivery to APCs has showed successful for gene delivery (Tang et al., 2007).

Regulation of MR expression

In 1992, Stahl proposed that MR expression may be an excellent marker for macrophage differentiation because expression of the receptor was tightly regulated in macrophages. A number of agents were shown to increase MR expression, such as 1,25 dihydroxy vitamin D3 (Clohisy et al., 1987), prostaglandin E (Schreiber et al., 1990), dexamethasone (Shepherd et al., 1985). In contrast, interferon- γ (Mokoena and Gordon, 1985) and immune complexes (Schreiber et al., 1991), decreased receptor expression.

MR contribution to disease pathogenesis

In addition to MR role in pathogen recognition, MR has been implicated in the development of kidney crescentic glomerulonephritis in mice based on results obtained using a model of nephrotoxic nephritis and MR-deficient animals (Chavele et al., 2010). Crescentic glomerulonephritis is not a specific disease but rather is a morphologic expression of severe glomerular injury (Couser, 1988). The nephrotoxic nephritis model is dependent on the interaction of immunoglobulins (Igs) with activating Fc receptors (FcRs) (Kaneko et al., 2006, Tarzi et al., 2003), as well as on macrophage- and T cell-mediated effector functions (Duffield et al., 2005, Kitching et al., 1999). MR deficiency protected mice against renal injury in response to nephrotoxic globulin. These animals displayed well-preserved renal architecture, normal renal function and minimal proteinuria (Chavele et al., 2010). This protection occurred despite similar humoral and T immune responses, but was associated with diminished macrophage and T cell infiltration. Proliferation of resident glomerular cells, e.g. mesangial cells, occurred after glomerular injury. MR deficient mesangial cells underwent increased apoptosis, whereas *Mr*^{-/-} macrophages had diminished FcR-mediated function; the interaction of the two cell types led to a predominantly less-inflammatory macrophage phenotype (Chavele et al., 2010). FcR and MR could interact through the binding of nephrotoxic globulin, with *Mr*^{-/-} macrophages and mesangial cells presenting impaired Fc-mediated phagocytosis compared with Wt controls. *MR*^{-/-} macrophages also produced less TNF- α in response to a range of LPS doses compared with their WT counterparts. The results suggest that signalling through MR in mesangial cells and macrophages may lead to cell activation and promotion of glomerulonephritis. Therefore, it is believed that MR

represents a therapeutic target in immune-mediated glomerulonephritis (Chavele et al., 2010).

Imaoka and co-workers showed that MR is overexpressed on alveolar macrophages in lungs of patients with severe chronic obstructive pulmonary disease and suggested it may be involved in the pathogenesis of this condition (Kaku et al., 2014). Recently soluble serum MR, generated at least in part by enzymatic shedding of MR⁺ immune cells, has been utilised as a prognostic biomarker in patients with multiple myeloma (Andersen et al., 2015), and with liver cirrhosis (Grønbæk et al., 2016).

Targeting of lectin receptors

For glycoproteins to be recognized by lectins, proper folding is required to allow its biological activity, therefore, removing N-glycosylation sites or trying to express glycosylated proteins in prokaryotes, which lack functional N-glycosylation machinery, is not suitable for the production of therapeutic glycoproteins (Lepenies and Seeberger, 2014). Instead, in order to artificially produce glycoproteins that are suitable for humans, alternative expression systems are required: (i) – a system that includes a functional glycosylation apparatus in bacteria, (ii) – protein expression in eukaryotic cells (yeasts, insect cells, protozoa, plants, and mammalian cells) or (iii) – a cell-free expression system (Johannssen and Lepenies, 2017).

The interaction between carbohydrates and lectins is usually very weak and the binding can be enhanced by using multivalent ligands. Multiple ligands on the same molecule create a cluster glycosidic effect that simply increase the binding constant.

Several types of synthesized multivalent glycans are known: glycoclusters, polymers, model antigens (glycosylated proteins and peptides), liposomes, dendrimers and nanoparticles (Johannssen and Lepenies, 2017). Parameters such as size, surface charge,

ligand density and conjugation methods impact targeting efficacy (Lepenies et al., 2013, Joshi et al., 2012). Ideal polymer synthesis should have controlled chain length, architecture, monomer sequence, chain folding and tertiary structures (Schmidt et al., 2011, Ouchi et al., 2011). Carbohydrates differ from amino acids and nucleotides by their versatility for isomer formation (Becer, 2012). Oligosaccharides have a high-density coding capacity due to their variations in anomeric status, linkage positions, ring size, branching, and introduction of site specific substitutions (Becer, 2012). These characteristics make oligosaccharides highly specific for receptor binding. Glycopolymers are an alternative structures to oligosaccharides (Bertozzi and Kiessling, 2001). The current challenge is to synthesize glycopolymers that are able to mimic oligosaccharides in its binding selectivity to lectins (Slavin et al., 2011). It is possible to control the polymer chain length and architecture using controlled/"living" polymerization techniques (Becer, 2012).

The use of glycan-based CLR-targeting possess many advantages: lower immunogenicity of carbohydrates and the opportunity to target several CLRs simultaneously (Johannssen and Lepenies, 2017). Glycan-ligand density and the spatial orientation of ligands can be manipulated, permitting a more flexible design. Development of ligands is cost- and time-consuming, requiring planning, investment and testing. Among lectins, MR is an important target for glycan-based targeting, whether one has the intention to exploit its endocytic features for gene delivery, or to modulate its ability to activate T cells.

1.4. Macrophages in health and disease

As mentioned previously, MR is mainly expressed by macrophages and dendritic cells and its expression varies according to the activation state of these cells. Macrophages are involved in host defence in all animals (Mills and Ley, 2014), participating actively in the inflammatory process, including the repair/healing phase (Mosser and Edwards, 2008). Macrophages are not only involved in immune functions but also have homeostatic roles, such as phagocytosis of cells fragments during development, removal of cellular debris and clearance of apoptotic cells (Kono and Rock, 2008). Phagocytosis of cellular components is able to dramatically change cell physiology, expression of surface proteins, and cytokines. Alteration in macrophage surface-protein expression in response to these stimuli could potentially be used to identify biochemical markers that are unique to these altered cells (Mosser and Edwards, 2008). Macrophages can detect endogenous danger signals that are present in the debris of necrotic cells through Toll-like receptors (TLRs) (Park et al., 2006). This makes macrophages one of the primary sensors of danger in the host.

Macrophages are known as initial responders in host defence. They recognise microbial-associated molecular patterns (MAMPS) and DAMPs through PRRs, initiate antimicrobial response, and instruct the adaptive immune response (Huen and Cantley, 2015). Macrophages can augment, modulate or suppress the local inflammatory milieu. *In vivo* studies of animal models of infectious or sterile organ injury suggest that macrophages are initially induced to a pro-inflammatory state which promotes removal of infected or damaged cells, followed by a wound-healing state. Macrophage categories were initially defined by *in vitro* responses to the prototypic T-helper 1 (Th1) cytokine, IFN γ (M1), or Th2 cytokines, interleukin IL-4 and IL-13 (M2), respectively (Gordon, 2003). This

system has expanded along time and now includes a growing set of inducers and transcriptional regulators that mediate a wide spectrum of activation states (Huen and Cantley, 2015) of which M1 and M2 are considered representative models of pro-inflammatory and wound healing activation states, respectively. An excessive response in either direction can lead to a disruption in homeostasis. A strong M2/healing response can lead to chronic infections, fibrosis, allergy, and immunosuppression in cancer (Mills, 2012). On the other side, an excessive inflammatory response plays a major role in atherosclerosis, autoimmunity, and other chronic inflammatory conditions.

Mononuclear phagocytes comprise monocytes, macrophages and dendritic cells (Geissmann et al., 2010). These cells are especially sensitive to Macrophage colony-stimulating factor (M-CSF), also known as CSF-1, a pleiotropic macrophage growth factor responsible for survival, differentiation and proliferation of monocytes (Stanley et al., 1997), in addition to spreading and motility of macrophages (Pixley and Stanley, 2004). M-CSF can either be secreted in the circulation as a glycoprotein, remain attached to proteoglycans or be expressed as a membrane-spanning glycoprotein on the surface of M-CSF-producing cells. M-CSF can be produced by vascular endothelial cells in response to bacterial endotoxin (Bartocci et al., 1987). Cytokines and steroid hormones are also known to increase production of M-CSF (Stanley, 2000). The tertiary structure of M-CSF is similar to the structure of granulocyte-macrophage colony-stimulating factor (GM-CSF), however, they do not share amino acid sequence homology (Pandit et al., 1992). Macrophages cultured in GM-CSF show a less-polar, less-spread morphology than macrophages grown in the presence of M-CSF (Pixley and Stanley, 2004).

M-CSF is normally present in tissues and plasma, and has been associated with M2-type macrophages. Whilst GM-CSF is only

present following injury or during infections, and has been associated with M1-type responses.

Due to the plurality of macrophage phenotypes, here, only the two classic macrophage polarization states is discussed - the pro-inflammatory M1-macrophage and the alternative activated M2-macrophages.

Classically activated M1 macrophages

IFN γ induces the M1 macrophage phenotype through binding to the IFN γ receptor complex (IFNGR) and leads to expression, among others, of pro-inflammatory chemokines. These chemokines include MCP1 (CCL2) and monokine induced by gamma interferon (MIG, CXCL9) that recruit monocytes and T cells, respectively, to sites of inflammation (Rauch et al., 2013). IFN γ can also induce expression of inducible nitric oxide synthase (iNOS) and increase the microbicidal activity of macrophages against intracellular pathogens. IFN γ is produced by cells of the immune system, this include natural killer (NK) cells, innate lymphoid cells (ILCs), cells involved in the adaptive immune response, such as T helper 1 (T_H1) cells and CD8⁺ cytotoxic T lymphocytes (CTLs). As mentioned above IFN- γ signals through IFNGR, which is expressed in many cell types. IFN γ can be induced by cytokines (IL-12 or IL-18) and by activation of PRRs (Ivashkiv, 2018).

Binding of IFN γ to its receptor activates the canonical Janus kinase (JAK)-signal transducer and activator of transcription (STAT) signalling pathway. It starts with the activation of the receptor-associated JAK1 and JAK2 protein-tyrosine kinases and subsequent tyrosine phosphorylation and activation of primarily STAT1, which translocates to the nucleus, binding to conserved IFN γ activation site (GAS) DNA elements and directly activating transcription of interferon-stimulated genes (ISGs) (Ivashkiv, 2018). ISGs encode products that have direct effector immune functions, such as

chemokines, antigen-presenting molecules (MHC), phagocytic receptors and various antiviral and antibacterial factors. IFN γ promotes host defence against intracellular pathogens, modulation of immune and inflammatory responses and associated tissue damage and tumour immunosurveillance (Ivashkiv, 2018).

Signalling by the JAK-STAT pathway is transient, with a peak signal occurring at 15-60 minutes and returning back to baseline at 2-4 hours after stimulation (Ivashkiv, 2018). Nevertheless, transcriptional responses of many direct STAT1 target genes peak several hours after IFN γ stimulation. A subset of ISGs shows delayed kinetics in a manner dependent on new protein synthesis (implying indirect regulation) and a pattern of sustained gene expression that persists beyond the duration of JAK-STAT1 signalling (Levy et al., 1988, Levy et al., 1990). This delayed and sustained kinetics of gene induction could be explained in part by a feedforward loop in which IFN γ induces *de novo* expression of transcription factors – interferon regulatory factors (IRFs) and STATs themselves, which cooperate to induce and sustain gene expression (Hu and Ivashkiv, 2009). Stimulation of IFN γ -induced macrophages by TLR ligands leads to super-induction of inflammatory cytokines and canonical nuclear factor- κ B target genes, event known as priming. IFN γ also induces gene-specific refractoriness to anti-inflammatory cytokines and IL-4 and IL-13.

The activation of transcription factors results in the induction of IL-1, IL-6, IL-12 and TNF α (Mosser, 2003, Lawrence and Natoli, 2011). Although these can cause tissue damage, proinflammatory M1 monocytes/macrophages can play an important role in clearance of apoptotic cells and debris after sterile injury (Arnold et al., 2007), where phagocytosis of myogenic precursor cells induce a switch to an anti-inflammatory profile.

IFN- γ induces the expression of the indoleamine 2,3-dioxygenase (IDO) gene in human cells. IDO is the main controller enzyme of the

Kynurenine pathway (KP), a pathway where the amino acid tryptophan is initially converted to N-Formylkynurenine, generating many intermediary products and nicotinamide adenine dinucleotide (NAD⁺) as the end product of the pathway. NAD⁺ is important cofactor involved in genome stability, stress tolerance and metabolism (Cervenka et al., 2017). IFN- γ inducible expression of the IDO gene is dependent of two upstream elements: I - a 14-base pair sequence homologous to an interferon-stimulated response element (ISRE) sequence found in IFN- α -inducible genes and II - a 9-base pair palindromic sequence homologous to an interferon- γ activated site (GAS) element found in IFN- γ -inducible genes (Chon et al., 1996). The ISRE homolog sequence and the PE II element recognized IFN- γ -regulated factors IRF-1 and p91 (STAT1), respectively (Chon et al., 1995). It has been established that IFN- γ induces the level of the IRF-1 factor (Pine et al., 1990), whereas p91 (STAT1) is activated by tyrosine phosphorylation of pre-existing p91 protein through the involvement of JAK1 and JAK2 enzymes activated by IFN- γ (Darnell et al., 1994). IDO activation is dependent on IRF-1 factor (Chon et al., 1995) when stimulated by IFN- γ but not by LPS (Fujigaki et al., 2006). The response of IDO gene to IFN- γ depends on a cooperative role of IFN- γ -responsive factors binding to the ISRE and GAS elements. LPS induction of IDO is mediated dominantly by an IFN- γ -independent mechanism (Fujigaki et al., 2001, Jung et al., 2007).

IDO activation limits availability of tryptophan. Because tryptophan is required for protein synthesis, withdrawal of this essential amino acid from the micro-environment arrests biosynthesis and subsequent growth of pathogens and proliferating cells (Schröcksnadel et al., 2006). Tryptophan deprivation leads to decreased mitosis (Hwu et al., 2000, Munn et al., 1999, Munn et al., 2002) and increased apoptosis in macrophages and dendritic cells (Terness et al., 2002, Frumento et al., 2002). Tryptophan depletion

works as a defence mechanism induced by IFN- γ in immunocompetent cells during immune response. It acts as an antimicrobial or antitumoral effector mechanism and limits the growth of intracellular pathogens or malignant cells (Pfefferkorn, 1984, de la Maza and Peterson, 1988, Ozaki et al., 1988).

A long list of clinical conditions is characterized by tryptophan degradation associated with increased immune activation, among these are Adult T-cell leukaemia, colon carcinoma, gynaecologic cancer and haematological neoplasias (Schröcksnadel et al., 2006). Cell malignancy is associated with an increased kynurenine/tryptophan ration.

Alternatively activated M2 macrophages

M2 macrophages have a broad range of functional activities ranging from wound healing, fibrosis, insulin sensitivity and immunosuppression *in vitro*. In mice these cells have been further subcategorized into M2a, M2b and M2c subtypes although it is unclear how this classification translates to the human system. The wound healing M2a subtype is characterized by expression of arginase-1 (ARG1), mannose receptor (CD206) and insulin-like growth factor (IGF1) (Martinez et al., 2009). The M2a phenotype is induced by binding of IL-4 and/or IL-13 to the IL-4R α receptor, and by activation of the JAK-STAT6 signalling pathway (Takeda et al., 1996). M2b macrophages are induced by immunocomplexes in combination with IL-1 β and LPS and M2c is induced after exposure to IL-10, TGF- β or glucocorticoids (Mantovani et al., 2004).

IL-4 is a cytokine produced by Th2 cells, basophils and mast cells. It was initially described as a growth factor for B cells stimulated by anti-IgM antibodies (Howard et al., 1982). IL-4 together with IL-13 drives type 2 immunity characterized by eosinophilia, mast cell hyperplasia, IgE secretion, smooth muscle contraction and epithelial remodelling (Chomarat and Banchereau, 1998, Nelms et al., 1999,

Fallon et al., 2002, McKenzie et al., 1998, McKenzie et al., 1999, Kühn et al., 1991). This cytokine signalling is involved in cell growth and survival (Chomarat and Banchereau, 1998, Nelms et al., 1999, Pernis and Rothman, 2002). This response can be helpful against helminth parasites but it is also implicated in allergy and asthma. IL-4 can stimulate two receptors, type I and type II. IL-4 receptors are composed of two transmembrane proteins which undergoes dimerization to form a type I or type II after IL-4 binds to IL-4R α chain. Receptor dimerization activates JAKs which starts a phosphorylation cascade (Kelly-Welch et al., 2003).

In vivo macrophages present themselves in a much more complex set of phenotypes than those observed *in vitro*; tissue-specific differentiation signals and the microenvironment contain numerous activation stimuli that vary not only among disease models but also temporally with respect to different stages of injury and repair (Sica and Mantovani, 2012). In response to this a model of 'spectrum of macrophage differentiation stages' has been proposed (Mosser and Edwards, 2008). In this model three main macrophage profiles were considered: host defence, wound healing and immune regulatory macrophages. According to this model populations of macrophages can actually present 'shades' of more than one of these profiles.

Macrophage origin can be diverse. Tissue macrophages may come from three sources: yolk sac, fetal liver and hematopoietic stem cells in the bone marrow. Once precursor cells reach the organs they differentiate into resident macrophages, which maintain homeostasis through phagocytosis of apoptotic bodies and production of growth factors and depending on the tissues, they are replenished through replication (microglia) or through monocyte recruitment (dermis). During inflammation, tissue resident macrophages are activated and there is recruitment of monocytes to the affected organ. There these cells become inflammatory mononuclear phagocytes. In chronic diseases, there is local

proliferation of macrophages. Under inflammatory conditions macrophages play roles that range from a pro-inflammatory profile with production of pro-inflammatory cytokines to more 'alternative' roles that contribute to resolution of inflammation and organ repair (Lin et al., 2009) (Alikhan et al., 2011).

Macrophages in disease

Tumour Associated Macrophages (TAMs) are an example of M2 macrophages that contribute to disease progression. In some tumours the percentage of macrophages among leukocytes can reach more than 50% (Mills et al., 2015). TAMs actively promote tumour growth (Laoui et al., 2014). Modulating macrophage polarization by decreasing M2 phenotype and increasing the M1 phenotype can slow or reverse tumour growth. Treatment of lung cancer in mice with clodronate-encapsulated liposome, a macrophage-depleting agent, significantly decreased tumour burden (Fritz et al., 2014).

In kidneys some studies demonstrated that systemic depletion of monocytes/macrophages, through administration of liposomal clodronate before ischemia reperfusion (IR), decreases morphologic kidney damage (Jo et al., 2006, Day et al., 2005). Other studies raised the possibility that the phenotype of the recruited macrophages play an important role in the degree of renal parenchymal injury (Wang et al., 2007, Vinuesa et al., 2008). In a mouse model of IR injury generated by unilateral renal pedicle clamping, macrophages were depleted by liposome clodronate. M2 macrophages transfer after liposome clodronate injection led to almost complete reversion of interstitial fibrosis, while transfer of M1 macrophages did not affect the degree of fibrosis (Kim et al., 2015). This led to the hypothesis that macrophages can be good targets for kidney injury therapy development and therapies targeted to a

macrophage receptor involved in immune response, homeostasis and cell activation would be suitable for this purpose.

Within this context, macrophage MR may become an important biological target in therapies aiming at reprogramming immune responses mediated by macrophages and DCs. Therefore the identification of selective receptor modulators is the initial step of this process (Azad et al., 2014). Although there are numerous options for MR ligands, largely based on mannose, there is still a lack of MR-blockers for the MR to be exploited as therapeutic agents. MR-specific glycopolymers offer a novel approach to harness the potential ability of MR to modulate macrophage and dendritic cell function.

1.5. Results leading to this project

Synthetic glycopolymers (GPs) are macromolecules featuring multiple copies of pendant carbohydrate moieties. GPs are multivalent, generally biocompatible, and have been utilised as multivalent ligands to investigate many biological processes, including cell-cell adhesion (Oezyurek et al., 2009, Muthukrishnan et al., 2006), development of new tissues, and reduction of infectious behaviour of virus and bacteria (Ogata et al., 2009). Binding between carbohydrates and lectins is weak but highly specific (Ting et al., 2010), with dissociation constants (K_d) in the range of 10^{-3} – 10^{-6} . One way to increase binding affinity is through multivalency which can be achieved with an increase in sugar density (Spain and Cameron, 2011). Multiple interactions provide extra specificity between carbohydrates and their binding proteins and at the same time offer extra binding strength (Ambrosi et al., 2005). In addition, the binding avidity of carbohydrate-containing polymers to lectin receptors often depends on the polymer chain size, which affects the ability to directly span over multiple copies of receptors across the membrane. Studies indicate that both the density and number of sugar binding units in biological multivalent ligands are key to determine the affinity of lectins and direct specific biological responses (Dam and Brewer, 2010). Sugar-based polymers have attracted substantial interest for biomedical applications, including gene, protein, drug, and antigen delivery (Zhang et al., 2015). Controlled radical polymerisation (CRP) is a family of polymerisation reactions which combines the functional group compatibility of conventional free radical polymerisation, with the ability to obtain polymers with narrow molecular weight dispersity typical of living polymerisations, and has been widely utilised to synthesise well-defined glycopolymers (Yilmaz and Becer, 2014). Atom-transfer radical polymerization (ATRP) is a CRP technique discovered in 1995

independently by Sawamoto (Kato et al., 1996) and Matyaszewski (Wang, 1995b). The living nature of ATRP allows for sequential addition of different monomers even in one-pot reaction to obtain block-copolymers of linear, star or comb-like topologies (Zhao, 2015). The possibility of building libraries of structurally well-defined macromolecules has paved the way for a number of investigations aimed at understanding the relationship between polymer structure and physical properties or function (Wojciech et al., 2012).

ATRP employs the reversible transfer of halogen atoms between growing chains and a redox active transition metal catalyst (Wang, 1995a). In ATRP, a transition metal, M_t^m (Cu^I), abstracts a halogen atom X (Br or Cl) from an organic halide, $R-X$, to form an oxidized species, $X-M_t^{m+1}$, and a carbon-centered radical $R\bullet$, which will thus generate radicals via redox reactions (Figure 5). The transition metal exists as a complex $X-M_t^{m+1}/L_n$ with L_n being a ligand. Radicals species ($R\bullet$) in turn react with the monomer of choice, in a propagation step which involves the stepwise growth of polymer chains. The equilibrium constant for the overall process, K_{eq} (also known as K_{ATRP}) is determined from the ratio of the activation (k_{act}) to deactivation constants (k_{deact}). Reaction conditions – e.g. choice of transition metal, ligand, temperature, concentration of the species involved, and nature of ATRP initiator and monomers – must be optimised to keep K_{eq} to an appropriate value to meet to contrasting needs, that is, to achieve an acceptable reaction rate without favouring detrimental irreversible termination reactions. A low equilibrium constant will lead to a slow polymerisation process whereas high K_{eq} results in high concentration of radical species, resulting in fast irreversible termination processes and ultimately loss of control over the polymer macromolecular features. The rate of polymerisation is much slower than the activation/deactivation process and hence the concentration of the active radicals remains

low compared to the R-X species (Wang, 1995b, Braunecker and Matyjaszewski, 2007).

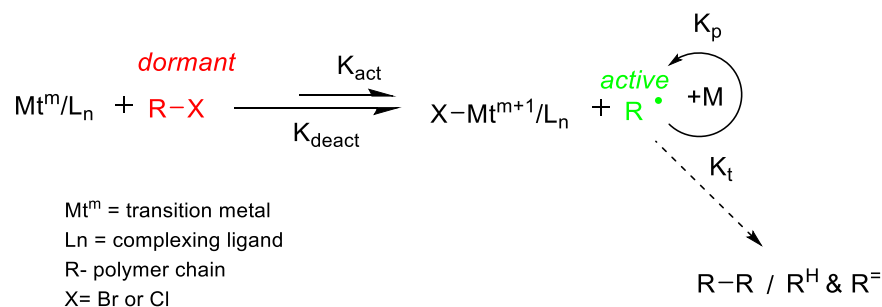


Figure 5. The general mechanism of ATRP (Matyjaszewski, 1999).

For this study two families of multivalent glycopolymers for selective targeting of the different lectin domains of MR (Figure 6) were prepared through a synthetic strategy that includes ATRP. Macroligands displaying D-galactopyranose-3-O-sulfate (SO₄-3-Gal) repeating units were expected to provide selective binding to CR domain, whilst glycopolymers containing D-mannopyranose (Man) units were designed to recognise the CTLDs. All polymers had a mucin-like structure (Godula and Bertozzi, 2012), with the sugar binding units grafted to the polymer backbone through a glycoside linker, leaving groups at C3 and C4 of the sugar rings, available for lectin binding. The avidity of binding of carbohydrate-containing polymers to lectin receptors often depends on the polymer chain length, which also directly affects the ability of these multivalent ligands to span over multiple copies of receptors at cell membranes. To isolate the contribution of the nature of the carbohydrate repeating units on binding, it is therefore critical that all glycopolymers investigated possess the same average chain length. This was achieved here by first synthesising a 'master' polymer precursor possessing chemoselective handles that are inert towards the polymerization conditions, which was then quantitatively functionalised with the required sugar units – D-mannopyranose

(Man), D-galactopyranose-3-O-sulfate (SO₄-3-Gal), and non-MR binding control sugar D-galactopyranose (Gal). More specifically, this approach, previously developed by Mantovani and Haddleton (Ladmiral et al., 2006) was used, which involved sequential Cu^I-catalyzed ATRP, to prepare the required polymer reactive precursor, and Cu(I)-catalysed Huisgen cycloaddition (also known as alkyne-azide cycloaddition, CuAAC), to introduce Man, SO₄-3-Gal, and Gal carbohydrate binding units, and a fluorescent tag, Oregon Green, to facilitate the detection of glycopolymers in subsequent *in vitro* assays. In this library of multivalent ligands three parameters were systematically varied, namely *i*) nature of MR-binding sugar (SO₄-3-Gal vs. Man), *ii*) density of a MR-binding sugar grafted on each polymer chain - 33, 66, and 100% of the polymer repeating units functionalised with the required sugar ligand, the remaining being occupied by non-MR binding galactose (Gal) molecules, and *iii*) length of glycopolymer chain - 32 or 187 average number of polymer repeating units. The latter were chosen to generate glycopolymers with average molecular weight M_n of 12-17 and 71-89 kDa, respectively below and above the 40-60 kDa threshold for glomerular kidney filtration which were expected to behave very differently *in vivo* due to their potentially different half-life in systemic circulation. Glycopolymers with 100% non-MR binding units, (Gal_{100%})₃₂ and (Gal_{100%})₁₈₇ were also prepared and utilised as negative controls for subsequent *in vitro* and *in vivo* studies.

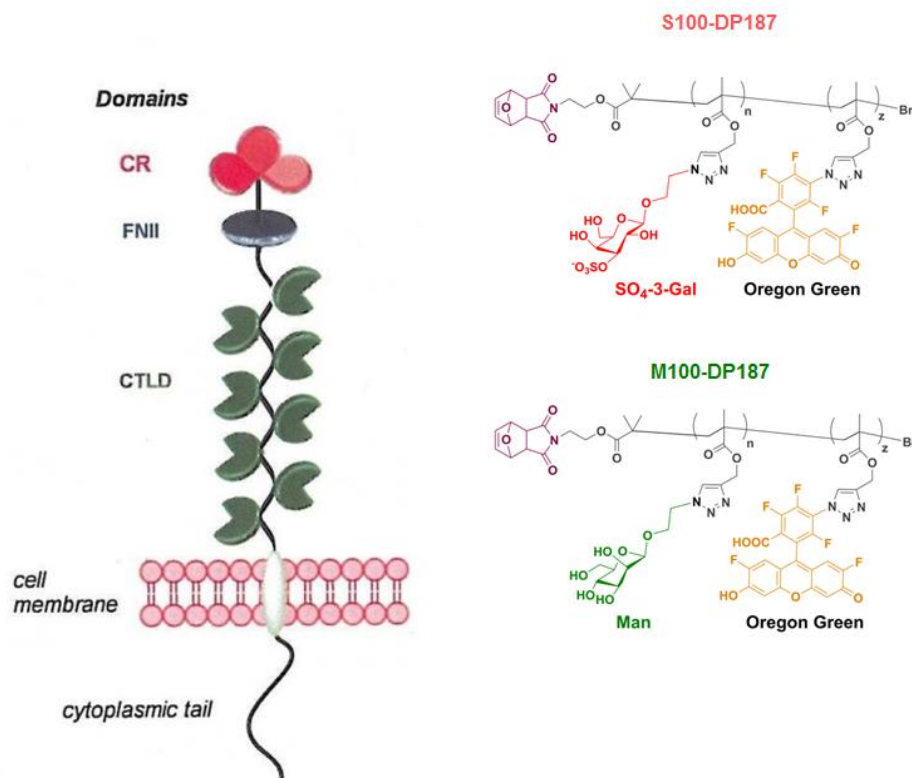


Figure 6. Mannose receptor structure and polymers chemical identity. Left. Mouse CR domain: binds to polymers containing SO₄-3-Gal-containing glycopolymers, and the CTLD domains, which bind to Man sugar moieties,. Right: chemical structure of the glycopolymers possessing $n = 187$, and presenting either SO₄-3-Gal (S100-DP187), or Man (M100-DP187) repeating units. DP is the degree of polymerisation, the average number of repeating units in each polymer chain. Glycopolymers were fluorescently labelled with 2,4,5,7,7' – pentafluorofluorescein (Oregon Green, $\lambda_{ex/em}$ 488/530 nm)(Magennis et al., 2017).

Whilst ideal to generate families of glycopolymers for the initial screening of MR-binding glycopolymer ligands, from a synthetic standpoint the ATRP - CuAAC approach is relatively cumbersome, thus once effective MR ligands were identified, an alternative approach for their synthesis which would allow for facile large-scale synthesis of these ligands was identified. Accordingly, a simple route that involves reversible addition-fragmentation chain transfer (RAFT) polymerisation was identified, and utilised to synthesise CR-binding glycopolymers. RAFT process is a versatile method for

conferring living characteristics on radical polymerizations providing unprecedented control over molecular weight, molecular weight distribution, composition and architecture. It is suitable for most monomers polymerizable by radical polymerization and is robust under a wide range of reaction conditions (Moad et al., 2008). RAFT polymerisation can be seen as a free radical polymerisation reaction, where polymers are generated from functional monomers and a source of radicals, with the addition of an extra component, called chain-transfer agent (CTA, or simply RAFT agent), which allows to control both the polymer molecular weight and molecular weight distribution.

More specifically, the overall RAFT process provides insertion of monomer units into the C–S bond of the RAFT agent structure (1) as shown in (Figure 7). (Moad et al., 2005).

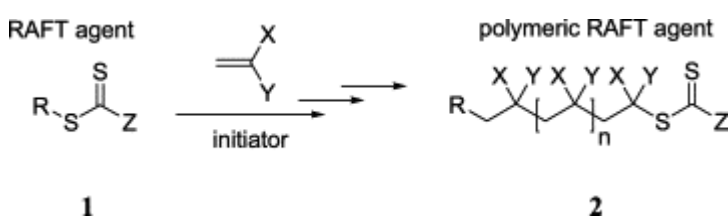


Figure 7. General mechanism of RAFT polymerisation.

Accordingly, S100-DP240, containing SO₄-3-Gal units, and its negative control analogue Gal-containing G100-DP240 were thus synthesised by RAFT polymerisation.

Preliminary studies in our lab, executed by Dr. Mastrotto (unpublished data), using CHO cells transfected with MR (MR⁺-CHO) and wild-type murine bone-marrow derived macrophages (BMDM) showed efficient polymer uptake by MR⁺-CHO for both Oregon Green-tagged mannosylated and galactose-3-O-sulfated glycopolymers (Figure 8a). No cell uptake was detected in MR⁻-CHO, or when (Gal_{100%})₃₂, which is unable to bind MR, was employed, confirming that uptake of Man and GPs was indeed mediated by MR.

Confocal microscopy analysis confirmed that the observed increase in fluorescence of MR⁺-CHO was due to cell internalization, rather than simple adhesion of GPs to MR⁺ at the cell membrane (Figure 8b).

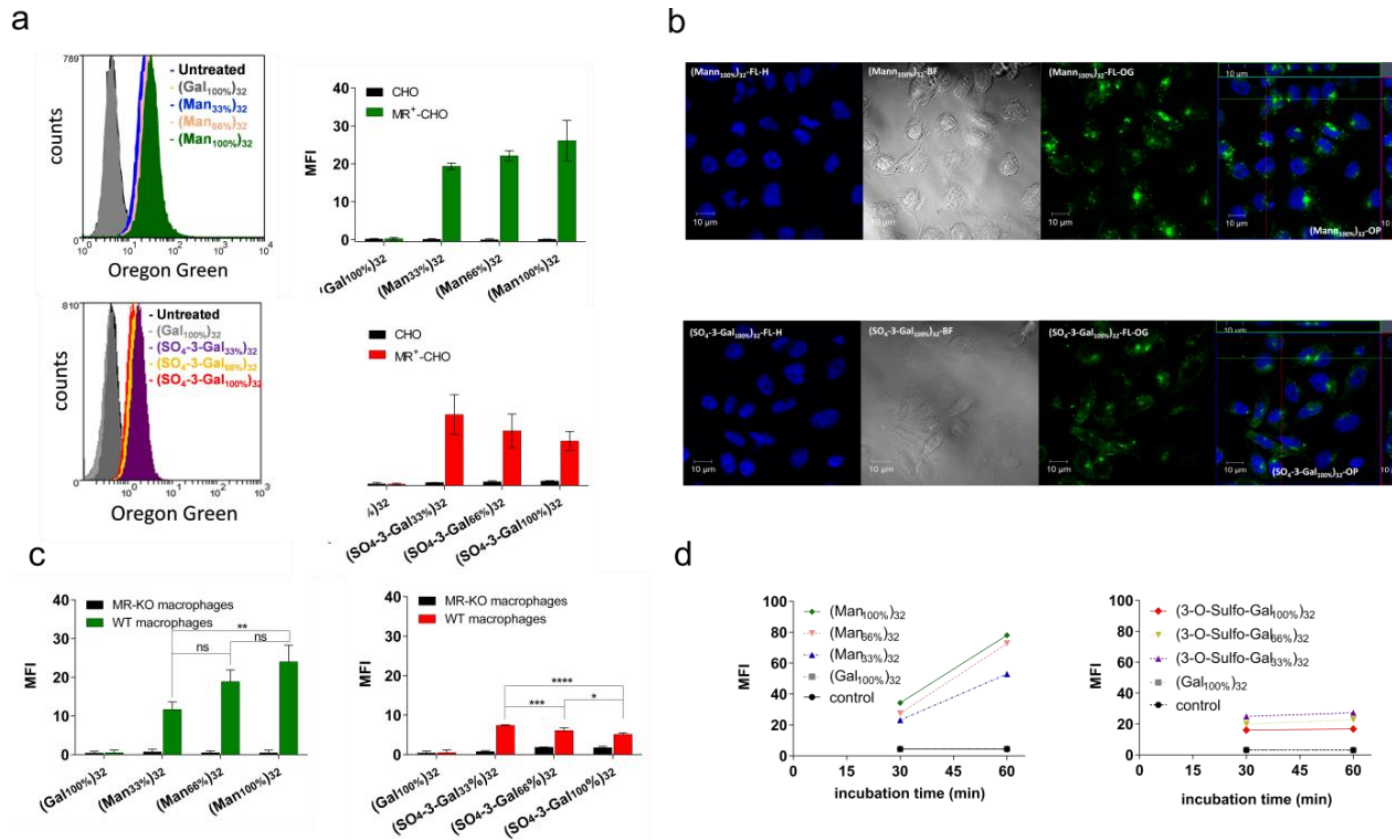


Figure 8. Internalisation of glycopolymers by CD206-presenting cells: **a.** Flow cytometry analysis of the uptake of mannosylated and 3-O-sulfo-galactosylated glycopolymers (GPs) with different sugars epitope densities. MR⁺-CHO and MR⁻-CHO cells were incubated with GPs (1.0 μg mL⁻¹) for 30 minutes at 37°C. After washing, cells were collected and analyzed by FACS. **b.** Confocal microscopy analysis of MR⁺-CHO following incubation with Oregon Green (OG) tagged GPs (100 μg mL⁻¹) for 1 h at 37°C. Cells were stained with HOECHST (H) for nuclei and imaged under bright field (BF) and fluorescence (FL) mode. **c.** Uptake of GPs by WT and MR-

KO macrophages quantified by FACS after incubation with 1.0 μg mL⁻¹ GPs solutions for 30 minutes at 37°C. **d.** Time-dependent uptake of GPs (1.0 μg mL⁻¹) by MR⁺-CHO cells. After treatment at various incubation times, cells were washed and uptake of Oregon Green-tagged GPs was quantified by FACS (credits Dr. Mastrotto).

MR⁺-CHO internalisation of Man GPs was found to be time-dependent, and increased when cell exposure was prolonged from 30 to 60 minutes. In contrast, total uptake of SO₄-3-Gal GPs remained virtually unchanged from 30 to 60 min, indicating that after the 30 min time point SO₄-3-Gal GPs could no longer be internalised (Figure 8d). Importantly, at the range of concentrations employed in this study all GPs were found to be virtually non-toxic upon incubation of at least 24 h, as assessed by LDH assay.

Having already established the influence of density of sugar binding units on cell uptake, starting from these experiments only 100%-Gal, Man, and SO₄-3-Gal with low (DP 32) and high (DP 187) molecular weight were employed. SO₄-3-Gal GPs reduced surface MR expression (Figure 9a) without affecting total MR (Figure 9b) and these findings correlated with the fact that binding of SO₄-3-Gal-GP, unlike Mann GP is pH-independent (Figure 9c) indicating that SO₄-3-Gal GP have the potential to retain MR within the endosomal compartment.

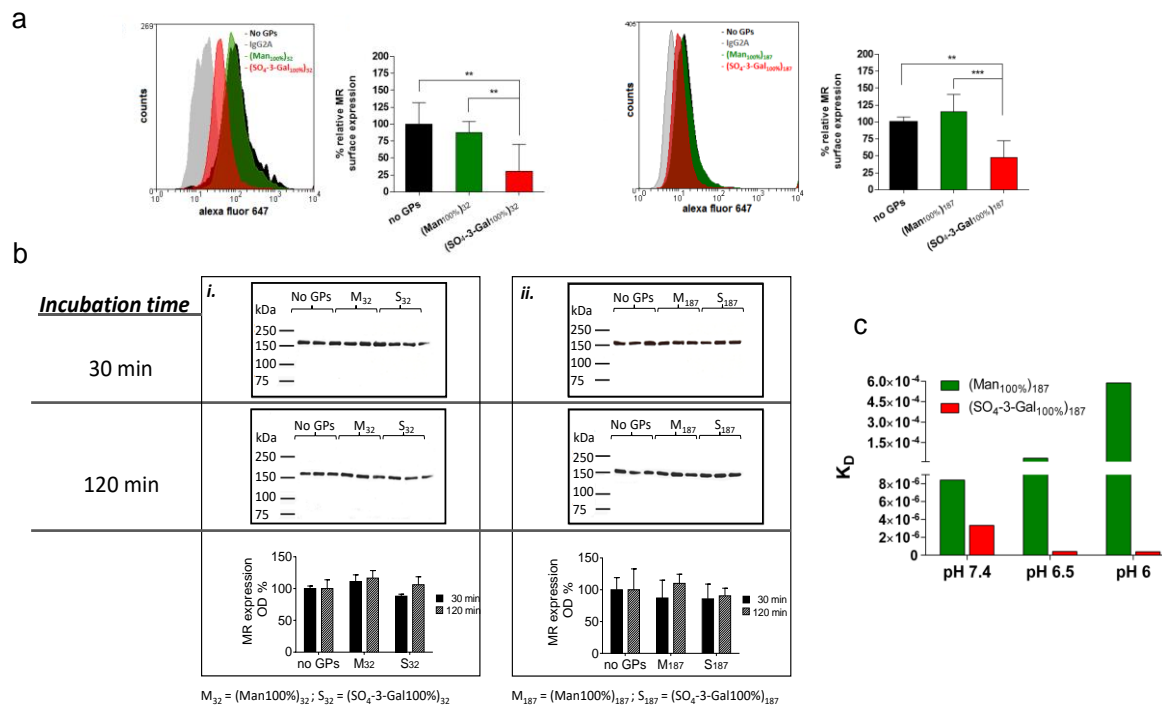


Figure 9. Mechanism of modulation of MR endocytic activity *in vitro*, and MR activity inhibition *in vivo*. To elucidate whether the inhibition occurs by an intracellular pathway leading to MR degradation, or by forming stable GP-MR complexes which prevent recycling of receptor back to the cell surface, following incubation with sulfated GPs, MR at the cell surface and total cell MR were quantified. **a.** Quantification of MR at the cell surface. Cells were incubated for 120 min with 15 μ M (Man_{100%})₃₂ or (SO₄-3-Gal_{100%})₃₂ glycopolymers (concentration refers to individual sugar repeating units), or cell medium only (positive control cells), then MR was immunostained and membrane-bound MR quantified by FACS. Data are the means \pm SD of duplicates of two independent experiments. **b.** Quantification of total cell MR. Blot analysis of cell lysates

from MR⁺-CHO cells treated with (Man_{100%})₃₂ or (SO₄-3-Gal_{100%})₃₂ solutions (A) 0.64 or (B) 15 mM in sugar repeating units) for 30 or 120 minutes. Untreated MR⁺-CHO cells were used as controls. MR expression was estimated by optical densitometry of western blots gels. Data are representative of two independent experiments performed in duplicate or triplicate. **c.** pH strongly affects binding of mannosylated GPs to the CLTD region of MR, but not binding of sulfated GPs to CR domain. The 7.4-6.0 pH range was chosen to simulate the conditions which GP-MR complexes encounter by going from cell membrane to endosomes. Dissociation constant K_D values were estimated by surface plasmon resonance (SPR) analysis, using immobilized MR, in 10 mM HEPES, 5 mM CaCl₂, 0.005% tween-20, 150 mM NaCl, pH 7.4, 6.5, 6. Higher values indicate more favorable dissociation of GP-MR complexes, which would facilitate the recycling of MR receptor to the cell membrane (credits Dr. Mastrotto).

These results indicated that with appropriate choice of polymer carbohydrate binding units one can switch from continuous delivery to MR -presenting cells, to inhibition of MR -mediated endocytosis. The latter aspect is of particular interest as it would open the way for the development of MR inhibitors, with potential important clinical implications in diseases or conditions where MR⁺ DCs and/or macrophages play a major role.

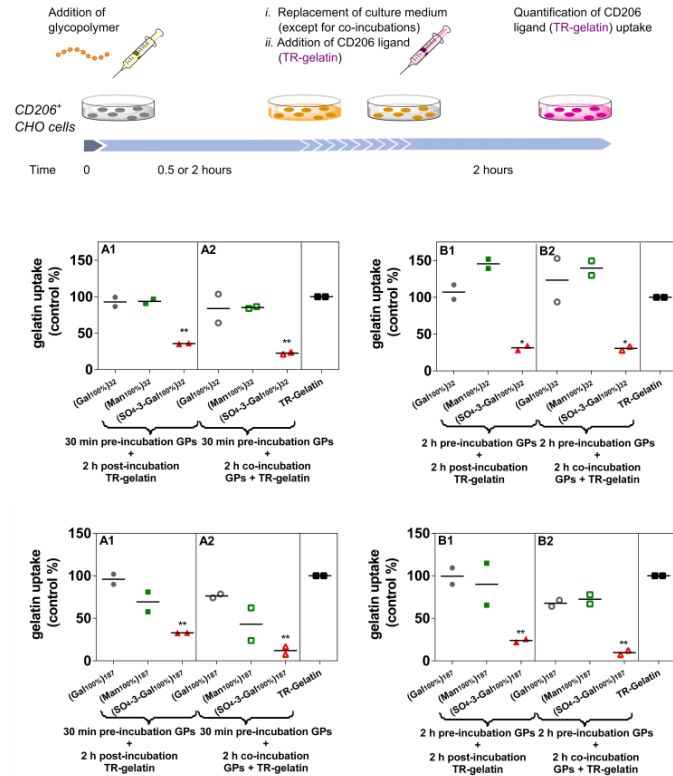
To explore this hypothesis experimentally, it was then tested the ability of sulfated GPs to inhibit uptake of other MR ligands. Collagen was chosen as its carbohydrate-independent binding to the FNII domain of MR and subsequent cell uptake have been characterised, by us (Martinez-Pomares et al., 2006b) and Dickamer's group (Napper et al., 2006b). In this work denatured collagen (gelatin) was fluorescently tagged with Texas Red (TR, $\lambda_{ex/em}$ 596/615 nm) to facilitate the quantification its MR -mediated cell uptake. MR⁺-CHO cells were chosen for this part of our study as they are more robust than WT macrophages, which allowed to carry out prolonged time-course experiments.

Initially, MR⁺-CHO were pre-treated with either (SO₄-3-Gal_{100%})₃₂ or (SO₄-3-Gal_{100%})₁₈₇ (15 μ M in sugar binding units) for 30 or 120 min, then Gelatin-TR was added to a final concentration of 10 μ g/ml. After 2 hours of co-incubation, cell uptake was quantified by FACS. Data clearly showed that internalisation of Gelatin-TR was significantly reduced compared with untreated cells incubated with Gelatin-TR for 2 h (positive control). MR⁺-CHO pre-incubated with analogous Man- and non-binding Gal-GPs showed similar Gelatin-TR uptake to that observed in untreated cells (Figure 10a). These uptake patterns did not significantly change by increasing the duration of polymer pre-incubation from 30 to 120 min. Remarkably, similar trends were also observed when after the initial pre-incubation GPs were removed from the culture media, and cells were treated with Gelatin-TR in the absence of glycopolymers, strongly suggesting that after initial

polymer pre-incubation, sustained inhibition of MR-mediated endocytosis could be attained even in the absence of sulfated GPs in the media.

To investigate the duration of this inhibition of MR endocytic activity, time course inhibition experiments were carried out. Accordingly, cells were initially incubated with either (SO₄-3-Gal_{100%})₃₂ or (SO₄-3-Gal_{100%})₁₈₇ for 2 h, then GPs were removed from the culture medium. Gelatin-TR was then added and uptake over time was monitored (Figure 10b). For both sulfated GPs full recovery of endocytic MR was observed after 48 hours. (SO₄-3-Gal_{100%})₃₂ gave the best inhibition profile, with Gelatin-TR uptake only re-starting to increase after 24-30 hours. From a therapeutic viewpoint it is important that not only the inhibitory effect is sustained, so as to reduce the frequency of the required drug intake, but also that this phenomenon is fully reversible, ensuring that MR activity is fully restored at the end of the treatment.

a



b

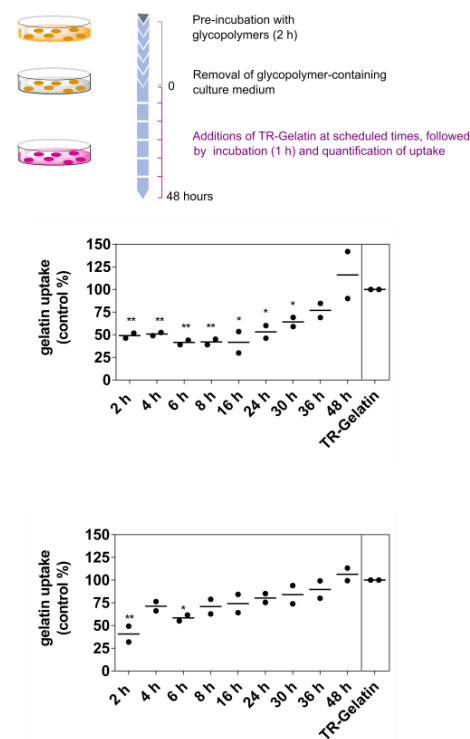


Figure 10. GPs inhibit CD206 (MR) endocytic activity *in vitro*. **a.** GPs can direct cell uptake of gelatin mediated by MR in MR⁺-CHO through its FN II domain. Cells were pretreated for (A) 30 minutes or (B) 2 hours with a range of GPs with different sugar epitopes and molecular weight (15 μ M in sugar binding units). Control cells were incubated over the same period with cell medium. Cells were then incubated for further 2 hours with fluorescently-tagged gelatin (Texas Red gelatin, 10 μ g mL⁻¹) in the presence (co-incubation) or in the absence of glycopolymers. Data is expressed as a percentage of gelatin uptake of untreated MR⁺-CHO control cells (right column of each panel, TR-Gelatin), as quantified by flow cytometry. **b.** Inhibition of CD206 endocytic activity elicited by a single initial treatment with sulfated GPs was monitored over time. MR⁺-CHO cells were incubated for 2 hours with (A) (SO₄-3-Gal100%)₃₂ or (B) (SO₄-3-Gal100%)₁₈₇ (15 μ M in sugar binding units). Control

cells were incubated over the same period with cell medium. Cells were then washed and incubated with cell medium. At scheduled time the medium was replaced with an 80- μ g mL⁻¹ of TR-Gelatin solution and incubated for 1 hour. Data is expressed as a percentage of gelatin uptake of untreated MR⁺-CHO control cells (right column of each panel, TR-Gelatin), as quantified by flow cytometry. Data were analyzed by two-way ANOVA with Bonferroni post-tests, * $p < 0.05$, ** $p < 0.01$. (credits Dr. Mastrotto).

In addition to MR, a range of other lectins are known to recognise mannose-rich molecular patterns *in vivo* – e.g. Dendritic Cell-Specific Intercellular adhesion molecule-3-Grabbing Non-integrin (DC-SIGN, CD209) (van Kooyk and Geijtenbeek, 2003) and Mannose-Binding Lectin (MBL), which can activate the lectin pathway of the complement system (Eddie Ip et al., 2009). Selective targeting of MR *in vivo* using mannosylated ligands appears to be challenging unless disease-specific delivery strategies, e.g. local administration, are utilised. Conversely, lectins able to selectively recognise SO₄-3-Gal motifs with sufficient avidity are less common. Using libraries of sulfated Gal polymers, Kiessling and coworkers showed that for relatively strong binding of P-selectin an additional sulfate group at C6 of the Gal units was required (Manning et al., 1997). Targeting the CR domain appeared therefore a suitable route for selective binding of MR.

This work shows that under the conditions investigated mannosylated multivalent ligands targeting CTLD domain are internalised by MR⁺-CHO cells and BMD murine macrophages in a continuous manner. In contrast, glycopolymers displaying galactose 3-O-sulfate units, designed to bind the CR domain acted as efficient MR blockers.

1.6 Hypothesis and aims

The hypothesis of this project is that MR-binding polymers that interact with the CR domain of mouse MR will be recognised by human MR and modulate MR-function in human myeloid cells.

The main aims of this project are:

- 1) Investigate the recognition of polymers S100-DP187, M100-DP187 and G100-DP187 (Table 2) by the CR domain of human MR and human myeloid cells;
- 2) Investigate the effect of glycopolymers on MR function in human myeloid cells;
- 3) Investigate the effect of glycopolymers on MR distribution within human myeloid cells.

Code	Targeted domain	Molecular weight (kDa)	Number of polymer repeating units
S100-DP187	CR	89.2	187
M100-DP187	CTLD	70.7	187
G100-DP187	No binding-Control	70.7	187
S100-DP240	CR	81.2	214
G100-DP240	No binding-Control	60	216

Table 2. List of polymers used in this present work.

Chapter 2 - Materials and Methods

2.1. Analysis of polymer binding to human CR domain

2.1.1. Materials

96-well MAXISORP Nunc-Immuno plate (#439454, Thermo Scientific), glycopolymers S100-DP187, M100-DP187 and G100-DP187 (developed by Dr. Mastrotto), Dulbecco's Phosphate Buffered Saline (#D8537, Sigma-Aldrich), human CR domain-mouse IgG2b Fc region chimera (huCR-Fc) (Martinez-Pomares et al., 2005), mouse CTLD4-7 domain-human IgG1 Fc region chimera (muCTLD4-7-Fc) (Zamze et al., 2002), anti-mouse IgG Fc-specific antibody alkaline phosphatase conjugate (#715-055-151, Jackson Immuno Research), anti-human IgG Fc-specific antibody alkaline phosphatase conjugate (#A9544, Sigma-Aldrich), SIGMAFAST p-nitrophenyl phosphate tablets (#N2770-5SET, Sigma-Aldrich), Tris-buffered saline (TBS) buffer [10 mM Tris-HCl, pH 7.5, 10 mM Ca²⁺, 154 mM NaCl, 0.05% (v/v) Tween 20 (P1379, Sigma-Aldrich)], Alkaline Phosphatase (AP) buffer (100mM Tris-HCl, 100 mM NaCl, 1mM MgCl₂, pH 9.5).

2.1.2. Methodology

MAXISORP 96-well plates were coated with 5 µg/ml of glycopolymers in 50 µl PBS and incubated overnight at 4 °C. Wells were washed three times with 200 µl of TBS buffer. Different concentrations (0.2, 1, 5, 10 µg/ml in TBS) of huCR-Fc (Martinez-Pomares *et al.*, 2005) and muCTLD4-7-F (Linehan et al., 2001) chimeric proteins were added to respective wells (each concentration in duplicate) and incubated for 2 hours. The huCR-Fc chimera consists of the human MR CR domain fused with the Fc

portion of a mouse IgG2b, whilst the muCTLD4-7-Fc chimera consists of the mouse MR CTLD 4 to 7 domains fused to the Fc portion of human IgG1. Washing step was executed 3x with 200 μ l of TBS buffer per well to remove unbound protein. To detect binding of huCR-Fc or moCTLD4-7-Fc protein chimera to the glycopolymers, an anti-mouse IgG Fc-specific antibody or anti-human IgG Fc-specific antibody (both alkaline phosphatases conjugated and diluted 1:1000 in TBS) was added and incubated for 1 hour. Wells were washed again 3x with 200 μ l of TBS buffer and 2x with 200 μ l of AP buffer. Alkaline phosphatase activity was detected by adding 200 μ l of SIGMAFAST p-nitrophenyl phosphate diluted in AP buffer to each well (Figure X). OD₄₀₅ was quantified in a Multiskan FC (Thermo Scientific). Data was processed in Excel and Graphpad Prism 6.

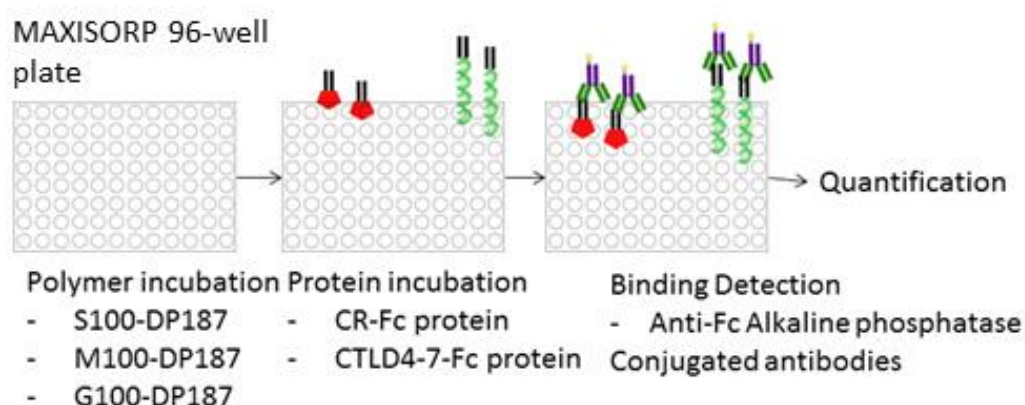


Figure 11. Summary of polymer binding assay. After coating wells of a MAXISORP 96-well plate with glycopolymers overnight, the plate was incubated with chimera proteins (huCR-Fc and muCTLD4-7-Fc) for two hours followed by incubation with anti-Fc alkaline phosphatase conjugated secondary antibody for one hour. Alkaline phosphatase activity was quantified after addition of substrate and measurement of OD at 405 nm.

2.2. Isolation and preparation of human monocytes

2.2.1. Materials

Buffy coat (Sheffield Blood Bank, UK), T75ml flask (#156502, Thermo Scientific), Dulbecco's Phosphate Buffered Saline (DPBS) (#D8537, Sigma-Aldrich), Histopaque-1077 (#10771, Sigma-Aldrich), 50 ml Falcon tubes (#227270, Greiner bio-one), 15 ml falcon tubes (#10384601, Greiner bio-one), MACs buffer (0.5% FBS, 2mM EDTA, PBS), Fetal Bovine Serum (#F7524, Sigma-Aldrich), EDTA (#E7889, Sigma-Aldrich), Quadro MACS separation unit (#130-090-976, Miltenyl Biotec), Pre-separation filters 30 µm (#130-041-407, Miltenyl Biotec), MACS Separation Columns – LS Columns (#130-042-401, Miltenyl Biotec), Trypan Blue (#T8154, Sigma), RPMI-1640 media (#R0883, Sigma-Aldrich), RPMI-1640 media without phenol red (#R7509, Sigma-Aldrich), Human AB Serum (#H4522, Sigma-Aldrich), 1M HEPES (#H0887, Sigma-Aldrich), Glutamax 100x (#35050-038, Gibco), L-glutamine (#56859, Sigma-Aldrich), 24-well low attachment plates (#cc228, Corning), hrM-CSF (#216-MCC, R&D Systems), hrGM-CSF (#130-093-864, Miltenyl Biotec), Human IL-4 (#130-093-920, Miltenyl Biotec).

2.2.2. Methodology

Blood monocytes were isolated from buffy coats as follows. Buffy coat blood (~70 ml) was diluted in DPBS to a total volume of 140 ml in a T75 flask and distributed among four 50 ml Falcon tubes containing 15 ml Histopaque-1077 each. The tubes were centrifuged at 800 x g for 30 minutes at a low acceleration/deceleration setting. The white buffy coat layer was collected with Pasteur pipettes and transferred to two clean 50 ml Falcon tubes. The tubes were filled to 50 ml with DPBS and then centrifuged at 350 x g for 10 minutes.

The supernatant was discarded, the remaining cell pellet was washed with 50 ml DPBS and centrifuged for 10 min at 250 x g. A third wash was done as in the last condition. The cell pellets were then placed together in the same tube and the tube was filled with 50 ml DPBS. A small amount of cells was diluted 1:10 in PBS (10 μ l + 90 μ l), then 1:2 in Trypan blue (10 μ l + 10 μ l) and counted, the remaining cells were centrifuged at 350 x g for 5 minutes resuspended in MACs buffer (80 μ l per 10^7 cells) and incubated with CD14 magnetic microbeads (10 μ l per 10^7 cells) on ice, in the dark for 15 min (Singh, 2012). Cells were washed with 20 ml MACS buffer and centrifuged at 350 xg for 5 min. The supernatant was discarded and the pellet was resuspended in 3 ml cold MACS buffer and applied through a LS MACS magnetic column as recommended by manufacturer. The column was washed with 3 ml MACS buffer twice before being removed from the magnet, a volume of 5 ml of MACS buffer was added to the column and cells were flushed out in a 15 ml falcon tube. A small number of cells were diluted 1:5 (10 μ l + 40 μ l), then 1:2 in Trypan blue (10 μ l + 10 μ l) and counted. The 15 ml tube containing the CD14+ cells was filled with media to the top and centrifuged at 350 x g for 5 minutes in order to remove any excess unbound CD14 beads and also to dilute the MACS buffer. Supernatant was discarded and the pellet was finally resuspended in RPMI-1640 medium containing 15% AB serum (Sigma-Aldrich, UK), 2mM L-glutamine or glutamax 1X and 10 mM HEPES. The final concentration was adjusted to 2×10^6 cells/ml. A initial volume of 500 μ l was added per well to 24-well low attachment plates (CC228, Corning) (Singh, 2012). The cells were incubated in the presence of M-CSF (50 ng/ml) or GM-CSF (50 ng/ml) at 37 °C for 7 days. In some conditions IL-4 (25 ng/ml) was added to the media. Fresh media (500 μ l) with supplements and cytokines was added per well at day 3 (Figure 12).

Cell separation by density gradient centrifugation

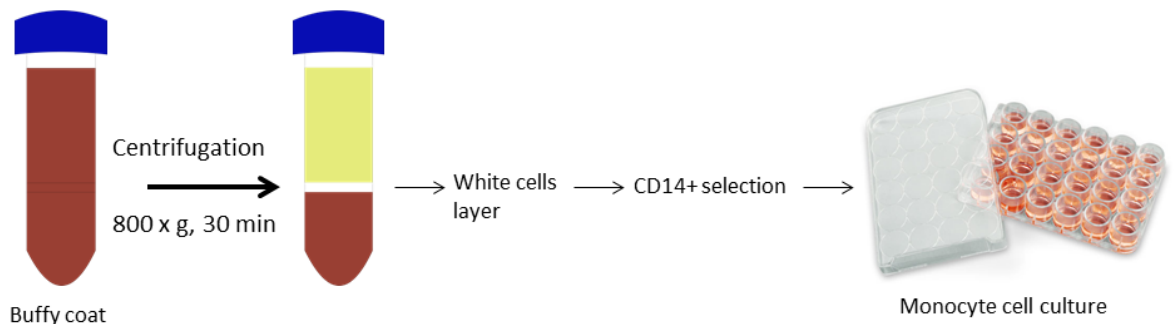


Figure 12. Summary of isolation and preparation of human monocytes.

2.3. Analysis of polymer binding and uptake by human macrophages

2.3.1. Material

X-Vivo 15 (#BE02-061Q, Lonza), Dulbecco's Phosphate Buffered Saline (#D8537, Sigma-Aldrich), glycopolymers S100-DP187, M100-DP187 and G100-DP187 (developed by Dr. Mastrotto), gelatin (#04055, Fluka) labelled with Texas Red, X-Vivo 15 (#BE02-061Q, Lonza), Formaldehyde (#15710-S, EMS), FACS tubes (#115101, Greiner bio-one).

2.3.2. Methodology

Macrophages grown on low adherence 24-well plate for 7 days as described on section 2.2.2 were placed on ice for 20 minutes to allow cells to detach. Macrophages were harvested by gently pipetting and collected into 15 ml Falcon tubes and centrifuged at 350 x g, 4 °C for 5 minutes. The cell pellet was washed with 10 ml X-Vivo 15

centrifuged at 350 x g, 4 °C for 5 minutes. Cells were resuspended in 1 ml X-Vivo 15 and counted. The number of cells was adjusted to 100.000 per 200 µl in X-Vivo 15. Cells were transferred to 1.5 ml Eppendorf tubes (200 µl/tube) and 200 µl of 2x polymer concentration in X-Vivo 15 were added to each tube. For the dose effect assay the concentrations ranged as below (Table 3). The tubes were sealed with foil then placed in the 37 °C incubator for one hour or on ice for one hour.

Polymer	Sugar units (molecular weight)			Concentrations used (µM -sugar units)		
	Mannose (373 Da)	3-SO ₄ -Gal (475 Da)	Galactose (373 Da)	Polymer uptake	Gelatin assay	Dose effect
S100-DP187	/	100%	/	4.2	40, 160, 640	0.5, 2.5, 12.5, 67.5
M100-DP187	100%	/	/	5.3	40, 160, 640	0.5, 2.5, 12.5, 67.5
G100-DP187	/	/	100%	5.3	40, 160, 640	0.5, 2.5, 12.5, 67.5

Table 3. Polymer type, molecular weight and polymer concentration used in different assays. Table

After incubation, cells were washed with 400 µl of X-Vivo 15 and centrifuged at 1000 rpm (in a benchtop centrifuge, model Prism R), 4 °C, for 5 minutes. Supernatant was aspirated with a micropipette and pellet was washed in 400 µl of ice-cold PBS and centrifuged at 1000 rpm, at 4 °C for 5 minutes. Supernatant was aspirated and a volume of 200 µl of PBS was added to each tube and the content was transferred to FACS tubes containing 200 µl of 1% formaldehyde in PBS. Fluorescence quantification was done in a flow cytometer (FC 500, Beckman Coulter) and analysed using Kaluza software.

2.4. Analysis of cell surface markers

2.4.1. Materials

X-Vivo 15 (#BE02-061Q, Lonza), Dulbecco's Phosphate Buffered Saline (#D8537, Sigma-Aldrich), Bovine Serum Albumin Fraction V [BSA] (#K41-001, PAA Laboratories), CD14 ECD antibody (#IM2707, IOTest Beckman Coulter), IgG2a Mouse ECD Isotype (#A09144, IOTest Beckman Coulter), CD16 PE antibody (#A07766, IOTest Beckman Coulter), IgG1 Mouse PE Isotype (#IM2707, IOTest Beckman Coulter), CD206 PE antibody (#IM2741, IOTest Beckman Coulter), CD11b FITC antibody (#IM0530, IOTest Beckman Coulter), IgG1 Mouse FITC Isotype (#A07795, IOTest Beckman Coulter), HLA-DR PerCP/Cy5.5 antibody (#307629, Biolegend), IgG2a PerCP/Cy5.5 Isotype (#400257, Biolegend), Mouse Serum (#M5905, Sigma-Aldrich), Formaldehyde (#15710-S, EMS).

2.4.2. Methodology for cell surface markers quantification (no polymer)

Cells grown on low adherence 24-well plate for 7 days as described on section 2.2.2 were placed on ice for 20 minutes to allow cells to detach. Macrophages were harvested by gently pipetting the media in the well, collected into 15 ml Falcon tubes and centrifuged at 350 x g, 4 °C for 5 minutes. Cells were washed with 10 ml X-Vivo 15 at 350 x g, 4 °C for 5 minutes. Pellet was resuspended in 1.5 ml of PBA (0.5% BSA in PBS) containing 5% mouse serum at 4 °C for 1 hour to block Fc receptors. Cells were centrifuged at 350 xg, 4 °C for 5 minutes and cell number adjusted to 50.000 in 45 µl of PBA. Cells were transferred to 1.5 ml Eppendorf tubes (45 µl/tube) and 5 µl of antibody marker or isotype control were added to each tube, according to Table 4 below, followed by incubation in the dark for one hour at 4 °C.

Antibody	Fluorophore	Catalog #	Label	specificity	concentration
CD14	ECD	IM2707	IOTest	human	5 μ l/ 10 ⁶ cells
CD16	PE	A07766	IOTest	human	
CD206	PE	IM2741	IOTest	human	
CD11b	FITC	IM0530	IOTest	human	
IgG2a	ECD	A09144	IOTest		
IgG1	FITC	A07795	IOTest		
IgG1	PE	A07796	IOTest		
HLA-DR	PerCP/Cy5.5	307629	Biolegend	human	
IgG2a, k	PerCP/Cy5.5	400257	Biolegend		

Table 4. List of antibodies used for macrophage profile analysis by flow cytometry (no polymer).

After three washes with 200 μ l of PBA at 350 x g, 4 °C for 5 minutes, cells were resuspended in 200 μ l of PBA. The final content was transferred to respective FACS tubes containing 200 μ l 1% formaldehyde in PBA. Fluorescence was quantified on FC500 or on Astrios (Beckman Coulter) flow cytometer and analysed using Kaluza software.

2.4.2. Methodology for cell surface markers quantification after polymer treatment

CD-14+ monocytes were incubated for 6 days at 37 °C in a low-attachment plate in the presence of M-CSF (50 ng/ml). On day 6, a volume of 100 μ l of glycopolymers (to achieve a final concentration of 48 μ M) plus cytokines IFN- γ (to achieve a final concentration of 20 ng/ml per well) and M-CSF (50 ng/ml) in media was added to each well. The plate was then incubated for 24h at 37 °C. On day 7 the plate was placed on ice for 20 min and cells were harvested and

collected into 15 ml tubes. The volume of 10 ml of ice-cold X-Vivo 15 was added to each tube and centrifuged at 350 x g, 4 °C for 5 min. Supernatant was discarded, the pellet was resuspended in 200 µl PBA containing 5% mouse serum and incubated at 4 °C for 45 minutes. The suspension was centrifuged at 350 x g, 4 °C for 5 min. Supernatant was discarded and the pellet was resuspended in 1 ml PBA, cells were counted and then diluted to 50.000 cells to 45 µl PBA. A volume of 45 µl of cell suspension was added to each Eppendorf and 5 µl of respective antibody or isotype control (Table 5) was added to each tube.

Antibody	Fluorophore	Catalog #	Label	specificity	concentration
CD206	Alexa-Fluor 647	321116	Biolegend	human	5 µl/ 10 ⁶ cells
Mouse IgG1	Alexa-Fluor 647	400130	Biolegend		
CD11b	PerCP/Cy5.5	301327	Biolegend	human	
Mouse IgG1	PerCP/Cy5.5	400149	Biolegend		
HLA-DR	PerCP/Cy5.5	307629	Biolegend	human	
IgG2a, k	PerCP/Cy5.5	400257	Biolegend		

Table 5. List of antibodies used for macrophage cell surface marker quantification after polymer treatment.

Cells were incubated in the dark, at 4 °C for 1 hour. A volume of 200 µl of PBA was added to each tube then centrifuged at 350 x g, 4 °C for 5 min, supernatant was discarded. Each tube was washed again two times under same conditions and the final pellet was resuspended in 200 µl of PBA. A volume of 200 µl of 1% formaldehyde in PBS was added to each FACS tube and the sample preparation was transferred to these tubes. FACS tubes were kept

in the cold room, overnight in the dark (wrapped in foil). Samples were quantified on the following day on Astrios flow cytometer (Beckman Coulter).

2.5. Inhibition of gelatin uptake by human macrophages

2.5.1. Material

X-Vivo 15 (#BE02-061Q, Lonza), Dulbecco's Phosphate Buffered Saline (#D8537, Sigma-Aldrich), glycopolymers S100-DP187, M100-DP187 and G100-DP187 (developed by Dr. Mastrotto), Gelatin - porcine skin (#04055, Fluka) labelled with Texas-red (provided by Dr Mastrotto), Formaldehyde (#15710-S, EMS).

2.5.2. Methodology

Monocyte-derived macrophages grown on 24-well plate for 7 days were placed on ice for 20 minutes to allow cells to detach. Macrophages were harvested by gently pipetting, collected into 15 ml Falcon tubes and centrifuged at 350 x g at 4 °C for 5 minutes. The number of cells was adjusted to 200.000 per 100 µl in X-Vivo 15. Cells were transferred to 1.5 ml Eppendorf tubes (100 µl/tube) and 100 µl of polymers diluted in X-Vivo 15 were added to each tube. The tubes were incubated at 37 °C for one hour or six hours. A volume of 50 µl of Texas red-labelled gelatin 5x concentrated was added to the cells to achieve a final concentration of 10 µg/ml and cells were incubated for an additional hour at 37 °C. Cells were washed with 300 µl of X-Vivo 15 and centrifuged at 1000 rpm (benchtop centrifuge, model Prism R), 4 °C, for 5 minutes. Another wash was done with 300 µl PBS and cells were resuspended in 200 µl of PBS and transferred to FACS tubes containing 200 µl of 1% formaldehyde in PBS. Fluorescence quantification was done in

Astrios (Beckman Coulter) and analysed using Kaluza software. Oregon Green channel (GPs): Laser 488nm, emission spectrum 500-526nm. Texas Red channel (Gelatin): Laser 561nm, emission spectrum 604-624nm.

2.6. Macrophage preparation for protein extraction

2.6.1. Materials

RPMI-1640 media (#R0883, Sigma-Aldrich), Human AB Serum (#H4522, Sigma-Aldrich), 1M HEPES (#H0887, Sigma-Aldrich), Glutamax 100x (#35050-038, Gibco), 24-well low attachment plates (#cc228, Corning), hrM-CSF (#216-MCC, R&D Systems), Human IL-4 (#130-093-920, Miltenyi Biotec), recombinant human IFN- γ (#285-IF-100, R&D Systems).

2.6.2. Methodology

Below are two types of macrophage preparation:

1- On day 6, M-CSF and M-CSF + IL-4 treated macrophages cultured on 24-well low attachment plates were incubated with cytokines and polymers. Culture media (RPMI-1640 medium containing 15% AB serum, 1x glutamax and 10 mM HEPES) containing 25 ng/ml of IL-4, 50 ng/ml of M-CSF and 40 μ M of polymer S100-DP187 or G100-DP187 were prepared and 100 μ l of this mix was added per well and 6 wells were allocated per condition. Plates were further incubated at 37 °C for 24 hours. On the following day, plates were placed on ice for 20 minutes and harvested into a 15 ml falcon tube and centrifuged at 350 x g for 5 minutes. Protein extraction from this pellet is described in 2.8.2.1 -

2- The second macrophage preparation had no addition of glycopolymers. Day five M-CSF treated macrophages in low-attachment plates were incubated at 4 °C for 45 minutes. Cells were harvested and transferred (1x10⁶ cells per 2 ml per well) to a 6-well

plate and incubated for 24 hours at 37 °C in the presence of cytokines M-CSF (50 ng/ml), IL-4 (25 ng/ml), IFN- γ (20 ng/ml), LPS (20 ng/ml) in culture media (RPMI-1640 medium containing 15% AB serum, 1x glutamax and 10 mM HEPES). On day 7 the protein lysate preparation was done according to 2.8.2.2.

2.7. Culture of MRC5 cells

2.7.1. Materials

DMEM (D6046, Sigma-Aldrich, UK), AB serum (H4522, Sigma-Aldrich, UK), Glutamax (35050-038, Gibco), HEPES (H0887, Sigma-Aldrich), T75 flask (430641 U, Corning). Frozen MRC5 cells (provided by Dr. Sally Wheatley, University of Nottingham).

2.7.2. Methodology

MRC5 cells were immediately thawed under warm water. The tube was centrifuged at 1,500 rpm for 5 min in a benchtop centrifuge, the supernatant was discarded and the pellet was resuspended in 10 ml of media (DMEM, 15% AB serum, 1x glutamax and 10 mM HEPES) and transferred to a T75 flask and incubated at 37 °C, 5% CO₂. On day 2 the media was replaced and the cells were incubated for 6 more days.

2.8. Cell lysate preparation

2.8.1. Materials

Dulbecco's Phosphate Buffered Saline (#D8537, Sigma-Aldrich), 24-well polystyrene tissue culture plate (#3524, Costar), 6-well plate (#EP0030720130, Eppendorf), Lysis buffer (10mM Tris-HCl – pH 8, 2% Triton X-100, 150 mM NaCl, 10mM EDTA), Tris-HCl pH 8 (#T3038, Sigma), Triton X-100 (#T8787, Sigma-Aldrich), NaCl,

EDTA (#E7889, Sigma-Aldrich), Protease inhibitors (#11836170001, Roche).

2.8.2. Methodology

1- Lysis of macrophage cultured in low attachment plates: Seven days monocyte-derived macrophages were placed on ice for 20 minutes and cells were harvested from wells and placed into 15 ml tubes. Cells were centrifuged at 350 x g, 4 °C for 5 minutes. The pellet was washed twice with 1 ml cold PBS and PBS was discarded after wash. Lysis buffer with protease inhibitors was added at 400 µl per 2×10^6 cells and incubated at 4 °C for 45 minutes.

2- Lysis of macrophages cultured in tissue culture plates. Ice cold lysis buffer with protease inhibitors was added to the well incubated at 4 °C for 45 minutes. In general, 100 or 400 µl lysis buffer was used per 10^6 cells.

Lysis of MRC5 cells. Media was removed and flask was washed twice with PBS. Lysis buffer was added at 10 ml per T75 flask. Samples were centrifuged at 2000 rpm, 4 °C for 5 min to pellet nuclei. In all instance's samples were centrifuged at 2000 rpm, 4 °C for 5 min to pellet nuclei. Supernatant was collected and centrifuged at 12.000 rpm for 30 minutes, 4 °C. Supernatant was collected and protein concentration was quantified using Pierce BCA protein assay kit (#23225, ThermoFisher Scientific). Samples were kept frozen at -20 °C.

2.9. Western Blot analysis

2.9.1. Materials

Ammonium persulfate (#A3678-100G, Sigma), Sodium dodecyl sulfate (#L3771-100G, Sigma), Temed (#161-0800, Bio-Rad), Acrylamide/Bis Solution 30% (#161-0158, Bio-Rad), Tris/Glycine/SDS (TGS) Buffer 10x (#161-0772, Bio-Rad), Tris/Glycine (TG) Buffer 10x (#161-0771, Bio-Rad), PT Buffer (0.1% Tween-20 in PBS), Tween-20 (#P1379, Sigma-Aldrich), Dulbecco's Phosphate Buffered Saline (#D8537, Sigma-Aldrich), Blocking buffer (5% non-fat milk in PT Buffer), Nitrocellulose Blotting Membrane (#10600016, Amersham), Resolving Gel Buffer – Tris-HCl pH 8.8 (#161-0798, Bio-Rad), Stacking Gel Buffer – Tris-HCl pH 6.8 (#161-0799, Bio-Rad), Loading Buffer – 4x (0.25M Tris-HCl pH 6.8, 8% SDS, 40 % Glycerol, Bromophenol Blue), Transfer Buffer (10 % TG buffer, 20% methanol, 70% Milli-Q H₂O), purified mouse anti-human CD206 (MMR) Antibody (#321102, Biolegend), Anti-Endo180 antibody A5/158 [hybridoma] (provided by Dr. Clare Isacke, ICR-London), Rabbit monoclonal [EP1006Y] antibody to HSP60 control (ab45134, ABCam), IRDye 680RD Goat anti-Rabbit (#926-68071, Licor), IRDye 800CW Goat anti-Mouse (#926-32210, Licor), Color prestained protein ladder (#P7712S, New England BioLabs).

2.9.2. Methodology

A 6% SDS-PAGE was prepared according to the following table:

Deionized Water	5.25 ml
TrisHCl pH 8.8	2.5 ml
Acrylamide	2 ml
10 % SDS	100 µl
10 % APS	100 µl
Temed	15 µl

Table 6. SDS-PAGE gel (6%) preparation protocol.

The solution was quickly poured in the middle of a pair of glasses on a gel apparatus. It was then allowed 40 min to polymerize. A stacking gel solution was prepared and poured on top of the separating gel:

Deionized Water	1.5 ml
0.5 M Tris-HCl, pH 6.8	625 µl
10 % SDS	325 µl
Acrylamide/Bis-acrylamide	25 µl
10 % APS	25 µl
TEMED	2.5 µl

Table 7. Stacking gel preparation protocol.

A 1.5 dentate slice was placed to create the wells and the gel was allowed to polymerize for 40 min. The gel was placed into the running apparatus and filled with 1x TGS buffer. Loading buffer 4 x was added to protein samples and boiled at 100 °C for at least 5 min. The tubes were centrifuged for a few seconds prior loading. The

gels were run at 100 V for 90 min. The gels were removed and transferred overnight to a membrane, at 200 mA.

On the following day, the membrane was removed from the apparatus and blocked for 1 hour in blocking buffer. The buffer was discarded and primary antibody in blocking buffer was added. For Endo180 detection, the membrane was incubated for 1 hour on a shaker with 10 ml of A5/158 hybridoma supernatant diluted 1:5 in blocking buffer (Sheikh et al., 2000). Whilst for MR detection, the membrane was incubated for 1 hour on a shaker with 10 ml of blocking buffer containing anti-MR antibody (diluted 1:1000). Anti-HSP60 primary antibody was diluted 1:10000 in the same solution as Endo180 or MR. Primary antibodies were removed and membrane was washed 3X with PT buffer. For MR and Endo180 quantification, the membrane was incubated for 1 hour on a shaker in the presence of IRDye 800CW anti-mouse IgG (925-32210, Licor) diluted 1:10000 in blocking buffer, whilst IRDye 680RD Goat anti-Rabbit (1:15000) was used to quantify the housekeeping gene HSP60. The membrane was washed 3X with PBS and the volume discarded. The membranes were kept in distilled water and quantified on Licor Odyssey 9120. Alternatively, detection of MR and Endo180-primary antibody was done with anti-mouse IgG peroxidase conjugate secondary antibody (715-036-150, Jackson Immunoresearch) diluted 1:1000 in blocking buffer. ECL reagent (NEL103001EA, Perkin Elmer) was used for detection on a KODAK film.

2.10. Indoleamine 2, 3 dioxygenase (IDO) activity assay

2.10.1. Materials

Acetic acid glacial (#A/0400/PB17, Fisher Scientific), 24-well polystyrene tissue culture plate (#0030722116, Eppendorf), L-Tryptophan (#T8941-25G, Sigma-Aldrich) Recombinant human IFN- γ (285-IF-100, R&D), LPS (#tlrl-pekllps, Invivogen), Hydrochloric acid (#J/4320/17, Fisher Scientific), Trichloroacetic acid (#T/3000/50, Fisher Scientific), L-Tryptophan (#T8941-25G, Sigma-Aldrich), 4-(Dimethylamino) benzaldehyde (#156477-25G, Sigma-Aldrich), 96-well plate (#439454, Thermo scientific).

2.10.2. Methodology

Cells grown as in section 2.2 were transferred to a polystyrene tissue culture plate on day 5. A total of 250.000 cells in 500 μ l RPMI-1640 media without phenol red were added per well in the presence of cytokines and supplements as previously mentioned (section 2.2). On day 6, the following cytokines were added to the media in combination with the glycopolymers: IFN- γ (20 ng/ml), LPS (20 ng/ml) and glycopolymers S100-DP240, G100-DP240 plus 100 μ M of L-Tryptophan (from a solution of 60 mM of L-Tryptophan diluted in media from a previous stock solution of 300 mM of L-Tryptophan in 1 M HCl). Cells were incubated for a further 24h. Cell media were collected and centrifuged at 350 x g, 5 min and the supernatant was transferred to another tube. For 100 μ l of supernatant, 50 μ l of 30% trichloroacetic acid was added and centrifuged for 5 min at full speed (1720 x g) in a benchtop centrifuge. In a 96-well plate, 100 μ l of the soluble phase and 100 μ l of Ehrlich's reagent (100 mg p-dimethylbezaldehyde in 5 ml glacial acetic acid) were added per well, incubated for 30 min, and quantified at 492 nm wavelength.

2.11. Fluorescence microscopy

2.11.1. Materials

Triton X-100 (#T8787, Sigma-Aldrich), Paraformaldehyde (#15710-S, EMS), X-Vivo 15 (#BE02-061Q, Lonza), 12 mm coverslips, Purified anti-human CD206 (MMR) Antibody (mouse) (#321102, Biolegend), Anti-Mannose receptor antibody (Rabbit) (#ab64693, ABCam), EEA1 (C45B10) Rabbit mAb (#3288, Cell Signaling Technology), LAMP1 (D4O1S) Mouse mAb (#15665, Cell Signaling Technology), Alexa Fluor 488-conjugated AffiniPure Donkey Anti-Mouse IgG (H+L) (#715-545-150, Jackson ImmunoResearch), Alexa Fluor 647-conjugated AffiniPure Donkey Anti-Rabbit IgG (H+L) (#711-605-152, Jackson ImmunoResearch), Dulbecco's Phosphate Buffered Saline (#D8537, Sigma-Aldrich), Dulbecco's Phosphate Buffered Saline plus CaCl₂ and MgCl₂ (#14040-091, Gibco), Donkey Serum (#D9663, Sigma), DAPI , Ibidi mounting medium (#50001, Ibidi).

2.11.1. Methodology

Before harvesting the cells, coverslips were treated with 1 M HCl for 1 hour to increase cell adherence. Coverslips were then washed several times with media with phenol red, until the media did not change colour. The coverslips were then washed twice with sterile distilled water and left to dry. Coverslips were then sterilized for 15 min under UV light and transferred to the bottom of a 24-well plate. On day 6 macrophages were harvested from the plates by placing them on ice for 20 min and then transferring the content to 15 ml tubes. Cells were centrifuged at 350 x g, 4 °C, for 5 min. Supernatant was poured off and the pellet was resuspended in 5 ml of X-Vivo 15 per each tube and centrifuged at 350 x g, 4 °C, for 5 min. Supernatant was poured off and cells were resuspended in 1 ml X-Vivo 15 and counted. A total of 250,000-300,000 cells were

placed on wells containing coverslips in the presence of 350 μ l X-Vivo 15 and cytokines. Cells were left overnight to attach to the coverslips. On the following day, some wells were incubated with 80 μ M of polymer S100-DP240 for 4 hours. The media was then removed and wells were washed twice with 500 μ l of PBS (with CaCl_2 and MgCl_2). The cells were then fixed by adding 250 μ l of 4% paraformaldehyde in PBS for 20 minutes while on ice. Wells were rinsed with 500 μ l of PBS (with CaCl_2 and MgCl_2), followed by two 5 min washes with 500 μ l of PBS (with CaCl_2 and MgCl_2) at RT. This is the standard washing step for the immunofluorescence assay. Cells were permeabilized with 250 μ l of 0.15 % Triton-X100 in PBS for 30 minutes. Triton-X100 solution was removed from the wells and washed according to the standard washing step. To block unspecific binding of antibodies, the cells were incubated for 1 hour with 250 μ l of 5% filtered donkey serum in PBS at RT. The blocking buffer was removed and 200 μ l of primary antibodies were added to respective wells. Purified anti-human CD206 Antibody (mouse) (10 μ g/ml), Anti-Mannose receptor antibody (Rabbit) (1 μ g/ml), Anti-Endo180 antibody (Mouse) (dilution 1:3), Anti-EEA1 (C45B10) Rabbit mAb (dilution 1:50), Anti-LAMP1 (D4O1S) Mouse mAb (dilution 1:50), all diluted in blocking buffer 5% donkey serum in PBS. Samples were incubated at RT for 12 hours at 4 $^{\circ}$ C. Wells were washed according to the standard washing step and then incubated with 250 μ l of secondary antibodies – Anti-mouse Alexa Fluor 488 and Anti-rabbit Alexa Fluor 647 (8 μ g/ml) diluted in blocking buffer (5% donkey serum). Wells were washed according to standard washing step. To stain the nucleus 250 μ l of DAPI were added per well at 1 μ g/ml in PBS for 5 minutes at RT. Wells were washed according to standard washing step. Coverslips were then removed from the wells and left to dry for a few seconds and then placed on glass slides with 3 μ l of Ibbidi mounting medium. Coverslips were then sealed with nail polish and left overnight to set.

During the optimization process, the slides were analysed by fluorescence microscope. After optimization process, the slides were analysed by confocal Zeiss 880. Images were processed by Fiji software for colocalization analysis and for line intensity profile calculation.

Chapter 3 – The interaction of MR-binding glycopolymers with human macrophages

With the success of the lab synthesized glycopolymer S100-DP187 in diminishing acute tubular injury in a mouse model of ischemia-reperfusion, it became necessary to study its function in a human setting looking forward at its therapeutic potential. Before testing its biological effects, it was essential to investigate whether these polymers bind the human CR domain of MR. In a binding assay where different polymers were tested against MR protein domains, polymer S100-DP187 showed binding to the CR domain of MR. Upon confirmation of polymer binding the next step was to validate its binding to human cells that express MR. Monocyte-derived macrophages were the cell type of choice, therefore polymer binding to these cells would be expected. Glycopolymer association with macrophages had to be tested, as well as, the increase in polymer dose and the effect of temperature in polymer uptake. The presence of macrophage cell markers had to be detected in these cells, giving more confidence about its identity. This initial step is necessary to determine the polymer specificity to its respective MR domain and how is the interaction between these and human cells expressing MR. With this in mind specific aims were set:

- 1 – Determine polymer S100-DP187 binding to human cysteine-rich domain of MR.
- 2 - Determine polymer uptake by human monocyte-derived macrophages and quantify polymer uptake under different concentrations.
- 3 – Determine the effect of temperature on polymer uptake by monocyte-derived macrophages.

4- Investigate binding competition between alternative sulfated polymer S100-DP240 vs S100-DP187.

3.1. Polymer S100-DP187 binds the cysteine-rich (CR) domain of human MR

S100-DP187 was previously shown to bind the CR domain of mouse MR, even though sequence analysis between mouse CR domain and human CR domain shows 85% identity (Figure 13), it was important to test if it was also recognised by the CR domain of human MR, prior to analysing its interaction with human macrophages. To investigate recognition of glycopolymer S100-DP187 by the CR domain of human MR, a lectin binding assay was done as described in materials and methods. A clear-bottom plate was pre-incubated with different glycopolymers overnight and excess/unbound glycopolymer as washed the following day. This step was followed by incubation with chimeric human cysteine-rich domain (HuCR)-Fc protein and mouse C-type lectin-like domain 4-7 (CTLD4-7)-Fc protein. The binding between glycopolymers and the MR domains was quantified. The interaction between polymer S100-DP187 and recombinant HuCR was dependent on protein concentration although saturation was not reached at the concentrations tested (Figure 14). HuCR did not interact with polymers M100-DP187 and G100-DP187. Mouse CTLD4-7 binding to polymer M100-DP187 also was dependent on protein concentration (Figure 14), however, the binding seemed to saturate at 5.0 µg/ml protein concentration.

```

Mouse 23
RQFLIYNEDHKRCVDALS AISVQTATCNPEAESQKFRWVSDSQIMSVAFKLC LGVPSKTD
RQFLIYNEDHKRCVDA+S +VQTA CN +AESQKFRWVS+SQIMSVAFKLC LGVPSKTD
RQFLIYNEDHKRCVDAVSPSAVQTAACNQDAESQKFRWVSESQIMSVAFKLC LGVPSKTD
Human 23

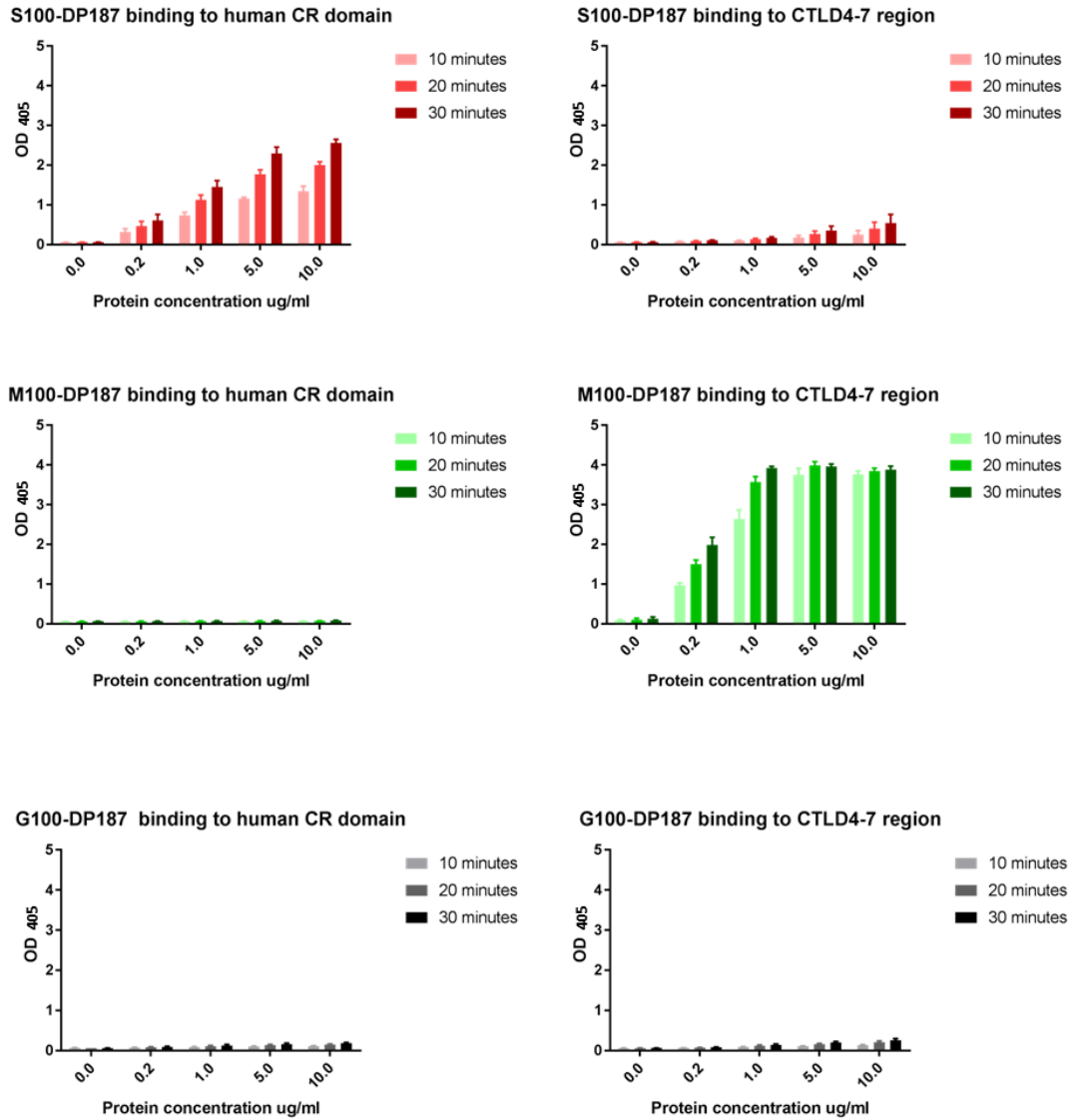
Mouse 83
WASVTLYACDSKSEYQKWECKNDTLFGIKGT ELYFNYGNRQEKNIKLYKGSGLWSRWKVY
W ++TLYACDSKSE+QKWECKNDTL GIKG +L+FNYGNRQEKNI LYKGSGLWSRWK+Y
WVAITLYACDSKSEFQKWECKNDTLLGIKGEDLFFNYGNRQEKNIMLYKGSGLWSRWKIY
Human 83

```

Figure 13. Analysis of MR Cysteine-rich (CR) domain sequence alignment between species *Mus musculus* and *Homo sapiens*. Protein sequence alignment from MR CR domain of species *Mus musculus* (Q61830, MRC1 MOUSE, Uniprot) and *Homo sapiens* (P22897, MRC1 HUMAN, Uniprot) were directly compared by Blastp at <http://blast.ncbi.nlm.nih.gov/>.

Neither HuCR nor CTLD4-7 showed significant binding to polymer G100-DP187, as expected.

In summary, the binding specificity of CTLD4-7 protein to the mannosylated GP (M100-DP187) and the HuCR protein binding to the sulfo-galactosylated GP (S100-DP187), as well as the lack of binding to galactosylated GP (G100-DP187), is in accordance to what is expected for the CTLD4-7 region and CR domain of MR (Leteux et al., 2000, Liu et al., 2000, Taylor et al., 1992, Taylor and Drickamer, 1993) and confirm the potential for human MR to recognise S100-DP187.



N=2

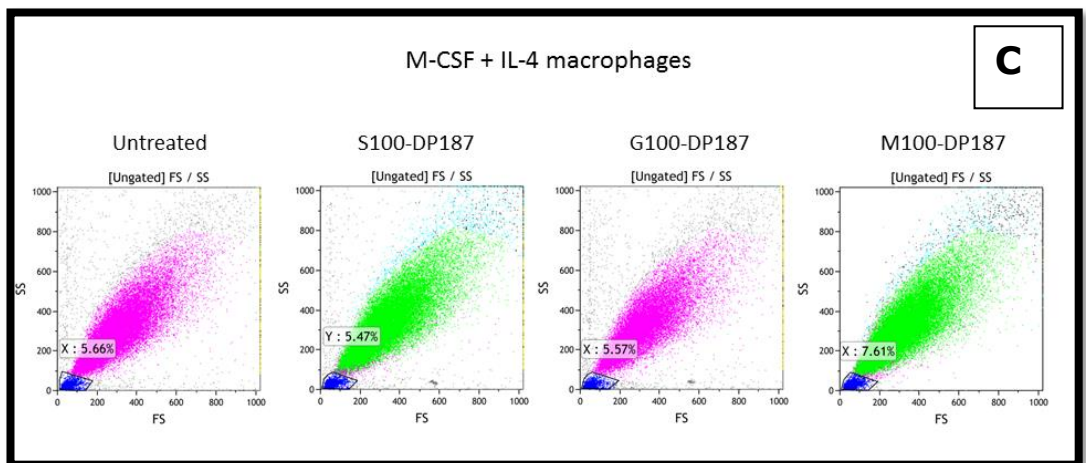
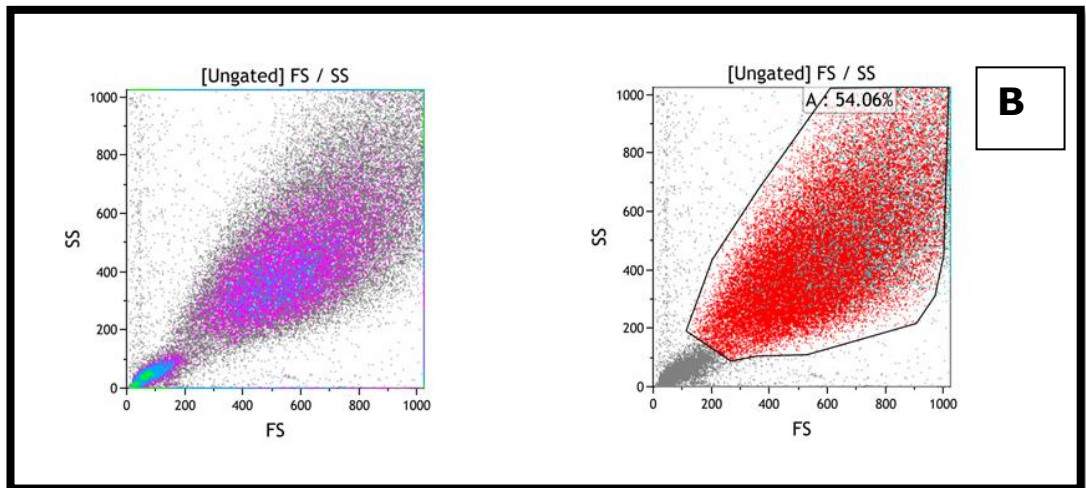
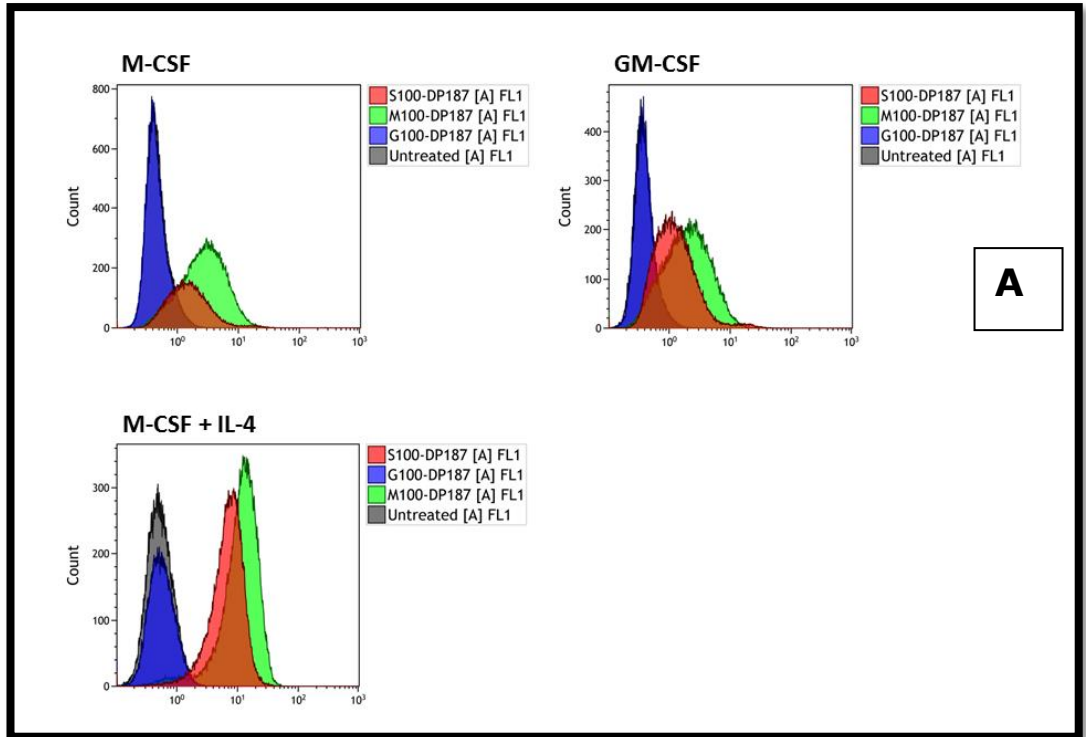
Figure 14. Recognition of polymer S100-DP187 by the CR domain of human MR and of polymer M100-DP187 by the CTLD4-7 region of mouse MR. Plates coated with 5 μ g/ml of glycopolymers M100-DP187, S100-DP187 and G100-DP187 were incubated with proteins huCR-Fc (Martinez-Pomares *et al.*, 2005) and muCTL4-7-F (Linehan *et al.*, 2001) for 2 hours and binding was quantified through alkaline phosphatase activity. HuCR-Fc and muCTL4-7-F binds to sulfo-galactose and mannose sugars, respectively. Binding was detected through the activity of an alkaline phosphatase secondary antibody at OD₄₀₅ Mean OD for n=2, in duplicate.

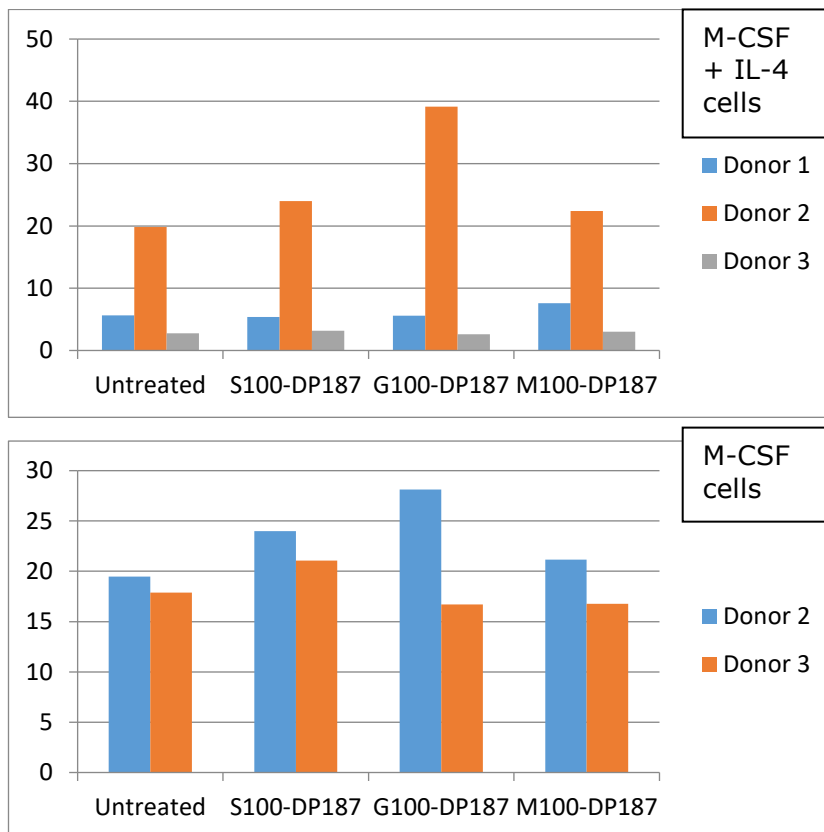
3.2. Association of MR-binding polymers with human monocyte-derived macrophages

To determine if MR-binding polymers could interact with human macrophages, monocyte-derived macrophages generated in the presence of M-CSF, GM-CSF or M-CSF and IL-4 were tested for their ability to associate with different polymers (S100-DP187: 4.2 μ M, M100-DP187 and G100-DP187: 5.3 μ M). The Oregon Green labelling of the polymers was exploited to quantify its binding to macrophages by flow cytometry. Cells used in the assay derived from human buffy coats and went through a positive selection for CD14 expression – a molecular marker mostly expressed in monocytes and macrophages. The maturation process of these cells took 7 days in the presence of different cytokines, including M-CSF, GM-CSF and IL-4. The goal in this stage was to verify polymer binding to macrophages which underwent different maturation protocols. Day 7 monocyte-derived macrophages (100.000 cells/200 μ l) in X-Vivo 15 were incubated with 200 μ l of S100-DP187 (4.2 μ M), M100-DP187 (5.3 μ M), G100-DP187 (5.3 μ M) for 1 hour at 37 °C and fluorescence was quantified using a FC500 flow cytometer. In the Forward Scatter (FS) vs Side Scatter (SS) plot, events in the left and bottom area of the graph, which represent cell debris and damaged cells, were excluded for the analysis (Figure 15, Panel B). The number of dead cells found in the FS/SS plot was not significantly affected by the use of glycopolymers (Figure 15, Panel C and D). Regardless of treatment (M-CSF or M-CSF + IL-4), cells incubated at 37 °C with polymers S100-DP187 and M100-DP187 showed increased Mean Fluorescence Intensity (MFI) in the FL1 channel (emission filter 525nm/40) in comparison with untreated or G100-DP187-treated cells (Figure 15, Panel A). The MFI was slightly higher for cells incubated with the mannosylated polymer M100-DP187 under all conditions. One explanation for this could be due to a difference in labelling efficiency

between polymers. IL-4+M-CSF treated macrophages showed higher fluorescence when incubated with polymers than M-CSF only-treated macrophages. A higher MFI for IL-4 treated cells was expected as this type of cells are known to express more MR (Stein et al., 1992). Glycoconjugates with galactose in the terminal position are known not to bind to alveolar macrophages, which are known to express MR (Shepherd et al., 1981). Thus, absence of fluorescence emitted from cells incubated in the presence of polymer G100-DP187 confirmed that this polymer could be used as a negative control for further experiments.

As the recognition of glycoproteins by alveolar macrophages is serum-independent (Stahl et al., 1978), the binding of glycopolymers S100-DP187 and M100-DP187 to monocyte-derived macrophages also occurred normally in X-Vivo 15, a serum-free medium. These preliminary results suggest that both S100-DP187 and M100-DP187 polymers can specifically associate with different types of human macrophages, corroborating the expectations from the binding assay where the two polymers showed binding to HuCR and CTLD4-7 domains, respectively.





D

Figure 15. Binding of polymers S100-DP187 and M100-DP187 to human macrophages generated in the presence of M-CSF, GM-CSF or M-CSF + IL-4. Top **Panel A.** Human macrophages generated in the presence of M-CSF, GM-CSF or M-CSF+IL-4 were incubated with polymers S100-DP187, M100-DP187 or G100-DP187 and processed for flow cytometry analysis. Fluorescence was detected in macrophages incubated with polymers S100-DP187 and M100-DP187 independently of the type of macrophage differentiation. M-CSF + IL-4 cells incubated with polymers S100-DP187 and M100-DP187 displayed increased mean fluorescence intensity, as expected. **Panel B.** Example of gating strategy used throughout flow cytometry experiments. **Panel C.** Example of percentage of dead cells in IL-4 treated cells. **Panel D.** Percentage of dead cells and debris found on the left-bottom corner in FS/SS plots of M-CSF and IL-4 + M-CSF treated macrophages. M-CSF: n=2, M-CSF + IL-4, n= 3.

3.3. Phenotypic characterisation of human macrophages

To confirm that monocytes incubated with M-CSF or M-CSF and IL-4 expressed the expected cellular markers after 7 days of culture, cells were subjected to analysis of cell surface markers using flow cytometry. Five markers (CD14, CD16, CD206, CD11b, HLA-DR) were chosen according to their previous detection in macrophages (Griffin et al., 1981, Kümmerle-Deschner et al., 1998, Rószler, 2015, Ling et al., 2014, Rogers et al., 2014). Markers CD206, CD11b and HLA-DR were present in both cell types and were up-regulated by IL-4 (Figure 16). Of note isotype controls showed negligible binding under all conditions. The surface markers CD14 and CD16 are known to be present mostly in monocyte populations. After 7 days of incubation the macrophages did not show high expression of CD14 or CD16 and the fluorescence was similar for specific antibodies and isotype controls. Likely CD14 and CD16 are downregulated in these cells as they mature. CD14 is known to be downregulated in monocytes by IL-4 in the presence of serum (Ruppert et al., 1993). In this study the quantification of surface MR is of particular interest. As reported previously, IL-4 increases CD206 expression (Martinez-Pomares et al., 2003, Egan et al., 2004) which is in accordance with our results regarding increased cell association of MR-binding polymers in IL-4-treated human macrophages.

The ability to recognize mannose glycoconjugates is restricted to macrophages, compared to monocytes, and is absent on polymorphonuclear leukocytes or lymphocytes (Stahl et al., 1978). Hence in agreement with the presence of macrophage markers in these monocyte-derived macrophages, uptake of MR ligands further gives more confidence regarding the identification of the cells used in our lab as macrophages.

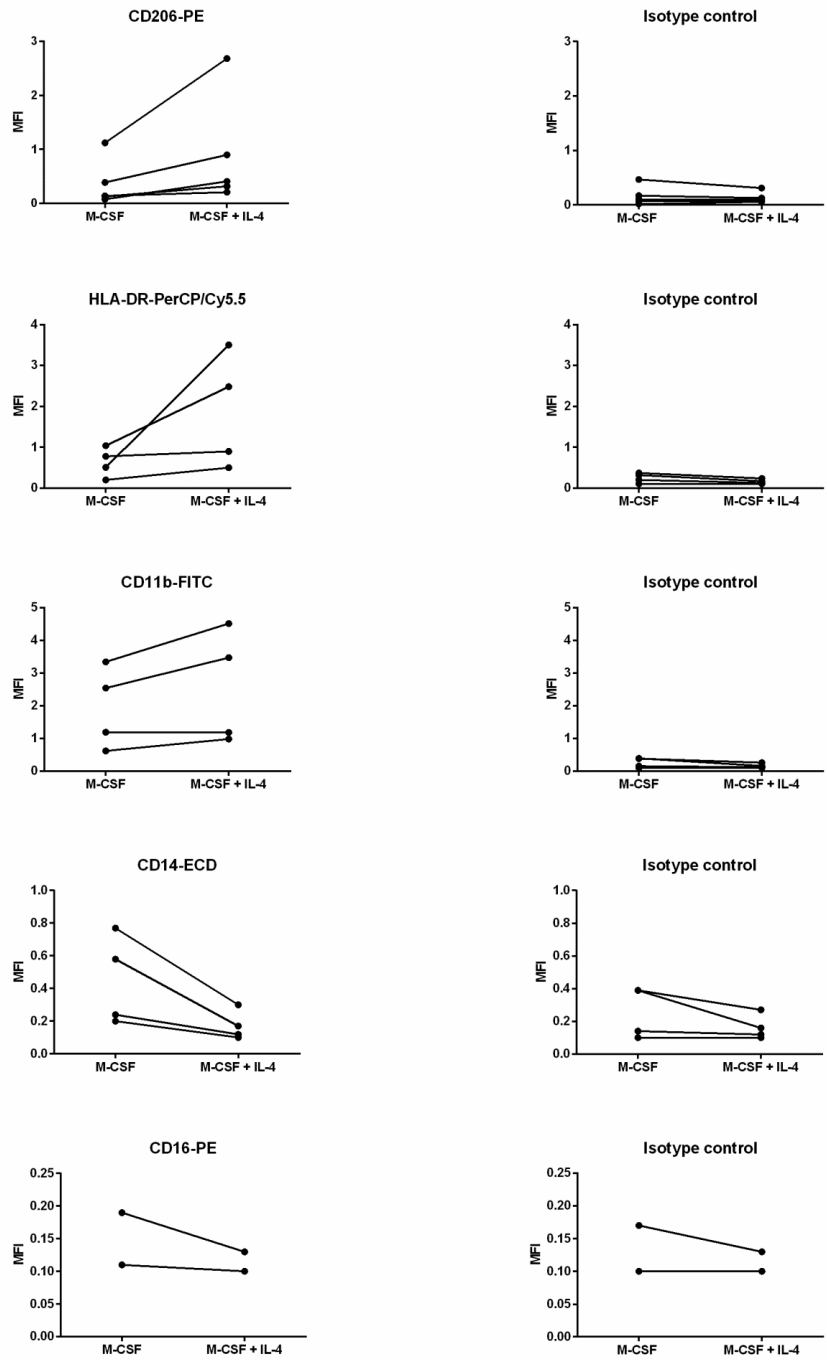
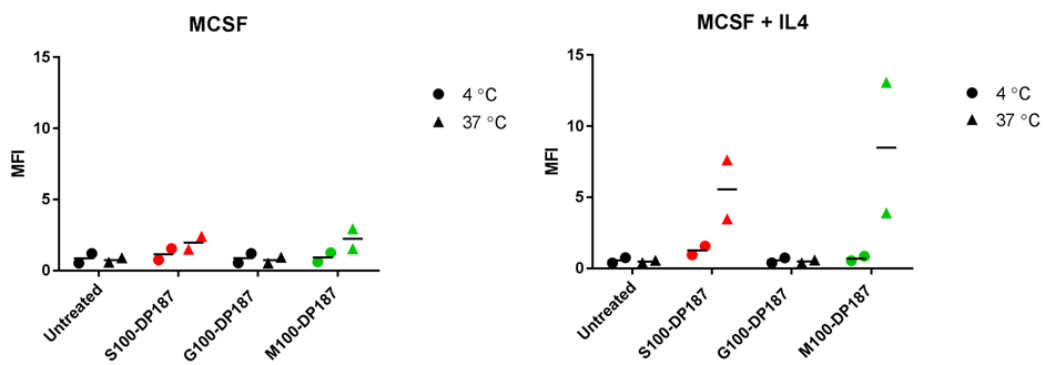
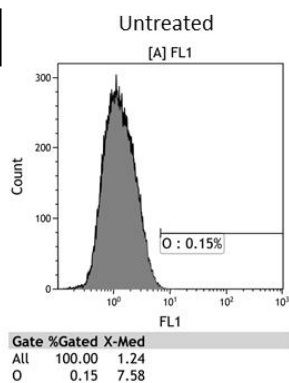
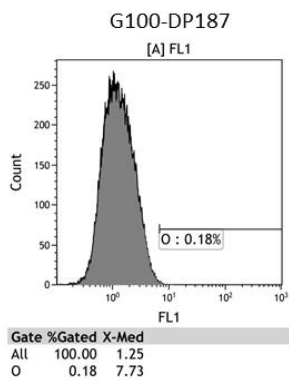
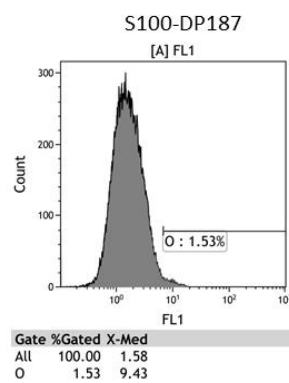
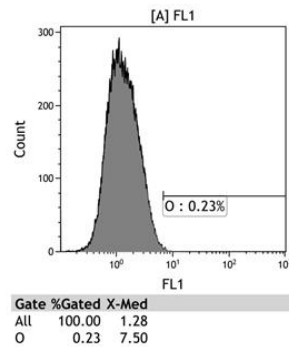
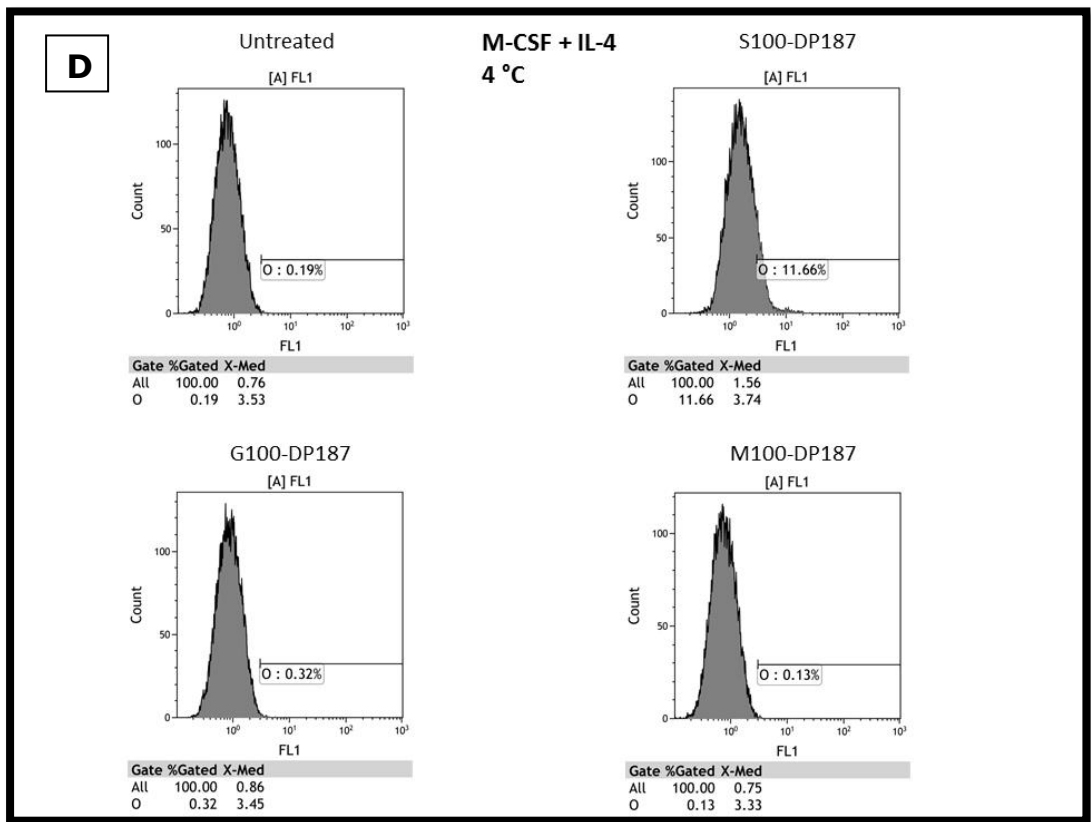
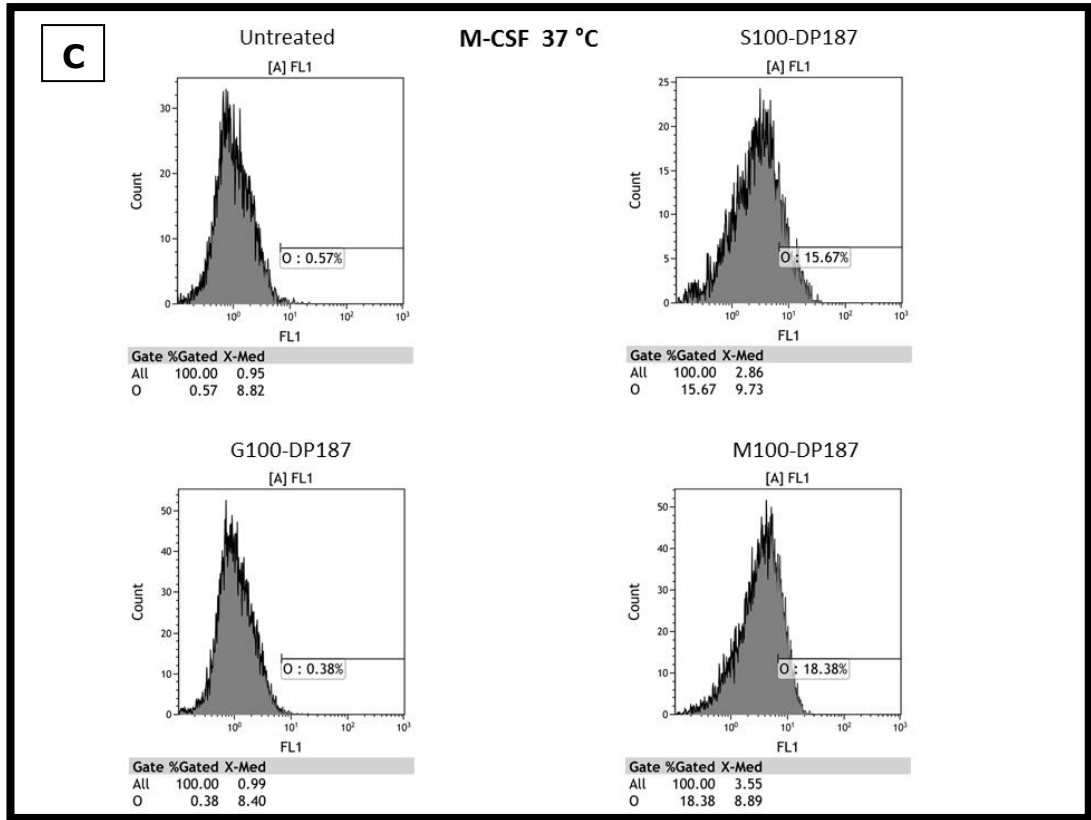


Figure 16. Mean fluorescence intensity for cell surface markers in M-CSF and M-CSF + IL-4 macrophage cultures. Human macrophages generated in the presence of M-CSF or M-CSF+IL-4 were incubated with labelled cell surface antibodies (CD206, CD11b, HLA-DR, CD14 and CD16) for 1 hour and processed for flow cytometry analysis. Established macrophage markers, such as CD11b, CD206 and HLA-DR were present in both cell conditions. An increase in fluorescence intensity for these markers is observed in the presence of IL-4. However, in these same conditions, CD14 was downregulated and become absent in the presence of IL-4. For each cell marker there is the corresponding isotype control on the second column. Paired t-test analysis shown (No significant differences). CD206, N=5; HLA-DR, CD11b, CD14, N=4; CD16, N=2.

3.4. Effect of temperature on the association of MR-binding polymers to human macrophages.

Active internalization of molecules by cells is temperature-dependent. This is particularly relevant for MR, which is mostly restricted to the early endosomal compartment and mediates ligand uptake through recycling from the plasma membrane to endosomes. To determine if polymer association to macrophages is mediated by an active process leading to internalisation, rather than binding to the plasma membrane, human macrophages were incubated with polymers at the temperatures of 4 °C and 37 °C. As shown in Figure (Figure 17A), cell fluorescence after incubation with polymers was affected by changes in temperature. At 4 °C, macrophages showed much lower MFI compared to cells incubated at 37 °C. This is particularly noticeable in IL-4 treated macrophages where an average 4.3 x MFI increase was observed between the 4 °C and 37 °C for the sulfated polymer S100-DP187. For polymer M100-DP187 the average MFI increase from 4 °C to 37 °C was 12.2 x higher MFI (Figure 17A). IL-4 treated cells incubated at 4 °C with S100-DP187 showed a higher percentage of cells expressing fluorescence above the threshold 'O' (Figure 17B). In this case, there are more S100-DP187 glycopolymers binding to macrophage's surface at 4 °C. However, this small number of cells showing higher fluorescence was not enough to significantly increase the overall MFI at 4 °C in the S100-DP187-treated cells. Temperature is known to affect receptor binding and endocytosis of glycoproteins (Stahl et al., 1980). Results suggest a temperature effect on binding and uptake of polymers by macrophages, explaining the low polymer MFI at 4 °C.

A**Effect of temperature on polymer-macrophage association****B****M-CSF 4 °C****M100-DP187**



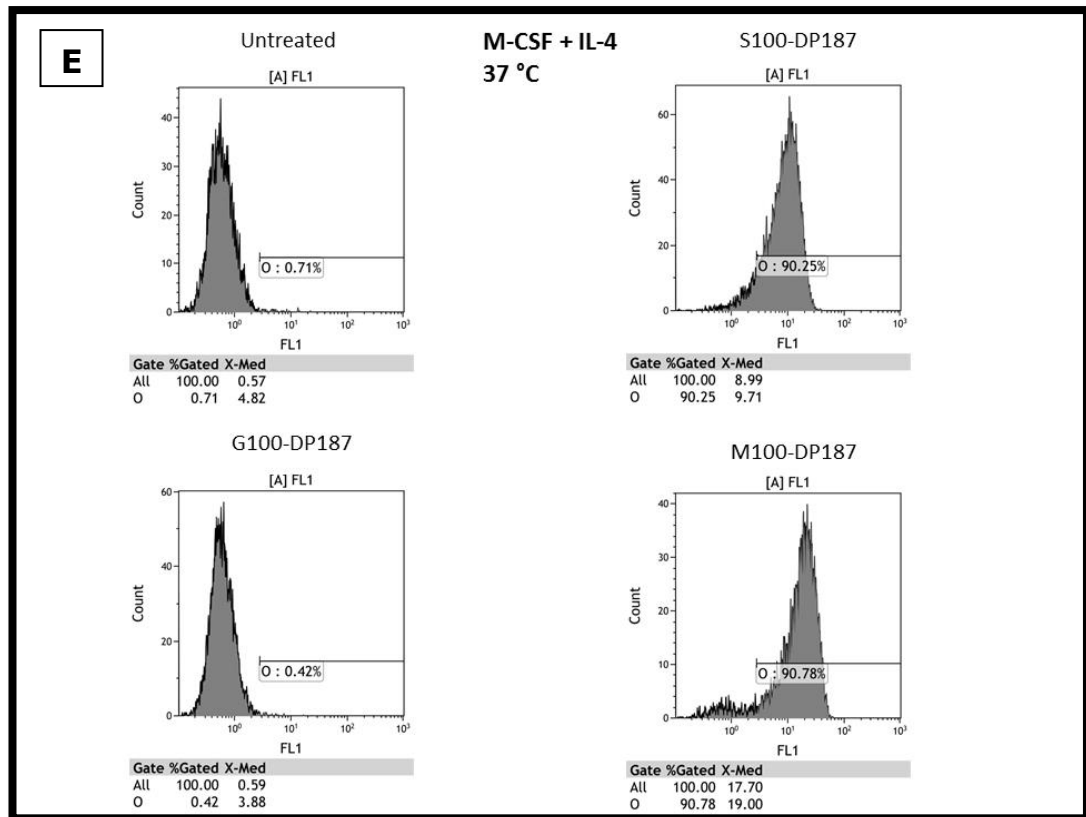


Figure 17. Temperature effect on polymer association to human macrophages. Human macrophages generated in the presence of M-CSF or M-CSF+IL-4 were incubated with polymers S100-DP187, G100-DP187 or M100-DP187 for 1 hour at 4 °C or 37 °C and processed for flow cytometry analysis. **Panel A:** Fluorescence was detected in macrophages incubated with polymers S100-DP187 and M100-DP187 after 1-hour incubation at 37 °C whilst low temperature (4 °C) in polymer association to macrophages. The difference between the 4 °C and 37 °C treatments was more prominent in IL-4 treated cells. Even with no significant difference in MFI between different polymer treatments at 4 °C (**Panel B**), an increase of cells above the threshold 'O' was observed, indicating that some cells are able to associate with the polymer S100-DP187 even at low temperatures (**Panel D**). At higher temperatures (37 °C), polymers S100-DP187 and M100-DP187 are associated with macrophages (**Panel C and E**). Polymer concentrations used: S100-DP187: 4.2 μM, M100-DP187 and G100-DP187: 5.3 μM. n=2.

3.5. Polymer association to macrophages is dose-dependent.

To determine if polymer uptake was dependent on polymer concentration, cells were incubated with different polymer amounts for 1 hour at 37 °C. Increasing polymer concentrations led to higher MFI for both M100-DP187 and S100-DP-187 (Figure 18). This increase not only depended on polymer concentration but also on the presence of cytokines. Confirming previous findings, IL-4-treated cells displayed higher fluorescence compared to M-CSF cells. Saturability is observed in clearance of glycosylated macromolecules (Stahl et al., 1978). In M-CSF treated macrophages, saturability was observed at 15 μ M polymer concentration. From 0.6 to 75 μ M, no galactose polymer binding was observed for either M-CSF or IL-4 treated macrophages. In IL-4 treated macrophages, no saturation was found and the slightly higher MFI trend for all concentrations of M100-DP187, in comparison with S100-DP187, corroborates what was observed in the previous sections.

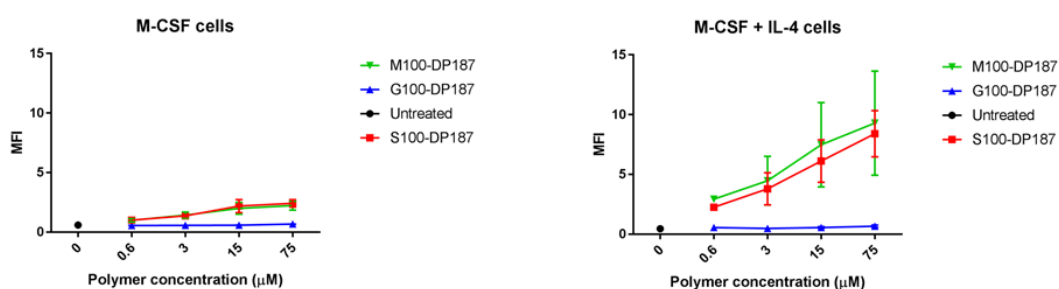


Figure 18. Effect of polymer dose on their association with human macrophages. Human macrophages generated in the presence of M-CSF or M-CSF+IL-4 were incubated with polymer concentrations (0.5 μ M, 3 μ M, 15 μ M, 75 μ M) S100-DP187, G100-DP187 or M100-DP187 for 1 hour at 4 °C or 37 °C and processed for flow cytometry analysis. Increase in S100-DP187 and M100-DP187 polymer concentrations led to increased binding/uptake to macrophages at 37°C. IL-4-treated cells showed, approximately, 3-fold increase in MFI compared to M-CSF cells and no saturation point was observed. N=2.

3.6. Uptake of polymer S100-DP187 by human macrophages can be competed with polymer S100-DP240

As explained previously, polymers used in this study were synthesized by two different techniques – ATRP (Atom transfer radical polymerization) and RAFT (Reversible addition-fragmentation chain transfer). In order to test if the newly synthesized RAFT polymers were able to compete with ATRP sulfated polymers for the same binding site, IL-4 treated macrophages were incubated with the RAFT polymers S100-DP240 and G100-DP240, which were unlabelled, for 1 hour at 37 °C and then further incubated for 2 or 6 hours in the presence of the Oregon Green-labelled ATRP polymer, S100-DP187 (Figure 19). The hypothesis was if both types of sulfated polymers bind to the same domain of MR, it would be expected a decrease in S100-DP187 fluorescence due to competition between the two polymers. At 2 hours incubation with the labelled polymer, no significant decrease in fluorescence intensity was observed. At 6 hours incubation, a small decrease in S100-DP187 fluorescence was observed in the S100-DP240-treated cells, but not in the G100-DP-240-treated cells. Surprisingly, no dose effect in correlation with the increase of unlabelled polymer was observed (Figure 20).

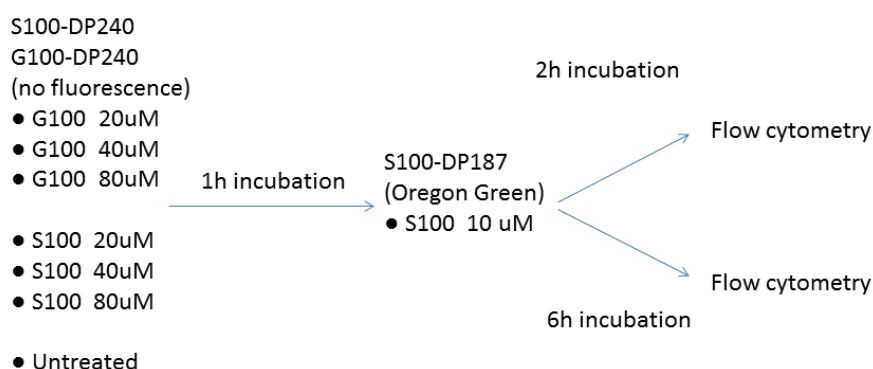


Figure 19. Summary of the competition assay between S100-DP240 and S100-DP187.

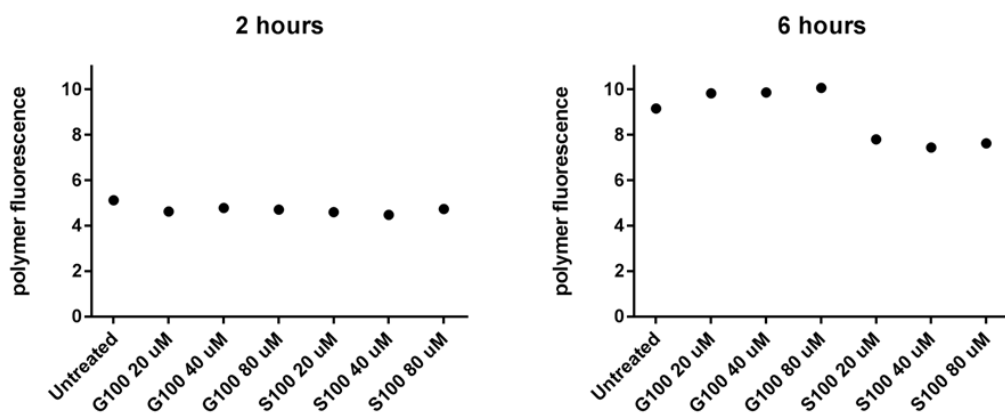


Figure 20. RAFT synthesized polymer, S100-DP240, competes with ATRP synthesized polymer, S100-DP187. After 6-hour incubation a decrease in polymer S100-DP187 fluorescence was observed when these samples were previously incubated with S100-DP240. After 2-hour incubation no significant competition was observed.

3.7. Discussion

Molecular recognition plays an important role in living organisms (Mammen et al., 1998). Recognition in biological systems can happen through protein-protein, carbohydrate-protein and antigen-antibody interactions and its strength depends on the electrostatic, hydrophobic and hydrogen bonding interactions. Because individual molecular interactions are weak, to have a stronger binding effect it is necessary to increase the number of molecular interactions. This phenomenon is known as multivalency. Carbohydrate interactions are known to be specially affected by multivalency (Lee and Lee, 1995). The glycopolymers generated by our group were initially synthesized by the method of atom-transfer radical polymerization (ATRP). Glycopolymers with 187 sugar binding units, termed, M100-DP187, G100-DP187 (M_n 70 kDa) and S100-DP187 (M_n 89 kDa) have been used in this study. This nomenclature refers to polymers labelled with Oregon green and bearing repeating units of mannose (M100-DP187), galactose (G100-DP187) or SO₄-3-Galactose (S100-DP187). Glycopolymers M100-DP187 and S100-DP187 were designed to target the two domains of MR, the CTLDs and CR domain, respectively. For comparison purposes, polymer G100-DP187 was specifically used as negative control for the experiments. Due to successful results showing the protective ability of polymer S100-DP187 in an animal model of ischemia reperfusion injury (manuscript in preparation), testing these polymers in human cells was considered as the initial step for future clinical studies. Initial binding assay results showed that the SO₄-3-Galactose polymer (S100-DP187) synthesized by our group is able to bind in a concentration dependent manner to the CR domain of human MR. The same polymer showed binding to monocyte-derived macrophages generated after 7 days of *in vitro* culture, independently of the differentiation method used, whether treated

with M-CSF, GM-CSF or M-CSF plus IL-4. The amount of binding/internalization observed was dependent on the macrophage treatment, with IL-4 treated macrophages showing a higher binding/internalization, likely caused by MR up-regulation by IL-4 (Stein et al., 1992).

Uptake of mannose-BSA by alveolar macrophages was shown to proceed linearly over time and one explanation for that was receptor recycling within the cell (Tietze et al., 1980). In other words, when the receptor-ligand complex is internalized, the ligand is dissociated from the receptor inside the cell, allowing the receptor to be recycled back to the membrane (Tietze et al., 1980). The process involves binding to a specific receptor and association with coated pits on the membrane and internalization in coated vesicles. The ligand may follow degradation in the lysosomes (Goldstein et al., 1979). The idea of receptor recycling came after the observation that (I) cells possess the ability to internalize ligands that far exceeds the number of receptors on the membrane and (II) uptake proceeds in the absence of protein synthesis (Tietze et al., 1982). At any given time, a large fraction of MR remained inside the rat alveolar macrophages (Stahl et al., 1980) an observation that has been reproduced in many instances using mouse and human macrophages as well as CHO cells expressing MR. In section 3.5, polymer binding/uptake by M-CSF cells saturated at 15 μ M, with further increase in polymer concentration not leading to any increase in MFI. Saturability and ligand specificity is necessary to define binding as receptor-mediated. In cells treated with IL-4, increasing concentrations of polymers led to a higher MFI in comparison with the M-CSF only treated cells. No saturability was observed for the IL-4 treated cells, probably due to a larger receptor pool. Intracellular receptor pool for MR may be 4-fold larger than the cell-surface receptor pool (Stahl et al., 1980). In rat alveolar macrophages, uptake could reach 2×10^6 molecules/h per cell. This suggests that each receptor, on average,

might take 11 minutes for each cycle, from cell surface to internalization and back to surface again. Acidification may also seem to be necessary for recycling of unoccupied receptors (Tietze et al., 1982). An important difference between the two types of polymers need to be mentioned. In MR⁺-CHO cells binding to MR by polymer M100-DP187 is calcium and pH-dependent, with a decrease in pH dramatically diminishing the avidity of this polymer to the receptor. In contrast, polymer S100-DP187 binding to MR is calcium and pH independent. This points to a significant difference in action between these two polymers.

Lower temperature was shown to affect polymer internalization of cells treated with labelled glycopolymers. This is in agreement with previous results where uptake of mannose-BSA by rat alveolar macrophages occurred only at 37 °C and binding/ internalization was time- and concentration-dependent (Stahl et al., 1980) and indicate that increase in fluorescence after incubation of macrophages with the polymers is due to cellular uptake rather than association with the plasma membrane.

After the initial tests with the ATRP polymers, a new family of polymers were synthesized by reversible addition-fragmentation chain-transfer polymerization (RAFT). The advantage of using this family of polymers is its increased biocompatibility due to lack of heavy metals during in the polymerization reaction. To verify if these could be used as a substitute to the initial ATRP polymers, a competition assay between the two types of polymers was designed in order to assure they compete for the same binding site. RAFT polymers were synthesized with no fluorescent labelling in contrast to the ATRP polymers which are labelled with Oregon Green. In IL-4 treated macrophages, after one-hour incubation with RAFT polymers (S100-DP240 and G100-DP240) followed by two hours incubation with the ATRP polymer (S100-DP187), no polymer competition was observed. One possible explanation for the lack of competition here

is that this type of cells has a large intracellular receptor pool and due to constant receptor cycling, the total time frame of three hours was not enough to cause a significant difference. For comparison purposes, uptake inhibition of mannose-BSA was only seen after the bulk of receptors were internalized by alveolar macrophages (Tietze et al., 1980). However, at six hours incubation with S100-DP187, a small decrease in polymer uptake was observed when cells were previously incubated with S100-DP240, indicating possible competition between the two types of polymers. To complement this experiment, a binding assay that includes S100-DP240 and the same chimeric protein (HuCR) used in section 3.1 would further confirm that this polymer binds to the same CR domain of MR as polymer S100-DP187. This was actually accomplished by Dr. Mastrotto (unpublished data) who confirmed through an independent assay that polymer S100-DP240 do bind the CR domain of MR. The successful interaction between these polymers and the human macrophage mannose receptor assured the reliability of these polymers and opened the possibility for further exploration of its biological effects.

Chapter 4 - Effect of MR-binding glycopolymers in human macrophages

The confirmation of S100-DP187 polymer internalization by human macrophages and its binding to the CR domain of human MR opened up the possibility for further exploration of its effect on human macrophages. Collagen turnover is an important process in tissue remodelling that allows for organ growth and cell migration (Madsen et al., 2013). Receptors like Endo180 in fibroblasts (Madsen et al., 2007) and MR in macrophages (Martinez-Pomares et al., 2006b) play a role in collagen turnover. Collagen binding to MR is mediated through the FNII domain (Napper et al., 2006b) and is independent of carbohydrate binding (Martinez-Pomares et al., 2006b). As the polymer S100-DP187 binds the CR domain of MR in a pH-independent manner, leading to trapping of the receptor within cells, it would be expected that collagen uptake by this receptor would be affected. In this chapter the blocking ability of S100-DP187 was tested by incubating monocyte-derived macrophages for a period of time with glycopolymers followed by incubation with fluorescently-labelled gelatin. Inhibition of gelatin uptake was quantified by flow cytometry. Total MR pool after incubation with polymers was also investigated. In addition, changes in cell surface markers and in cell metabolism in response to this polymer would provide an indication of its biological capabilities and potential for its use in clinical therapy. With this in mind, the ability of glycopolymers to affect macrophage polarization was tested, either by cell surface markers analysis or by detection of metabolic changes. Macrophages incubated with polymers were tested for changes in cell surface markers by flow cytometry. To complement the phenotypic analysis, tryptophan metabolism was also analysed through an indoleamine 2, 3-dioxygenase (IDO) activity assay. IDO plays an important role

in health and disease (Cervenka et al., 2017, Schröcksnadel et al., 2006), and is affected by MR activity (Salazar et al., 2016, Royer et al., 2010).

The aims of this chapter are:

- 1- To confirm inhibition of gelatin uptake by polymer S100-DP187 in human macrophages.
- 2- To study changes in cell surface markers caused by uptake of S100-DP187 polymer.
- 3- To detect changes in tryptophan metabolism caused by polymer S100-DP240.
- 4- To quantify total MR protein in the cell after incubation with S100-DP187.

4.1. Effect of glycopolymers on gelatin binding/uptake by human macrophages

Uptake of collagen from the extracellular matrix is a necessary step in tissue regeneration. Collagen is broken down by matrix metalloproteinases (MMPs) and internalized by fibroblasts and macrophages. In mouse macrophages, collagen binds to the Fibronectin-type II (FNII) domain of MR (Martinez-Pomares et al., 2006b) and is internalized for digestion in the lysosomes. Our earlier results showed that gelatin uptake by CHO-MR and mouse macrophages cells could be inhibited by S100 polymers (both DP-32 and DP-187) with this inhibition lasting more between 16 to 24 h in CHO-MR cells. In the previous chapter it was shown that glycopolymers bind to human MR and human macrophages, but the ability of these polymers to affect collagen uptake was not investigated. In order to test the polymers capacity to block collagen uptake by human macrophages, macrophages were assessed for their ability to bind/internalize the FNII ligand gelatin after pre-

incubation with polymers. Gelatin, the product of thermal denaturation and disintegration of collagen was used for this assay. Gelatin labelled with Texas Red was provided by Dr Francesca Mastrotto. Mature macrophages (day 7, M-CSF and M-CSF+IL-4) incubated in the presence of glycopolymers for 1 or 6 hours followed by incubation with gelatin (10 µg/ml) for 1 hour were analysed by flow cytometry. In one sample there was only the addition of gelatin but no glycopolymer. Kaluza software was used for analysis of the cells which were gated using the same strategy as the previous chapter. After gating the cell population, channels for polymers labelled with Oregon Green (Laser 488nm, emission spectrum 500-526nm) and for gelatin labelled with Texas Red (Laser 561nm, emission spectrum 604-624nm) were created for calculation of MFI. Gelatin uptake was increased by treatment with M-CSF + IL-4 compared to M-CSF treatment. M2 macrophages are known for participating in extracellular matrix degradation (Madsen and Bugge, 2013), thus a more active gelatin uptake would be expected in macrophages treated with IL-4. Gelatin uptake was not affected by incubation with polymer S100-DP187 (48 µM) for 1 hour in M-CSF macrophages but a slight reduction was seen in M-CSF + IL-4 treated cells (Figure 21), panel A). These results contrast with CHO-MR cells which showed significant reduction in gelatin uptake after 1h incubation with S100-DP187 (Figure 10). This could reflect differences in MR biology between both types of cells and/or the activity of another collagen binding receptor in human macrophages.

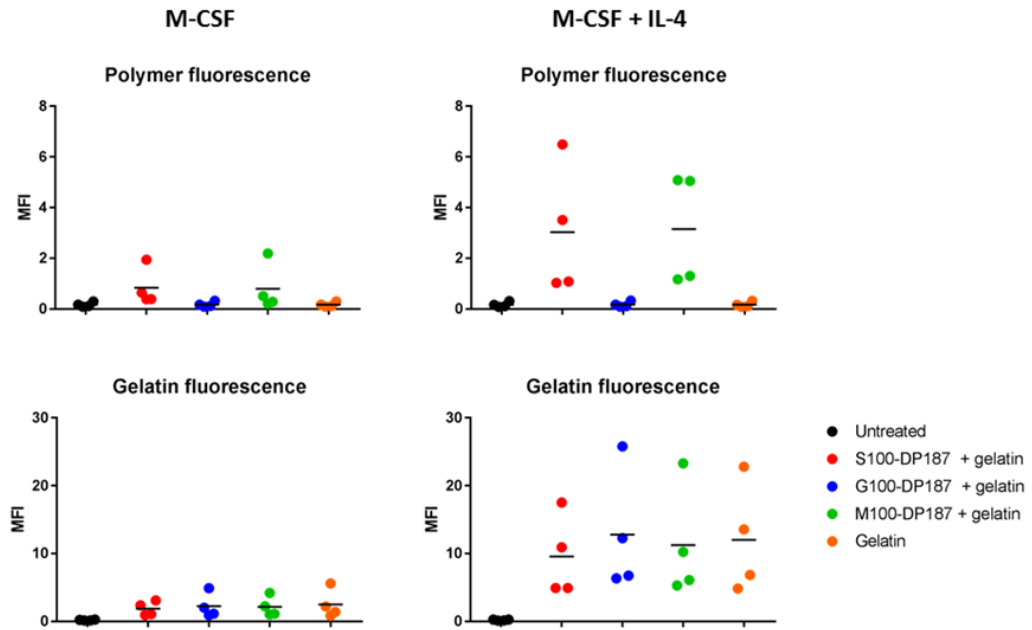


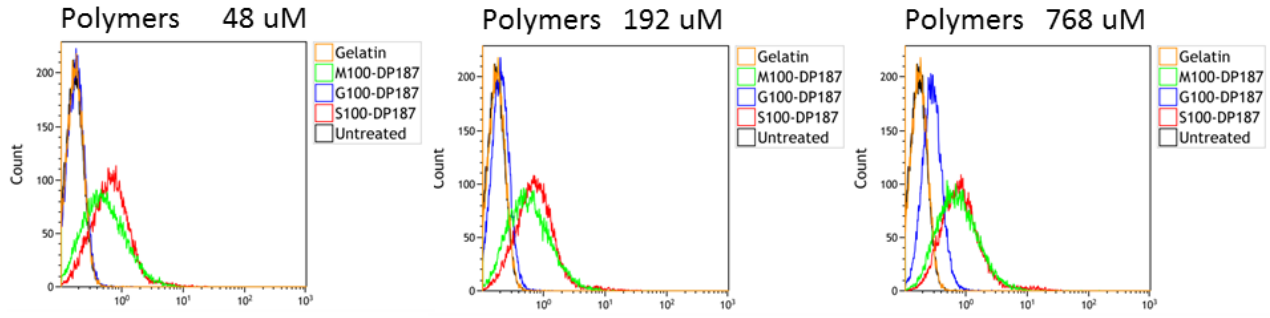
Figure 21. Effect of polymers (1-hour incubation) on gelatin uptake by human macrophages. Incubation with polymer S100-DP187 for 1 hour at 37 °C prior to gelatin incubation (10 µg/ml) for 1 hour caused a slight reduction in gelatin uptake by IL-4-treated macrophages. Polymer concentration: 48 µM. n=4.

Two other polymer concentrations were used- 192 µM and 768 µM, to test their effect on gelatin uptake after 1-hour incubation. In M-CSF treated macrophages, none of the three concentrations tested (48, 192 and 768 µM) showed major inhibition of gelatin uptake (Figure 22, A). Polymer G100-DP187 at 768 µM associated with M-CSF macrophages and with M-CSF + IL-4 macrophages at 192 and 768 µM (Figure 22, B), something not observed at 48 µM. Incubation with 192 µM and 768 µM S100-DP187 decreased gelatin uptake in IL-4-treated cells and the effect seems to be dose dependent (Figure 22, B). Increasing concentrations of M100-DP187 also led to a reduction in gelatin uptake, however, the inhibition was not as efficient as the one caused by polymer S100-DP187. Based on these observations it was concluded that in comparison with CHO-MR cells,

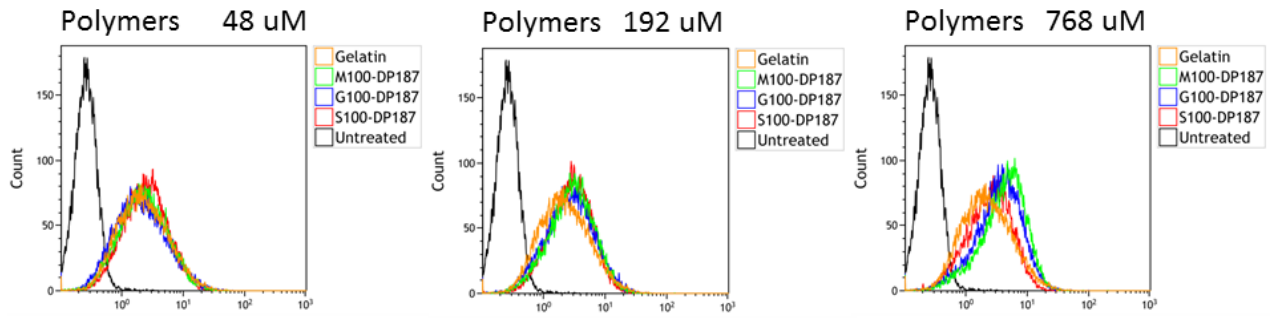
incubation with polymer S100-DP187 at 48 μM for 1 hour does not significantly inhibit gelatin uptake in human macrophages.

**M-CSF macrophages
Oregon Green fluorescence**

A

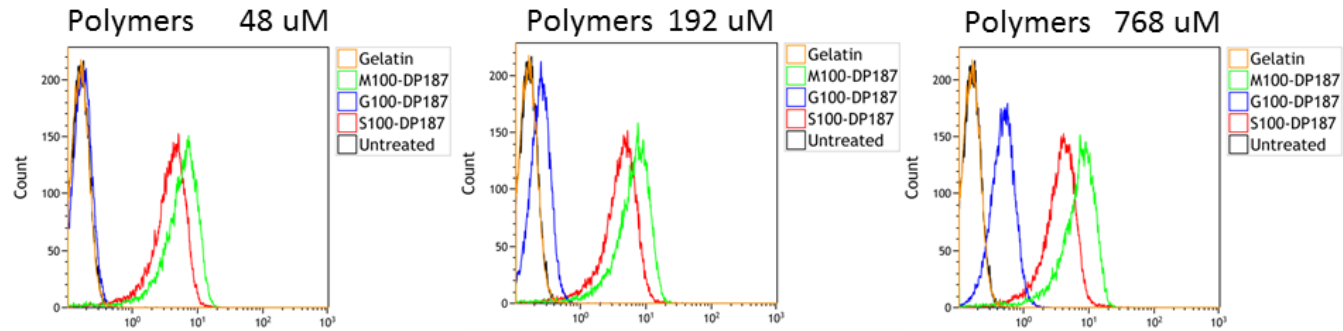


Texas Red fluorescence

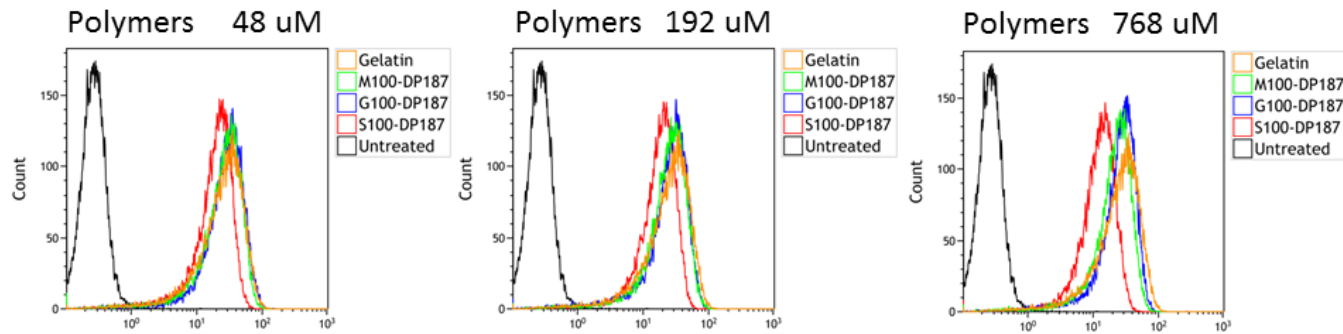


**M-CSF + IL-4 macrophages
Oregon Green fluorescence**

B



Texas Red fluorescence



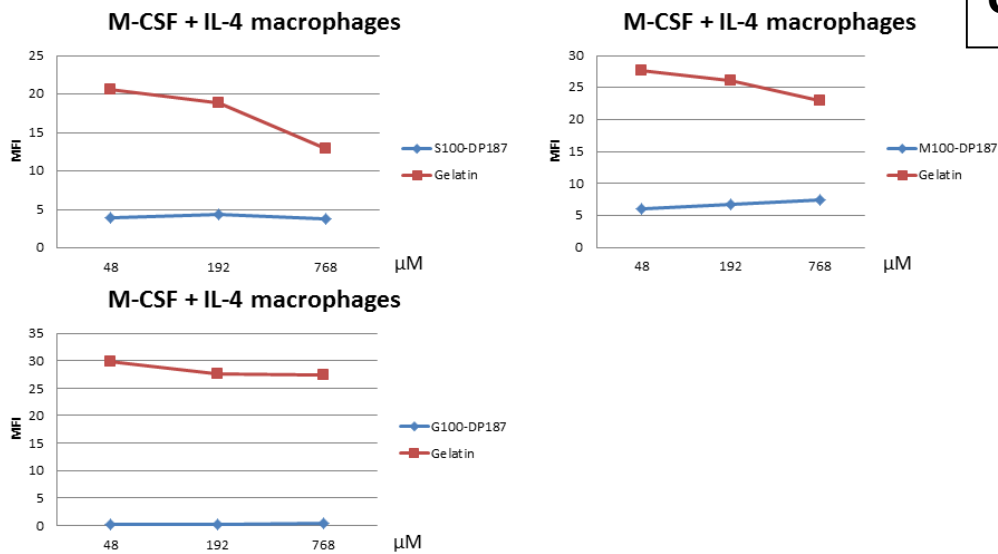


Figure 22. Effect of different polymer concentrations (1-hour incubation) on gelatin binding to human macrophages. Monocyte-derived macrophages were incubated with polymers for 1 hour at 37 °C prior to gelatin incubation (10 μg/ml) for 1 hour. Polymer concentrations: 48 μM, 192 μM, 768 μM. **Panel A.** Glycopolymers and gelatin MFI histogram for M-CSF treated macrophages. **Panel B.** Glycopolymers and gelatin MFI histogram for M-CSF + IL-4 treated macrophages. An increase from 48 μM to 768 μM in polymer S100-DP187 concentration provoked a decrease in gelatin uptake by IL-4 treated macrophages, as it can be observed by the decrease in Texas Red fluorescence for cells incubated with this polymer. **Panel C.** Glycopolymers and gelatin MFI for IL-4 treated macrophages. Reduction in gelatin uptake in IL-4 treated macrophages was also observed in M100-DP187 treated cells but the inhibition was not as efficient as the one caused by polymer S100-DP187. Data analysed in Kaluza shows MFI for the Oregon Green labelled polymers (Laser 488nm, emission spectrum 500-526nm) and Texas Red labelled gelatin (Laser 561nm, emission spectrum 604-624nm) for the three different concentrations. n=1.

A 6 hours incubation with S100-DP187 (48 μ M) followed by a 1-hour gelatin (10 μ g/ml) incubation led to more prominent reduction in gelatin fluorescence in IL-4-treated macrophages (Figure 23). This effect was also observed with S100-DP240 (40 μ M). The difference in inhibition efficiency between assays suggests that polymer time of incubation plays a significant role in gelatin uptake inhibition.

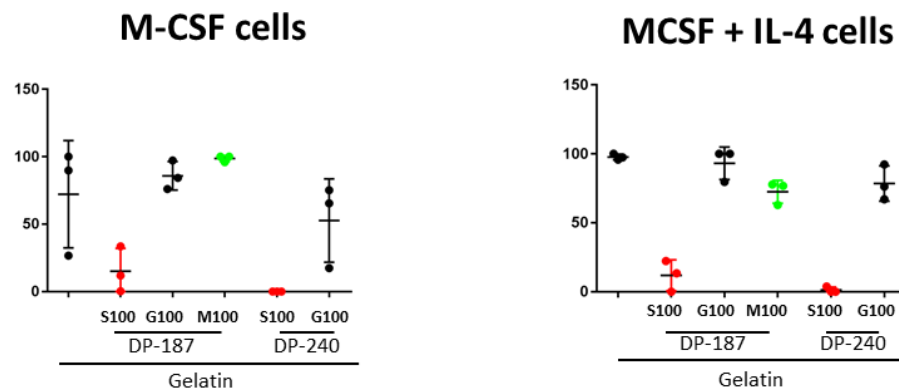


Figure 23. Effect of polymers (6-hour incubation) on gelatin uptake by human macrophages. Prominent gelatin uptake inhibition was observed in IL-4 treated cells in the presence of either sulfated polymers (S100-DP187 and S100-DP240) after 6 hours incubation at 37 °C followed by gelatin incubation for 1 hour. Data was normalized from 0 (lowest MFI in each experiment) to 100 (highest MFI in each experiment). S100-DP187, G100-DP187, M100-DP187: 48 μ M and S100-DP240, G100-DP240: 40 μ M. n=3.

4.2. Endo180 is expressed in human macrophages

Differences in gelatin uptake inhibition for one-hour polymer incubation between CHO⁺MR cells and human macrophages pointed to divergent uptake processes between the two cell types. This could be caused by another collagen binding receptor that present in human macrophages and could compensate for the impaired gelatin uptake inhibition by S100-DP187 in these cells. Endo180 is a known collagen binding receptor in fibroblasts but has been found in human monocyte-derived macrophages and co-localize with CD14 in macrophages from human skin sections (Sheikh et al., 2000). This receptor is also known as mannose receptor 2 due to its structural similarities to MR. Endo180 (CD280) contains the same three main regions than MR: the cysteine-rich domain; the FNII domain and eight CTLDs domains, however, the cysteine-rich domain in this receptor does not bind sulfated sugars (East and Isacke, 2002), excluding the possibility that polymer S100-DP187 would also affect the function of this receptor. We employed western blotting to test for the presence of Endo180 in human macrophages. Protein lysate from the fibroblastic cell line, MRC5, was used as a positive control for the presence of Endo180. Macrophages treated for seven days in the presence of M-CSF or M-CSF + IL-4 were lysed on day 7 and the protein lysate was used for Endo180 detection. M-CSF and M-CSF + IL-4-treated macrophages showed expression of Endo180, however, in order to detect this receptor, the amount of protein loaded per well for macrophages (20 µg) had to be higher than for MRC5 cells (6 µg) (Figure 24). The presence of this additional collagen binding receptor in human macrophages could explain the decreased gelatin inhibition uptake by polymer S100-DP187 in these cells when compared to CHO-MR. Differences in band sizes between MRC5 and M-CSF + IL-4 macrophages and M-CSF macrophages could be explained by changes in protein glycosylation in Endo180 (Su et al.,

2005). An intriguing observation of this preliminary assay was that Endo180, unlike MR, was downregulated by IL-4.

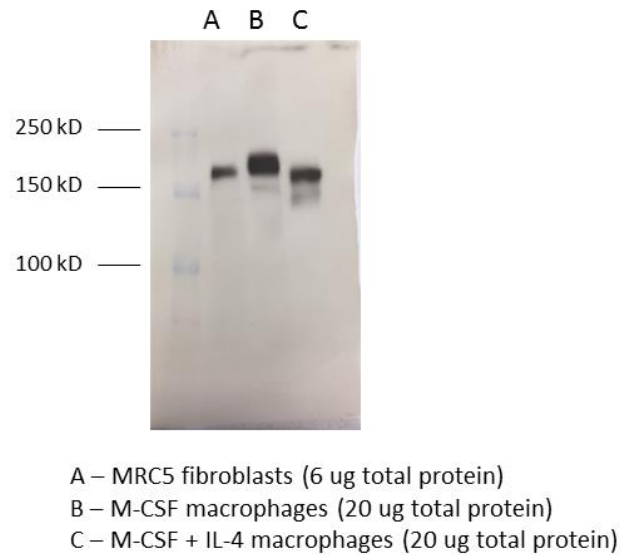


Figure 24. Analysis of Endo180 expression in human macrophages. M-CSF and M-CSF + IL-4 macrophages were cultured for seven days, on day 7, cells were lysed and protein lysates (20 μ g protein/well) were used for Endo180 detection. Membrane was incubated with A5158 antibody primary antibody (dilution 1:5) for 1 hour, followed by incubation with secondary antibody anti-mouse peroxidase (dilution 1:1000) for 1 hour. As positive control MRC5 protein lysate was used at 6 μ g per well.

4.3. Cell surface markers expression after polymer incubation

For a molecule to be considered a “mannose receptor blocker” in addition to inhibiting its activity it should also reduce the presence of the receptor at the cell surface. To investigate whether the glycopolymer S100-DP187 could block MR presence at the cell surface, monocyte-derived macrophages were initially incubated with 48 μ M of S100-DP187, M100-DP187 and G100-DP187 for 1 hour followed by incubation with anti-MR antibody labelled with Alexa-Fluor 647 for 1 hour. Cells were fixed and antibody fluorescence was quantified by flow cytometry and analysed by Kaluza software. M-CSF + IL-4 macrophages incubated with S100-DP187 showed decreased MR cell surface expression in comparison with untreated cells or cells treated with G100-DP187 (Figure 25), although not significant. M-CSF cells did not present any changes in MR expression after one-hour polymer treatment.

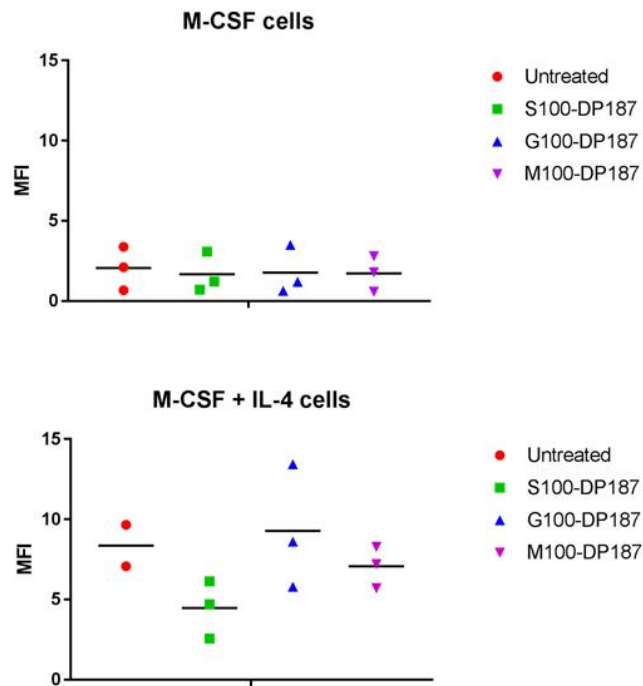


Figure 25. Cell surface markers expressions in macrophages are affected by polymer S100-DP187. Day 7 macrophages were incubated in the presence of polymers (48 μ M) for 1 hour prior to anti-MR antibody labelling for 1 hour and fluorescence was quantified by flow cytometry. MFI Kaluza scale: Legacy. N=3.

Next, changes in surface markers during M1 activation in the presence of polymers were tested. IFN- γ was used to obtain M1 cells as follows; cells on day 6 were co-incubated with IFN- γ (20 ng/ml) and polymers for 24 hours, after this period, macrophages were harvested from the plates and labelled for cell markers, such as MR, HLA-DR and CD11b for 1 hour. Anti-MR antibody was labelled with Alexa Fluor 647 (Laser 642, emission filter 671/30), whilst anti-HLA-DR and anti-CD11b antibodies were labelled with PerCP-Cy5.5 (Laser 488, emission filter 710/45). Samples were labelled individually for each antibody and data was analysed by Kaluza software. It was observed in the analysis that isotype control samples for PerCP-Cy5.5 in the presence of S100-DP187 was

showing a higher fluorescence than isotype control samples for the untreated and G100-DP187 treated samples. This was interpreted as the Oregon Green labelled polymer S100-DP187 interfering in the channel used for PerCP-CY5.5 analysis. Thus, HLA-DR and CD11b MFI were affected by spillover from S100-DP187 fluorescence. The results changed dramatically in this scenario of 24 hours polymer incubation. A reduction in MR surface expression was detected both in M-CSF-treated, as well as in IFN- γ -treated macrophages (Figure 26) when these cells were incubated in the presence of S100-DP187 (48 μ M). However, a significant reduction was only observed in IFN- γ -treated cells incubated with S100-DP187 compared against IFN- γ -treated cells treated with no polymer ($p=0.0162$) or against IFN- γ -treated cells incubated with G100-DP187 ($p=0.0229$). Intriguingly, no reduction in MR expression was observed in the presence of IFN- γ which was unexpected. CD11b, another marker found in mature macrophages, showed to be less expressed in IFN- γ -treated cells in the presence of S100-DP187 compared against IFN- γ -treated cells incubated with no polymer (Figure 26). IFN- γ upregulates HLA-DR, a MHCII cell surface receptor found in activated macrophages but in the presence of polymer S100-DP187, HLA-DR marker is not increased at the same rate as IFN- γ -treated cells in the presence of no polymer. This surface marker failed to be upregulated, suggesting that these cells could not be properly activated in the presence of S100-DP187 (Figure 26). Data for HLA-DR and CD11b were not compensated and the graph shows the influence of S100-DP187 fluorescence spillover.

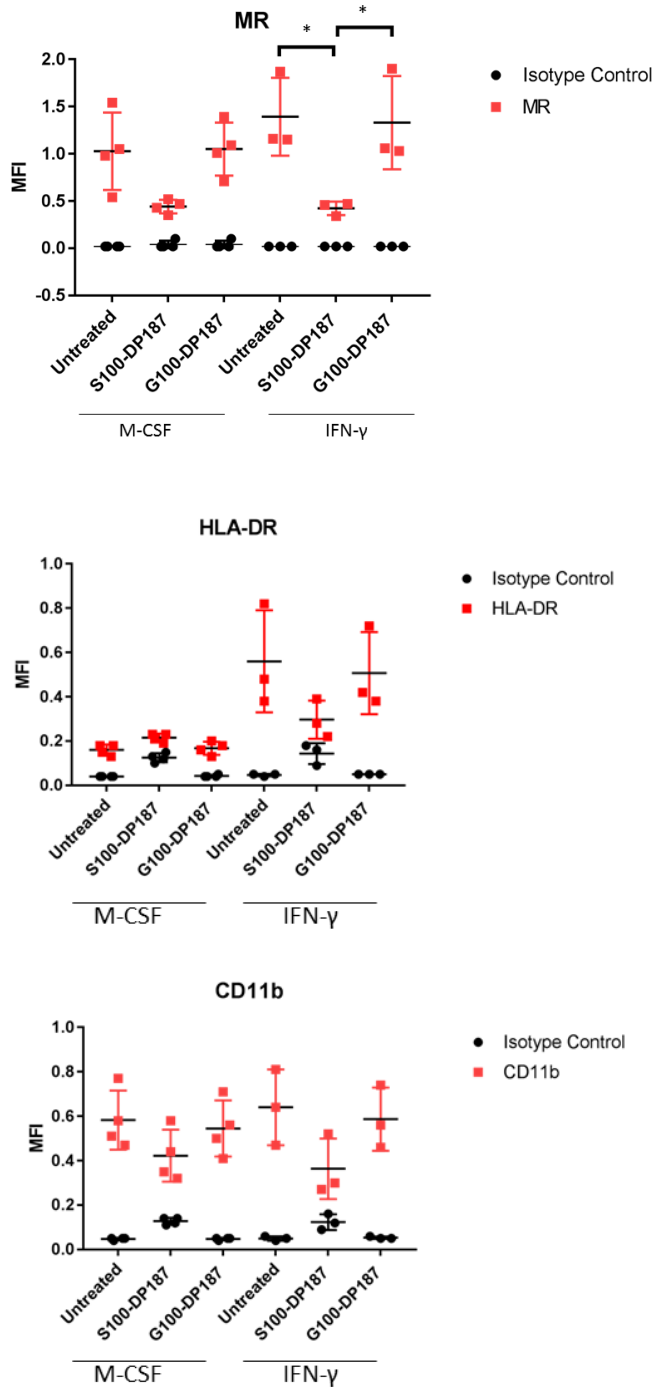


Figure 26. Cell surface markers expression in macrophages are affected by polymer S100-DP187. M-CSF-treated macrophages for 6 days were activated by IFN- γ (20 ng/ml) and co-incubated in the presence of S100-DP187 and G100-DP187 (48 μ M) for 24 hours. On the following day, cells were labelled with antibodies against MR, CD11b and HLA-DR, fixed, and labelling quantified by flow cytometry. Statistical analysis (ANOVA) of MR expression showed a reduction of MR in IFN- γ treated macrophages incubated with S100-DP187 in comparison with untreated cells ($p=0.0162$).

4.4. IDO activity is affected by polymer S100-DP240

To further investigate the capacity of polymer S100-DP187 to modulate macrophage phenotype, it was necessary not only to analyse its ability to inhibit MR surface expression but also to quantify metabolic changes associated with MR activity. Dendritic cells, which express MR, play a key role in induction of Th2-mediated inflammation in allergic diseases (Kuipers and Lambrecht, 2004). Allergens bind to the C-type lectin like domain of MR and are able to affect dendritic cells ability to polarize T cells through indoleamine 2,3-dioxygenase (IDO) activity (Royer et al., 2010). IDO is an enzyme present in many cell types, including macrophages, which participate in Tryptophan metabolism, by converting L-Tryptophan to N-formylkynurenine, which is further converted to L-kynurenine by the enzyme formamidase. Kynurenine production is associated with reduction in the activity of natural killer cells, dendritic cells and reduction in T cells proliferation. High levels of kynurenine can also increase the proliferation and migratory capacity of cancer cells, as well as help tumors escape the immune system (Cervenka et al., 2017). Because of the importance of kynurenine in modulating the immune system and its connection with MR, it was decided to investigate its production and possible modulation by unlabelled polymer S100-DP240. IDO activity is induced by IFN- γ (Moffett and Namboodiri, 2003) and LPS (Salazar et al., 2016), whilst the polysaccharide mannan, which binds MR, decreases its induction. The chosen method to quantify tryptophan metabolites was through the use of Ehrlich's reagent, which contains 4-(Dimethylamino)benzaldehyde that forms a coloured condensation product in contact with primary amines present in kynurenine. Monocyte-derived macrophages grown for 5 days on low-attachment plates were transferred to a polystyrene tissue culture plate and

cultured in the presence of M-CSF (50 ng/ml). On day 6, cells were treated with a combination of cytokines, lipopolysaccharide and glycopolymers and further incubated for 24 hours at 37 °C. On day 7, supernatants were collected, proteins were removed from the media by Trichloroacetic acid. Kynurenine was detected in the media by Ehrlich solution and quantified at 492 nm. The combination of IFN- γ (20 ng/ml) and LPS (20 ng/ml) increased kynurenine synthesis significantly, more than the amount of the two individual treatments combined. Incubation with polymer S100-DP240 reduced kynurenine production in a dose-dependent manner, whilst polymer G100-DP240 had no apparent effect (Figure 27).

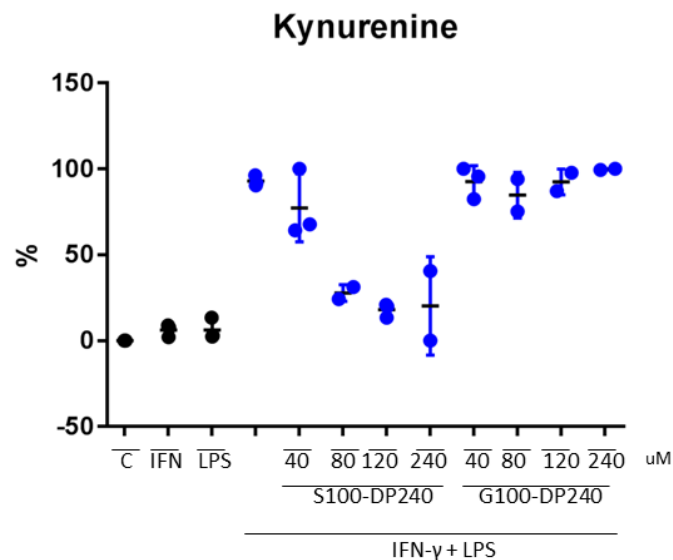
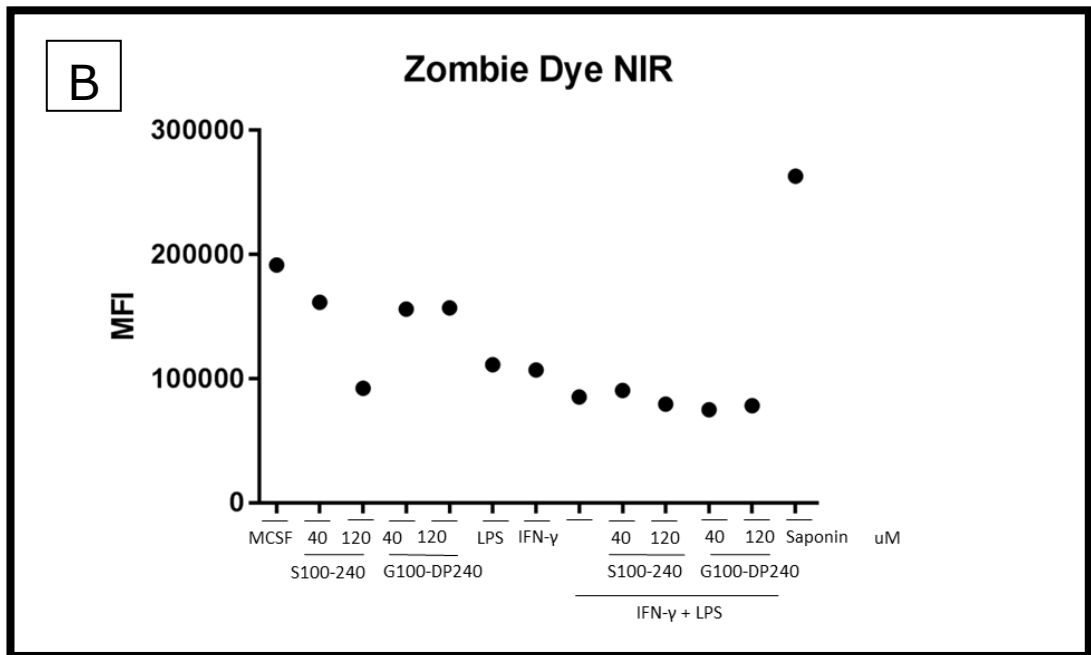
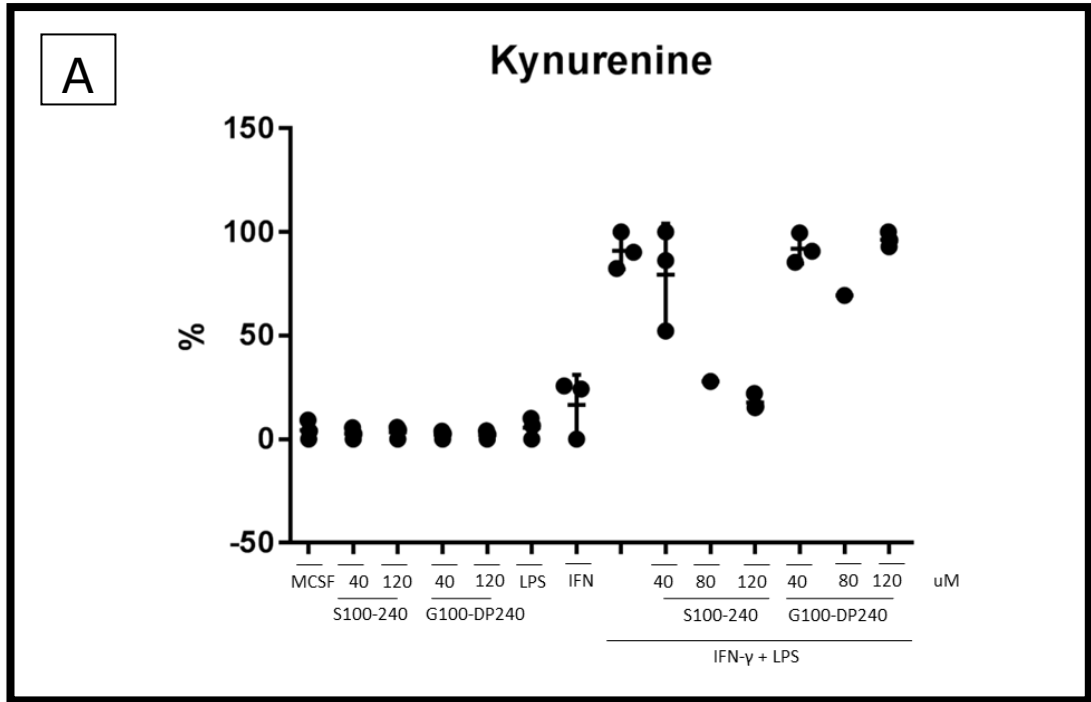


Figure 27. S100-DP240 reduces IDO activity in IFN- γ /LPS treated macrophages. Day 6 macrophages on a polystyrene tissue culture plate were treated with IFN- γ (20 ng/ml), LPS (20 ng/ml) and different concentrations of glycopolymers (40, 80, 120, 240 μ M) for 24 hours. On day 7, supernatant was collected and used for kynurenine condensation with Ehrlich's reagent and quantified at 492 nm. Data were normalized from 0 (lowest kynurenine concentration in each experiment) to 100 (highest kynurenine concentration in each experiment). N=2. For 40 μ M of S100-DP240 and G100-DP240: N=3.

To ensure the reduction in kynurenine was not due to cell death, an alternative method using the low-attachment plate was used where the detached cells were analysed by flow cytometry whilst the supernatant was used for kynurenine quantification. In this method cells were stimulated directly in the low-attachment plate with IFN- γ (20 ng/ml) and LPS (20 ng/ml) on day 6 and incubated at 37 °C for 24 hours. On day 7, supernatant was collected and centrifuged at 350 x g for 5 minutes in order to remove any floating cells. The supernatant was used for kynurenine quantification as described previously. The reduction in IDO activity was also observed in activated macrophages treated with S100-DP240 (Figure 28, Panel A). In parallel, cells were collected from the plate and used for staining with Zombie dye NIR for 30 minutes, which penetrate cells that possess damaged membranes (Figure 28, Panel B). Cells treated with detergent saponin 0.015% for 5 minutes were used as positive control for membrane damage. Results show that cells treated with S100-DP240 do not have higher fluorescence for Zombie dye NIR when analysed by flow cytometry, excluding the possibility of cell damage caused by polymer S100-DP240.



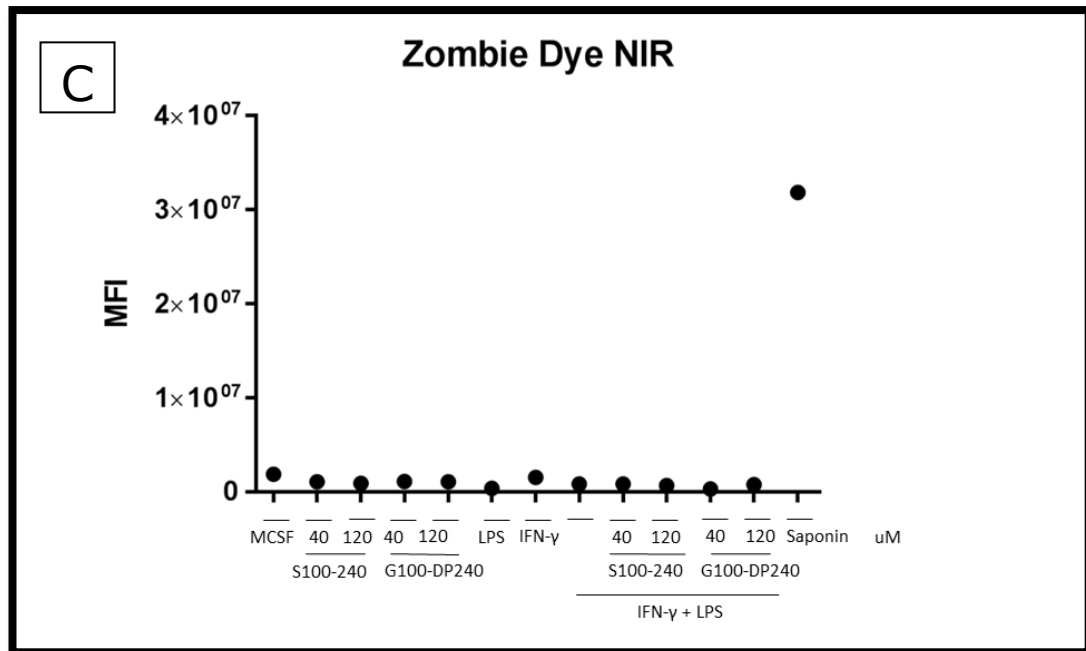


Figure 28. S100-DP240 effect in kynurenine production was not due to a decrease in cell viability. Panel A. Day 6 macrophages on low-attachment plates were treated with M-CSF only (50 ng/ml), IFN- γ (20 ng/ml), LPS (20 ng/ml) and different polymer concentrations (40, 80, 120 μ M) for 24 hours at 37 $^{\circ}$ C. On day 7, supernatant was collected for kynurenine quantification. Data from experiments are normalized to a scale of 0 – 100. N=3. **Panel B and C.** Data from two independent assays showing cells incubated with Zombie dye NIR for 30 minutes, fixed, and quantified by flow cytometry. Positive control cells were treated with saponin (0.015%) for 5 minutes. Fluorescence is shown on Kaluza full scale.

From the same group of cells, surface markers were also analysed. Macrophages were incubated with antibodies against MR (Alexa Fluor 647) and against HLA-DR (PerCP-Cy5.5) for 1 hour at 4 $^{\circ}$ C, fixed and analysed by flow cytometry (Astrios EQ). Due to great variation in MR MFI, data was reorganized such as that MFI from M-CSF treated cells (untreated) were set to 100% and the MFI from M-CSF cells treated with polymers (40, 120 μ M) were recalculated in comparison with the first. In the case of cells treated with IFN- γ (20 ng/ml) and LPS (20 ng/ml), macrophages treated with this combination (IFN- γ + LPS) was set to 100% and the other conditions were recalculated accordingly. A trend showing a decrease in MR

surface expression in IFN- γ (20 ng/ml) and LPS (20 ng/ml) treated macrophages incubated in the presence of polymer S100-DP240 (40, 120 μ M) corroborate the blocking capacity of this polymer (Figure 29, Panel A). Something that was also observed here is that MR expression in IFN- γ treated macrophages is higher than in cells treated with the combination of IFN- γ and LPS. This points to the possibility that MR is differentially regulated in IFN- γ - vs IFN- γ + LPS-treated cells even though both conditions are discussed in the literature as pro-inflammatory.

For marker HLA-DR, the MFI values shown by Kaluza full scale was used to plot the graph. At 120 μ M of S100-DP240, HLA-DR was significantly decreased ($p=0.0112$) in IFN- γ (20 ng/ml) + LPS (20 ng/ml) treated cells (Figure 29, Panel B).

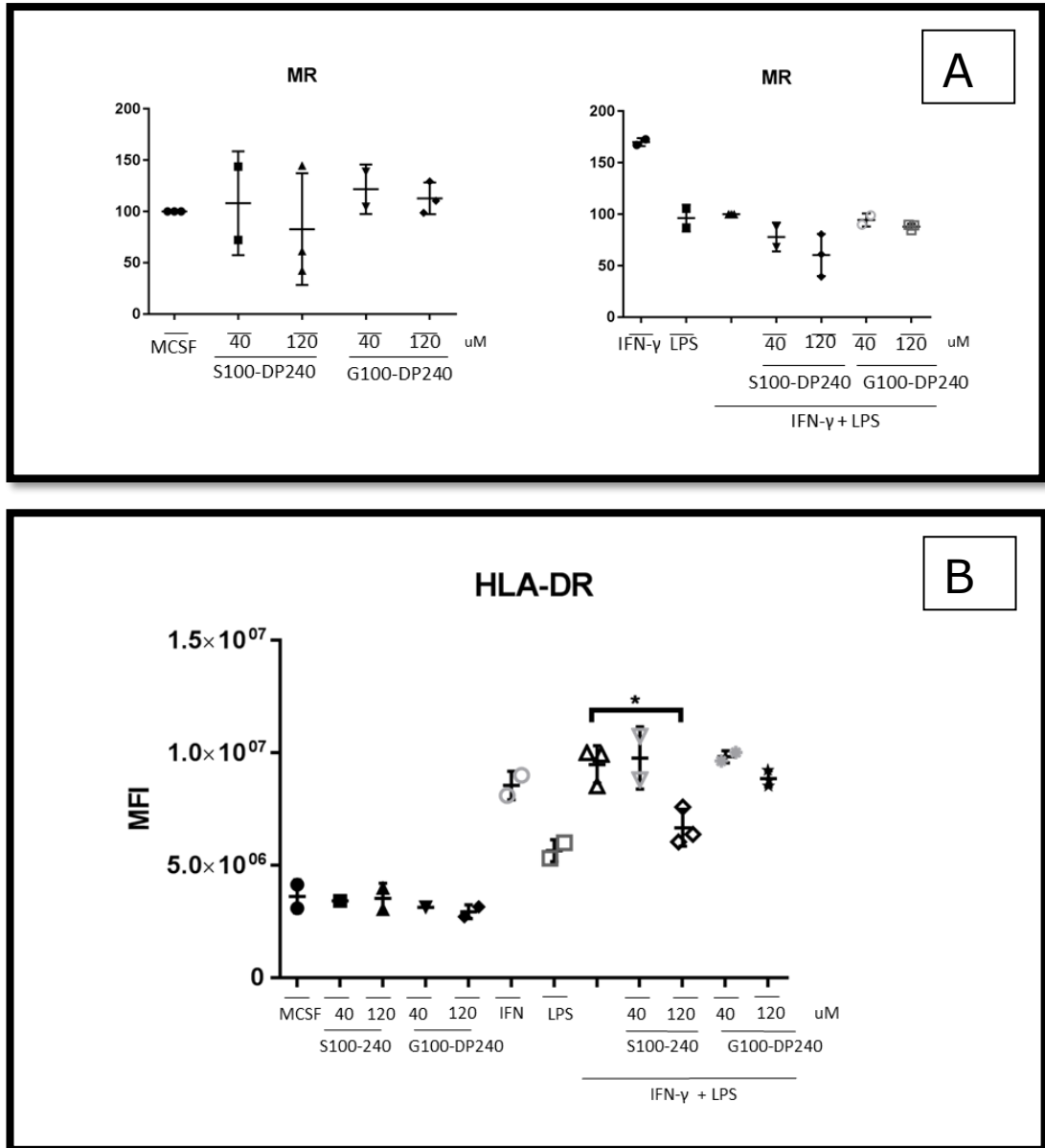


Figure 29. Polymer S100-DP240 inhibit HLA-DR expression in M1 activated macrophages. Day 6 macrophages activated by IFN-γ + LPS for and co-incubated in the presence of S100-DP240 and G100-DP240 (40, 120 μM) for 24 hours were labelled with antibodies against MR (Panel A) and HLA-DR (Panel B) for 1 hour at 4 °C and quantified by flow cytometry.

4.5. Total MR and Endo180 expression after incubation with polymer S100-DP187

The inhibition in cell surface markers by polymers S100-DP187 and S100-DP240 revealed its ability to affect MR presence on the surface but whether the receptor is being internalized for degradation or whether that affects the whole MR pool is unknown. To determine if total MR expression in macrophages was affected by polymer treatment, macrophages were incubated with M-CSF (50 ng/ml) and IL-4 (25 ng/ml) for 7 days and, by day 7, polymer S100-DP187 at 48 μ M, 96 μ M or 192 μ M for 2 hours, at 37 $^{\circ}$ C was added to the plate. Lysates from M-CSF and M-CSF + IL-4 macrophages were used in western blot and quantified. IL-4 clearly increased total MR expression in human macrophages. Treatment with polymer S100-DP187 did not cause decreased total MR expression in IL-4 treated macrophages. In M-CSF cells from donor 2, MR expression from treatment S100-DP187 (192 μ M) is decreased in comparison with the other lanes. However, because there was no loading control the analysis lacks accuracy.

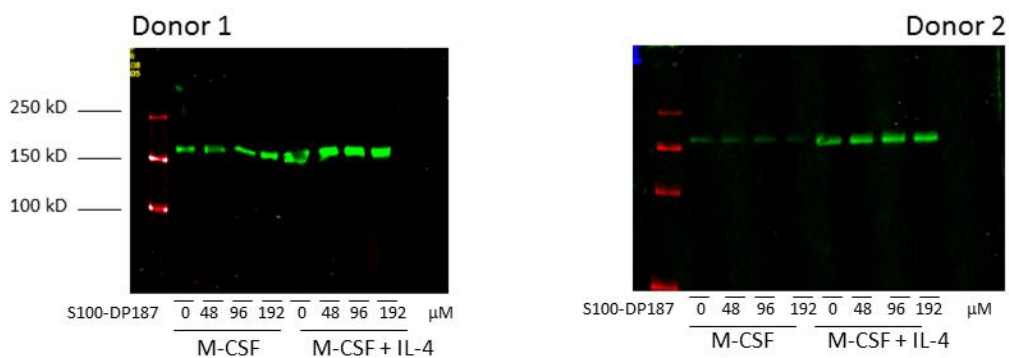
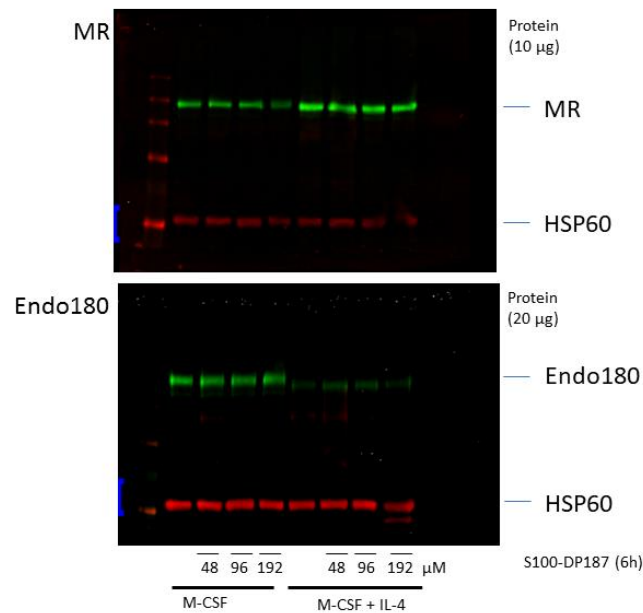


Figure 30. Analysis of total MR expression by human macrophages after treatment with polymers for 2 hours. Macrophages were grown in the presence of M-CSF (50 ng/ml) and IL-4 (25 ng/ml) for 7 days and by day 7 were incubated with polymer S100-DP187 (48, 96, 192 μ M) for 2 hours at 37 $^{\circ}$ C. Cells were lysed and processed for total MR detection. A purified mouse anti-human CD206 (MMR) antibody (dilution 1:1000) was used for detection of MR, after one-hour incubation, the secondary antibody IRDye 800CW Goat anti-Mouse (dilution 1:10000) was added and incubated for 1 hour. Each gel corresponds for a distinct cell donor.

To complement the previous experiment, an assay using 6 hours polymer incubation which also incorporated a loading control alongside Endo180 detection was performed. Macrophages incubated for 7 days with M-CSF (50 ng/ml) and IL-4 (25 ng/ml) and, on day 7, different concentrations of S100-DP187 were added to the plate for 6 hours, at 37 °C. Cells were lysed and protein was extracted for MR and Endo180 detection. For loading control, heat shock protein 60 (HSP60) was chosen. Mouse anti-MR antibody and anti-Endo180 were used as primary antibodies to detect MR and Endo180, respectively, and a rabbit monoclonal antibody was used to detect HSP60. For detection of the mouse and rabbit antibody the infrared dye IRDye 800CW Goat anti-Mouse and IRDye 680RD Goat anti-Rabbit antibodies, were used respectively. The intensity of the bands was quantified through Licor scanner Odyssey and plotted as the ratio of the intensity of the band of interest/intensity of HSP60 protein band. The two proteins displayed different regulation, even though they are part of the same family. While incubation with IL-4 for 7 days upregulates MR expression, it has an opposite effect downregulating Endo180. MR and Endo180 total expression did not show any degradation in the presence of increasing doses of S100-DP187 (Figure 31).

A



B

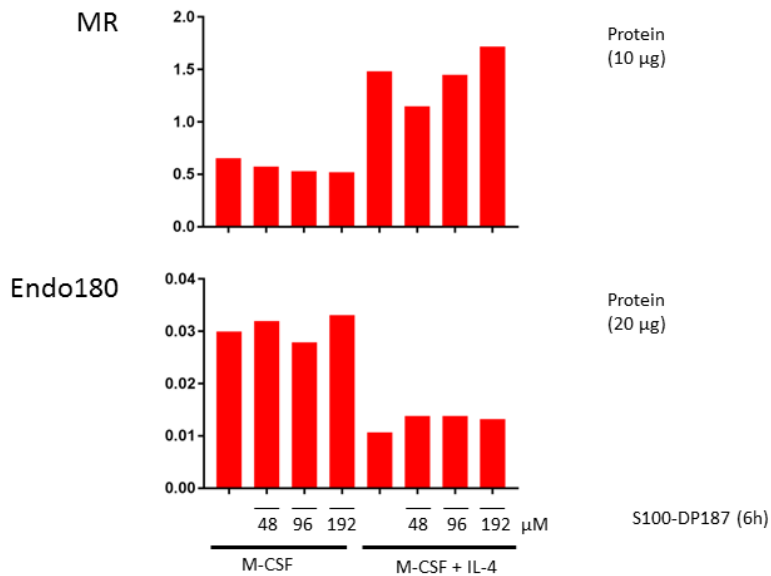
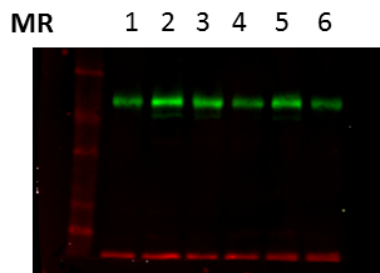


Figure 31. MR and Endo180 possess opposite regulation in the presence of IL-4. Panel A. Day 7 M-CSF and M-CSF + IL-4 treated macrophages incubated with S100-DP187 (48, 96 or 192 μ M) for 6 hours were lysed for MR, Endo180 and HSP60 detection through western blot. **Panel B.** Bands intensities were quantified using Licor and plotted as the ratio between MR/HSP60 and Endo180/HSP60. $n=1$. One membrane (10 μ g of proteins) was used for MR detection: purified mouse anti-human CD206 (MMR) antibody (dilution 1:1000) was used as primary antibody against MR and primary rabbit monoclonal antibody was used against HSP60 (dilution 1:10000), after one hour incubation with the primary antibodies, the secondary

antibodies IRDye 800CW Goat anti-Mouse (dilution 1:10000) and IRDye 680RD Goat anti-Rabbit (1:15000) were added and incubated for 1 hour. The other membrane (20 µg of proteins) was used for Endo180 detection: Anti-Endo180 antibody A5/158 [hybridoma] primary antibody (dilution 1:5) was used as primary antibody against Endo180 and primary rabbit monoclonal antibody was used against HSP60 (dilution 1:10000), after one hour incubation, the secondary antibodies IRDye 800CW Goat anti-Mouse (dilution 1:10000) and IRDye 680RD Goat anti-Rabbit (1:15000) were added and incubated for 1 hour.

4.6. MR and Endo180 expression in M2 and M1 macrophages

MR is considered a macrophage polarization indicator. Classically, M1 macrophages are known to have downregulated MR while M2 macrophages have upregulated MR. In a previous section, macrophages treated with IFN- γ showed that MR surface expression was not being downregulated. This contradicted the literature which shows IFN- γ to downregulate MR in mouse (Harris et al., 1992) and humans (Ambarus et al., 2012), although, the reduction in MR expression was only observed in human macrophages after 4 days of stimulation. To further explore this, day 5 monocyte-derived macrophages, incubated with M-CSF only, were transferred from low-attachment plates to a polystyrene plate and incubated with M-CSF (50 ng/ml) overnight at 37 °C. On day 6, the cells were stimulated with different cytokines (M-CSF: 50 ng/ml, IL-4: 25 ng/ml, IFN- γ : 20 ng/ml) and LPS (20 ng/ml) and incubated for 24 hours. On the following day, supernatant was removed and cells were lysed for western blot. Only cells treated with a combination of IFN- γ and LPS showed downregulation in MR expression (Figure 32). Surprisingly, IFN- γ (20 ng/ml) treatment alone did not cause downregulation in MR, not even at the higher dose of 100 ng/ml. MR regulation in human monocyte-derived macrophages activated by IFN- γ (20 ng/ml) for 24 hours resembles that of IL-4 (25 ng/ml), an anti-inflammatory cytokine, rather than that obtained by the combination of IFN- γ and LPS.



- 1 – M-CSF
- 2 – IL-4
- 3 – IFN- γ (20 ng/ml)
- 4 - IFN- γ + LPS (20 ng/ml)
- 5 - IFN- γ (100 ng/ml)
- 6 - IFN- γ + LPS (100 ng/ml)

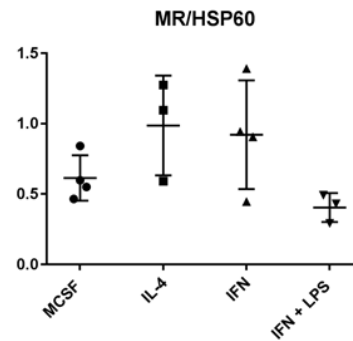


Figure 32. IFN- γ alone does not promote downregulation of MR in human monocyte-derived macrophages after 24 hours treatment. Day 6 macrophages treated with M-CSF (50 ng/ml), IL-4 (25 ng/ml), IFN- γ (20 ng/ml), IFN- γ (100 ng/ml), IFN- γ (20 ng/ml) + LPS (20 ng/ml), IFN- γ (100 ng/ml) + LPS (100 ng/ml) and incubated for 24 hours at 37 °C. On the bottom right, the ratios of MR/HSP60 band intensities were plotted for 4 different donors: (concentrations: IL-4 (25 ng/ml), IFN- γ (20 ng/ml), IFN- γ (20 ng/ml) + LPS (20 ng/ml)).

Endo180 expression on the other hand showed the same pattern of expression of MR when treated with IFN- γ and LPS or IFN- γ alone, being slightly downregulated in the presence of IFN- γ and LPS after 24 hours and being slightly upregulated by IFN- γ alone. Downregulation of Endo180 when cells were treated with IL-4 (25 ng/ml) for 24 hours only was also observed (Figure 33).

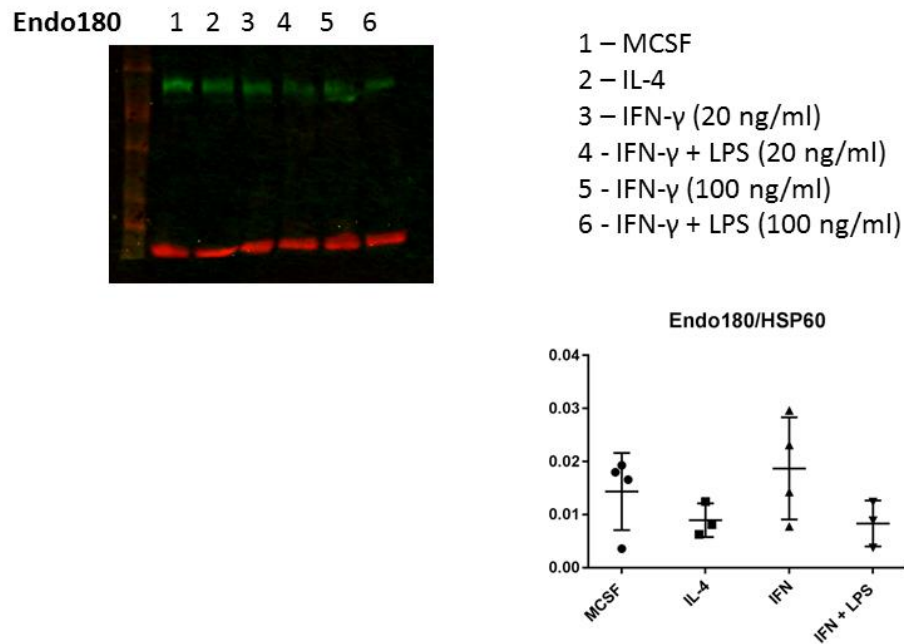


Figure 33. Endo180 is downregulated by IL-4 and IFN- γ + LPS. Day 6 macrophages treated with IL-4 (25 ng/ml), IFN- γ (20 ng/ml), IFN- γ (100 ng/ml), IFN- γ (20 ng/ml) + LPS (20 ng/ml), IFN- γ (100 ng/ml) + LPS (100 ng/ml) and incubated for 24 hours at 37 °C. On the bottom right, the ratios of Endo180/HSP60 band intensities were plotted for 4 different donors: (concentrations: IL-4 (25 ng/ml), IFN- γ (20 ng/ml), IFN- γ (20 ng/ml) + LPS (20 ng/ml)).

4.7. Discussion

MR is an important receptor in macrophages that is involved in collagen turnover (Martinez-Pomares et al., 2006b) and it was of interest to test if MR-modulators could affect this important process. The mechanism of collagen turnover consists of two mechanistically distinct collagen catabolic pathways: the first is an extracellular pathway, where membrane-bound and soluble proteases degrade collagen, and a second (endocytic) pathway, in which collagen is first internalized by cells and then degraded by lysosomal proteases (Madsen et al., 2007). This process is of particular interest during resolution of inflammation in which tissue remodelling occurs (Martinez-Pomares et al., 2006b) and also in malignant tumors, where extracellular matrix degradation allows for physical expansion and facilitates tumor growth (Hynes, 2009). Previous work (Madsen et al., 2013) showed that collagen introduced into the dermis of mice underwent cellular endocytosis which was predominately executed by a population of M2-like macrophages. Genetic ablation of MR and Endo180 in these mice impaired the intracellular collagen degradation pathway. MR also showed its contribution in collagen endocytosis by tumor associated macrophages (TAMs) associated with Lewis lung carcinoma (LLC) cells injected subcutaneously in mice (Madsen et al., 2017). Thus, finding a way to modulate macrophage collagen turnover could have its clinical application. The ability of S100-DP187 to modulate collagen uptake by human macrophages was investigated using different periods of time and under different concentrations. Gelatin uptake was increased by IL-4 and could only be efficiently inhibited by polymer S100-DP187 after 6-hour incubation. This led to the hypothesis that another receptor could possibly be mediating gelatin uptake in these cells. The presence of Endo180, another known collagen binding receptor, in monocyte-derived macrophage may explain the less efficient

gelatin inhibition by S100-DP187 in these cells compared to CHO-MR cells or mouse macrophages which do not possess Endo180. MR surface expression was affected by polymer S100-DP187 and it was also affected by time of incubation. Longer periods (24h) of polymer incubation led to a significant decrease in MR expression in IFN- γ -treated macrophages. The process also affected negatively other surface molecules in IFN- γ treated cells, such as HLA-DR, an MHC class II molecule involved in activation of T cells. Besides this, CD11b also had its expression affected in IFN- γ treated macrophages by S100-DP187. These results suggested that, maybe, these cells were not being properly activated by the cytokines and could have its metabolism affected by this polymer.

Kynurenine pathway is a major route for tryptophan metabolism in mammals (Mándi and Vécsei, 2012). In the first step of the process tryptophan is converted to kynurenine in a reaction catalysed by indoleamine 2,3-dioxygenase (IDO) and tryptophan 2,3-dioxygenase (TDO). Kynurenine is then metabolized into other catabolites through the action of enzymes within the kynurenine pathway (Stone and Darlington, 2002). Kynurenine is converted by kynurenine 3-hydroxylase to 3-hydroxykynurenine (3-HK) (Stone, 1993) which is further converted to quinolinic acid (QUIN), an agonist of the N-methyl-D-aspartate (NMDA) sensitive glutamate receptors (Stone and Perkins, 1981). Another arm of the kynurenine pathway leads to the production of kynurenic acid (KYNA), an antagonist of NMDA receptors (Swartz et al., 1990). IDO-mediated tryptophan catabolism appears to have a significant counter-regulatory role in damping down the activation of the immune system (Mándi and Vécsei, 2012), more particularly in the suppression of T cells (Mellor and Munn, 2004). Another hypothesis is that tryptophan metabolism modifies the properties of antigen presenting cells (APCs) (Grohmann et al., 2003). Kynurenine pathway can serve as a negative feedback loop for Th1 cells, but

may play a distinct role in up-regulating Th2 immune responses, one example is the induction of apoptosis of Th1 cells by tryptophan catabolites but the same effect is not observed in Th2 cells (Fallarino et al., 2002). IDO activation in dendritic cells (DCs) induces the generation of regulatory T cells (Puccetti and Grohmann, 2007), which may contribute to the negative feedback suppression of T cells responses. High levels of IDO will result in a decline of Th1 response, whilst an enhanced Th2 response is expected (Xu et al., 2008). IFN- γ (Chon et al., 1996) and LPS (Fujigaki et al., 2006) induce IDO gene transcription. This led to the investigation of tryptophan metabolism in macrophages which is known to have its conversion into its metabolites accelerated by IFN- γ (Moffett and Namboodiri, 2003). In dendritic cells, allergic responses are known to have the participation of MR and IDO (Royer et al., 2010). For these studies, the unlabelled polymer S100-DP240 was used to minimise interference with the assay. Macrophages incubated in the presence of S100-DP240 showed a decrease in kynurenine production and this happened independently of the type of culture plate they were seeded. This result complements the previous assay where cells treated with IFN- γ failed to upregulate HLA-DR in the presence of polymer S100-DP187, this reinforces the idea that these cells are not being properly activated by IFN- γ and may not function as expected. Cells used for the IDO activity assay also had its cells surface markers analysed. A decrease in HLA-DR surface marker was only detected at a higher polymer concentration (120 μ M), but the inhibitory effect in MR surface expression was not significant. The inhibition in MR expression in section 4.4 (Figure 29) was not as efficient as the one observed in section 4.3 (Figure 26), even though the incubation time was 24 hours in both cases. This could be due to differences between the two assays or between the polymers. First, in section 4.3, the polymer used was S100-DP187 at 48 μ M, whilst in section 4.4, polymer S100-DP240 was used instead at 40

μM . The second difference is that in section 4.4, cells that were used for flow cytometry were the same cells prepared for IDO assay, this means that these macrophages were incubated on day 6 not only with media and cytokines but also with 100 μM of L-Tryptophan diluted in HCl, for means of kynurenine production. This makes the comparison between the assays difficult and should not be treated as equivalent. With the decrease in MR surface expression it became necessary to confirm if the decrease also occurred at the total protein level.

Incubation with polymer S100-DP187 did not lead to a decrease in total MR expression, in contrast to MR surface expression. The explanation for this could be that MR is being internalized and trapped in an endosome and not being degraded in the lysosomes at a higher rate. MR degradation in the lysosomes was not quantified, but if MR degradation occurred at a high rate in the presence of S100-DP187, synthesis of MR would be expected at a similar rate to compensate its loss. An important fact observed is that MR and Endo180, very similar proteins structurally, are differentially regulated by IL-4. MR was upregulated while Endo180 was downregulated by this cytokine. Regarding the influence of IFN- γ , cell surface markers analysis showed that MR surface expression was high in cells incubated with IFN- γ alone. This contradicts the literature which says IFN- γ downregulates MR and that MR is a marker for macrophage polarization, where MR is upregulated in M2 macrophages and downregulated in M1 macrophages. This led to further investigation of protein expression under different circumstances.

High total MR expression was confirmed in macrophages treated with IFN- γ for 24 hours, in agreement with the cell surface labelling results. In mice it is accepted that MR is downregulated in cells treated with IFN- γ , so the differences found could be explained by inter-species variations. However, some papers claim that MR

activity is also downregulated in human macrophages under the influence of IFN- γ . By looking at the protocols of stimulation of these human macrophages by IFN- γ , one can find great diversity in procedures. In one case, macrophages were treated for 4 days under IFN- γ stimulation (Ambarus et al., 2012). Another one that analysed MR sugar uptake under stimulation by IFN- γ only noticed a reduction in sugar uptake after 48 hours of incubation with IFN- γ (Mokoena and Gordon, 1985).

Still one question remained: If both types of polymers, S100-DP187 and M100-DP187, bind to MR but only one of them is able to decrease MR surface expression and inhibit gelatin uptake, why only S100-DP187 has these special properties even when collagen binding to MR is independent of carbohydrates? Is the complex S100-DP187-MR being trapped inside the endosomes for longer?

Chapter 5 – MR co-localization

MR mediates clathrin-dependent endocytosis of its ligands into endosomal compartments. In these compartments, ligands dissociate from the receptor and MR recycles back to the cell membrane (Gazi and Martinez-Pomares, 2009). At any given time, most of MR molecules are inside the cell, with recycling turnover typically occurring in matter of minutes. Changes in acidity contribute to ligand-receptor dissociation in the endosome (Tietze et al., 1982). Previous tests in our lab showed that a change of pH from 7.5 to 6 did not affect binding of sulfated polymer to the CR domain of MR (Mastrotto et al., manuscript in preparation), suggesting that endosomal acidity does not affect dissociation of sulfated polymer-receptor complex in the endosome. It was shown previously that sulfated multivalent ligands S100-DP187 and S100-DP240 significantly decreased the cell surface amount of MR compared to untreated macrophages, whilst there was minimum MR degradation. These results reinforce the original hypothesis that blocking of MR-mediated endocytosis was due to trapping of the receptor into stable ligand-receptor complexes from which the latter could no longer dissociate. In MR⁺CHO cells, confocal microscopy showed that these complexes were not localized at the cell membrane but rather spatially confined within recycling endosomal compartments. To investigate if polymer-receptor complexes were found in endosomal compartments of human macrophages treated with polymer S100-DP240, it was necessary to examine if in these cells MR was indeed internalized to endosomes where it would co-localize with the endosomal marker EEA1 (Early endosome antigen 1) and how this co-localisation was affected by treatment with the S100-DP240 polymer. The increased co-localization between MR and EEA1 in the S100-DP240 treated cells would corroborate the hypothesis of

polymer trapping in the endosome of human cells. Receptor degradation in the lysosomes would be detected by co-localization between MR and the Lysosomal-associated membrane protein 1 (LAMP1). Thus, the goals for the chapters are:

- I. To detect MR, EEA1 and LAMP1 in monocyte-derived macrophages.
- II. To investigate differences in co-localization of MR and EEA1 in human macrophages in the presence and absence of S100-DP240 polymers.

In parallel attempts were made to study the localisation of Endo180 in relation to MR in human macrophages

5.1. Detection of MR and Endo180 by Immunofluorescence

The first step in the optimization of the immunolabeling procedure was to detect MR and Endo180 by immunofluorescence (IF) microscopy in preparations of human macrophages. Before harvesting the cells from the low-attachment plates, glass coverslips (12 mm) were treated with 1 M HCl for 1 hour to increase cell adherence. Coverslips were then washed several times with media with phenol red, until the media did not change colour. The coverslips were then washed twice with sterile distilled water and left to dry. Coverslips were then sterilized for 15 min under UV light and transferred to the bottom of a new 24-well plate. On day 6, cells were harvested from the low-attachment plates by placing them on ice for 20 min and then transferring the content to 15 ml tubes. Cells were centrifuged at 350 x g, 4 °C, for 5 min. Supernatant was poured off and the pellet was resuspended in 5 ml of X-Vivo 15 for each tube and centrifuged at 350 x g, 4 °C, for 5 min. Supernatant was poured off and cells were resuspended in 1 ml X-Vivo 15 and counted. A total of 250,000 cells were placed on each well in the presence of 350 µl media with no phenol red and containing cytokines. Two populations of macrophages were tested, macrophages generated in the presence of M-CSF (50 ng/ml, M0) and macrophages generated in the presence of M-CSF and IL-4 (50 ng/ml and 25 ng/ml, respectively, M2). Cells were left overnight to attach to the coverslips at 37 °C. The media was then removed and wells were washed twice with 500 µl of PBS (with CaCl₂ and MgCl₂). The cells were then fixed by adding 250 µl of 4% paraformaldehyde in PBS for 20 min while on ice. Wells were rinsed with 500 µl of PBS (with CaCl₂ and MgCl₂), followed by two 5 min washes with 500 µl of PBS (with CaCl₂ and MgCl₂) at RT. This is the standard washing

step for the immunofluorescence assay. Cells were permeabilized with 250 μ l of 0.2 % Tween-20 in PBS for 30 min. Tween-20 solution was removed from the wells and washed according to the standard washing step. To block nonspecific binding of antibodies, the cells were incubated for 1 h with 250 μ l of blocking buffer (5% filtered donkey serum in PBS) at RT. The blocking buffer was removed and 200 μ l of primary antibodies were added to respective wells. Purified anti-human Anti-Endo180 antibody (Mouse) (hybridoma dilution 1:5), Anti-MR antibody (Rabbit) (1 μ g/ml), all diluted in blocking buffer. Samples were incubated at RT for 1 hour. Wells were washed according to the standard washing step and then incubated with 250 μ l of secondary antibodies – Anti-mouse Alexa Fluor 488 and Anti-rabbit Alexa Fluor 647 (10 μ g/ml) diluted in blocking buffer for 1 hour. Wells were washed again according to standard washing step. To stain the nucleus 250 μ l of DAPI were added per well at 1 μ g/ml in PBS for 5 minutes at RT. Wells were washed according to standard washing step. The coverslips were then removed from the wells and left to dry for a few seconds and then placed on glass slides with 3 μ l of Vectashield mounting medium. Coverslips were then sealed with nail polish and left overnight to dry. Slides were then analysed and scanned by confocal Zeiss LSM 880C on the following day. Conditions in the microscope (lens 60x oil microscope, Speed: 7, Averaging: 2, Bit depth: 16-bit, pinhole: 1AU, laser power, channel gain) were set up by technical assistance and maintained for all the pictures. The images were processed using Volocity software from an average of 25 scanned Z-stack sections of the cells, the channels were split and a montage was made with the different channels (DAPI, green channel, red channel).

In this initial trial it was possible to detect Endo180 expression in human macrophages through IF. Endo180 distribution in the cell changed according to the type of macrophage, whilst M-CSF treated macrophages displayed a more dispersed distribution of Endo180,

the protein was found more concentrated around the nucleus in IL-4 treated cells. The change in distribution is possibly due to differences in the shape of the cells. On the other hand, MR was not detected in this initial trial (Figure 34).

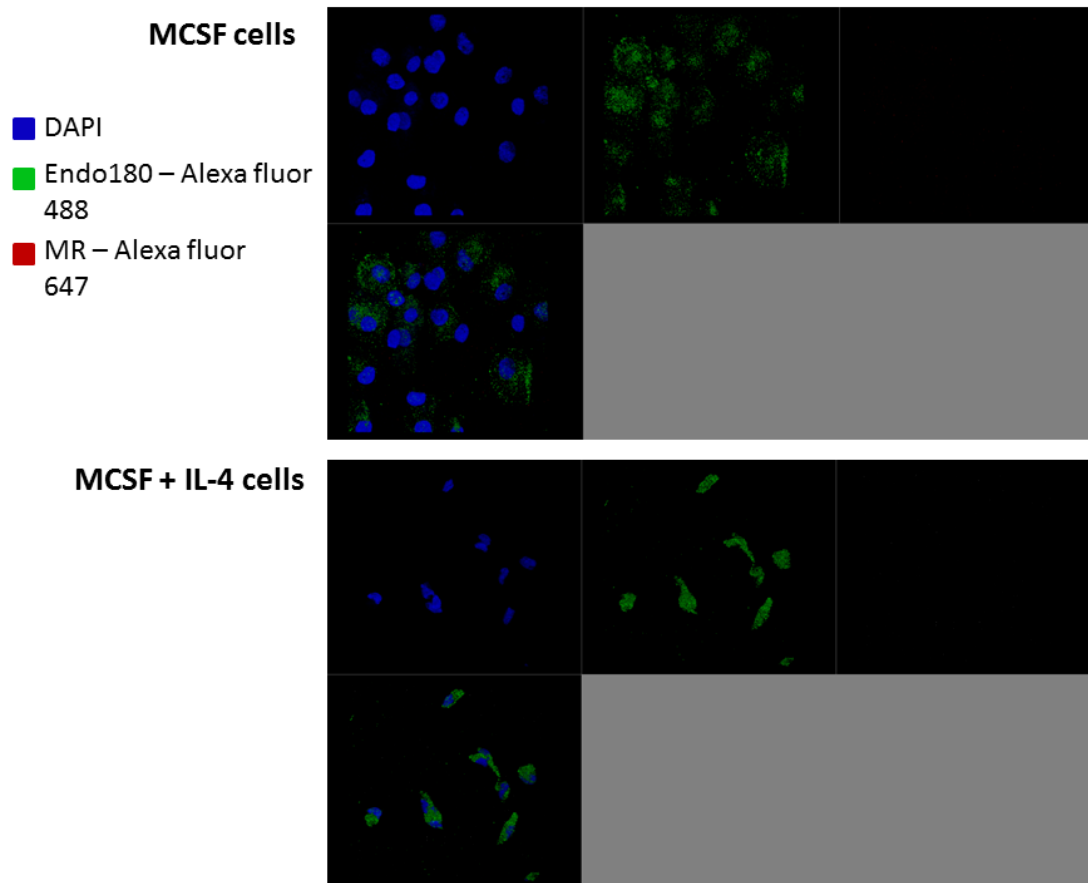


Figure 34. Detection of Endo180 and MR in human macrophages by immunofluorescence. Coverslips were prepared with M-CSF and M-CSF+IL-4-treated macrophages. Cells were fixed with 4% paraformaldehyde for 20 minutes and permeabilized with 0.2 % Tween-20 in PBS for 30 min. To avoid binding to nonspecific antigens, macrophages were incubated for 1 h with 5% filtered donkey serum in PBS at RT. For Endo180 detection, an anti-Endo180 antibody (Mouse) (hybridoma dilution 1:5) was used, whilst an anti-MR antibody (Rabbit) (1 $\mu\text{g}/\text{ml}$) was used for MR detection, all diluted in blocking buffer containing 5% donkey serum and incubated for 1 h. For detection secondary antibodies, anti-mouse Alexa Fluor 488 and Anti-rabbit Alexa Fluor 647 (10 $\mu\text{g}/\text{ml}$) diluted in blocking buffer were added at RT for 1 hour. To stain the nucleus 250 μl of DAPI were added per well at 1 $\mu\text{g}/\text{ml}$ in PBS for 5 minutes at RT. Vectashield mounting medium was placed in the centre of the coverslips and then sealed with nail polish and left overnight to set. Upper image represents M-CSF only treated macrophages, whilst bottom image represents M-CSF + IL-4 treated macrophages. Slides were analysed by Zeiss LSM 880C microscope.

5.2. Antibody optimization for IF

Due to the inability to detect MR, IF protocol went through modifications in order to improve fluorescence brightness whilst at the same time minimizing nonspecific binding. To achieve this control coverslips were prepared. M-CSF treated macrophages on coverslips were incubated with one primary antibody followed by incubation with the two secondary antibodies or coverslips were incubated only with the secondary antibodies as follows:

I – Anti-MR antibody (rabbit) (1 $\mu\text{g/ml}$) + secondary Anti-mouse Alexa Fluor 488 (14 $\mu\text{g/ml}$) and Anti-rabbit Alexa Fluor 647 (15 $\mu\text{g/ml}$) antibodies.

II - Anti-Endo180 antibody from hybridoma (mouse) (dilution 1:5) + secondary Anti-mouse Alexa Fluor 488 (14 $\mu\text{g/ml}$) and Anti-rabbit Alexa Fluor 647 (15 $\mu\text{g/ml}$) antibodies.

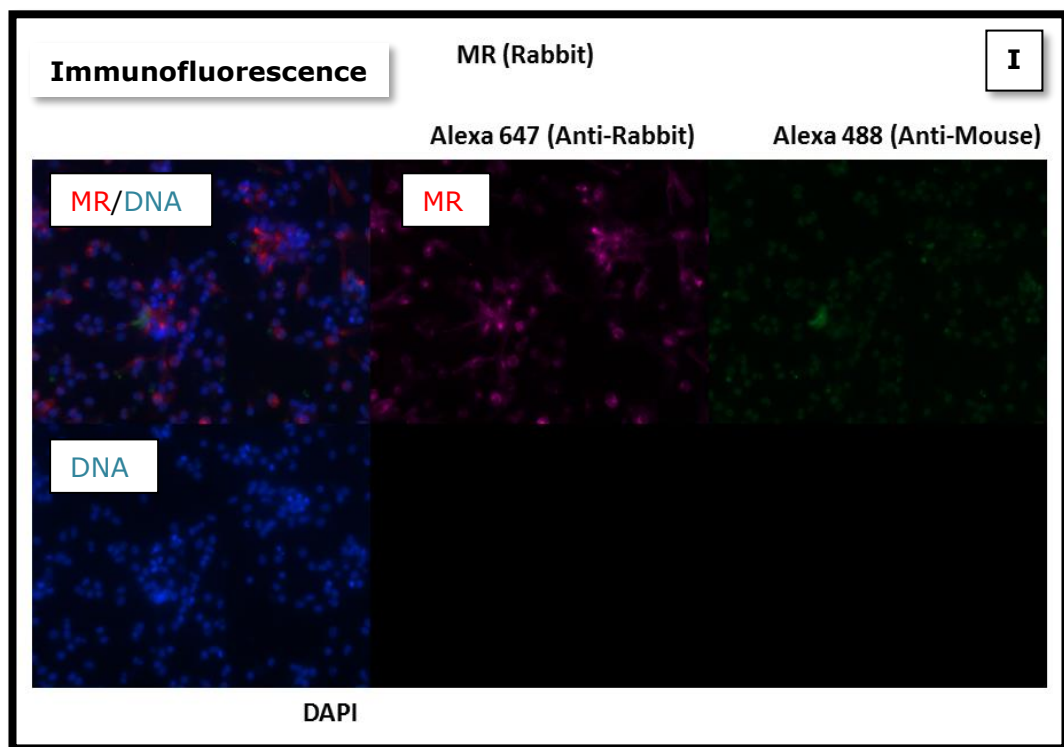
III – Secondary anti-rabbit Alexa Fluor 647 (15 $\mu\text{g/ml}$) antibody.

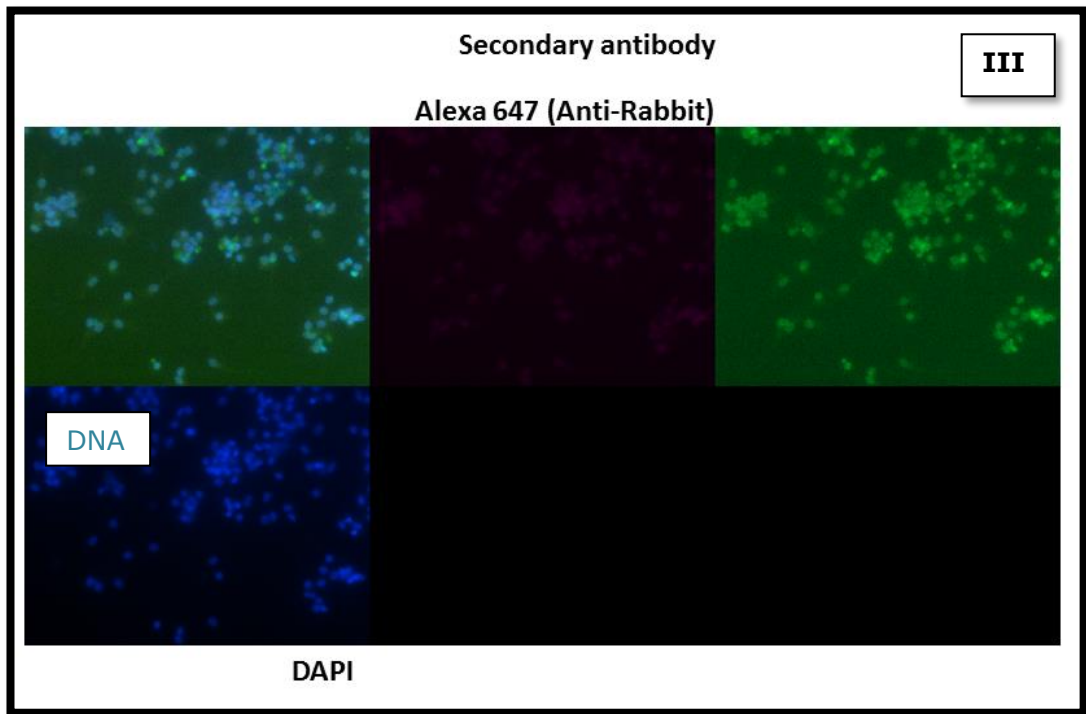
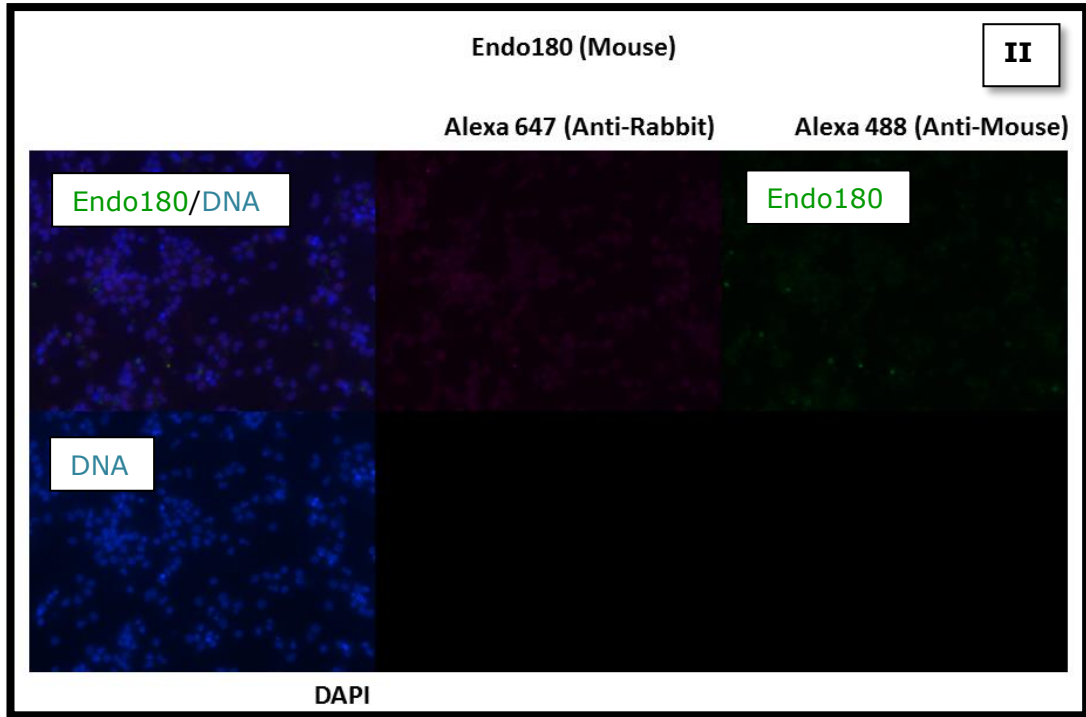
IV – Secondary anti-mouse Alexa Fluor 488 (14 $\mu\text{g/ml}$) antibody.

Incubation time for the primary antibody incubation was increased to 90 min, secondary antibody concentration was also increased and mounting media was changed from Vectashield to Ibidi mounting media. MR labelled with Alexa fluor 647 was detected in human macrophages (Figure 35, panel I) however, nonspecific fluorescence from the green (Alexa fluor 488) channel was also observed (Figure 35, panel I). Endo180 detection (Figure, panel II) was not much stronger than the control slide incubated with secondary antibody Alexa fluor 488 alone (Figure 35, panel IV), indicating staining did not work properly. Fluorescence from the slide incubated with secondary antibody Alexa fluor 647 alone showed an apparent weak signal (Figure 35, panel III) but it could be because the image looks

overexposed. Slide incubated with secondary antibody Alexa Fluor 488 only also looked overexposed. Coverslips were analysed and images were captured by Zeiss 200 M microscope with the help of technical assistance, which kept the same conditions when analysing similar fluorescence staining. The channels from the images were split on Fiji software and a montage was made with the different channels (DAPI, green channel, red channel).

This step showed that cell's fluorescence was not properly adjusted and further optimization in the protocol was performed.





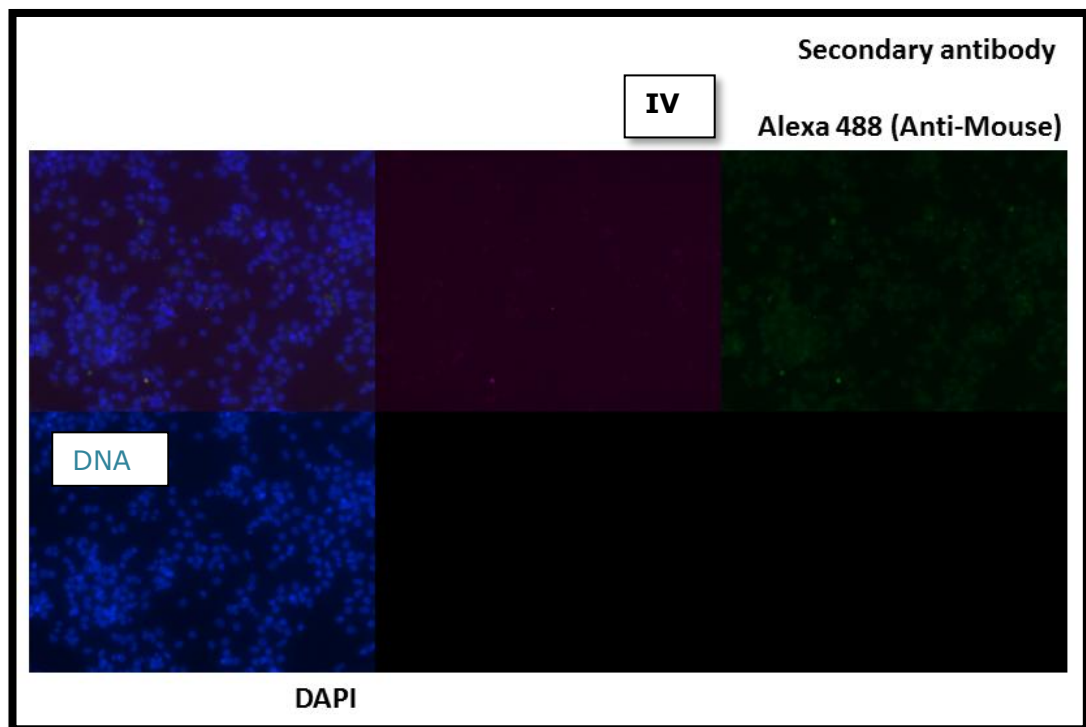


Figure 35. Detection of Endo180 and MR in human macrophages by immunofluorescence. Coverslips were prepared with M-CSF macrophages. Cells were fixed with 4% paraformaldehyde for 20 min and permeabilized with 0.2 % Tween-20 in PBS for 30 min. To avoid binding to nonspecific antigens, macrophages were incubated for 1 hour with 5% filtered donkey serum in PBS at RT. For Endo180 detection, an anti-Endo180 antibody (Mouse) (hybridoma dilution 1:5) was used, whilst an anti-Mannose receptor antibody (Rabbit) (1 $\mu\text{g}/\text{ml}$) was used for MR detection, all diluted in blocking buffer and incubated for 90 min. For detection secondary antibodies, anti-mouse Alexa Fluor 488 (14 $\mu\text{g}/\text{ml}$) and Anti-rabbit Alexa Fluor 647 (15 $\mu\text{g}/\text{ml}$) diluted in blocking buffer were added at RT for 1 h. To stain the nucleus 250 μl of DAPI were added per well at 1 $\mu\text{g}/\text{ml}$ in PBS for 5 minutes at RT. Ibidi mounting medium was placed in the centre of the coverslips and then sealed with nail polish and left overnight to set. Slides were analysed using a Zeiss 200 M microscope. Slides treated with: Panel I. Anti-MR antibody (rabbit) + secondary anti-mouse Alexa Fluor 488 and anti-rabbit Alexa Fluor 647 antibodies. Panel II. Anti-Endo180 antibody from hybridoma (mouse) + secondary Anti-mouse Alexa Fluor 48 and Anti-rabbit Alexa Fluor 647 antibodies. Panel III. Secondary anti-rabbit Alexa Fluor 647 antibody. Panel IV. Secondary anti-mouse Alexa Fluor 488 antibody.

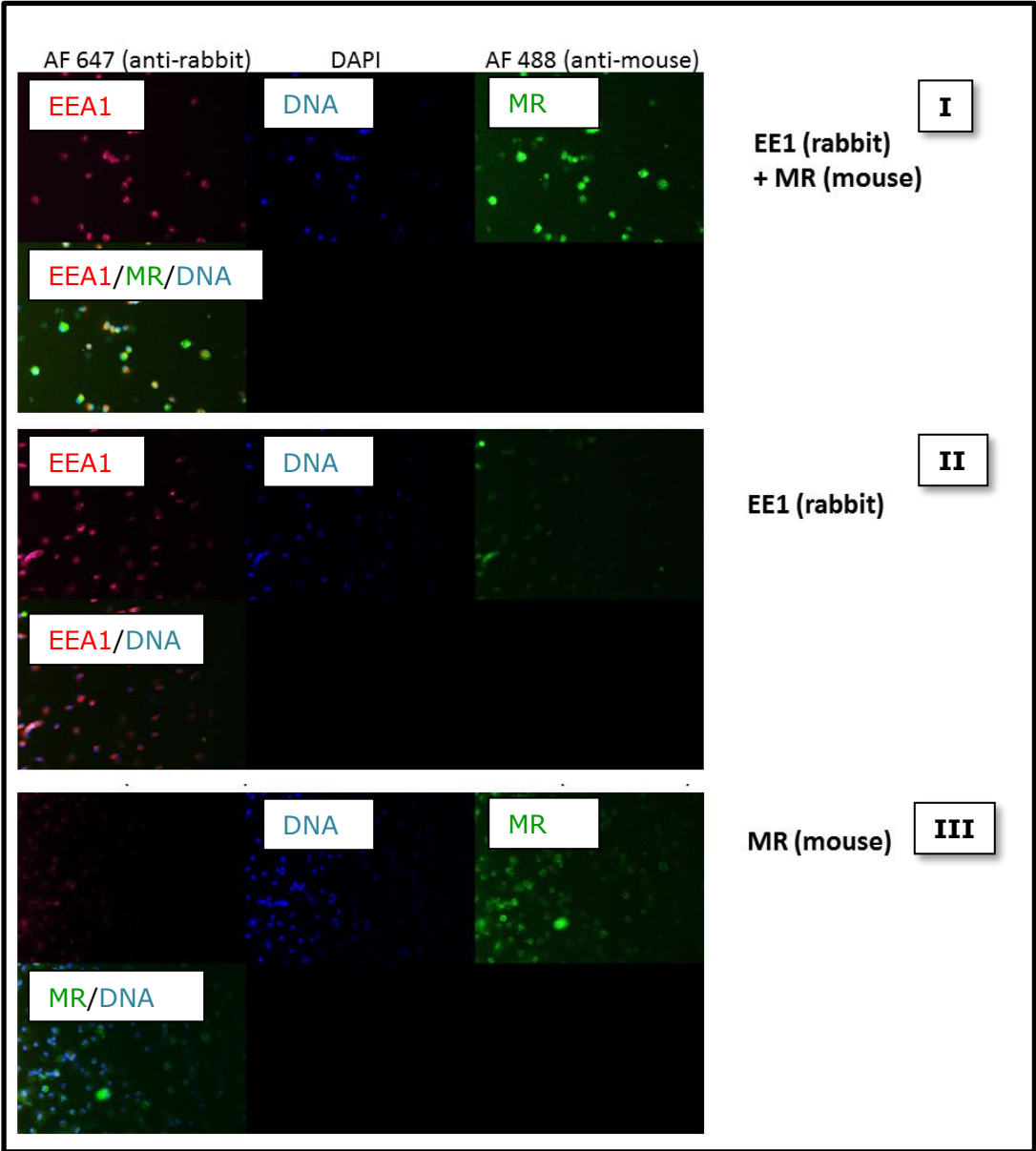
In a second step of optimization two new antibody were added to the process: anti-EEA1 and mouse anti-MR. In this step the goal was to optimize the detection of the new marker whilst improving fluorescence from the previous markers in M-CSF-treated macrophages. The reason of choosing fluorescence microscope at this stage was cost effectiveness compared to confocal microscope. The method of cell permeabilization changed to (0.15%) Triton-X100, which has been used in the laboratory in the past, for 30 min. Primary antibody incubation increased to 2 h. Secondary antibody concentration was slightly reduced. Hence, the following combinations of labellings below were performed:

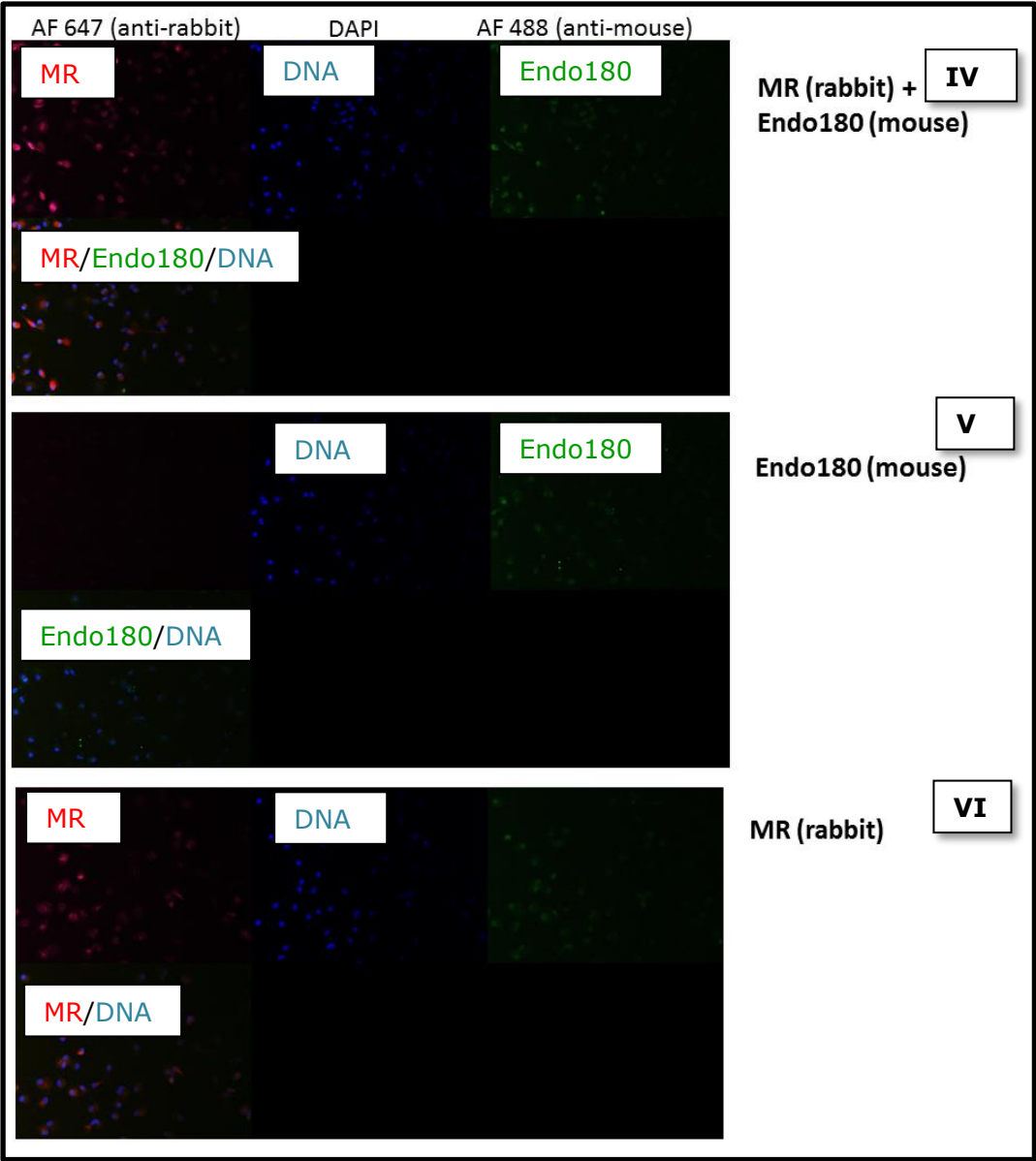
- I. Anti-MR antibody (mouse, 10 µg/ml) + anti-EEA1 (rabbit, 1:100 dilution) + secondary anti-mouse Alexa Fluor 488 (10 µg/ml) and Anti-rabbit Alexa Fluor 647 (10 µg/ml) antibodies.
- II. Anti-EEA1 antibody (rabbit, 1 µg/ml) + secondary Anti-mouse Alexa Fluor 488 (10 µg/ml) and Anti-rabbit Alexa Fluor 647 (10 µg/ml) antibodies.
- III. Anti-MR antibody (mouse, 10 µg/ml) + secondary Alexa Fluor 488 (10 µg/ml) and Anti-rabbit Alexa Fluor 647 (10 µg/ml) antibodies.
- IV. Anti-MR antibody (rabbit, 1 µg/ml) + anti-Endo180 (mouse, 1:2 dilution) antibody + secondary Anti-mouse Alexa Fluor 488 (10 µg/ml) and Anti-rabbit Alexa Fluor 647 (10 µg/ml) antibodies.
- V. Anti-Endo180 (mouse, 1:2 dilution of hybridoma supernatant) antibody + secondary Anti-mouse Alexa Fluor 488 (10 µg/ml) and Anti-rabbit Alexa Fluor 647 (10 µg/ml) antibodies.
- VI. Anti-MR antibody (rabbit, 1 µg/ml) + secondary Anti-mouse Alexa Fluor 488 (10 µg/ml) and Anti-rabbit Alexa Fluor 647 (10 µg/ml) antibodies.

VII. Secondary Anti-mouse Alexa Fluor 488 (AF 488, 10 µg/ml).

VIII. Secondary Anti-rabbit Alexa Fluor 647 (AF 647, 10 µg/ml).

MR, Endo180, EEA1 were detected and showed higher fluorescence than the negative controls. EEA1 + MR (Figure 36, panel I) double labelling coverslips showed higher fluorescence than single labelling slides for MR (mouse), EEA1. Coverslips were analysed using a Zeiss Exciter widefield fluorescence microscope.





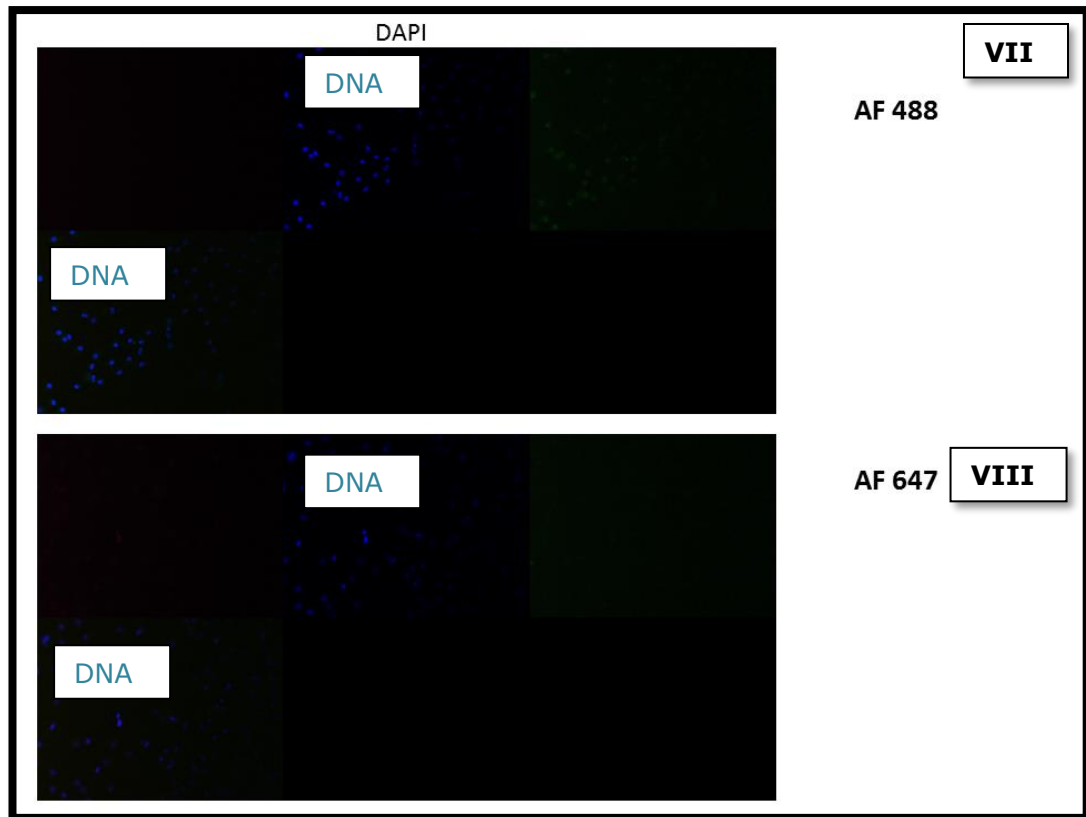


Figure 36. Optimization process for MR, Endo180 and EEA1 detection by immunofluorescence. Coverslips were prepared with M-CSF macrophages. Cells were fixed with 4% paraformaldehyde for 20 min and permeabilized with 0.15% Triton-X100 in PBS for 30 min. To avoid binding to nonspecific antigens, macrophages were incubated for 1 h with 5% filtered donkey serum in PBS at RT. For Endo180 detection, an anti-Endo180 antibody (Mouse, hybridoma dilution 1:2) was used, whilst two anti-MR antibody (Rabbit, 1 μ g/ml) and anti-MR antibody (mouse, 10 μ g/ml) was used for MR detection. For EEA1, anti-EEA1 (rabbit, 1:100 dilution) was used. All antibodies were diluted in blocking buffer containing 5% donkey serum and incubated for 2 h. For secondary antibodies, anti-mouse Alexa Fluor 488 (10 μ g/ml) and Anti-rabbit Alexa Fluor 647 (10 μ g/ml) diluted in blocking buffer were added at RT for 1 h. To stain the nucleus 250 μ l of DAPI were added per well at 1 μ g/ml in PBS for 5 minutes at RT. Ibbidi mounting medium was placed in the centre of the coverslips and then sealed with nail polish and left overnight to set. Slides were analysed by Zeiss Exciter widefield fluorescence microscope. Slides were incubated with the following conditions: **Panel I.** Anti-MR antibody (mouse) + anti-EEA1 (rabbit) + secondary anti-mouse Alexa Fluor 488 and Anti-rabbit Alexa Fluor 647 antibodies. **Panel II.** Anti-EEA1 antibody (rabbit) + secondary anti-mouse Alexa Fluor 488 and anti-rabbit Alexa Fluor 647 antibodies. **Panel III.** Anti-MR antibody (mouse) + secondary anti-mouse Alexa Fluor 488 and anti-rabbit Alexa Fluor 647 antibodies. **Panel IV.** Anti-MR antibody (rabbit) + anti-Endo180 (mouse) antibody + secondary anti-mouse Alexa Fluor 488 and anti-rabbit Alexa Fluor 647 antibodies. **Panel V.** Anti-Endo180 (mouse) antibody + secondary anti-mouse Alexa Fluor 488 and anti-rabbit Alexa Fluor 647 antibodies. **Panel VI.** Anti-MR antibody (rabbit) + secondary anti-mouse Alexa Fluor 488 and anti-rabbit Alexa Fluor 647

antibodies. **Panel VII.** Secondary anti-mouse Alexa Fluor 488. **Panel VIII.** Secondary anti-rabbit Alexa Fluor 647.

Data showed specific labelling for MR (both using the mouse and rabbit antibodies) and EE1. No specific labelling for Endo180 could be observed.

5.2. MR colocalization to EEA1 and LAMP1

Although MR and EE1 were detected by fluorescent microscopy previously, there was a need to improve brightness, thus, primary antibody incubation was increased to overnight incubation at 4 °C. Secondary antibody incubation was maintained at the same amount of time, but concentration was slightly decreased in order to further reduce nonspecific fluorescence.

For co-localization analysis, several coefficients are used to determine how much one single marker colocalizes with a second marker. Co-localization can be observed with the help of confocal microscopes. When two or more antigens are detected immunohistochemically in the same location within a section, they are said to be colocalized. Co-localization is established when correspondent antibodies with different excitation spectra when staining of antigens visualized in different colours overlap (Zinchuk et al., 2007). Colocalization refers to the existence of the signal at the same pixel location when examining multi-channel fluorescence microscopy images (Zinchuk et al., 2007). It is presented by three images consisting of fluorescence for red and green channels, as well as a third merged image where the channels are combined and overlapping pixels turn yellow when they have the same intensity. It is crucial that the analysis includes exclusively antigens of interest and excludes any nonspecific events generated by background and noise. The analysis is performed by computer software such as Fiji. The software estimates the degree of colocalization according to specialized algorithms within the selected region of interest (ROI). The analysis is based on evaluation of colour components of the selected pair of channels. Pearson correlation coefficient (PCC) is used to describe the correlation of the intensity distributions between channels and it takes into account the similarities between

signal shapes (Figure 37). The coefficient values range between -1 and 1, when the value is 0 it indicates no significant correlation, whilst 1 indicates perfect correlation and -1 indicates complete negative correlation.

$$\text{PCC} = \frac{\sum_i (R_i - \bar{R}) \times (G_i - \bar{G})}{\sqrt{\sum_i (R_i - \bar{R})^2 \times \sum_i (G_i - \bar{G})^2}}$$

Figure 37. Pearson's correlation coefficient formula. R_i and G_i refer to the intensity values of the red and green channels, respectively, of pixel i , \bar{R} and \bar{G} refer to the mean intensities of the red and green channels, respectively, across the entire image. (Dunn et al., 2011).

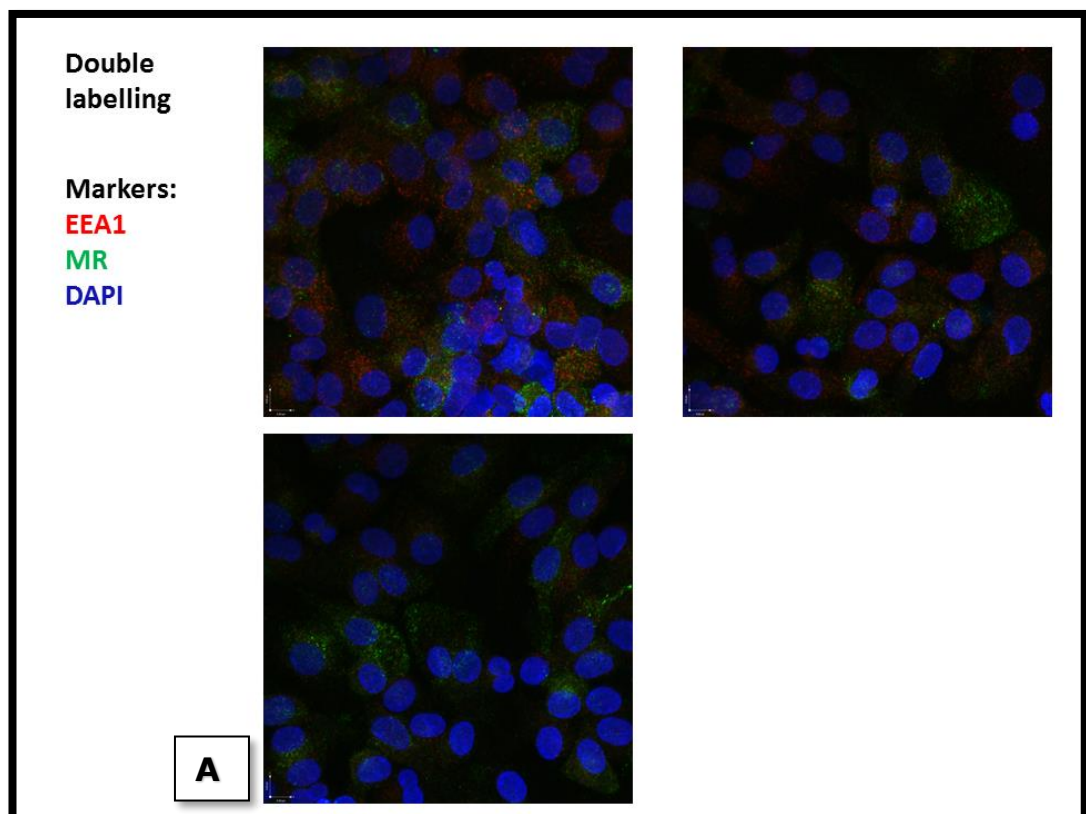
It is expected that signal in each image needs to be sufficient to distinguish from noise and background, uncontaminated by autofluorescence and free of signal bleed-through between the two images (Dunn et al., 2011).

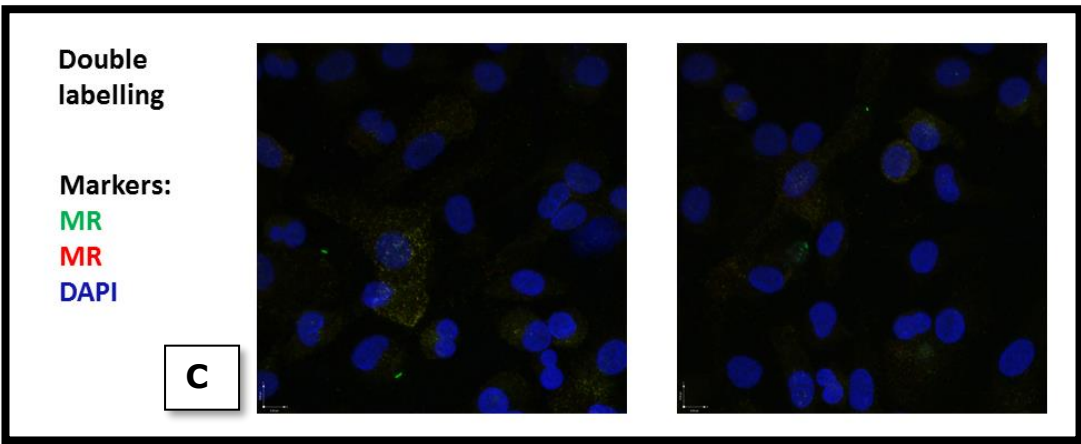
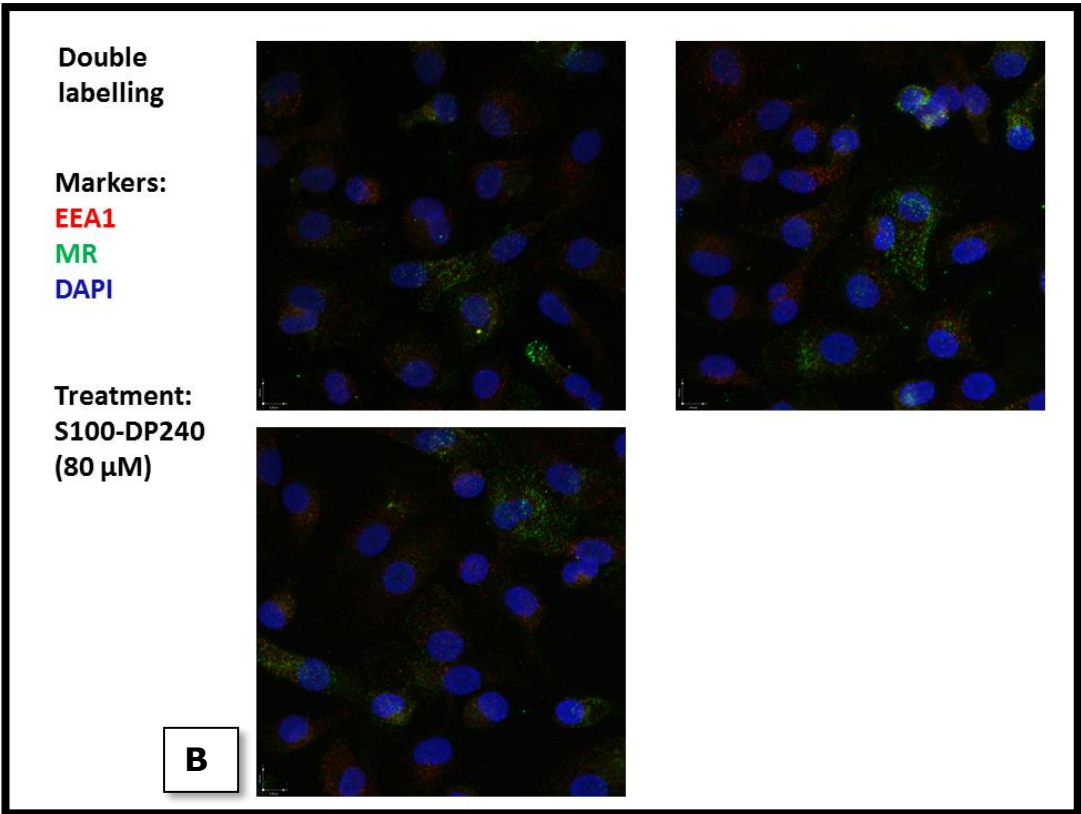
Co-localization can be thought of as consisting of two components: co-occurrence, the simple spatial overlap of two probes, and correlation, in which two probes not only overlap with one another but co-distribute in proportion to one another within and between structures (Dunn et al., 2011). Co-localization may be visually apparent only under very specific labelling conditions, when the fluorescence of the two probes occurs in a fixed and nearly equal proportion. In general, the most reliable method for visually comparing the relative distribution of two probes is a side-by-side comparison of the two images.

As mentioned above the same set of conditions discussed in the last section was repeated in this section, with the difference that the secondary antibodies were reduced to 8 $\mu\text{g/ml}$ and the primary antibody incubation was increased to overnight (4 $^{\circ}\text{C}$). In order to compare the effect of polymer S100-DP240 in colocalization of MR and EEA1, macrophages were incubated with S100-DP240 polymer (80 μM) for 4 hours at 37 $^{\circ}\text{C}$. A new control coverslip including MR

(rabbit) vs MR (mouse) was prepared in order to verify the degree of co-localization of the two antibodies.

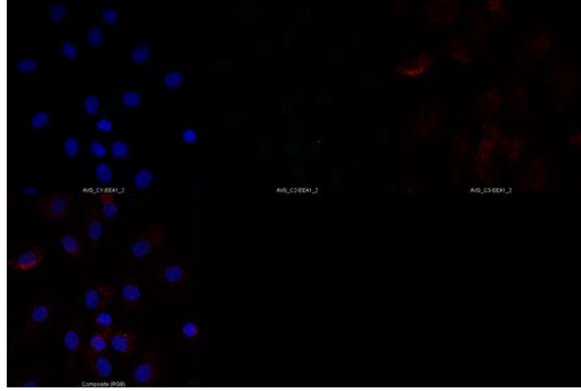
Overall the pictures looked suitable for colocalization analysis. Single labelling coverslips of EEA1, MR (mouse) and MR (rabbit) antibodies showed minimum amount of nonspecific fluorescence and coverslips incubated with secondary antibodies only showed low fluorescence (Figure 38, Panel F), as expected. For each condition, images below represent different fields from the same slide.



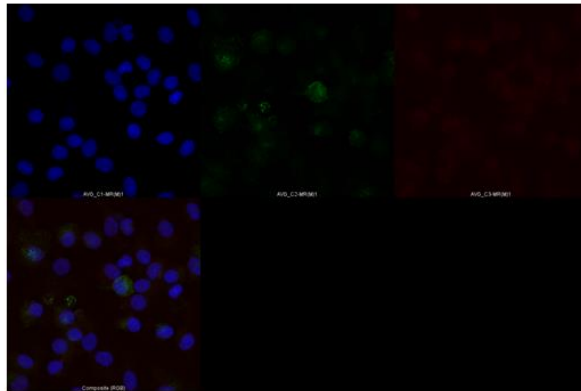


Single labelling

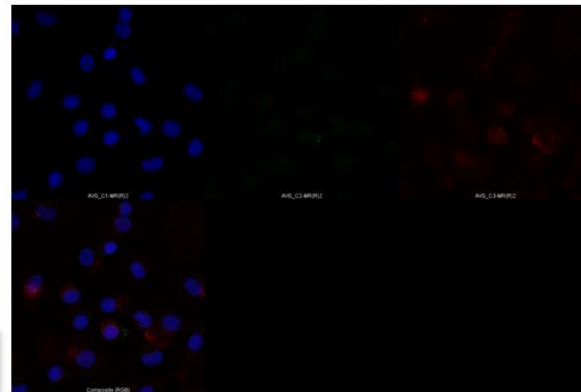
EEA1



MR



MR



D

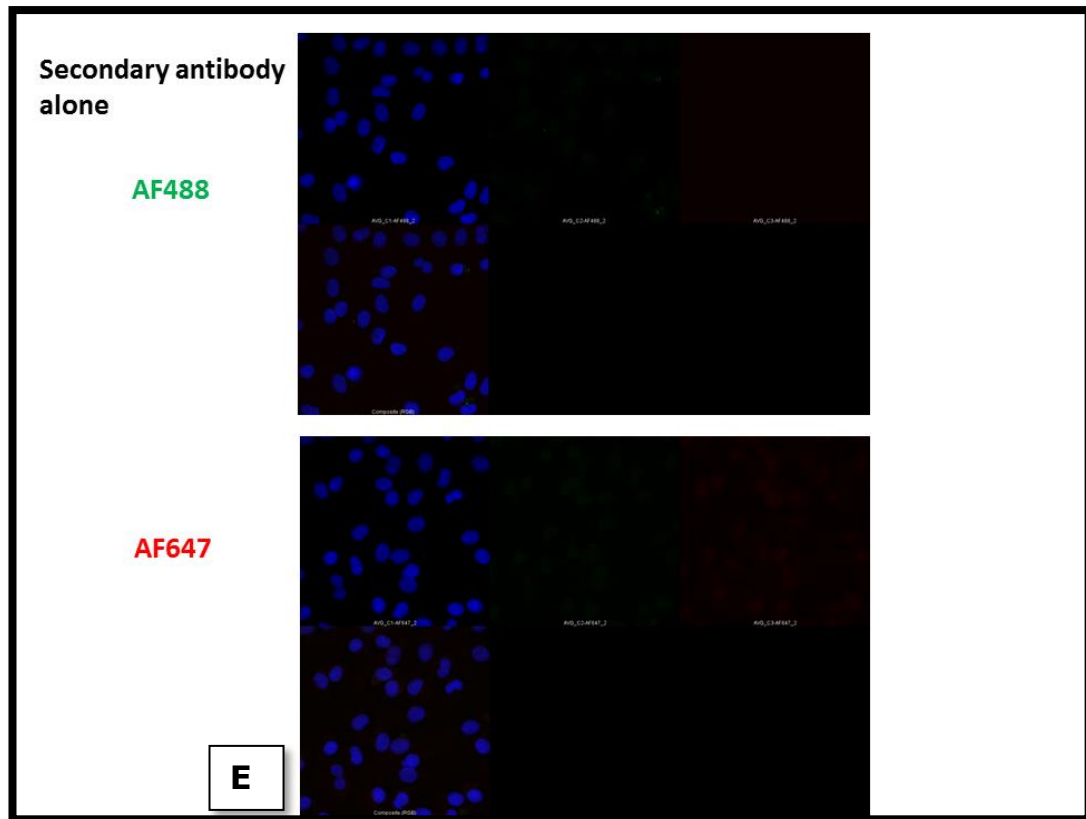


Figure 38. Colocalization of MR vs EEA1 and MR vs MR by confocal microscopy. Coverslips were prepared with M-CSF macrophages. One set of samples was treated with 80 μ M of S100-DP240 for 4 h at 37 $^{\circ}$ C. Cells were fixed with 4% paraformaldehyde for 20 min and permeabilized with 0.15% Triton-X 100 in PBS for 30 min. To avoid binding to nonspecific antigens, macrophages were incubated for 1 h with 5% filtered donkey serum in PBS at RT. For Endo180 detection, an anti-Endo180 antibody (Mouse, hybridoma dilution 1:5) was used, whilst an anti-MR antibody (Rabbit, 1 μ g/ml) and anti-MR antibody (mouse, 10 μ g/ml) was used for MR detection. For EEA1, anti-EEA1 (rabbit, 1:50 dilution), was used respectively, all diluted in blocking buffer containing 5% donkey serum and incubated overnight at 4 $^{\circ}$ C. For secondary antibodies, anti-mouse Alexa Fluor 488 (8 μ g/ml) and Anti-rabbit Alexa Fluor 647 (8 μ g/ml) diluted in blocking buffer were added at RT for 1 h. To stain the nucleus 250 μ l of DAPI were added per well at 1 μ g/ml in PBS for 5 minutes at RT. Ibbidi mounting medium was placed in the centre of the coverslips and then sealed with nail polish and left overnight to dry. Slides were visualised using a Zeiss LSM 880C confocal microscope. Panel A. Double labelled slide for MR (mouse) and EEA1 (rabbit) plus two secondary antibodies (AF488, AF647). Panel B. Cells treated with 80 μ M of S100-DP240 for 4 hours and double labelled with MR (mouse) and EEA1 (rabbit) plus two secondary antibodies (AF488, AF647) and. Panel C. Double labelled slide with MR (rabbit) and MR (mouse) plus two secondary antibodies (AF488, AF647). Panel D. Single labelling of primary antibodies MR (mouse), EEA1 (mouse), MR (rabbit) plus secondary antibodies AF488 and AF647. Panel E. Cells incubated with one secondary antibody.

5.2.2. Analysis of colocalization of MR vs EEA1 and MR vs MR

Confocal images were opened in Fiji software, converted to a Z projection and the background was subtracted from the images. The three channels (DAPI, green and red) were split from the original file and a region of interest (ROI) was selected around the cell before running the analysis tool coloc 2, which compares the degree of colocalization between the green and red channel. For all the examples tested, the results from the software analysis showed a warning message that the automatic threshold calculated by the software was higher than the channel's mean, this way affecting coefficients like Mander's and in a minor proportion the Pearson correlation coefficient (PCC), thus Mander's coefficient was discarded. For the examples of MR vs EEA1 colocalization analysis, PCC from four selected cells of the same donor (n=1) showed (Figures 41, 42, 43, 44) values of 0.15, 0.10, 0.12, 0.24, in a scale of 0 (no significant correlation) and 1 (perfect correlation) between the two markers, indicating a low correlation between the channels. Observation of the image using a 3D Volocity software tool showed the presence of MR and, to a lesser degree EEA1, in the nucleus (Figure 39). The presence is confirmed when each layer of the confocal image is analysed (Figure 40) individually and was also observed in other cells. This affected the manner in which line intensity profile areas were chosen, in other words, the nucleus was avoided when drawing the line for intensity profiles. The profiles in these examples reinforce the low correlation found between these two markers. For the examples of MR vs EEA1 colocalization in macrophages treated with 80 μ M of S100-DP240, PCC from four selected cells of the same donor (n=1) showed (Figures 45, 46, 47, 48) values of 0.18, 0.10, 0.14, 0.05, indicating again a low correlation between channels. Line intensity profiles reinforce the low correlation between markers. In

both treatments, some pockets of correlation are observed in the line intensity profiles, however, one cannot infer significant differences between the two types of treatment.

In the positive control example of MR-mouse (AF488) vs MR-rabbit (AF647), the resulting PCC was of 0.51 (Figure 50) and 0.56 (Figure 51), a moderate coefficient for two antibodies that should be targeting the same receptor. However, the line intensity profile showed a higher correlation between the two lines and the analysis of the two channels side by side showed that the two images are very similar. In these cells, the line was drawn over the nucleus region but did not affect the correlation between the lines. The yellowish aspect of overlapped channels indicates a good degree of colocalization. MR (green) and MR (red) was also observed in the nucleus (Figures 50 and 51), confirming previous observation.

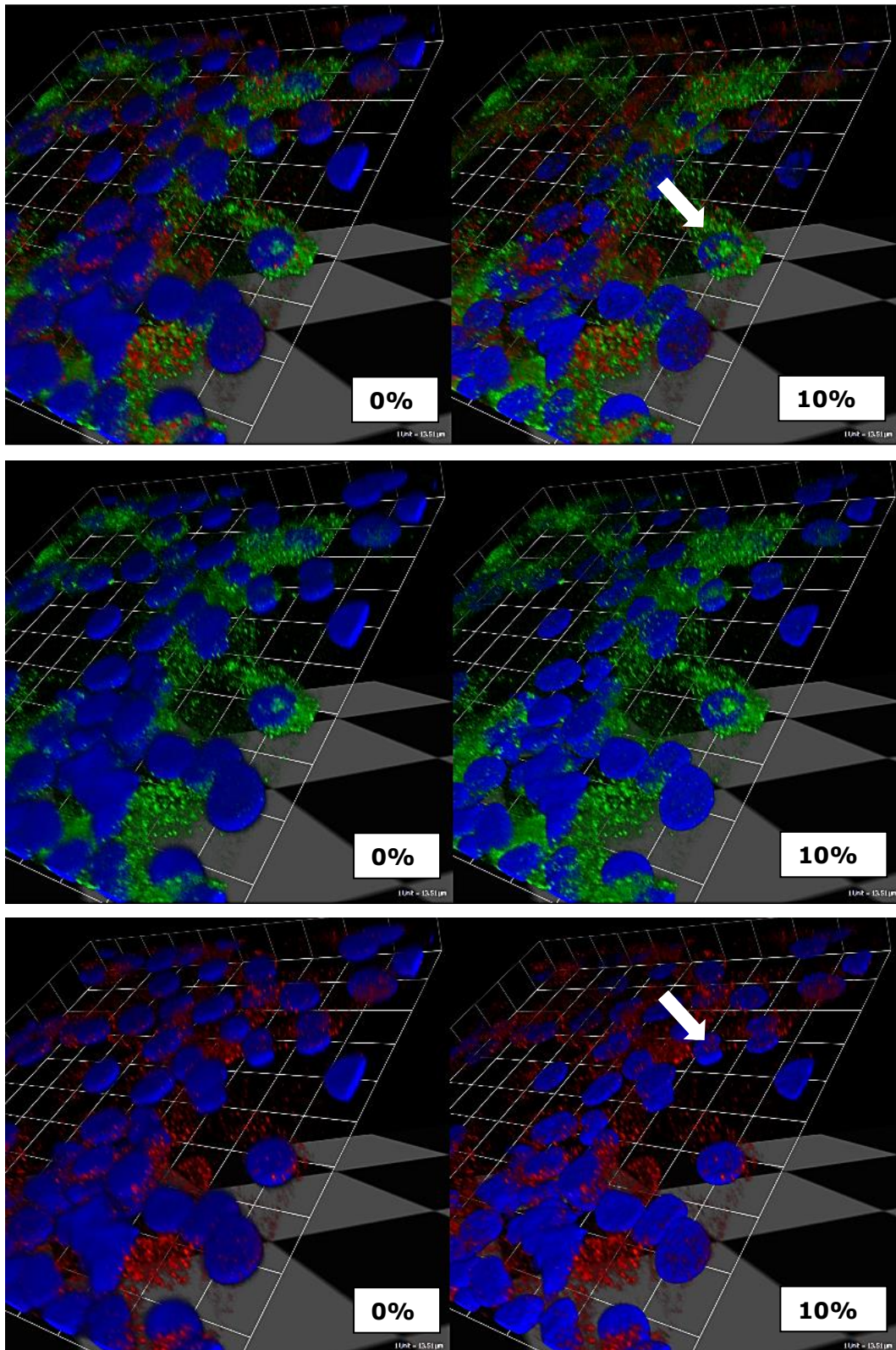


Figure 39. MR and EEA1 localization in the cell nucleus. Volocity software 3D image showing MR and EEA1 localization in the cell nucleus. Image is stained for MR-mouse (green) and EEA1-rabbit (red). Black level (transparency) in the blue channel varies from 0% to 10%. **Top panel. MR and EEA1 channels. Middle panel. MR channel. Bottom panel. EEA1 channel.** Original images were adjusted to +20% brightness and +25% sharpen for display purposes.

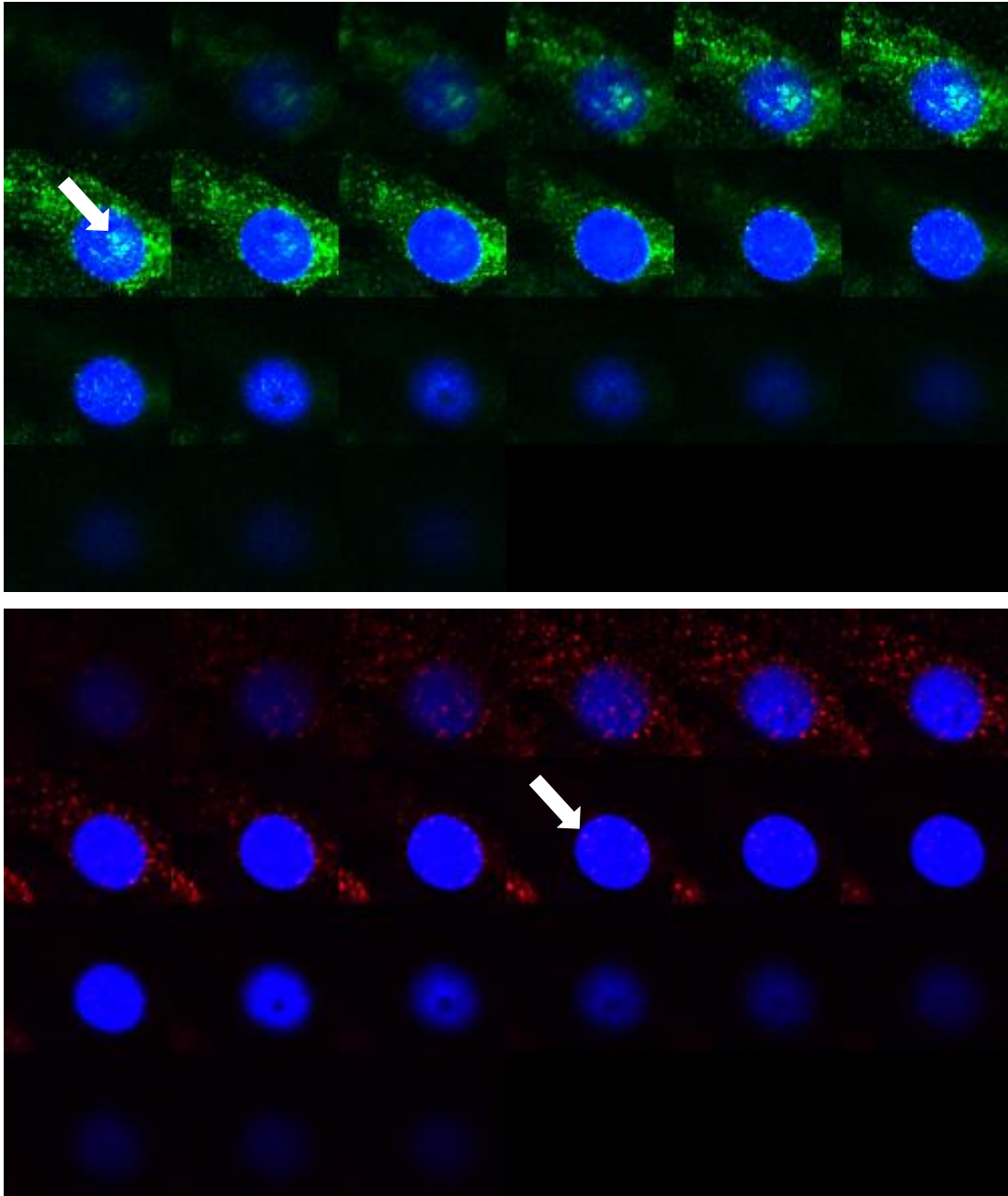


Figure 40. Image showing confocal layers from a cell stained with MR (green), EEA1 (red), DNA (blue). Areas where MR and EEA1 are found in the nucleus are shown by white arrows. Top pannel. MR channel. Bottom pannel. EEA1 channel.

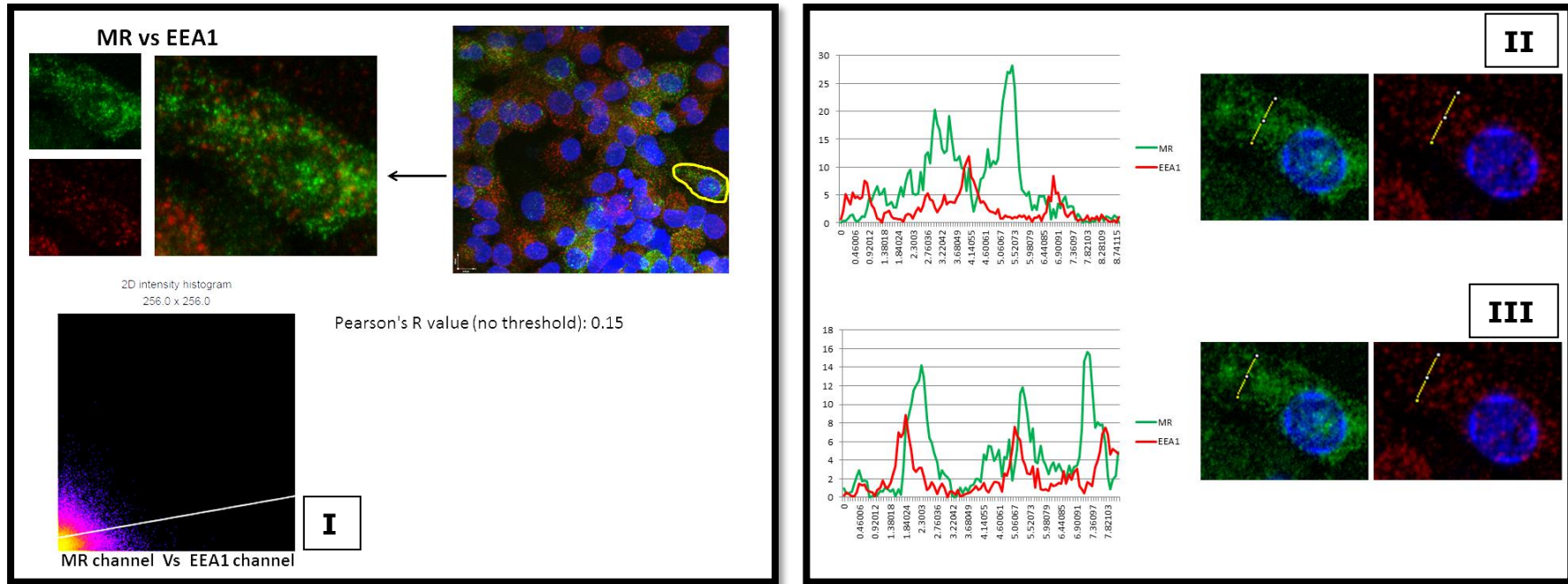


Figure 41. Example 1: Colocalization analysis and line intensity profiles of MR (green) vs EEA1 (red) in human macrophages. Before running colocalization analysis (coloc 2) in Fiji software, confocal image is converted to a Z projection and undergo background subtraction. The channels are split and a region of interest (ROI) is drawn in order to select the area for software analysis. Pearson's R value of 0.15 is given as a result of pixel colocalization between the green and red channel of the selected region. A 2 D histogram for the two channels is shown at the bottom (I). Line intensity profiles for different locations of the Z projections are shown on the side (II and III). Images on the left were adjusted to +40% brightness and images on the right panel were adjusted to -40% contrast and +40% brightness only for display purposes.

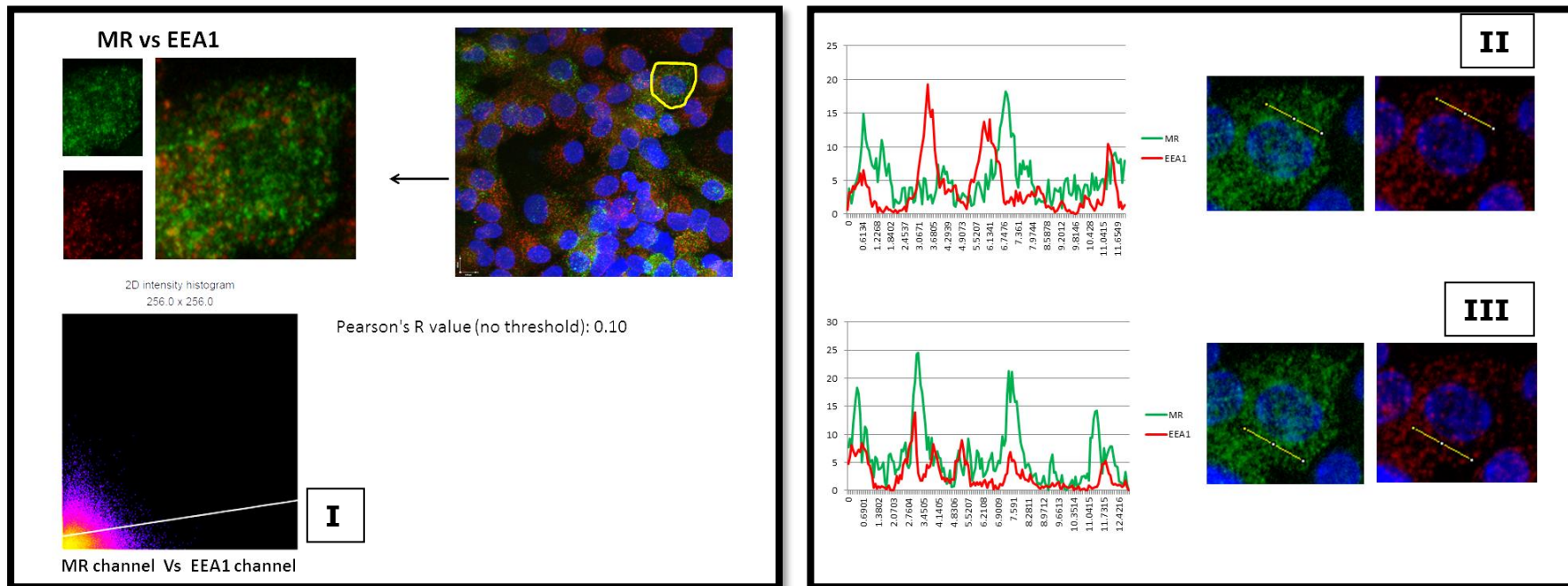


Figure 42. Example 2: Colocalization analysis and line intensity profiles of MR (green) vs EEA1 (red) in human macrophages. Before running colocalization analysis (coloc 2) in Fiji software, confocal image is converted to a Z projection and undergo background subtraction. The channels are split and a region of interest (ROI) is drawn in order to select the area for software analysis. Pearson's R value of 0.10 is given as a result of pixel colocalization between the green and red channel of the selected region. A 2 D histogram for the two channels is shown at the bottom (I). Line intensity profiles for different locations of the Z projections are shown on the side (II and III). Images on the left were adjusted to +40% brightness and images on the right panel were adjusted to -40% contrast and +40% brightness only for display purposes.

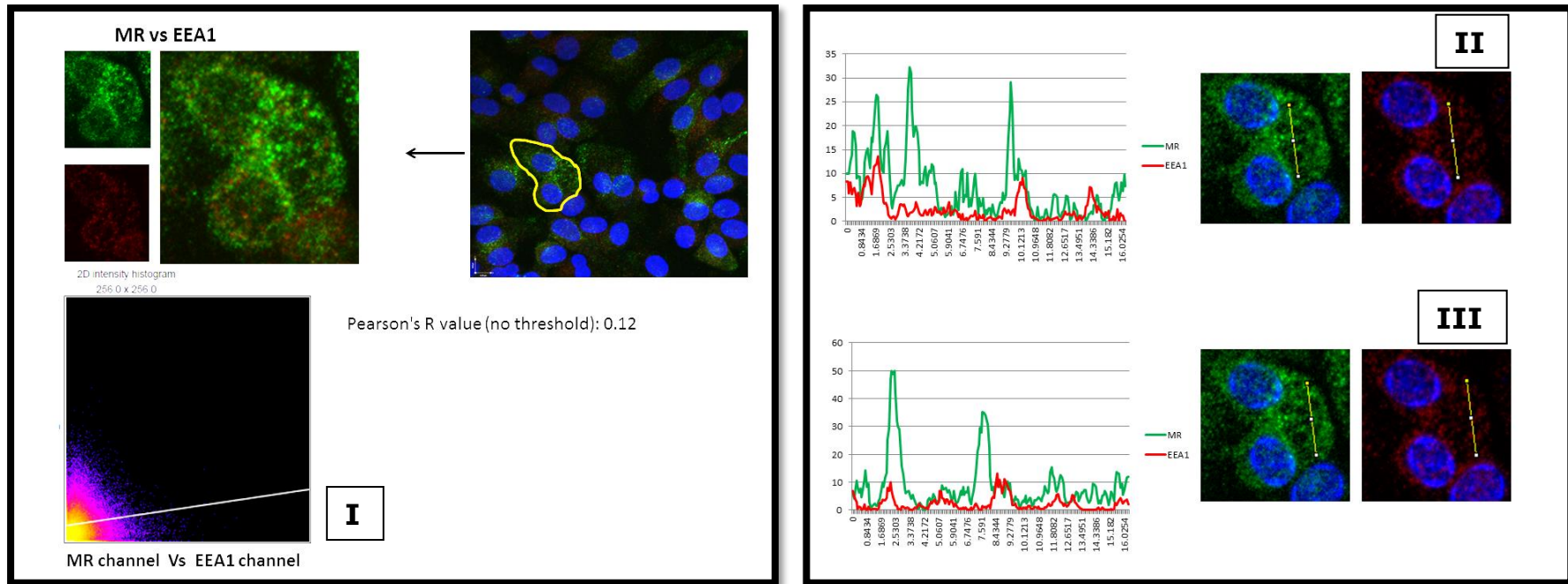


Figure 43. Example 3: Colocalization analysis and line intensity profiles of MR (green) vs EEA1 (red) in human macrophages. Before running colocalization analysis (coloc 2) in Fiji software, confocal image is converted to a Z projection and undergo background subtraction. The channels are split and a region of interest (ROI) is drawn in order to select the area for software analysis. Pearson's R value of 0.12 is given as a result of pixel colocalization between the green and red channel of the selected region. A 2 D histogram for the two channels is shown at the bottom (I). Line intensity profiles for different locations of the Z projections are shown on the side (II and III). Images on the left were adjusted to +40% brightness and images on the right panel were adjusted to -40% contrast and +40% brightness only for display purposes.

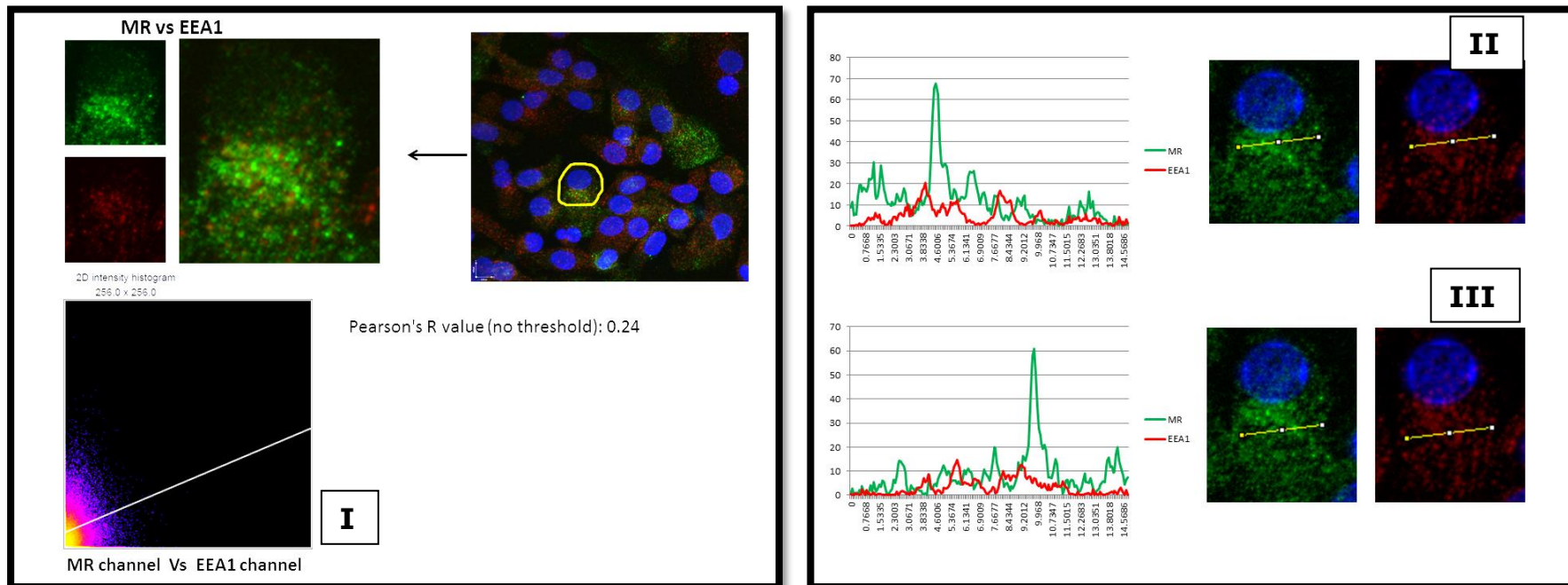


Figure 44. Example 4: Colocalization analysis and line intensity profiles of MR (green) vs EEA1 (red) in human macrophages. Before running colocalization analysis (coloc 2) in Fiji software, confocal image is converted to a Z projection and undergo background subtraction. The channels are split and a region of interest (ROI) is drawn in order to select the area for software analysis. Pearson's R value of 0.24 is given as a result of pixel colocalization between the green and red channel of the selected region. A 2 D histogram for the two channels is shown at the bottom (I). Line intensity profiles for different locations of the Z projections are shown on the side (II and III). Images on the left were adjusted to +40% brightness and images on the right panel were adjusted to -40% contrast and +40% brightness only for display purposes.

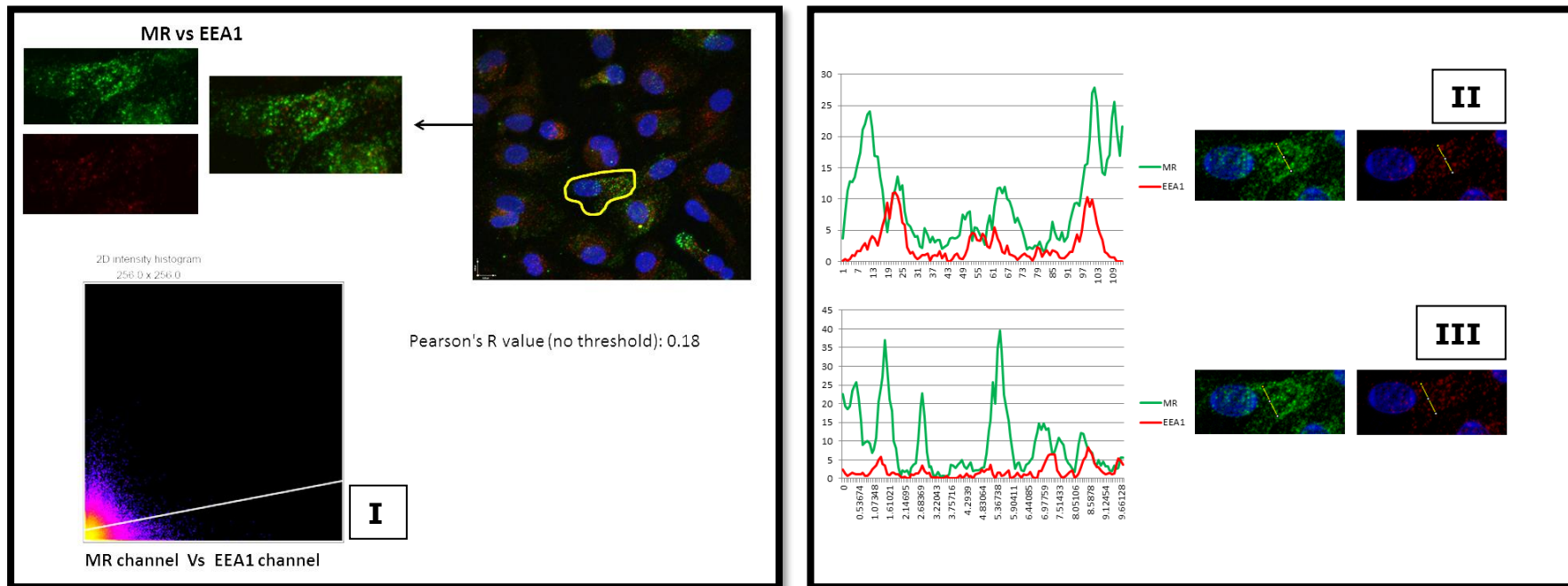


Figure 45. Example 1: Colocalization analysis and line intensity profiles of MR (green) vs EEA1 (red) in human macrophages treated with S100-DP240 for 4 hours. Before running colocalization analysis (coloc 2) in Fiji software, confocal image is converted to a Z projection and undergo background subtraction. The channels are split and a region of interest (ROI) is drawn in order to select the area for software analysis. Pearson's R value of 0.18 is given as a result of pixel colocalization between the green and red channel of the selected region. A 2 D histogram for the two channels is shown at the bottom (I). Line intensity profiles for different locations of the Z projections are shown on the side (II and III). Images on the left were adjusted to +40% brightness and images on the right panel were adjusted to -40% contrast and +40% brightness only for display purposes.

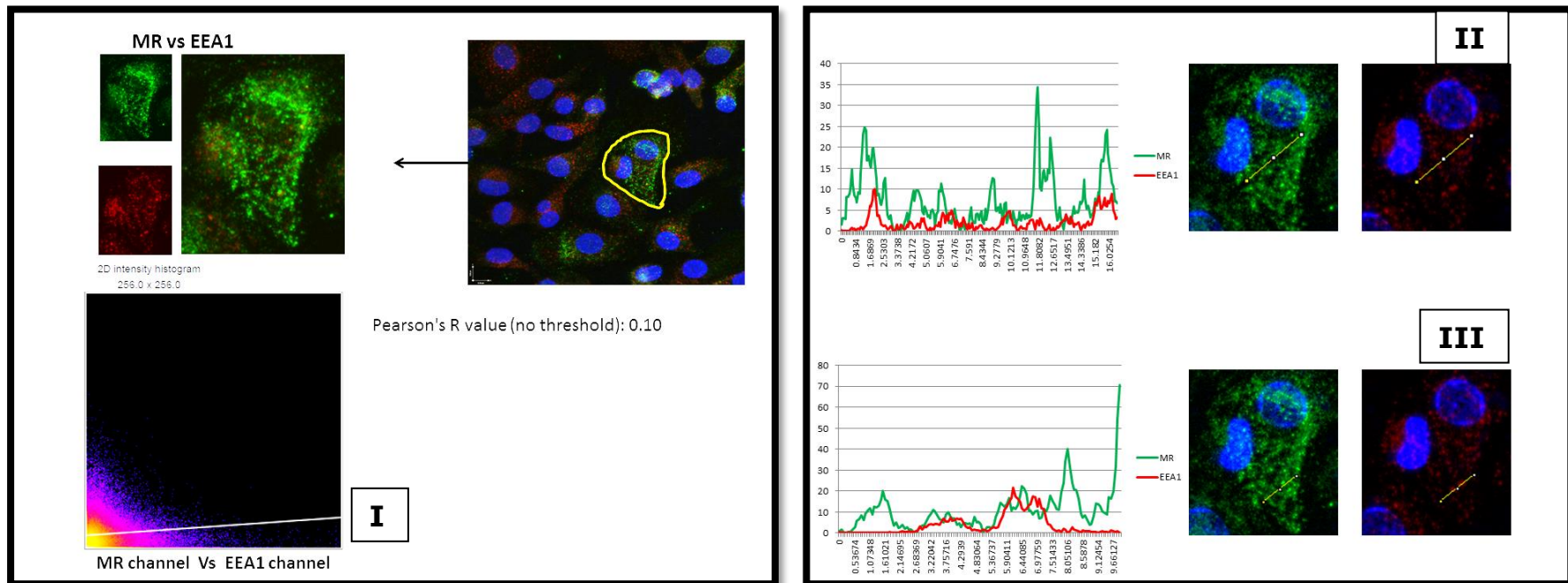


Figure 46. Example 2: Colocalization analysis and line intensity profiles of MR (green) vs EEA1 (red) in human macrophages treated with S100-DP240 for 4 hours. Before running colocalization analysis (coloc 2) in Fiji software, confocal image is converted to a Z projection and undergo background subtraction. The channels are split and a region of interest (ROI) is drawn in order to select the area for software analysis. Pearson's R value of 0.10 is given as a result of pixel colocalization between the green and red channel of the selected region. A 2 D histogram for the two channels is shown at the bottom (I). Line intensity profiles for different locations of the Z projections are shown on the side (II and III). Images on the left were adjusted to +40% brightness and images on the right panel were adjusted to -40% contrast and +40% brightness only for display purposes.

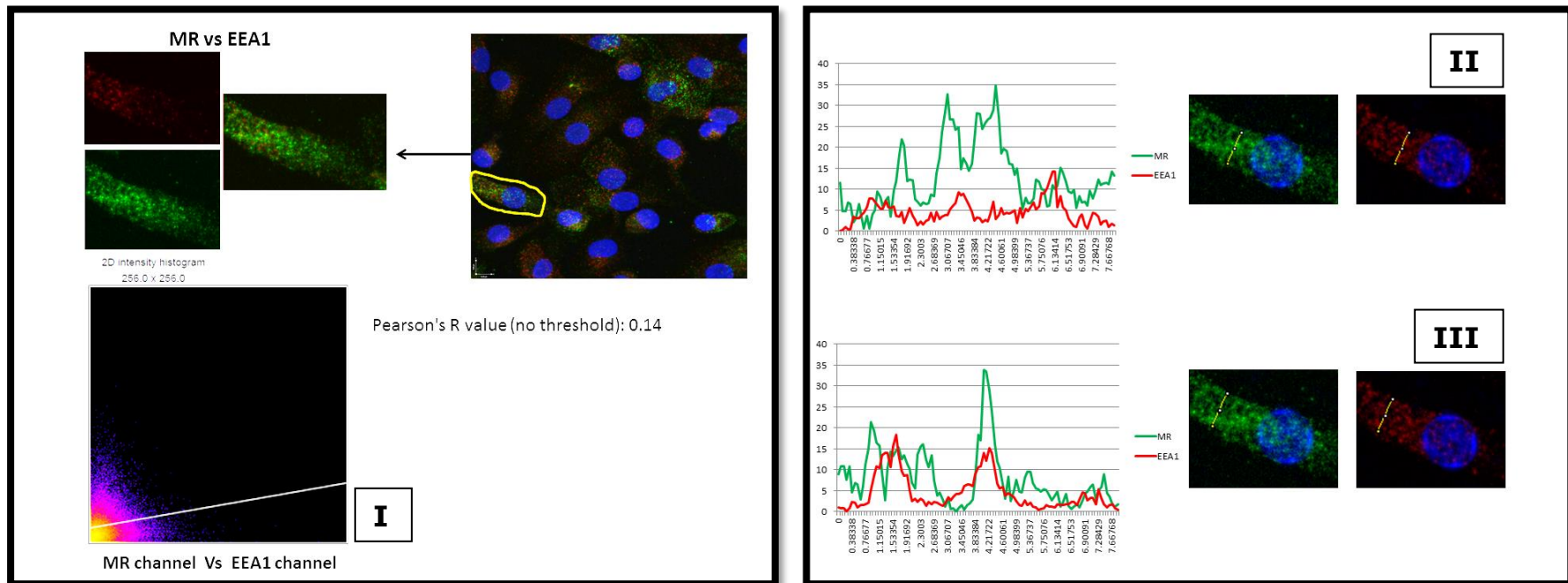


Figure 47. Example 3: Colocalization analysis and line intensity profiles of MR (green) vs EEA1 (red) in human macrophages treated with S100-DP240 for 4 hours. Before running colocalization analysis (coloc 2) in Fiji software, confocal image is converted to a Z projection and undergo background subtraction. The channels are split and a region of interest (ROI) is drawn in order to select the area for software analysis. Pearson's R value of 0.14 is given as a result of pixel colocalization between the green and red channel of the selected region. A 2 D histogram for the two channels is shown at the bottom (I). Line intensity profiles for different locations of the Z projections are shown on the side (II and III). Images on the left were adjusted to +40% brightness and images on the right panel were adjusted to -40% contrast and +40% brightness only for display purposes.

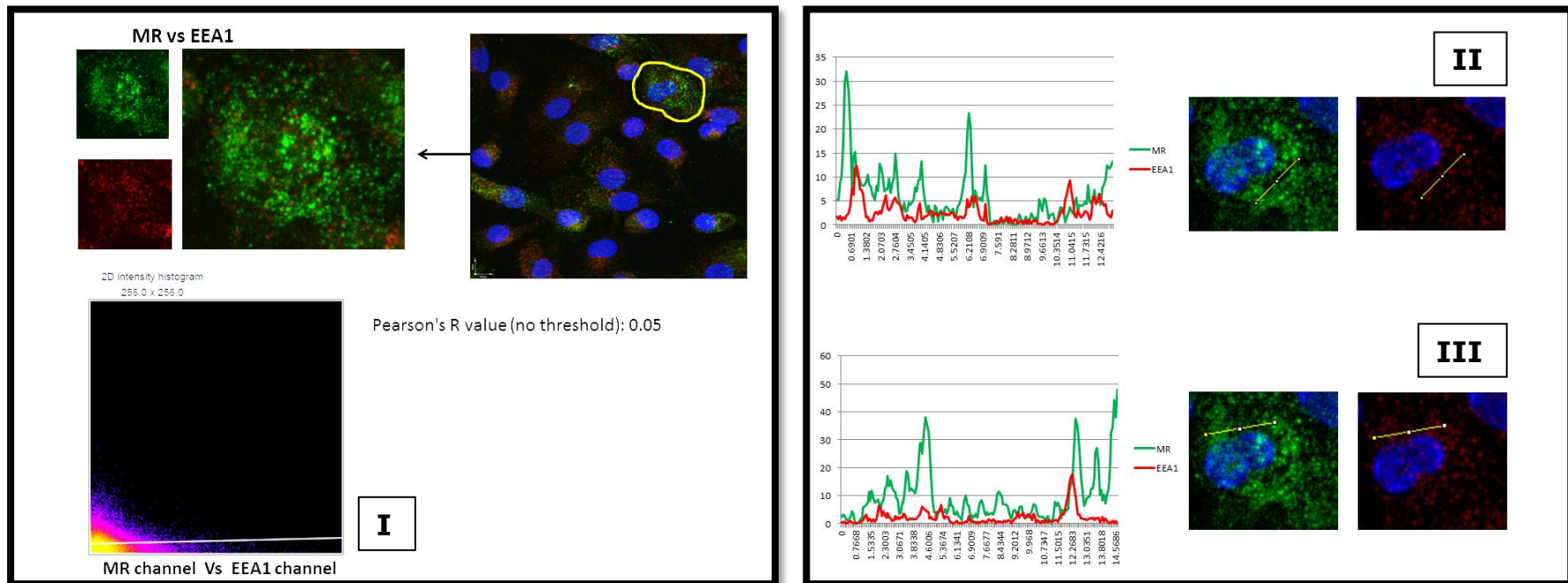


Figure 48. Example 4: Colocalization analysis and line intensity profiles of MR (green) vs EEA1 (red) in human macrophages treated with S100-DP240 for 4 hours. Before running colocalization analysis (coloc 2) in Fiji software, confocal image is converted to a Z projection and undergo background subtraction. The channels are split and a region of interest (ROI) is drawn in order to select the area for software analysis. Pearson's R value of 0.05 is given as a result of pixel colocalization between the green and red channel of the selected region. A 2 D histogram for the two channels is shown at the bottom (I). Line intensity profiles for different locations of the Z projections are shown on the side (II and III). Images on the left were adjusted to +40% brightness and images on the right panel were adjusted to -40% contrast and +40% brightness only for display purposes.

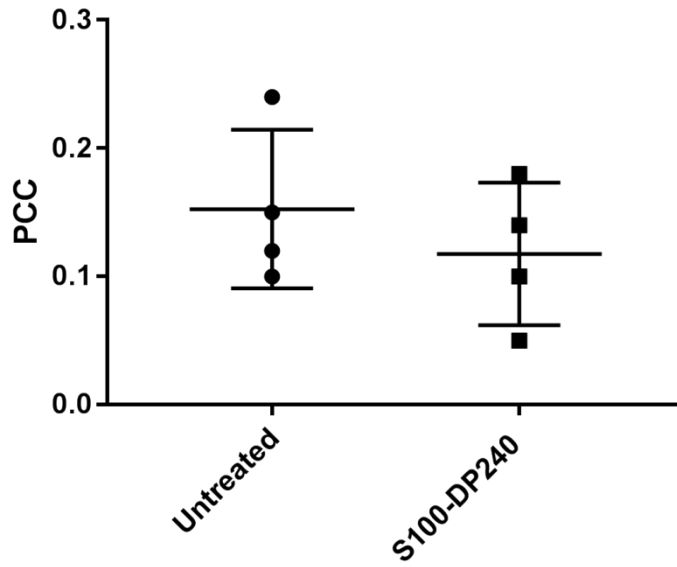


Figure 49. PCC values for MR vs EEA1 in untreated and in polymer S100-DP240 treated macrophages. PCC values were calculated by coloc 2 in Fiji software for selected cells. Each dot represents the PCC value of a selected cell from the same donor (n=1).

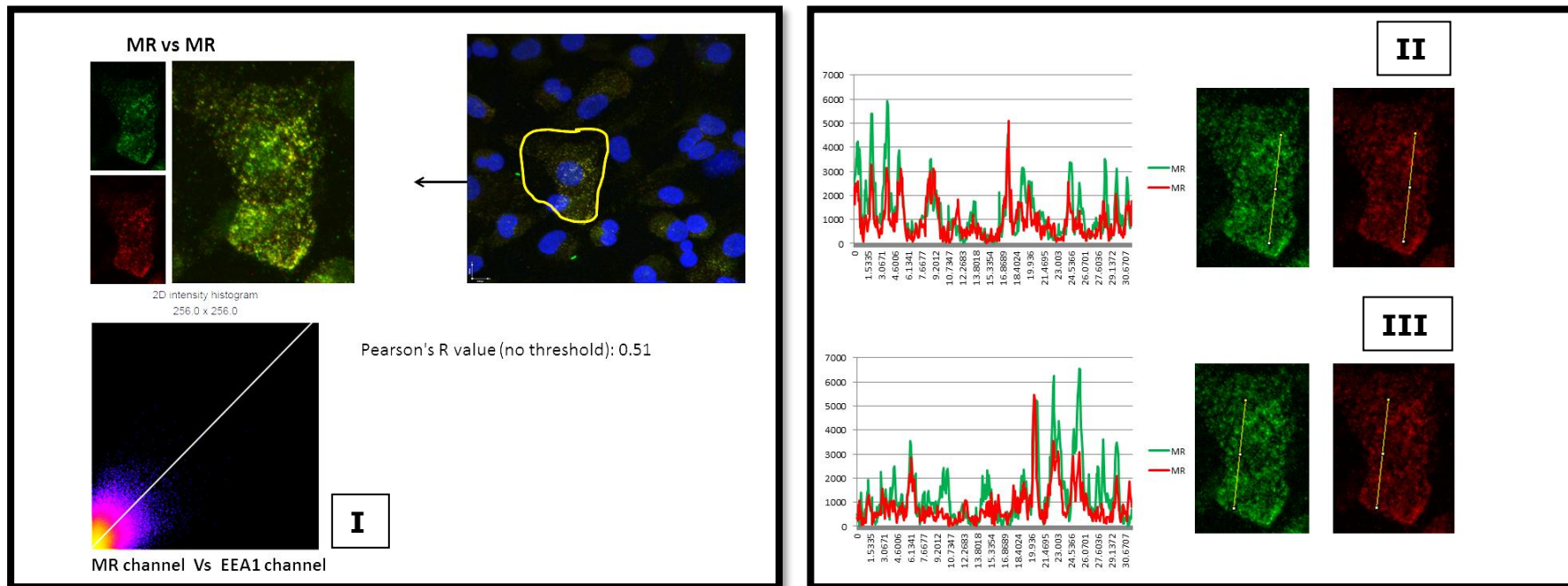


Figure 50. Example 1. Colocalization analysis and line intensity profiles of MR (green) vs MR (red) in human macrophages. Before running colocalization analysis (coloc 2) in Fiji software, confocal image is converted to a Z projection and undergo background subtraction. The channels are split and a region of interest (ROI) is drawn in order to select the area for software analysis. Pearson's R value of 0.51 is given as a result of pixel colocalization between the green and red channel of the selected region. A 2 D histogram for the two channels is shown at the bottom (I). Line intensity profiles for different locations of the Z projections are shown on the side (II and III). Images on the left were adjusted to +40% brightness and images on the right panel were adjusted to -40% contrast and +40% brightness only for display purposes.

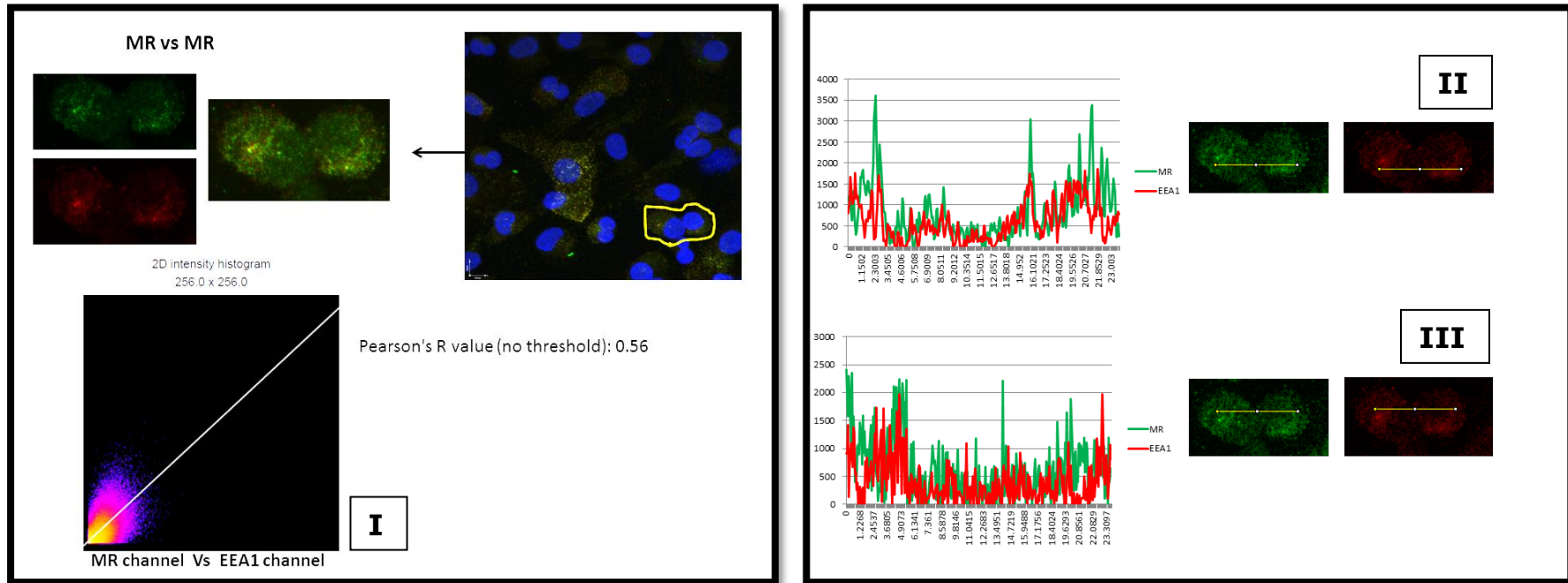


Figure 51. Example 2. Colocalization analysis and line intensity profiles of MR (green) vs MR (red) in human macrophages. Before running colocalization analysis (coloc 2) in Fiji software, confocal image is converted to a Z projection and undergo background subtraction. The channels are split and a region of interest (ROI) is drawn in order to select the area for software analysis. Pearson's R value of 0.56 is given as a result of pixel colocalization between the green and red channel of the selected region. A 2 D histogram for the two channels is shown at the bottom (I). Line intensity profiles for different locations of the Z projections are shown on the side (II and III). Images on the left were adjusted to +40% brightness and images on the right panel were adjusted to -40% contrast and +40% brightness only for display purposes.

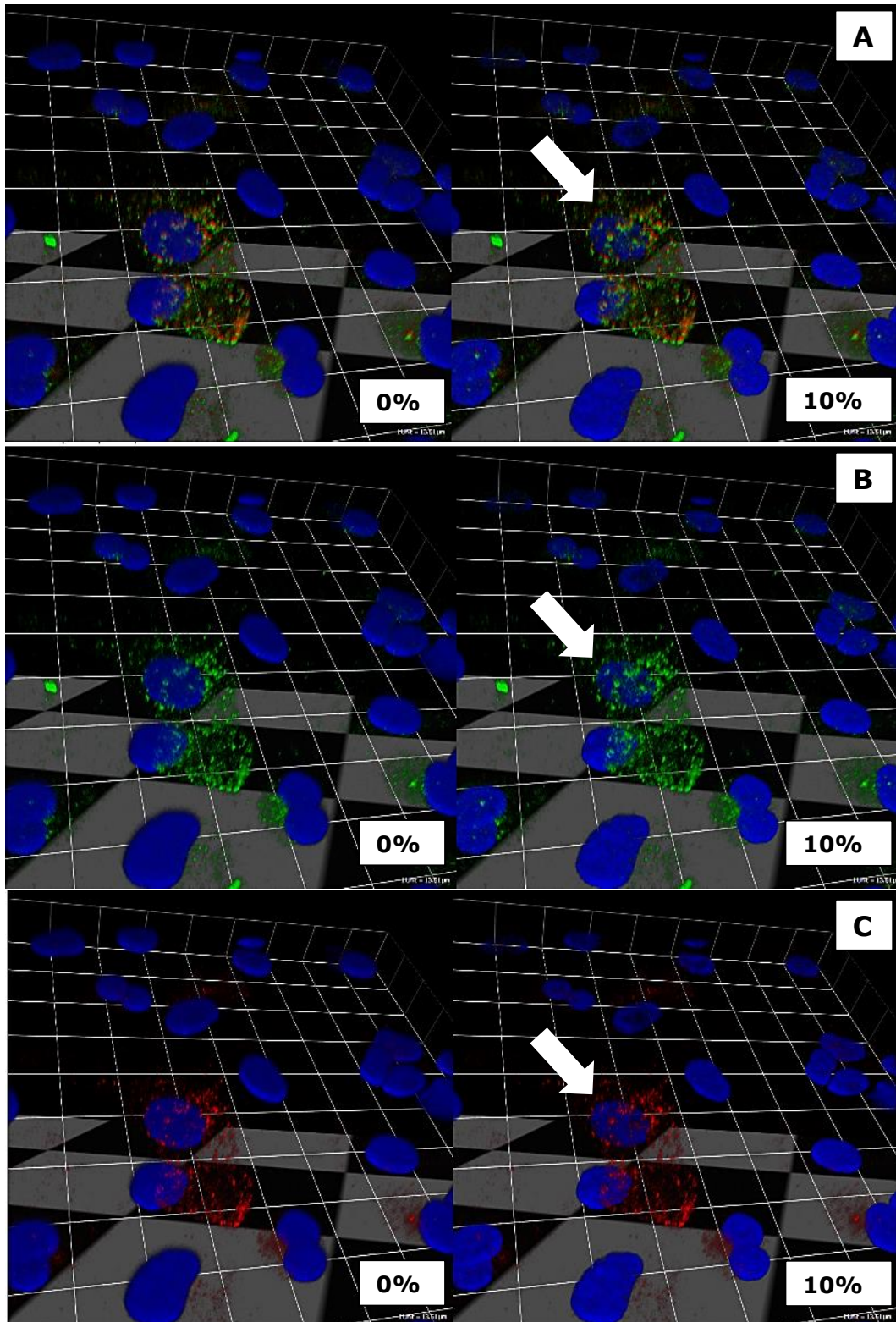


Figure 52. MR localization in the cell nucleus. Volocity software 3D image showing MR localization in the cell nucleus. Image is stained for MR-mouse (green) and MR-rabbit (red). Black level (transparency) in the blue channel varies from 0% to 10%. **Top panel. MR (mouse) and MR (rabbit) channels. Middle panel. MR channel (mouse). Bottom panel. MR channel (rabbit).** Original images were adjusted to +20% brightness and +25% sharpen for display purposes.

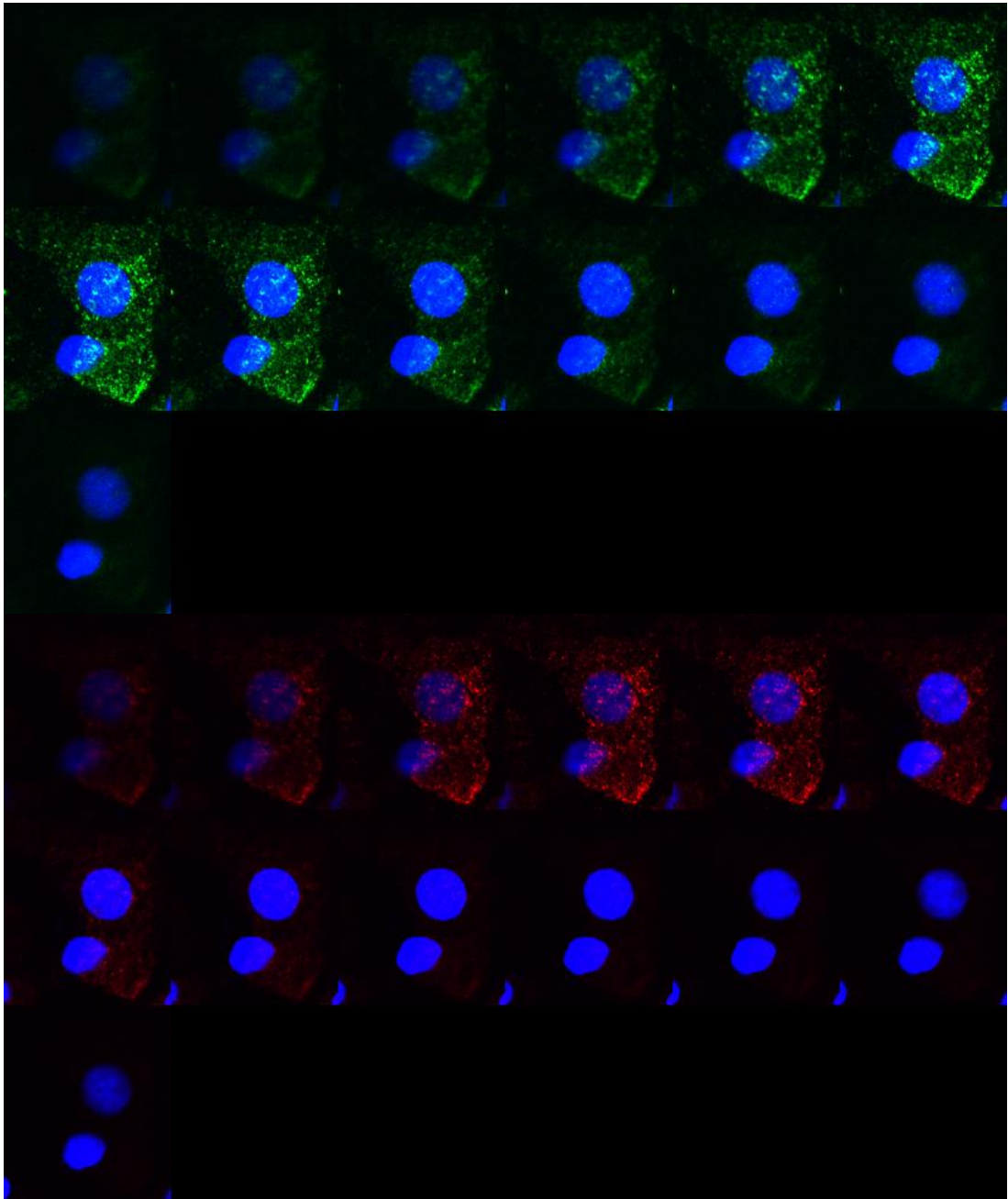


Figure 53. Image showing confocal layers from a cell stained with MR (mouse-green), MR (rabbit-red), DNA (blue). Areas where MR (mouse) and MR (rabbit) are found in the nucleus.

5.3. Discussion

From the previous work with MR⁺-CHO cells our group hypothesized that polymer S100-DP187 exerts its action by trapping MR in the endosomes, leading to a decrease in the number of receptors at the cell surface. To investigate if the same mechanism is present in human macrophages, the first step was to detect MR and other markers in human macrophages through immunofluorescence (IF). Microscopy protocol had to be optimized not only to detect specific markers in the cells, but also to control signal brightness and nonspecific fluorescence. A major concern was that the secondary antibodies against a particular species could cross-react with antibodies from a different species which would hamper efforts to establish co-localization of two markers.

Initially MR was not detected in the cells; as a consequence, the incubation time for the primary antibody was increased together with the concentration for the secondary antibody. In the following stage all the markers were detected but this time the problem was with nonspecific fluorescence from samples incubated with secondary antibody only. Endo180 detection in the IF microscope was dim compared with the image from confocal Zeiss LSM 880. This could be due to different reasons, e.g. changes in protocol, differences between microscopes. Lowering the concentration of the secondary antibody decreased the nonspecific fluorescence, at the same time that increasing the time of incubation of the primary antibody improved the overall detection of the markers. The optimization process revolved around finding the right concentration for the antibodies, more specifically, the secondary antibodies, at the same time that the incubation period for the primary antibody was determined. When images displayed a good fluorescence signal

for the markers and minimum nonspecific fluorescence in the channels, the focus changed to colocalization analysis.

Images studies of untreated macrophages resulted in a low degree of colocalization for MR and EEA1, indicated by both PCC values and line intensity profiles. Lines were drawn in different regions of the cell in order to observe variability within the cytoplasm. The low MR x EEA1 colocalization score contrasted with what is discussed in the literature about the location of MR in the early endosome (Gazi and Martinez-Pomares, 2009). Previous work (Vigerust et al., 2012) demonstrated that MR and EEA1 do colocalize in a human macrophage hybridoma cell line contradicting the results from the present analysis in human monocyte-derived macrophages. Images from macrophages treated with polymer S100-DP240 for 4 hours did not show significant changes in the PCC values when compared to untreated macrophages. Observation of line intensity profiles did not indicate a high degree of colocalization and did not show significant differences to untreated macrophages. Overall, similar to untreated macrophages, these cells also showed low degree of colocalization. However, line intensity profiles from untreated macrophages and macrophages treated with polymer S100-DP240 showed that there are some pockets in the graphs where MR and EEA1 display similar intensities, possibly indicating that in some regions in the cell colocalization may occur. One limitation of the line intensity profile analysis is that it was done for the Z projection of the whole cell. A more detailed comparison of layer by layer of the cell could have shown different results.

A matter of concern about the images is the presence of MR in the nucleus. MR is known to recycle between the endosome and the membrane, but its presence in the nucleus has not been previously reported. A smaller quantity of EEA1 was also observed in the nucleus. One possible explanation is that the permeabilization step mediated by Triton-X100 is producing pores in the nuclear

membrane (**L van de Ven** et al., 2009, Tissera et al., 2010), allowing proteins from the cytoplasm to enter the nucleus. If this is the case, there is a possibility that endosomes, which has a lipidic structure, is also affected by this procedure, thus limiting the reliability of the colocalization analysis. It also needs to be pointed out that this analysis is from cells from one donor and do not possess any statistical validity.

As experimental control, coverslips incubated with rabbit anti-MR antibody and a mouse anti-MR antibody were also analysed. PCC score was not as high (0.51 and 0.56) as expected for two antibodies that should be targeting the same receptor. Observation of the two MR channels side by side gives the impression they are greatly colocalized, however, analysis like that are not quantitative and can be deemed subjective. Overlapped line intensity profiles of the two channels (MR x MR) supports high colocalization of the two antibodies. The contradictions of the results possibly indicate that the images do not have the quality required for analysis by coloc 2 tool. A future step would be to discuss with specialists in colocalization analysis what could be done to improve the conditions of this assay.

The confirmation of the hypothesis that sulfated glycopolymers act by trapping MR in the endosomes of human macrophages is an important step in the elucidation of the mechanism of action of these polymers. The development of an appropriate MR binding polymer able to inhibit MR-mediated endocytosis would be of particular interest as it would open the way for the development of MR inhibitors, with potential important clinical implications in diseases or conditions where MR⁺ DCs and/or macrophages play a major role.

Chapter 6 - Final Discussion

Since lectin-carbohydrate binding is characteristically weak, multivalent ligand targeting is an attractive strategy to enhance the avidity of such weak binding interactions. A new generation of sugar-based polymers with complex architectures, compositions, and well-defined molecular weights have been developed in the past few years. These characteristics greatly enrich polymer diversity and enable a range of functions in biomaterials and biomedicine (Miura, 2007). Compared with other synthetic polymers, sugar-based biomaterials have the advantage of being biocompatible, biodegradable, non-immunogenic, making them particularly suitable for *in vivo* applications (Zhang et al., 2015). Over the years, sugar-based biomaterials have attracted substantial interest for biomedical applications, including drug, gene and antigen delivery, as well as diagnostic tools.

By taking advantage of MR endocytic capacity, a mannosylated cargo-delivery system has been developed to deliver Amphotericin B to macrophages infected by *Leishmania* protozoans (Asthana et al., 2015). The advantage of delivering the anti-leishmanial chemotherapeutic Amphotericin B using mannosylated chitosan nanocapsules is that it improves selective delivery of Amphotericin B into infected macrophages, therefore reducing the side effects of this medication to the host. In cancer immunotherapy, glycan-modified liposomes have been used to encapsulate tumor antigens and deliver them to DCs (Unger et al., 2012). Lewis^x-modified liposomes targets the lectin DC-SIGN expressed at the surface of DCs and were used to deliver the melanoma antigen MART-1 to these cells, consequently boosting activation of CD4⁺ and CD8⁺ T cells activation by DCs. As an alternative attempt to deliver DNA to cells, a vector composed of a high mannose N-glycan conjugated to a polyacridine peptide was designed. This compound binds to

plasmid DNA and targets DC-SIGN expressed by DC-SIGN⁺-CHO cells. Plasmid DNA-peptide-manosylated sugar complexes were internalized by DC-SIGN⁺-CHO cells, opening the possibility for receptor-mediated gene delivery (Anderson et al., 2010). In diagnostic applications, presence in the amniotic fluid of sialic acid and fucose glycotopes of plasma fibronectin has been used to monitor the evolution of pregnancy (Jain et al., 2012), as these glycotypes are associated with implantation, growth and differentiation of fetal tissues and changes according to pregnancy stages.

Synthesis of polymeric materials has attracted tremendous interest because of the precise control over architecture, stereochemistry, and composition. Sugars are considered building blocks, in which each unit has inherent chirality (D- and L- configuration), and unique degradation properties *in vitro* (Zhang et al., 2015), giving them exceptional abilities in polymer synthesis. Glycopolymers are sugar-functionalized polymers where sugar moieties are conjugated as pendant groups (Zhang et al., 2015). Synthetic glycopolymers can be synthesized either by polymerization of glycosylated monomers or by post-functionalization of pre-synthesized polymer scaffolds. Hence efforts have focused on the controlled synthesis of well-defined glycopolymers (Voit and Appelhans, 2010) by atom transfer radical polymerization (ATRP)(Bhatia et al., 2011), and reversible addition fragmentation chain transfer (RAFT) polymerization (Ahmed and Narain, 2011). These methods facilitate preparation of polymers with low dispersity indices (heterogeneity of size of molecules) and well-controlled molecular weights and monomer sequences, generating precisely prepared bioactive carries.

C-type lectin receptors (CLRs) belong to a large family of receptors that share a structurally carbohydrate-recognition domain (CRD) and often bind to glycan structures in a Ca²⁺-dependent manner (van Kooyk and Rabinovich, 2008). CLRs can be exploited to

modulate functions of CLR-expressing cells such as endocytosis or cell activation as well as for drug delivery. In innate immunity, CLRs are mainly expressed by antigen presenting cells (APCs) such as DCs and macrophages. They serve as pattern-recognition receptors (PRRs) and bind to pathogen-associated molecular patterns (PAMPs) (Sancho and Reis e Sousa, 2012) but may also sense self-antigens released by tissue damage or dead cells (Sancho and Reis e Sousa, 2013). Thus, myeloid CLRs such as DC-SIGN, mannose receptor (MR), and others are crucial to initiate immune responses against a number of pathogens including bacteria, viruses, parasites, and fungi. MR recognizes not only mannose-terminated glycans, but also fucose-terminated glycans on the surface of pathogens, thus it is capable of sensing bacterial, viral, and fungal ligands (Vautier et al., 2012). The receptor also binds to sulfated sugars in a calcium-independent manner through its N-terminal CR domain, giving the ability to recognize sulfated oligosaccharides found in pituitary hormones such as lutropin and thyrotropin. MR also binds collagen through its fibronectin type II domain (East and Isacke, 2002). Besides its effect in pathogen recognition, MR is involved in cell activation, antigen presentation to T cells, and control of homeostasis, such as clearance of endogenous products, and cell adhesion (Taylor et al., 2005).

MR is a suitable biological target for drug carriers due to its endocytic ability and drug delivery properties. Suitable carriers must facilitate transport across the membrane and deliver their cargo inside the cells. MR has been shown to be particularly suitable for targeting of tumour-associated macrophages (TAMs) in cancer, for infectious diseases and for vaccine delivery (Azad et al., 2014). In the cancer tissue microenvironment, TAMs have been described to play a role in tumour invasion, proliferation and metastasis (Mantovani et al., 1992). These macrophages are M2-like and express high levels of MR (Allavena et al., 2010). Mannose-coated liposomes have been

developed for imaging of TAMs and consequently track cancer growth by positron emission tomography (Locke et al., 2012). These liposomes also hold the potential for delivery of therapeutic agents to the tumour microenvironment. Targeting the macrophage MR has shown to be a potential strategy for the treatment of Tuberculosis. *M. tuberculosis* is a prototypic intracellular pathogen of macrophages which cause both active and latent tuberculosis (Azad et al., 2014). In order to target these intracellular pathogens, nanocarriers optimized specifically for macrophage MR has been developed for drug delivery (D'Addio et al., 2013). In the field of vaccine delivery, targeting antigens to endocytic receptors such as MR represents an attractive strategy to enhance the efficacy of vaccines (Keler et al., 2004). These APC-targeted vaccines have the ability to guide exogenous protein antigens into endosomes that process the antigens for major histocompatibility complex class I and II presentation. The MR and other C-type lectins have the ability to sample antigens and link the innate and adaptive immune responses. Delivery of antigens has achieved effective induction of cellular and humoral immune response (Keler et al., 2004). While there are examples of agonists and drug carriers targeting MR, there is lack of MR blockers in the literature.

With the intention of targeting MR in a very controlled way, our group developed a library of glycopolymers, with different sugar moieties conjugated as pendant groups and with different lengths. Glycopolymers synthesised by ATRP had chains varying between 32 - 187 average number of polymer repeating units, with average molecular weight M_n of 12-17 and 71-89 kDa, respectively; below and above the 40-60 kDa threshold for glomerular kidney filtration. We expected both sets of glycopolymers would behave very differently *in vivo* due to their potentially different half-life in circulation. Glycopolymers with 100% non-CD206 binding units, (Gal)₃₂ and (Gal)₁₈₇ were also prepared and utilised as negative

controls for subsequent *in vitro* and *in vivo* studies. A new set of polymers with average molecular weight M_n 60-81 kDa were also synthesized by RAFT.

The hypotheses of this project were that MR-binding polymers developed in our lab could be recognised by human MR and modulate MR-function in human myeloid cells. The main aims of this project were to: 1) Investigate the recognition of polymers S100-DP187, M100-DP187 and G100-DP187 by the CR domain of human MR and human myeloid cells; 2) Investigate the effect of glycopolymers on MR function in human myeloid cells; and 3) Investigate the effect of glycopolymers on MR distribution within human myeloid cells.

Macrophages are distributed throughout the human body and patrol tissues while maintaining homeostasis. Macrophages in tissues are derived from embryonic precursors that seed the tissues before birth and maintain themselves by self-renewal (Ginhoux and Jung, 2014). However, blood monocytes, derived from haematopoietic cells in the bone marrow, can infiltrate and differentiate into macrophages in the tissues. The contribution of monocytes to the population of resident tissue macrophages is tissue dependent. While in lung and brain macrophages are of embryonic origin and are maintained by replication, in the dermis and lamina propria macrophages are replenished through the constant recruitment of blood monocytes, rather than replication (Gordon et al., 2017).

In order to translate previous mouse work in the lab to the human setting it was important to use a biological model of human myeloid cells expressing MR. Tissue macrophages are not generally available, whilst blood monocytes can be easily obtained from donors. Thus monocyte-derived macrophages provide a suitable model for research in this area. Although myeloid cell lines provide a convenient supply of cells, lines such as the human monocytic leukaemia cell line THP-1, and the human myeloid leukaemia cell

line U937, which possess uniform genetic makeup (Chanput, 2015), do not express MR. In addition, these cell lines fail to represent the diversity found in humans.

Analysis of Polymer Uptake by Human Macrophages

Uptake of S100 and M100 GPs was initially observed in MR⁺-CHO cells and mouse macrophages (Mastrotto et al, manuscript in preparation) and this thesis confirmed uptake by human monocyte-derived macrophages. S100-DP187 was recognized by the human CR domain of MR (Figure 14) and by human macrophages (Figure 15). In human macrophages, S100 and M100 polymer uptake was dependent on temperature of incubation (Figure 17) and escalated with the increase in polymer concentration (Figure 18), all signs of receptor mediated uptake. In addition, polymer uptake was increased in IL-4 –treated macrophages which is consistent with the increased MR expression in these cells (see below).

Knockout mouse macrophages failed to show uptake of S100 and M100 polymers, indicating MR was the sole receptor responsible for polymer uptake. Unfortunately, our lab is not currently set up to perform specific down regulation of MR in human macrophages using siRNA which would have confirmed the specificity of the uptake of S100 and M100 GPs by MR. Other approaches such as antibody-mediated MR blocking has also been unsuccessful in our laboratory.

Effect of S100 polymers on MR biology

Our initial results in MR⁺-CHO cells suggested that after cell uptake of S100 multivalent ligands further MR-mediated endocytosis was prevented. The effect was achieved after 30 minutes incubation with S100 polymers (Figure 8, d), whilst the same was not observed in for Man GPs. This phenomenon could be explained by *i*) an alteration of cell trafficking of MR which would eventually lead to its degradation, or *ii*) the formation of very stable S100 GPs-MR complexes unable to dissociate and restricting receptor recycling, either at the cell membrane or within endosomal compartments.

(i) MR degradation

To verify whether reduced MR-mediated ligand uptake was due to intracellular receptor degradation, total cellular MR in MR⁺-CHO cells was estimated by western blotting. After incubation with GPs at 15 μ M, for 30 and 120 min, Western Blot analysis of cell lysates indicated that the total amount of MR in the cell remained virtually unchanged compared to untreated MR⁺-CHO cells, for all polymers investigated (Figure 9, b). A similar pattern was observed in human macrophages incubated for 2 (Figure 30) and 6 hours (Figure 31) with 48 μ M to 192 μ M of S100 GPs, corroborating the idea that the total MR number remains constant regardless of the increase in polymer concentration.

(ii) MR surface expression inhibition

In regards to the ability to block MR expression on the cell surface, sulfated multivalent ligands S100-DP32 and S100-DP187 significantly decreased the proportion of MR at the cell surface compared to untreated MR⁺-CHO cells after 120 min incubation, in contrast, mannosylated analogues did not cause the same effect (Figure 9, a). In human macrophages, a significant reduction in surface MR was not observed after 1-hour incubation (Figure 25)

using 48 μ M S100-DP187, however, after 24 hours incubation a significant reduction of MR was observed for IFN- γ + M-CSF and M-CSF only treated macrophages (Figure 26). IFN- γ and LPS are known as pro-inflammatory agents that polarize macrophages to type M1 or classically activated phenotype (Glass and Natoli, 2016). In this context, polymers were also tested to see whether they possess the ability to interfere with the expression of M1 markers. An alternative stimulus to use to obtain M1 macrophages is TNF α . TNF α is a pro-inflammatory cytokine and, like LPS, it can also activate macrophages that have already been primed by IFN- γ (Parameswaran and Patial, 2010).

The results showing reduced surface expression of MR could reinforce the original hypothesis that blocking of MR-mediated endocytosis was due to trapping of the receptor into stable ligand-receptor complexes from which the latter could no longer dissociate. But there is also a possibility that these polymers are simply blocking the recognition of these receptors by the labelled antibody, explaining why there is less surface MR expression. In the mouse model this is an unlikely scenario because the antibody used to detect MR (5D3) binds the CTLD4-7 region of MR (Martinez-Pomares, 2012) and is not a blocking antibody. Hence binding of S100 GPs to MR should not affect 5D3 binding.

In addition to reduced MR surface expression, IFN- γ treated macrophages incubated for 24 hours in the presence of S100-DP187 also showed reduced expression of HLA-DR and CD11b compared to untreated cells. No assay was done to determine if these polymers could be binding non-specifically to these receptors and blocking their recognition by the antibodies. Of interest, recent work in the lab has indicated reduced STAT-1 phosphorylation in response to IFN- γ in the presence of S100-DP240 (S. Muntaka, unpublished). Another interesting possibility is that S100-DP187 could be interfering with the action of IFN- γ /LPS which would explain why

levels of MHCII were much reduced in the S100-DP187-treated samples. This could be tested by analysing STAT-1 and NF κ B activation in the presence of S100-DP187. Our lab has consistently detected increased production of MCP-1 by IFN- γ -treated macrophages (Muntaka et al., 2019). Analysis of MCP-1 production by S100-DP-187-treated cells failed to show any significant changes (data not shown).

(iii) MR localization

Confocal microscopy of MR⁺-CHO showed that MR-S100 GPs complexes were not localized at the cell membrane but rather spatially confined within recycling endosomal compartments labelled with the early endosomal marker EE1. The limited experimental data on the localisation of MR and EE1 in human macrophages untreated or treated with S100-DP240 could not confirm these findings. The degree of colocalization between MR and EEA1 based on the PCC score was very low, contradicting what is known in the literature about the presence of MR in the early endocytic compartment (Gazi and Martinez-Pomares, 2009). Further no significant PCC difference between untreated and S100-DP240 GPs-treated macrophages was observed. Due to uncertainties regarding the quality of the colocalization analysis in human macrophages and the quality of the pictures, further co-localization analysis needs to be performed in these cells. Some changes in the permeabilisation protocol could be applied, such as, Triton X-100 could be substituted to Tween 20 or the time of incubation with Triton X-100 could be decreased. There is also a choice of using other endosomal markers instead of EEA1, like Rab4, Rab5 and transferrin. It would be of interest to learn if these markers co-localize with MR. Detection of MR in the cell nucleus was surprising as no previous reports of MR nuclear localisation exist. The validity of this finding is supported by the fact that both anti-MR antibodies gave the same staining pattern.

Although an artefact caused by the labelling procedure cannot be ruled out.

(iv) Collagen uptake inhibition

To explore the inhibitory capacity of S100 GPs in MR activity, the ability of sulfated GPs to inhibit uptake of other MR ligands was tested. Collagen was chosen because of its carbohydrate-independent binding to the FNII domain of MR and subsequent cell uptake have been described by our group (Martinez-Pomares et al., 2006a) and Dickamer's group (Napper et al., 2006a). This mechanism is of particular interest during resolution of inflammation in which tissue remodelling occurs (Martinez-Pomares et al., 2006b), one recent example highlighted the process of collagen endocytosis mediated by MR in TAMs found in Lewis lung carcinoma (LLC) cells (Madsen et al., 2017).

In our previous study, MR⁺-CHO cells were pre-treated with either S100-DP32 or S100-DP187 (15 μ M in sugar binding units) for 30 or 120 min, then Gelatin-Texas Red (TR) was added to a final concentration of 10 μ g/ml (Figure 10). After 2 hours of co-incubation, data clearly showed that internalisation of Gelatin-TR was significantly reduced by S100 GPs compared with untreated cells incubated with Gelatin-TR for 2 hours (positive control). These uptake patterns did not significantly change by increasing the duration of polymer pre-incubation from 30 to 120 min neither by washing the cells prior to adding the gelatin. The lack of effect of washing/removing the polymers from the cells probably indicates the GPs had already been internalized and found as GP-MR in the endosomes. Remarkably, similar trends were also observed when human macrophages were incubated with 48 μ M of S100-DP187 GPs for 6 hours followed by 1-hour Gelatin-TR incubation (Figure 23). The same trend was not observed in human macrophages incubated

for 1 hour with S100-DP187 GPs (Figure 21), suggesting that time of incubation is an important factor to observe significant effects in human cells, in contrast to MR⁺-CHO cells or mouse macrophages. Even though it seems counterintuitive, it was easier to observe gelatin uptake inhibition in human macrophages treated with IL-4, which contains a higher MR cellular pool. The reasons for these findings are unclear at this time. Little is known about the cellular biology of MR in human macrophages with many characteristics assumed based on findings in mouse macrophages

Endo180 as an alternative collagen receptor in human monocyte-derived macrophages

The differences in blocking efficiency of S100 GPs between MR⁺-CHO cells/mouse macrophages and human macrophages led to the hypothesis that another receptor could be mediating gelatin uptake in human cells. The presence of Endo180, another known collagen binding receptor, in monocyte-derived macrophage may explain the less efficient gelatin inhibition by S100-DP187 in these cells compared to MR⁺-CHO cells or mouse macrophages, which do not possess Endo180. Western blotting analysis showed that indeed human monocyte-derived macrophages express Endo180 and that, in contrast to MR, M-CSF treated macrophages showed higher levels of Endo180 when compared to IL-4 treated macrophages, indicating downregulation of Endo180 by IL-4 (Figure 31). Endo180 bands detected in IL-4 treated macrophage seems to slightly differ in size to bands from M-CSF treated macrophages (Figure 24), suggesting potential differences in glycosylation. Endo180 is a receptor that was initially found in fibroblasts (East and Isacke, 2002) and the concentrations of antibody that is normally used to detect this receptor in fibroblasts was not enough for detection in human macrophages, forcing the use of higher concentrations of antibodies and higher protein loading in the gel. Due to difficulty of detection

of Endo180 in human macrophages, the presence and regulation of Endo180 in human macrophages should be also confirmed by qPCR. Endo180 associate with uPAR-associated protein forming the complex uPARAP/Endo180 which is connected to matrix turnover (Engelholm et al., 2009). uPARAP internalize collagen and gelatin and route this material to the lysosomes (Engelholm et al., 2009). Hence, this receptor is expected to be localized with markers such as LAMP1 (Kjoller, 2004), which might differ from MR which is expected to be localized in the endosomes. It is not known if the presence of Endo180 in human macrophages is the only factor responsible for differences in gelatin uptake between MR⁺-CHO cells and human macrophages and between the two types of human macrophages in this study (M-CSF vs IL-4). Another factor could be the differences in protocols. In MR⁺-CHO cells, 30 min of incubation with S100-DP187 followed by 2 hours incubation with labelled gelatin was enough to detect significant reduction in gelatin uptake (Figure 10). In human macrophages incubated for 1 hour with S100-DP187 followed by 1-hour gelatin incubation had no significant reduction in gelatin uptake (Figure 21). To confirm if Endo180 is the cause of inefficient gelatin uptake inhibition in human macrophages, Endo180 could be silenced by siRNA and collagen uptake inhibition in these cells would be quantified and, in the presence, and absence of S100 GPs.

In agreement with these findings in human cells a short incubation of one hour with S100 polymers was not sufficient to decrease significantly MR surface expression. A significant change was only observed at 24 hours incubation (Figure 26). The difficulty in inhibiting MR in human cells compared to mouse macrophages or MR⁺-CHO could be due to differences in the endocytic pathways or in a higher MR intracellular pool in human cells that would repopulate the membrane with more receptors, taking a longer period of time

to observe a significant inhibition in MR surface expression in human macrophages.

Modulation of IDO activity using S100-GPs

The main allergen from house dust mite (HDM) – Der p 1 -, in the presence of low levels of LPS downregulates indoleamine 2,3-dioxygenase (IDO) through engagement of MR on human DCs, leading to a Th2 immune response (Royer et al., 2010). These data show the involvement of MR in inducing Th2 allergic immune responses through regulation of IDO activity in human DCs with the participation of Toll-like receptor 4 (TLR4) signaling. The kynurenine pathway is a major route for tryptophan metabolism in mammals (Mándi and Vécsei, 2012). In the first step of the process tryptophan is converted to kynurenine in a reaction catalysed by indoleamine 2,3-dioxygenase (IDO). IDO-mediated tryptophan catabolism appears to have a significant counter-regulatory role in damping down the activation of the immune system (Mándi and Vécsei, 2012), more particularly in the suppression of T cells (Mellor and Munn, 2004). IFN- γ (Chon et al., 1996) and LPS (Fujigaki et al., 2006) are known to induce IDO gene transcription. MR engagement by mannan (plant polysaccharide made of mannose) can downregulate IDO activity and impairs Th1 cell priming induced by LPS (Salazar et al., 2016). This led to the study of tryptophan metabolism in macrophages activated by IFN- γ and LPS in the presence of unlabelled S100-DP240 GPs. Macrophages activated by IFN- γ and LPS and incubated in the presence of S100-DP240 showed a decrease in kynurenine production (Figure 27), which was dependent on polymer concentration. This effect was seen independently of the type of culture plate macrophages were seeded on (Figure 27 and Figure 28, a). It is not clear whether engagement of MR by S100 GPs would lead to a Th2 response based on the down modulation of IDO provoked by allergen Der p 1 (Royer et al., 2010) or mannan (Salazar et al., 2016). By targeting MR with glycosylated

(3-sulfo-LewisA or tri-GlcNAc) OVA conjugates it was possible to skew T cells towards Th1 response (Singh et al., 2011). Thus, different MR targeting may lead to different outcomes. Hence it is not safe to hypothesize which T cell response would be stimulated by SO₄-3-Gal GPs, if any at all. This could be tested in the future by detecting Th2/Th1 cell markers in T cells from a Macrophage-T or DCs- T cell co-culture incubated in the presence of different cytokines and SO₄-3-Gal or Man GPs.

Cells used for the IDO activity assay also had their cell surface markers analysed. A decrease in HLA-DR surface marker (Figure 29, B) was only detected at a higher polymer concentration (120 µM) and the inhibitory effect in MR surface expression (Figure 29, A) was not significant (IFN-γ + LPS treated), even when incubated with the GPs for 24 hours. The addition of LPS together with IFN-γ may also be the cause of no significant reduction in MR caused by S100-DP240, in contrast to the significant reduction in MR in cells treated with IFN-γ only and S100-DP187. This makes the comparison between the assays difficult and as they may not be treated as equivalent.

With regards to the influence of IFN-γ, cell surface markers analysis showed that MR surface expression was high in cells incubated with IFN-γ alone for 24 hours in the absence of GPs in this case. This contradicts the literature which relates IFN-γ to downregulation of MR and considers MR as a marker for macrophage polarization, in which MR is upregulated in M2 macrophages and downregulated in M1 macrophages. This led to further investigation of protein expression under different circumstances in order to investigate total MR protein expression.

MR expression in M1 and M2 human macrophages

High MR protein expression was confirmed by western blot in macrophages treated with IFN-γ for 24 hours comparable to M-CSF-

macrophages, in agreement with the cell surface labelling results. In mice it is accepted that MR is downregulated in cells treated with IFN- γ , so the differences found could be explained by inter-species variations. However, some papers claim that MR activity is also downregulated in human macrophages under the influence of IFN- γ . By looking at the protocols of stimulation of these human macrophages by IFN- γ one can find great diversity in procedures. In one case, MR was downregulated in human macrophages that were treated for 4 days under IFN- γ stimulation (Ambarus et al., 2012). Another paper analysed MR sugar uptake under stimulation by IFN- γ and only noticed a reduction in sugar uptake after 48 hours of incubation with IFN- γ (Mokoena and Gordon, 1985). IFN- γ signalling is mediated by the JAK-STAT pathway, in particular activation of STAT1, which is typically transient, peaking at 15-60 minutes and then resolving, i.e. going back to the baseline at 2-4 hours after stimulation (Ivashkiv, 2018). However, it is apparent that IFN- γ induces a subset of interferon-stimulated genes (ISGs) with delayed kinetics in a manner dependent on new protein synthesis (implying indirect regulation) and also induces a pattern of sustained gene expression that persists beyond the duration of JAK-STAT signalling (Levy et al., 1988, Levy et al., 1990). This might relate to the differences observed in MR expression in human macrophages stimulated by IFN- γ in different periods of time. As mentioned above an assay performed in our lab showed that polymer S100-DP240 reduced STAT-1 activation, although the reduction was not significant.

Future perspectives

The polymers developed in our lab demonstrated many potential clinical applications. The ability of the SO₄-3-Gal GPs to reduce MR surface expression and to negatively affect collagen uptake by human and mouse macrophages may have the potential to interfere

with collagen turnover and consequently on tissue remodelling during inflammation. This may have application in conditions like invasive tumor growth, in which interstitial collagen from the extracellular matrix is extensively degraded and internalized by M2-like TAMs (Madsen et al., 2017). It has been postulated that the density of TAMs correlates with tumor prognosis (Biswas et al., 2013, Zhang et al., 2012). Deletion of MR in mice led to smaller tumor volumes, although not significant, and more intercellular collagen deposition in Lewis lung carcinoma tumors (Madsen et al., 2017). The effect of these GPs on tumor size is not known and might be tested in the future. Current work in the lab is testing the effect of these polymers on spheroids comprised of cancer cells-cancer associated fibroblasts and human macrophages and on tumour growth in mice. An added possibility is to use the knowledge accumulated in polymer synthesis and apply in the development of synthetic drug carriers that would target only TAMs.

Another important action of SO₄-3-Gal GPs that may have its application in cancer biology is the ability to modulate IDO activity in DCs and macrophages. Several tumor types show increased tryptophan metabolism, which in turn associates with poor prognosis (Juhász et al., 2012). Moreover, enhanced IDO activity was observed in tumors, such as in colon cancer, leading to increased cell proliferation in mice (Thaker et al., 2013). In mouse models of ovarian cancer, melanoma and renal cell carcinoma IDO expression correlates with increased angiogenesis (Nonaka et al., 2011). Tryptophan catabolites induce Th1-cell apoptosis and, in addition to inhibition of proliferation of these cells, IDO-dependent tryptophan catabolism could contribute *in vivo* to the regulation of T-cell responses through selective effects on specific lymphocyte subsets (Grohmann et al., 2003). Unequal death of Th1 and Th2 cells has been suggested to contribute to several disease states. The IDO-

kynurenine pathway can serve as a negative feedback loop for Th1 response (Xu et al., 2008). In relation to the IDO inhibition observed in macrophages treated with SO₄-3-Gal GPs, the assay mimics conditions related to infection, due to treatment with IFN- γ and LPS, and it is still unknown how these polymers would act in the context of cancer and preliminary tests are underway. However, it was already shown in an inflammatory model of acute kidney injury caused by ischemia reperfusion injury (IRI), that intravenous injection of S100-DP187 GPs in mice prior to IRI protected these animals against injury (unpublished data). This preliminary data indicated the potential anti-inflammatory effect of these polymers.

The results achieved in this thesis with the SO₄-3-Gal GPs are novel in relation to MR surface blocking, collagen uptake inhibition and IDO inhibition in human macrophages. It adds to the current targeting strategies of MR in immunization and enhanced cross-presentation (Apostolopoulos et al., 2000, Apostolopoulos et al., 2006, Singh et al., 2011) and in gene delivery (Tang et al., 2007). It also opens the possibility to explore cellular activities that could be affected by carbohydrate-based targeting approaches like modulation of cell growth, cell migration or other effector functions such as cytokine release as demonstrated recently using carbohydrate functionalized surfaces (Gentsch et al., 2010). Further work in this thesis highlights the need to consider Endo180 as an alternative collagen-uptake system in human macrophages. The intriguing differences in regulation between MR and Endo180 by IFN- γ and IL-4 in human macrophages deserves further investigation as can lead to novel findings regarding the role of M1 and M2 macrophages in collagen processing.

7. References

- AHMED, M. & NARAIN, R. 2011. The effect of polymer architecture, composition, and molecular weight on the properties of glycopolymer-based non-viral gene delivery systems. *Biomaterials*, 32, 5279-90.
- ALIKHAN, M. A., JONES, C. V., WILLIAMS, T. M., BECKHOUSE, A. G., FLETCHER, A. L., KETT, M. M., SAKKAL, S., SAMUEL, C. S., RAMSAY, R. G., DEANE, J. A., WELLS, C. A., LITTLE, M. H., HUME, D. A. & RICARDO, S. D. 2011. Colony-stimulating factor-1 promotes kidney growth and repair via alteration of macrophage responses. *Am J Pathol*, 179, 1243-56.
- ALLAVENA, P., CHIEPPA, M., BIANCHI, G., SOLINAS, G., FABBRI, M., LASKARIN, G. & MANTOVANI, A. 2010. Engagement of the mannose receptor by tumoral mucins activates an immune suppressive phenotype in human tumor-associated macrophages. *Clin Dev Immunol*, 2010, 547179.
- AMBARUS, C. A., KRAUSZ, S., VAN EIJK, M., HAMANN, J., RADSTAKE, T. R., REEDQUIST, K. A., TAK, P. P. & BAETEN, D. L. 2012. Systematic validation of specific phenotypic markers for in vitro polarized human macrophages. *J Immunol Methods*, 375, 196-206.
- AMBROSI, M., CAMERON, N. R. & DAVIS, B. G. 2005. Lectins: tools for the molecular understanding of the glycode. *Org Biomol Chem*, 3, 1593-608.
- ANDERSEN, M. N., ANDERSEN, N. F., RØDGAARD-HANSEN, S., HOKLAND, M., ABILDGAARD, N. & MØLLER, H. J. 2015. The novel biomarker of alternative macrophage activation, soluble mannose receptor (sMR/sCD206): Implications in multiple myeloma. *Leukemia Research*, 39, 971-975.
- ANDERSON, K., FERNANDEZ, C. & RICE, K. G. 2010. N-glycan targeted gene delivery to the dendritic cell SIGN receptor. *Bioconj Chem*, 21, 1479-85.
- APOSTOLOPOULOS, V., PIETERSZ, G. A., GORDON, S., MARTINEZ-POMARES, L. & MCKENZIE, I. F. 2000. Aldehyde-mannan antigen complexes target the MHC class I antigen-presentation pathway. *Eur J Immunol*, 30, 1714-23.
- APOSTOLOPOULOS, V., PIETERSZ, G. A., TSIBANIS, A., TSIKKINIS, A., DRAKAKI, H., LOVELAND, B. E., PIDDLESSEN, S. J., PLEBANSKI, M., POUNIOTIS, D. S., ALEXIS, M. N., MCKENZIE, I. F. & VASSILAROS, S. 2006. Pilot phase III immunotherapy study in early-stage breast cancer patients using oxidized mannan-MUC1 [ISRCTN71711835]. *Breast Cancer Res*, 8, R27.
- ARNOLD, L., HENRY, A., PORON, F., BABA-AMER, Y., VAN ROOIJEN, N., PLONQUET, A., GHERARDI, R. K. & CHAZAUD, B. 2007. Inflammatory monocytes recruited after skeletal muscle injury switch into antiinflammatory macrophages to support myogenesis. *J Exp Med*, 204, 1057-69.
- ASTHANA, S., GUPTA, P. K., JAISWAL, A. K., DUBE, A. & CHOURASIA, M. K. 2015. Overexpressed Macrophage Mannose Receptor Targeted Nanocapsules- Mediated Cargo Delivery Approach for Eradication of Resident Parasite: In Vitro and In Vivo Studies. *Pharm Res*, 32, 2663-77.
- AZAD, A. K., RAJARAM, M. V. & SCHLESINGER, L. S. 2014. Exploitation of the Macrophage Mannose Receptor (CD206) in Infectious Disease Diagnostics and Therapeutics. *J Cytol Mol Biol*, 1.
- BARTOCCI, A., MASTROGIANNIS, D. S., MIGLIORATI, G., STOCKERT, R. J., WOLKOFF, A. W. & STANLEY, E. R. 1987. Macrophages specifically regulate the concentration of their own growth factor in the circulation. *Proc Natl Acad Sci U S A*, 84, 6179-83.
- BECER, C. R. 2012. The glycopolymer code: synthesis of glycopolymers and multivalent carbohydrate-lectin interactions. *Macromol Rapid Commun*, 33, 742-52.
- BERTOZZI, C. R. & KIESSLING, L. L. 2001. Chemical glycobiology. *Science*, 291, 2357-64.

- BHATIA, S., MOHR, A., MATHUR, D., PARMAR, V. S., HAAG, R. & PRASAD, A. K. 2011. Biocatalytic Route to Sugar-PEG-Based Polymers for Drug Delivery Applications. *Biomacromolecules* [Online], 12.
- BISWAS, S. K., ALLAVENA, P. & MANTOVANI, A. 2013. Tumor-associated macrophages: functional diversity, clinical significance, and open questions. *Semin Immunopathol*, 35, 585-600.
- BONNANS, C., CHOU, J. & WERB, Z. 2014. Remodelling the extracellular matrix in development and disease. *Nat Rev Mol Cell Biol*, 15, 786-801.
- BORNHÖFFT, K. F., GOLDAMMER, T., REBL, A. & GALUSKA, S. P. 2018. Siglecs: A journey through the evolution of sialic acid-binding immunoglobulin-type lectins. *Dev Comp Immunol*, 86, 219-231.
- BRAUNECKER, W. & MATYJASZEWSKI, K. 2007. Controlled/living radical polymerization: features, developments and perspectives. *Prog. Polym. Sci.*, 32, 93-146.
- BROWN, G. D., WILLMENT, J. A. & WHITEHEAD, L. 2018. C-type lectins in immunity and homeostasis. *Nat Rev Immunol*, 18, 374-389.
- CERVENKA, I., AGUDELO, L. Z. & RUAS, J. L. 2017. Kynurenines: Tryptophan's metabolites in exercise, inflammation, and mental health. *Science*, 357.
- CHANPUT, W. P., VERA WICHERS, HARRY 2015. *THP-1 and U937 Cells*.
- CHAVELE, K. M., MARTINEZ-POMARES, L., DOMIN, J., PEMBERTON, S., HASLAM, S. M., DELL, A., COOK, H. T., PUSEY, C. D., GORDON, S. & SALAMA, A. D. 2010. Mannose receptor interacts with Fc receptors and is critical for the development of crescentic glomerulonephritis in mice. *J Clin Invest*, 120, 1469-78.
- CHOMARAT, P. & BANCHEREAU, J. 1998. Interleukin-4 and interleukin-13: their similarities and discrepancies. *Int Rev Immunol*, 17, 1-52.
- CHON, S. Y., HASSANAIN, H. H. & GUPTA, S. L. 1996. Cooperative role of interferon regulatory factor 1 and p91 (STAT1) response elements in interferon-gamma-inducible expression of human indoleamine 2,3-dioxygenase gene. *J Biol Chem*, 271, 17247-52.
- CHON, S. Y., HASSANAIN, H. H., PINE, R. & GUPTA, S. L. 1995. Involvement of two regulatory elements in interferon-gamma-regulated expression of human indoleamine 2,3-dioxygenase gene. *J Interferon Cytokine Res*, 15, 517-26.
- CLOHISY, D. R., BAR-SHAVIT, Z., CHAPPEL, J. C. & TEITELBAUM, S. L. 1987. 1,25-Dihydroxyvitamin D3 modulates bone marrow macrophage precursor proliferation and differentiation. Up-regulation of the mannose receptor. *J Biol Chem*, 262, 15922-9.
- COHEN, M. & VARKI, A. 2010. The sialome--far more than the sum of its parts. *OMICS*, 14, 455-64.
- COUSER, W. G. 1988. Rapidly progressive glomerulonephritis: classification, pathogenetic mechanisms, and therapy. *Am J Kidney Dis*, 11, 449-64.
- CUMMINGS, R. D. 2009. The repertoire of glycan determinants in the human glycome. *Mol Biosyst*, 5, 1087-104.
- CUMMINGS, R. D. & PIERCE, J. M. 2014. The challenge and promise of glycomics. *Chem Biol*, 21, 1-15.
- D'ADDIO, S. M., BALDASSANO, S., SHI, L., CHEUNG, L., ADAMSON, D. H., BRUZEK, M., ANTHONY, J. E., LASKIN, D. L., SINKO, P. J. & PRUD'HOMME, R. K. 2013. Optimization of cell receptor-specific targeting through multivalent surface decoration of polymeric nanocarriers. *J Control Release*, 168, 41-9.
- DAM, T. K. & BREWER, C. F. 2010. Lectins as pattern recognition molecules: the effects of epitope density in innate immunity. *Glycobiology*, 20, 270-9.
- DARNELL, J. E., KERR, I. M. & STARK, G. R. 1994. Jak-STAT pathways and transcriptional activation in response to IFNs and other extracellular signaling proteins. *Science*, 264, 1415-21.

- DAY, Y. J., HUANG, L., YE, H., LINDEN, J. & OKUSA, M. D. 2005. Renal ischemia-reperfusion injury and adenosine 2A receptor-mediated tissue protection: role of macrophages. *Am J Physiol Renal Physiol*, 288, F722-31.
- DE LA MAZA, L. M. & PETERSON, E. M. 1988. Dependence of the in vitro antiproliferative activity of recombinant human gamma-interferon on the concentration of tryptophan in culture media. *Cancer Res*, 48, 346-50.
- DRICKAMER, K. & TAYLOR, M. E. 2015. Recent insights into structures and functions of C-type lectins in the immune system. *Curr Opin Struct Biol*, 34, 26-34.
- DUFFIELD, J. S., TIPPING, P. G., KIPARI, T., CAILHIER, J. F., CLAY, S., LANG, R., BONVENTRE, J. V. & HUGHES, J. 2005. Conditional ablation of macrophages halts progression of crescentic glomerulonephritis. *Am J Pathol*, 167, 1207-19.
- DUNN, K. W., KAMOCCA, M. M. & MCDONALD, J. H. 2011. A practical guide to evaluating colocalization in biological microscopy. *Am J Physiol Cell Physiol*, 300, C723-42.
- EAST, L. & ISACKE, C. M. 2002. The mannose receptor family. *Biochim Biophys Acta*, 1572, 364-86.
- EAST, L., MCCARTHY, A., WIENKE, D., STURGE, J., ASHWORTH, A. & ISACKE, C. M. 2003. A targeted deletion in the endocytic receptor gene Endo180 results in a defect in collagen uptake. *EMBO Rep*, 4, 710-6.
- EAST, L., RUSHTON, S., TAYLOR, M. E. & ISACKE, C. M. 2002. Characterization of sugar binding by the mannose receptor family member, Endo180. *J Biol Chem*, 277, 50469-75.
- EDDIE IP, W. K., TAKAHASHI, K., ALAN EZEKOWITZ, R. & STUART, L. M. 2009. Mannose-binding lectin and innate immunity. *Immunological Reviews*, 230, 9-21.
- EGAN, B. S., ABDOLRASULNIA, R. & SHEPHERD, V. L. 2004. IL-4 modulates transcriptional control of the mannose receptor in mouse FSDC dendritic cells. *Arch Biochem Biophys*, 428, 119-30.
- ENGELHOLM, L. H., INGVARSEN, S., JÜRGENSEN, H. J., HILLIG, T., MADSEN, D. H., NIELSEN, B. S. & BEHRENDT, N. 2009. The collagen receptor uPARAP/Endo180. *Front Biosci (Landmark Ed)*, 14, 2103-14.
- ENGERING, A. J., CELLA, M., FLUITSMA, D., BROCKHAUS, M., HOEFESMIT, E. C., LANZAVECCHIA, A. & PIETERS, J. 1997. The mannose receptor functions as a high capacity and broad specificity antigen receptor in human dendritic cells. *Eur J Immunol*, 27, 2417-25.
- EVERTS, V., VAN DER ZEE, E., CREEMERS, L. & BEERTSEN, W. 1996. Phagocytosis and intracellular digestion of collagen, its role in turnover and remodelling. *Histochem J*, 28, 229-45.
- EZEKOWITZ, R. A., SASTRY, K., BAILLY, P. & WARNER, A. 1990. Molecular characterization of the human macrophage mannose receptor: demonstration of multiple carbohydrate recognition-like domains and phagocytosis of yeasts in Cos-1 cells. *J Exp Med*, 172, 1785-94.
- FALLARINO, F., GROHMANN, U., VACCA, C., BIANCHI, R., ORABONA, C., SPRECA, A., FIORETTI, M. C. & PUCCHETTI, P. 2002. T cell apoptosis by tryptophan catabolism. *Cell Death Differ*, 9, 1069-77.
- FALLON, P. G., JOLIN, H. E., SMITH, P., EMSON, C. L., TOWNSEND, M. J., FALLON, R. & MCKENZIE, A. N. 2002. IL-4 induces characteristic Th2 responses even in the combined absence of IL-5, IL-9, and IL-13. *Immunity*, 17, 7-17.
- FIELDS, G. B. 2013. Interstitial collagen catabolism. *J Biol Chem*, 288, 8785-93.
- FRITZ, J. M., TENNIS, M. A., ORLICKY, D. J., LIN, H., JU, C., REDENTE, E. F., CHOO, K. S., STAAB, T. A., BOUCHARD, R. J., MERRICK, D. T., MALKINSON, A. M. & DWYER-NIELD, L. D. 2014. Depletion of tumor-associated macrophages slows the growth of chemically induced mouse lung adenocarcinomas. *Front Immunol*, 5, 587.

- FRUMENTO, G., ROTONDO, R., TONETTI, M., DAMONTE, G., BENATTI, U. & FERRARA, G. B. 2002. Tryptophan-derived catabolites are responsible for inhibition of T and natural killer cell proliferation induced by indoleamine 2,3-dioxygenase. *J Exp Med*, 196, 459-68.
- FUJIGAKI, H., SAITO, K., FUJIGAKI, S., TAKEMURA, M., SUDO, K., ISHIGURO, H. & SEISHIMA, M. 2006. The signal transducer and activator of transcription 1 α and interferon regulatory factor 1 are not essential for the induction of indoleamine 2,3-dioxygenase by lipopolysaccharide: involvement of p38 mitogen-activated protein kinase and nuclear factor- κ B pathways, and synergistic effect of several proinflammatory cytokines. *J Biochem*, 139, 655-62.
- FUJIGAKI, S., SAITO, K., SEKIKAWA, K., TONE, S., TAKIKAWA, O., FUJII, H., WADA, H., NOMA, A. & SEISHIMA, M. 2001. Lipopolysaccharide induction of indoleamine 2,3-dioxygenase is mediated dominantly by an IFN- γ -independent mechanism. *Eur J Immunol*, 31, 2313-8.
- GARFOOT, A. L., SHEN, Q., WÜTHRICH, M., KLEIN, B. S. & RAPPLEYE, C. A. 2016. The Eng1 β -Glucanase Enhances Histoplasma Virulence by Reducing β -Glucan Exposure. *MBio*, 7, e01388-15.
- GAZI, U. & MARTINEZ-POMARES, L. 2009. Influence of the mannose receptor in host immune responses. *Immunobiology*, 214, 554-61.
- GEIJTENBEEK, T. B. & GRINGHUIS, S. I. 2016. C-type lectin receptors in the control of T helper cell differentiation. *Nat Rev Immunol*, 16, 433-48.
- GEISSMANN, F., MANZ, M. G., JUNG, S., SIEWEKE, M. H., MERAD, M. & LEY, K. 2010. Development of monocytes, macrophages, and dendritic cells. *Science*, 327, 656-61.
- GENTSCH, R., PIPPIG, F., NILLES, K., THEATO, P., KIKKERI, R., MAGLINAO, M., LEPENIES, B., PETER H. SEEBERGER, # & AND HANS G. BÉORNER*. 2010. Modular Approach toward Bioactive Fiber Meshes
- Carrying Oligosaccharides. *Macromolecules* [Online], 43.
- GINHOUX, F. & JUNG, S. 2014. Monocytes and macrophages: developmental pathways and tissue homeostasis. *Nat Rev Immunol*, 14, 392-404.
- GLASS, C. K. & NATOLI, G. 2016. Molecular control of activation and priming in macrophages. *Nat Immunol*, 17, 26-33.
- GODULA, K. & BERTOZZI, C. R. 2012. Density Variant Glycan Microarray for Evaluating Cross-Linking of Mucin-like Glycoconjugates by Lectins. *Journal of the American Chemical Society*, 134, 15732-15742.
- GOLDSTEIN, J. L., ANDERSON, R. G. & BROWN, M. S. 1979. Coated pits, coated vesicles, and receptor-mediated endocytosis. *Nature*, 279, 679-85.
- GORDON, S. 2003. Alternative activation of macrophages. *Nat Rev Immunol*, 3, 23-35.
- GORDON, S., MARTINEZ-POMARES, L. & 2017. Physiological roles of macrophages. *Pflügers Archiv - European Journal of Physiology*, 469.
- GRIFFIN, J. D., RITZ, J., NADLER, L. M. & SCHLOSSMAN, S. F. 1981. Expression of myeloid differentiation antigens on normal and malignant myeloid cells. *J Clin Invest*, 68, 932-41.
- GROHMANN, U., FALLARINO, F. & PUCETTI, P. 2003. Tolerance, DCs and tryptophan: much ado about IDO. *Trends Immunol*, 24, 242-8.
- GRØNBÆK, H., RØDGAARD-HANSEN, S., AAGAARD, N. K., ARROYO, V., MOESTRUP, S. K., GARCIA, E., SOLÀ, E., DOMENICALI, M., PIANO, S., VILSTRUP, H., MØLLER, H. J. & CONSORTIUM, C. S. I. O. T. E.-C. 2016. Macrophage activation markers predict mortality in patients with liver cirrhosis without or with acute-on-chronic liver failure (ACLF). *J Hepatol*, 64, 813-22.
- HARRIS, N., SUPER, M., RITS, M., CHANG, G. & EZEKOWITZ, R. A. 1992. Characterization of the murine macrophage mannose receptor: demonstration that the downregulation of receptor expression mediated

- by interferon-gamma occurs at the level of transcription. *Blood*, 80, 2363-73.
- HOWARD, M., FARRAR, J., HILFIKER, M., JOHNSON, B., TAKATSU, K., HAMAOKA, T. & PAUL, W. E. 1982. Identification of a T cell-derived b cell growth factor distinct from interleukin 2. *J Exp Med*, 155, 914-23.
- HU, X. & IVASHKIV, L. B. 2009. Cross-regulation of signaling pathways by interferon-gamma: implications for immune responses and autoimmune diseases. *Immunity*, 31, 539-50.
- HUDAK, J. E. & BERTOZZI, C. R. 2014. Glycotherapy: new advances inspire a reemergence of glycans in medicine. *Chem Biol*, 21, 16-37.
- HUEN, S. C. & CANTLEY, L. G. 2015. Macrophage-mediated injury and repair after ischemic kidney injury. *Pediatr Nephrol*, 30, 199-209.
- HWU, P., DU, M. X., LAPOINTE, R., DO, M., TAYLOR, M. W. & YOUNG, H. A. 2000. Indoleamine 2,3-dioxygenase production by human dendritic cells results in the inhibition of T cell proliferation. *J Immunol*, 164, 3596-9.
- HYNES, R. O. 2009. The extracellular matrix: not just pretty fibrils. *Science*, 326, 1216-9.
- IVASHKIV, L. B. 2018. IFN γ : signalling, epigenetics and roles in immunity, metabolism, disease and cancer immunotherapy. *Nat Rev Immunol*, 18, 545-558.
- JAIN, K., KESHARWANI, P., GUPTA, U. & JAIN, N. K. 2012. A review of glycosylated carriers for drug delivery. *Biomaterials*, 33, 4166-86.
- JO, S. K., SUNG, S. A., CHO, W. Y., GO, K. J. & KIM, H. K. 2006. Macrophages contribute to the initiation of ischaemic acute renal failure in rats. *Nephrol Dial Transplant*, 21, 1231-9.
- JOHANNSEN, T. & LEPENIES, B. 2017. Glycan-Based Cell Targeting To Modulate Immune Responses. *Trends Biotechnol*, 35, 334-346.
- JOHNSON, J. L., JONES, M. B., RYAN, S. O. & COBB, B. A. 2013. The regulatory power of glycans and their binding partners in immunity. *Trends Immunol*, 34, 290-8.
- JOSHI, M. D., UNGER, W. J., STORM, G., VAN KOOYK, Y. & MASTROBATTISTA, E. 2012. Targeting tumor antigens to dendritic cells using particulate carriers. *J Control Release*, 161, 25-37.
- JUHÁSZ, C., CHUGANI, D. C., BARGER, G. R., KUPSKY, W. J., CHAKRABORTY, P. K., MUZIK, O. & MITTAL, S. 2012. Quantitative PET imaging of tryptophan accumulation in gliomas and remote cortex: correlation with tumor proliferative activity. *Clin Nucl Med*, 37, 838-42.
- JUNG, I. D., LEE, C. M., JEONG, Y. I., LEE, J. S., PARK, W. S., HAN, J. & PARK, Y. M. 2007. Differential regulation of indoleamine 2,3-dioxygenase by lipopolysaccharide and interferon gamma in murine bone marrow derived dendritic cells. *FEBS Lett*, 581, 1449-56.
- JÜRGENSEN, H. J., MADSEN, D. H., INGVARSEN, S., MELANDER, M. C., GÅRDSVOLL, H., PATTHY, L., ENGELHOLM, L. H. & BEHRENDT, N. 2011. A novel functional role of collagen glycosylation: interaction with the endocytic collagen receptor uparap/ENDO180. *J Biol Chem*, 286, 32736-48.
- KAKU, Y., IMAOKA, H., MORIMATSU, Y., KOMOHARA, Y., OHNISHI, K., ODA, H., TAKENAKA, S., MATSUOKA, M., KAWAYAMA, T., TAKEYA, M. & HOSHINO, T. 2014. Overexpression of CD163, CD204 and CD206 on alveolar macrophages in the lungs of patients with severe chronic obstructive pulmonary disease. *PLoS ONE*, 9, 1-8.
- KANEKO, Y., NIMMERJAHN, F., MADAIIO, M. P. & RAVETCH, J. V. 2006. Pathology and protection in nephrotoxic nephritis is determined by selective engagement of specific Fc receptors. *J Exp Med*, 203, 789-97.
- KATO, M., KAMIGAITO, M., SAWAMOTO, M. & HIGASHIMURAS, T. 1996. Polymerization of Methyl Methacrylate with the Carbon. 1721--1723.

- KELER, T., RAMAKRISHNA, V. & FANGER, M. W. 2004. Mannose receptor-targeted vaccines. *Expert Opin Biol Ther*, 4, 1953-62.
- KELLY-WELCH, A. E., HANSON, E. M., BOOTHBY, M. R. & KEEGAN, A. D. 2003. Interleukin-4 and interleukin-13 signaling connections maps. *Science*, 300, 1527-8.
- KIM, M. G., KIM, S. C., KO, Y. S., LEE, H. Y., JO, S. K. & CHO, W. 2015. The Role of M2 Macrophages in the Progression of Chronic Kidney Disease following Acute Kidney Injury. *PLoS One*, 10, e0143961.
- KITCHING, A. R., HOLDSWORTH, S. R. & TIPPING, P. G. 1999. IFN-gamma mediates crescent formation and cell-mediated immune injury in murine glomerulonephritis. *J Am Soc Nephrol*, 10, 752-9.
- KONO, H. & ROCK, K. L. 2008. How dying cells alert the immune system to danger. *Nat Rev Immunol*, 8, 279-89.
- KUIPERS, H. & LAMBRECHT, B. N. 2004. The interplay of dendritic cells, Th2 cells and regulatory T cells in asthma. *Curr Opin Immunol*, 16, 702-8.
- KÜHN, R., RAJEWSKY, K. & MÜLLER, W. 1991. Generation and analysis of interleukin-4 deficient mice. *Science*, 254, 707-10.
- KÜMMERLE-DESCHNER, J. B., HOFFMANN, M. K., NIETHAMMER, D. & DANNECKER, G. E. 1998. Pediatric rheumatology: autoimmune mechanisms and therapeutic strategies. *Immunol Today*, 19, 250-3.
- L VAN DE VEN, A., ADLER-STORHYZ, K. & RICHARDS-KORTUM, R. 2009. Delivery of Optical Contrast Agents using Triton-X100, Part 1: Reversible permeabilization of live cells for intracellular labeling. J Biomed Opt [Online].**
- LADMIRAL, V., MANTOVANI, G., CLARKSON, G. J., CAUET, S., IRWIN, J. L. & HADDLETON, D. M. 2006. Synthesis of Neoglycopolymers by a Combination of "Click Chemistry" and Living Radical Polymerization. *J. Am. Chem. Soc.*, 128, 4823-4830.
- LAOUI, D., VAN OVERMEIRE, E., DE BAETSELIER, P., VAN GINDERACHTER, J. A. & RAES, G. 2014. Functional Relationship between Tumor-Associated Macrophages and Macrophage Colony-Stimulating Factor as Contributors to Cancer Progression. *Front Immunol*, 5, 489.
- LAWRENCE, T. & NATOLI, G. 2011. Transcriptional regulation of macrophage polarization: enabling diversity with identity. *Nat Rev Immunol*, 11, 750-61.
- LEE, Y. & LEE, R. 1995. Carbohydrate - Protein interactions: Basis of Glycobiology. *Accounts of Chemical Research*, 28.
- LEPENIES, B., LEE, J. & SONKARIA, S. 2013. Targeting C-type lectin receptors with multivalent carbohydrate ligands. *Adv Drug Deliv Rev*, 65, 1271-81.
- LEPENIES, B. & SEEBERGER, P. H. 2014. Simply better glycoproteins. *Nat Biotechnol*, 32, 443-5.
- LETEUX, C., CHAI, W., LOVELESS, R. W., YUEN, C. T., UHLIN-HANSEN, L., COMBARNOUS, Y., JANKOVIC, M., MARIC, S. C., MISULOVIN, Z., NUSSENZWEIG, M. C. & FEIZI, T. 2000. The cysteine-rich domain of the macrophage mannose receptor is a multispecific lectin that recognizes chondroitin sulfates A and B and sulfated oligosaccharides of blood group Lewis(a) and Lewis(x) types in addition to the sulfated N-glycans of lutropin. *J Exp Med*, 191, 1117-26.
- LEVY, D. E., KESSLER, D. S., PINE, R., REICH, N. & DARNELL, J. E. 1988. Interferon-induced nuclear factors that bind a shared promoter element correlate with positive and negative transcriptional control. *Genes Dev*, 2, 383-93.
- LEVY, D. E., LEW, D. J., DECKER, T., KESSLER, D. S. & DARNELL, J. E. 1990. Synergistic interaction between interferon-alpha and interferon-gamma through induced synthesis of one subunit of the transcription factor ISGF3. *EMBO J*, 9, 1105-11.

- LIN, S. L., CASTAÑO, A. P., NOWLIN, B. T., LUPHER, M. L. & DUFFIELD, J. S. 2009. Bone marrow Ly6Chigh monocytes are selectively recruited to injured kidney and differentiate into functionally distinct populations. *J Immunol*, 183, 6733-43.
- LINEHAN, S. A., MARTÍNEZ-POMARES, L., DA SILVA, R. P. & GORDON, S. 2001. Endogenous ligands of carbohydrate recognition domains of the mannose receptor in murine macrophages, endothelial cells and secretory cells; potential relevance to inflammation and immunity. *Eur J Immunol*, 31, 1857-66.
- LING, G. S., BENNETT, J., WOOLLARD, K. J., SZAJNA, M., FOSSATI-JIMACK, L., TAYLOR, P. R., SCOTT, D., FRANZOSO, G., COOK, H. T. & BOTTO, M. 2014. Integrin CD11b positively regulates TLR4-induced signalling pathways in dendritic cells but not in macrophages. *Nat Commun*, 5, 3039.
- LIU, Y., CHIRINO, A. J., MISULOVIN, Z., LETEUX, C., FEIZI, T., NUSSENZWEIG, M. C. & BJORKMAN, P. J. 2000. Crystal structure of the cysteine-rich domain of mannose receptor complexed with a sulfated carbohydrate ligand. *J Exp Med*, 191, 1105-16.
- LOCKE, L. W., MAYO, M. W., YOO, A. D., WILLIAMS, M. B. & BERR, S. S. 2012. PET imaging of tumor associated macrophages using mannose coated 64Cu liposomes. *Biomaterials*, 33, 7785-93.
- MADSEN, D. H. & BUGGE, T. H. 2013. Imaging collagen degradation in vivo highlights a key role for M2-polarized macrophages in extracellular matrix degradation. *Oncoimmunology*, 2, e27127.
- MADSEN, D. H., ENGELHOLM, L. H., INGVARSEN, S., HILLIG, T., WAGENAAR-MILLER, R. A., KJØLLER, L., GÅRDSVOLL, H., HØYER-HANSEN, G., HOLMBECK, K., BUGGE, T. H. & BEHRENDT, N. 2007. Extracellular collagenases and the endocytic receptor, urokinase plasminogen activator receptor-associated protein/Endo180, cooperate in fibroblast-mediated collagen degradation. *J Biol Chem*, 282, 27037-45.
- MADSEN, D. H., INGVARSEN, S., JÜRGENSEN, H. J., MELANDER, M. C., KJØLLER, L., MOYER, A., HONORÉ, C., MADSEN, C. A., GARRED, P., BURGDORF, S., BUGGE, T. H., BEHRENDT, N. & ENGELHOLM, L. H. 2011. The non-phagocytic route of collagen uptake: a distinct degradation pathway. *J Biol Chem*, 286, 26996-7010.
- MADSEN, D. H., JÜRGENSEN, H. J., SIERSBÆK, M. S., KUCZEK, D. E., GREY CLOUD, L., LIU, S., BEHRENDT, N., GRØNTVED, L., WEIGERT, R. & BUGGE, T. H. 2017. Tumor-Associated Macrophages Derived from Circulating Inflammatory Monocytes Degrade Collagen through Cellular Uptake. *Cell Rep*, 21, 3662-3671.
- MADSEN, D. H., LEONARD, D., MASEDUNSKAS, A., MOYER, A., JÜRGENSEN, H. J., PETERS, D. E., AMORNPHIMOLTHAM, P., SELVARAJ, A., YAMADA, S. S., BRENNER, D. A., BURGDORF, S., ENGELHOLM, L. H., BEHRENDT, N., HOLMBECK, K., WEIGERT, R. & BUGGE, T. H. 2013. M2-like macrophages are responsible for collagen degradation through a mannose receptor-mediated pathway. *J Cell Biol*, 202, 951-66.
- MAGENNIS, E. P., FRANCINI, N., MASTROTTO, F., CATANIA, R., REDHEAD, M., FERNANDEZ-TRILLO, F., BRADSHAW, D., CHURCHLEY, D., WINZER, K., ALEXANDER, C. & MANTOVANI, G. 2017. Polymers for binding of the gram-positive oral pathogen *Streptococcus mutans*. *PLOS ONE*, 12, e0180087.
- MAMMEN, M., CHOI, S. K. & WHITESIDES, G. M. 1998. Polyvalent Interactions in Biological Systems: Implications for Design and Use of Multivalent Ligands and Inhibitors. *Angew Chem Int Ed Engl*, 37, 2754-2794.
- MANNING, D. D., HU, X., BECK, P. & KIESSLING, L. L. 1997. Synthesis of sulfated neoglycopolymers: Selective P-selectin inhibitors. *Journal of the American Chemical Society*, 119, 3161-3162.

- MANTOVANI, A., BOTTAZZI, B., COLOTTA, F., SOZZANI, S. & RUCO, L. 1992. The origin and function of tumor-associated macrophages. *Immunol Today*, 13, 265-70.
- MANTOVANI, A., SICA, A., SOZZANI, S., ALLAVENA, P., VECCHI, A. & LOCATI, M. 2004. The chemokine system in diverse forms of macrophage activation and polarization. *Trends Immunol*, 25, 677-86.
- MARTH, J. D. & GREWAL, P. K. 2008. Mammalian glycosylation in immunity. *Nat Rev Immunol*, 8, 874-87.
- MARTINEZ, F. O., HELMING, L. & GORDON, S. 2009. Alternative activation of macrophages: an immunologic functional perspective. *Annu Rev Immunol*, 27, 451-83.
- MARTINEZ-POMARES, L. 2012. The mannose receptor. *J Leukoc Biol*, 92, 1177-86.
- MARTINEZ-POMARES, L., HANITSCH, L. G., STILLION, R., KESHAV, S. & GORDON, S. 2005. Expression of mannose receptor and ligands for its cysteine-rich domain in venous sinuses of human spleen. *Lab Invest*, 85, 1238-49.
- MARTINEZ-POMARES, L., REID, D. M., BROWN, G. D., TAYLOR, P. R., STILLION, R. J., LINEHAN, S. A., ZAMZE, S., GORDON, S. & WONG, S. Y. 2003. Analysis of mannose receptor regulation by IL-4, IL-10, and proteolytic processing using novel monoclonal antibodies. *J Leukoc Biol*, 73, 604-13.
- MARTINEZ-POMARES, L., WIENKE, D., STILLION, R., MCKENZIE, E. J., ARNOLD, J. N., HARRIS, J., MCGREAL, E., SIM, R. B., ISACKE, C. M. & GORDON, S. 2006a. Carbohydrate-independent recognition of collagens by the macrophage mannose receptor. *European Journal of Immunology*, 36, 1074-1082.
- MARTINEZ-POMARES, L., WIENKE, D., STILLION, R., MCKENZIE, E. J., ARNOLD, J. N., HARRIS, J., MCGREAL, E., SIM, R. B., ISACKE, C. M. & GORDON, S. 2006b. Carbohydrate-independent recognition of collagens by the macrophage mannose receptor. *Eur J Immunol*, 36, 1074-82.
- MATYJASZEWSKI, K. 1999. Lifetimes of Polystyrene Chains in Atom Transfer Radical Polymerization. *Macromolecules*, 32, 9051--9053.
- MCKENZIE, G. J., EMSON, C. L., BELL, S. E., ANDERSON, S., FALLON, P., ZURAWSKI, G., MURRAY, R., GRENCIS, R. & MCKENZIE, A. N. 1998. Impaired development of Th2 cells in IL-13-deficient mice. *Immunity*, 9, 423-32.
- MCKENZIE, G. J., FALLON, P. G., EMSON, C. L., GRENCIS, R. K. & MCKENZIE, A. N. 1999. Simultaneous disruption of interleukin (IL)-4 and IL-13 defines individual roles in T helper cell type 2-mediated responses. *J Exp Med*, 189, 1565-72.
- MELLOR, A. L. & MUNN, D. H. 2004. IDO expression by dendritic cells: tolerance and tryptophan catabolism. *Nat Rev Immunol*, 4, 762-74.
- MILLS, C. D. 2012. M1 and M2 Macrophages: Oracles of Health and Disease. *Crit Rev Immunol*, 32, 463-88.
- MILLS, C. D., LENZ, L. L. & LEY, K. 2015. Macrophages at the fork in the road to health or disease. *Front Immunol*, 6, 59.
- MILLS, C. D. & LEY, K. 2014. M1 and M2 macrophages: the chicken and the egg of immunity. *J Innate Immun*, 6, 716-26.
- MIURA, Y. 2007. Synthesis and biological application of glycopolymers. 45.
- MOAD, G., CHONG, Y., POSTMA, A., RIZZARDO, E. & THANG, S. 2005. Advances in RAFT polymerization: the synthesis of polymers with defined end-groups. *Polymer*, 46.
- MOAD, G., RIZZARDO, E. & THANG, S. 2008. Radical addition-fragmentation chemistry in polymer synthesis. 49.
- MOFFETT, J. R. & NAMBOODIRI, M. A. 2003. Tryptophan and the immune response. *Immunol Cell Biol*, 81, 247-65.

- MOKOENA, T. & GORDON, S. 1985. Human macrophage activation. Modulation of mannosyl, fucosyl receptor activity in vitro by lymphokines, gamma and alpha interferons, and dexamethasone. *J Clin Invest*, 75, 624-31.
- MOSSER, D. M. 2003. The many faces of macrophage activation. *J Leukoc Biol*, 73, 209-12.
- MOSSER, D. M. & EDWARDS, J. P. 2008. Exploring the full spectrum of macrophage activation. *Nat Rev Immunol*, 8, 958-69.
- MUNN, D. H., SHAFIZADEH, E., ATTWOOD, J. T., BONDAREV, I., PASHINE, A. & MELLOR, A. L. 1999. Inhibition of T cell proliferation by macrophage tryptophan catabolism. *J Exp Med*, 189, 1363-72.
- MUNN, D. H., SHARMA, M. D., LEE, J. R., JHAVER, K. G., JOHNSON, T. S., KESKIN, D. B., MARSHALL, B., CHANDLER, P., ANTONIA, S. J., BURGESS, R., SLINGLUFF, C. L. & MELLOR, A. L. 2002. Potential regulatory function of human dendritic cells expressing indoleamine 2,3-dioxygenase. *Science*, 297, 1867-70.
- MUNTAKA, S., ALMUHANNA, Y., JACKSON, D., SINGH, S., AFRYIE-ASANTE, A., CÁMARA, M. & MARTÍNEZ-POMARES, L. 2019. Gamma Interferon and Interleukin-17A Differentially Influence the Response of Human Macrophages and Neutrophils to *Pseudomonas aeruginosa* Infection. *Infect Immun*, 87.
- MUTHUKRISHNAN, S., NITSCHKE, M., GRAMM, S., OZYÜREK, Z., VOIT, B., WERNER, C. & MÜLLER, A. H. 2006. Immobilized hyperbranched glycoacrylate films as bioactive supports. *Macromol Biosci*, 6, 658-66.
- MÁNDI, Y. & VÉCSEI, L. 2012. The kynurenine system and immunoregulation. *J Neural Transm (Vienna)*, 119, 197-209.
- NAPPER, C. E., DRICKAMER, K. & TAYLOR, M. E. 2006a. Collagen binding by the mannose receptor mediated through the fibronectin type II domain. *The Biochemical journal*, 395, 579-586.
- NAPPER, C. E., DRICKAMER, K. & TAYLOR, M. E. 2006b. Collagen binding by the mannose receptor mediated through the fibronectin type II domain. *Biochem J*, 395, 579-86.
- NELMS, K., KEEGAN, A. D., ZAMORANO, J., RYAN, J. J. & PAUL, W. E. 1999. The IL-4 receptor: signaling mechanisms and biologic functions. *Annu Rev Immunol*, 17, 701-38.
- NONAKA, H., SAGA, Y., FUJIWARA, H., AKIMOTO, H., YAMADA, A., KAGAWA, S., TAKEI, Y., MACHIDA, S., TAKIKAWA, O. & SUZUKI, M. 2011. Indoleamine 2,3-dioxygenase promotes peritoneal dissemination of ovarian cancer through inhibition of natural killer cell function and angiogenesis promotion. *Int J Oncol*, 38, 113-20.
- OEZYÜREK, Z., FRANKE, K., NITSCHKE, M., SCHULZE, R., SIMON, F., EICHHORN, K. J., POMPE, T., WERNER, C. & VOIT, B. 2009. Sulfated glyco-block copolymers with specific receptor and growth factor binding to support cell adhesion and proliferation. *Biomaterials*, 30, 1026-35.
- OGATA, M., HIDARI, K. I., KOZAKI, W., MURATA, T., HIRATAKE, J., PARK, E. Y., SUZUKI, T. & USUI, T. 2009. Molecular design of spacer-N-linked sialoglycopolyptide as polymeric inhibitors against influenza virus infection. *Biomacromolecules*, 10, 1894-903.
- OHNISHI, H., OKA, K., MIZUNO, S. & NAKAMURA, T. 2012. Identification of mannose receptor as receptor for hepatocyte growth factor β -chain: novel ligand-receptor pathway for enhancing macrophage phagocytosis. *J Biol Chem*, 287, 13371-81.
- OHTSUBO, K. & MARTH, J. D. 2006. Glycosylation in cellular mechanisms of health and disease. *Cell*, 126, 855-67.
- OUCHI, M., BADI, N., LUTZ, J. F. & SAWAMOTO, M. 2011. Single-chain technology using discrete synthetic macromolecules. *Nat Chem*, 3, 917-24.

- OZAKI, Y., EDELSTEIN, M. P. & DUCH, D. S. 1988. Induction of indoleamine 2,3-dioxygenase: a mechanism of the antitumor activity of interferon gamma. *Proc Natl Acad Sci U S A*, 85, 1242-6.
- PANDIT, J., BOHM, A., JANCARIK, J., HALENBECK, R., KOTHS, K. & KIM, S. H. 1992. Three-dimensional structure of dimeric human recombinant macrophage colony-stimulating factor. *Science*, 258, 1358-62.
- PARAMESWARAN, N. & PATIAL, S. 2010. Tumor necrosis factor- α signaling in macrophages. *Crit Rev Eukaryot Gene Expr*, 20, 87-103.
- PARK, J. S., GAMBONI-ROBERTSON, F., HE, Q., SVETKAUSKAITE, D., KIM, J. Y., STRASSHEIM, D., SOHN, J. W., YAMADA, S., MARUYAMA, I., BANERJEE, A., ISHIZAKA, A. & ABRAHAM, E. 2006. High mobility group box 1 protein interacts with multiple Toll-like receptors. *Am J Physiol Cell Physiol*, 290, C917-24.
- PERNIS, A. B. & ROTHMAN, P. B. 2002. JAK-STAT signaling in asthma. *J Clin Invest*, 109, 1279-83.
- PFEFFERKORN, E. R. 1984. Interferon gamma blocks the growth of *Toxoplasma gondii* in human fibroblasts by inducing the host cells to degrade tryptophan. *Proc Natl Acad Sci U S A*, 81, 908-12.
- PINCETIC, A., BOURNAZOS, S., DILILLO, D. J., MAAMARY, J., WANG, T. T., DAHAN, R., FIEBIGER, B. M. & RAVETCH, J. V. 2014. Type I and type II Fc receptors regulate innate and adaptive immunity. *Nat Immunol*, 15, 707-16.
- PINE, R., DECKER, T., KESSLER, D. S., LEVY, D. E. & DARNELL, J. E. 1990. Purification and cloning of interferon-stimulated gene factor 2 (ISGF2): ISGF2 (IRF-1) can bind to the promoters of both beta interferon- and interferon-stimulated genes but is not a primary transcriptional activator of either. *Mol Cell Biol*, 10, 2448-57.
- PIXLEY, F. J. & STANLEY, E. R. 2004. CSF-1 regulation of the wandering macrophage: complexity in action. *Trends Cell Biol*, 14, 628-38.
- PUC CETTI, P. & GROHMANN, U. 2007. IDO and regulatory T cells: a role for reverse signalling and non-canonical NF-kappaB activation. *Nat Rev Immunol*, 7, 817-23.
- RABINOVICH, G. A., VAN KOOYK, Y. & COBB, B. A. 2012. Glycobiology of immune responses. *Ann N Y Acad Sci*, 1253, 1-15.
- RAUCH, I., MÜLLER, M. & DECKER, T. 2013. The regulation of inflammation by interferons and their STATs. *JAKSTAT*, 2, e23820.
- REDELINGHUYS, P. & BROWN, G. D. 2011. Inhibitory C-type lectin receptors in myeloid cells. *Immunol Lett*, 136, 1-12.
- ROGERS, N. M., FERENBACH, D. A., ISENBERG, J. S., THOMSON, A. W. & HUGHES, J. 2014. Dendritic cells and macrophages in the kidney: a spectrum of good and evil. *Nat Rev Nephrol*, 10, 625-43.
- ROYER, P. J., EMARA, M., YANG, C., AL-GHOULEH, A., TIGHE, P., JONES, N., SEWELL, H. F., SHAKIB, F., MARTINEZ-POMARES, L. & GHAEMMAGHAMI, A. M. 2010. The mannose receptor mediates the uptake of diverse native allergens by dendritic cells and determines allergen-induced T cell polarization through modulation of IDO activity. *J Immunol*, 185, 1522-31.
- RUPPERT, J., SCHÜTT, C., OSTERMEIER, D. & PETERS, J. H. 1993. Down-regulation and release of CD14 on human monocytes by IL-4 depends on the presence of serum or GM-CSF. *Adv Exp Med Biol*, 329, 281-6.
- RÓSZER, T. 2015. Understanding the Mysterious M2 Macrophage through Activation Markers and Effector Mechanisms. *Mediators Inflamm*, 2015, 816460.
- SALAZAR, F., HALL, L., NEGM, O. H., AWUAH, D., TIGHE, P. J., SHAKIB, F. & GHAEMMAGHAMI, A. M. 2016. The mannose receptor negatively modulates the Toll-like receptor 4-aryl hydrocarbon receptor-indoleamine

- 2,3-dioxygenase axis in dendritic cells affecting T helper cell polarization. *J Allergy Clin Immunol*, 137, 1841-1851.e2.
- SANCHO, D. & REIS E SOUSA, C. 2012. Signaling by myeloid C-type lectin receptors in immunity and homeostasis. *Annu Rev Immunol*, 30, 491-529.
- SANCHO, D. & REIS E SOUSA, C. 2013. Sensing of cell death by myeloid C-type lectin receptors. *Curr Opin Immunol*, 25, 46-52.
- SCHMIDT, B. V., FECHLER, N., FALKENHAGEN, J. & LUTZ, J. F. 2011. Controlled folding of synthetic polymer chains through the formation of positionable covalent bridges. *Nat Chem*, 3, 234-38.
- SCHNAAR, R. L. 2016. Glycobiology simplified: diverse roles of glycan recognition in inflammation. *J Leukoc Biol*.
- SCHREIBER, S., BLUM, J. S., CHAPPEL, J. C., STENSON, W. F., STAHL, P. D., TEITELBAUM, S. L. & PERKINS, S. L. 1990. Prostaglandin E specifically upregulates the expression of the mannose-receptor on mouse bone marrow-derived macrophages. *Cell Regul*, 1, 403-13.
- SCHREIBER, S., STENSON, W. F., MACDERMOTT, R. P., CHAPPEL, J. C., TEITELBAUM, S. L. & PERKINS, S. L. 1991. Aggregated bovine IgG inhibits mannose receptor expression of murine bone marrow-derived macrophages via activation. *J Immunol*, 147, 1377-82.
- SCHRÖCKSNADDEL, K., WIRLEITNER, B., WINKLER, C. & FUCHS, D. 2006. Monitoring tryptophan metabolism in chronic immune activation. *Clin Chim Acta*, 364, 82-90.
- SCHWEIZER, A., STAHL, P. D. & ROHRER, J. 2000. A di-aromatic motif in the cytosolic tail of the mannose receptor mediates endosomal sorting. *J Biol Chem*, 275, 29694-700.
- SHEIKH, H., YARWOOD, H., ASHWORTH, A. & ISACKE, C. M. 2000. Endo180, an endocytic recycling glycoprotein related to the macrophage mannose receptor is expressed on fibroblasts, endothelial cells and macrophages and functions as a lectin receptor. *J Cell Sci*, 113 (Pt 6), 1021-32.
- SHEPHERD, V. L. & HOIDAL, J. R. 1990. Clearance of neutrophil-derived myeloperoxidase by the macrophage mannose receptor. *Am J Respir Cell Mol Biol*, 2, 335-40.
- SHEPHERD, V. L., KONISHI, M. G. & STAHL, P. 1985. Dexamethasone increases expression of mannose receptors and decreases extracellular lysosomal enzyme accumulation in macrophages. *J Biol Chem*, 260, 160-4.
- SHEPHERD, V. L., LEE, Y. C., SCHLESINGER, P. H. & STAHL, P. D. 1981. L-Fucose-terminated glycoconjugates are recognized by pinocytosis receptors on macrophages. *Proc Natl Acad Sci U S A*, 78, 1019-22.
- SICA, A. & MANTOVANI, A. 2012. Macrophage plasticity and polarization: in vivo veritas. *J Clin Invest*, 122, 787-95.
- SINGH, S. 2012. *Innate Immune Recognition of Pseudomonas aeruginosa*. PhD, University of Nottingham.
- SINGH, S. K., STRENG-OUWEHAND, I., LITJENS, M., KALAY, H., BURGDORF, S., SAELAND, E., KURTS, C., UNGER, W. W. & VAN KOOYK, Y. 2011. Design of neo-glycoconjugates that target the mannose receptor and enhance TLR-independent cross-presentation and Th1 polarization. *Eur J Immunol*, 41, 916-25.
- SLAVIN, S., BURNS, J., HADDLETON, D. M. & BECER, C. R. 2011. Synthesis of glycopolymers via click reactions. *European Polymer Journal*.
- SPAIN, S. G. & CAMERON, N. R. 2011. A spoonful of sugar: the application of glycopolymers in therapeutics. *Polymer Chemistry [Online]*, 2.
- STAHL, P., SCHLESINGER, P. H., SIGARDSON, E., RODMAN, J. S. & LEE, Y. C. 1980. Receptor-mediated pinocytosis of mannose glycoconjugates by macrophages: characterization and evidence for receptor recycling. *Cell*, 19, 207-15.

- STAHL, P. D. 1990. The macrophage mannose receptor: current status. *Am J Respir Cell Mol Biol*, 2, 317-8.
- STAHL, P. D., RODMAN, J. S., MILLER, M. J. & SCHLESINGER, P. H. 1978. Evidence for receptor-mediated binding of glycoproteins, glycoconjugates, and lysosomal glycosidases by alveolar macrophages. *Proc Natl Acad Sci U S A*, 75, 1399-403.
- STANLEY, E. R. 2000. CSF-1. In *Cytokine Reference: A Compendium of Cytokine and Other Mediators Of Host Defense*, Academic Press.
- STANLEY, E. R., BERG, K. L., EINSTEIN, D. B., LEE, P. S., PIXLEY, F. J., WANG, Y. & YEUNG, Y. G. 1997. Biology and action of colony--stimulating factor-1. *Mol Reprod Dev*, 46, 4-10.
- STEIN, M., KESHAV, S., HARRIS, N. & GORDON, S. 1992. Interleukin 4 potently enhances murine macrophage mannose receptor activity: a marker of alternative immunologic macrophage activation. *J Exp Med*, 176, 287-92.
- STEINMAN, R. M. 1991. The dendritic cell system and its role in immunogenicity. *Annu Rev Immunol*, 9, 271-96.
- STONE, T. W. 1993. Neuropharmacology of quinolinic and kynurenic acids. *Pharmacol Rev*, 45, 309-79.
- STONE, T. W. & DARLINGTON, L. G. 2002. Endogenous kynurenines as targets for drug discovery and development. *Nat Rev Drug Discov*, 1, 609-20.
- STONE, T. W. & PERKINS, M. N. 1981. Quinolinic acid: a potent endogenous excitant at amino acid receptors in CNS. *Eur J Pharmacol*, 72, 411-2.
- SU, Y., BAKKER, T., HARRIS, J., TSANG, C., BROWN, G. D., WORMALD, M. R., GORDON, S., DWEK, R. A., RUDD, P. M. & MARTINEZ-POMARES, L. 2005. Glycosylation influences the lectin activities of the macrophage mannose receptor. *J Biol Chem*, 280, 32811-20.
- SWARTZ, K. J., DURING, M. J., FREESE, A. & BEAL, M. F. 1990. Cerebral synthesis and release of kynurenic acid: an endogenous antagonist of excitatory amino acid receptors. *J Neurosci*, 10, 2965-73.
- TAKEDA, K., TANAKA, T., SHI, W., MATSUMOTO, M., MINAMI, M., KASHIWAMURA, S., NAKANISHI, K., YOSHIDA, N., KISHIMOTO, T. & AKIRA, S. 1996. Essential role of Stat6 in IL-4 signalling. *Nature*, 380, 627-30.
- TAN, M. C., MOMMAAS, A. M., DRIJFHOUT, J. W., JORDENS, R., ONDERWATER, J. J., VERWOERD, D., MULDER, A. A., VAN DER HEIDEN, A. N., SCHEIDEGGER, D., OOMEN, L. C., OTTENHOFF, T. H., TULP, A., NEEFJES, J. J. & KONING, F. 1997. Mannose receptor-mediated uptake of antigens strongly enhances HLA class II-restricted antigen presentation by cultured dendritic cells. *Eur J Immunol*, 27, 2426-35.
- TANG, C. K., LODDING, J., MINIGO, G., POUNIOTIS, D. S., PLEBANSKI, M., SCHOLZEN, A., MCKENZIE, I. F., PIETERSZ, G. A. & APOSTOLOPOULOS, V. 2007. Mannan-mediated gene delivery for cancer immunotherapy. *Immunology*, 120, 325-35.
- TARZI, R. M., DAVIES, K. A., CLAASSENS, J. W., VERBEEK, J. S., WALPORT, M. J. & COOK, H. T. 2003. Both Fcγ receptor I and Fcγ receptor III mediate disease in accelerated nephrotoxic nephritis. *Am J Pathol*, 162, 1677-83.
- TATENO, H., OHNISHI, K., YABE, R., HAYATSU, N., SATO, T., TAKEYA, M., NARIMATSU, H. & HIRABAYASHI, J. 2010. Dual specificity of Langerin to sulfated and mannosylated glycans via a single C-type carbohydrate recognition domain. *J Biol Chem*, 285, 6390-400.
- TAYLOR, M. E., BEZOUSKA, K. & DRICKAMER, K. 1992. Contribution to ligand binding by multiple carbohydrate-recognition domains in the macrophage mannose receptor. *J Biol Chem*, 267, 1719-26.
- TAYLOR, M. E. & DRICKAMER, K. 1993. Structural requirements for high affinity binding of complex ligands by the macrophage mannose receptor. *J Biol Chem*, 268, 399-404.

- TAYLOR, M. E. & DRICKAMER, K. 2011. *Introduction to glycobiology*.
- TAYLOR, M. E. & DRICKAMER, K. 2014. Convergent and divergent mechanisms of sugar recognition across kingdoms. *Curr Opin Struct Biol*, 28, 14-22.
- TAYLOR, P. R., GORDON, S. & MARTINEZ-POMARES, L. 2005. The mannose receptor: linking homeostasis and immunity through sugar recognition. *Trends Immunol*, 26, 104-10.
- TERADA, M., KHOO, K. H., INOUE, R., CHEN, C. I., YAMADA, K., SAKAGUCHI, H., KADOWAKI, N., MA, B. Y., OKA, S., KAWASAKI, T. & KAWASAKI, N. 2005. Characterization of oligosaccharide ligands expressed on SW1116 cells recognized by mannan-binding protein. A highly fucosylated poly-lactosamine type N-glycan. *J Biol Chem*, 280, 10897-913.
- TERNESSE, P., BAUER, T. M., RÖSE, L., DUFTER, C., WATZLIK, A., SIMON, H. & OPELZ, G. 2002. Inhibition of allogeneic T cell proliferation by indoleamine 2,3-dioxygenase-expressing dendritic cells: mediation of suppression by tryptophan metabolites. *J Exp Med*, 196, 447-57.
- THAKER, A. I., RAO, M. S., BISHNUPURI, K. S., KERR, T. A., FOSTER, L., MARINSHAW, J. M., NEWBERRY, R. D., STENSON, W. F. & CIORBA, M. A. 2013. IDO1 metabolites activate β -catenin signaling to promote cancer cell proliferation and colon tumorigenesis in mice. *Gastroenterology*, 145, 416-25.e1-4.
- TIETZE, C., SCHLESINGER, P. & STAHL, P. 1980. Chloroquine and ammonium ion inhibit receptor-mediated endocytosis of mannose-glycoconjugates by macrophages: apparent inhibition of receptor recycling. *Biochem Biophys Res Commun*, 93, 1-8.
- TIETZE, C., SCHLESINGER, P. & STAHL, P. 1982. Mannose-specific endocytosis receptor of alveolar macrophages: demonstration of two functionally distinct intracellular pools of receptor and their roles in receptor recycling. *J Cell Biol*, 92, 417-24.
- TING, S. R. S., CHEN, G. & STENZEL, M. H. 2010. Synthesis of glycopolymers and their multivalent recognitions with lectins. *Polymer Chemistry*.
- TISSERA, H., KODIHA, M. & STOCHAJ, U. 2010. Nuclear envelopes show cell-type specific sensitivity for the permeabilization with digitonin. *Protocol Exchange*. Nature.
- UNGER, W. W., VAN BEELEN, A. J., BRUIJNS, S. C., JOSHI, M., FEHRES, C. M., VAN BLOOIS, L., VERSTEGE, M. I., AMBROSINI, M., KALAY, H., NAZMI, K., BOLSCHER, J. G., HOOIJBERG, E., DE GRUIJL, T. D., STORM, G. & VAN KOOYK, Y. 2012. Glycan-modified liposomes boost CD4⁺ and CD8⁺ T-cell responses by targeting DC-SIGN on dendritic cells. *J Control Release*, 160, 88-95.
- VAN GISBERGEN, K. P., AARNOUDSE, C. A., MEIJER, G. A., GEIJTENBEEK, T. B. & VAN KOOYK, Y. 2005. Dendritic cells recognize tumor-specific glycosylation of carcinoembryonic antigen on colorectal cancer cells through dendritic cell-specific intercellular adhesion molecule-3-grabbing nonintegrin. *Cancer Res* [Online], 65.
- VAN KOOYK, Y. & GEIJTENBEEK, T. B. H. 2003. DC-SIGN: escape mechanism for pathogens. *Nat Rev Immunol*, 3, 697-709.
- VAN KOOYK, Y. & RABINOVICH, G. A. 2008. Protein-glycan interactions in the control of innate and adaptive immune responses. *Nat Immunol*, 9, 593-601.
- VARKI, A. 2011. Evolutionary forces shaping the Golgi glycosylation machinery: why cell surface glycans are universal to living cells. *Cold Spring Harb Perspect Biol*, 3.
- VARKI, A., CUMMINGS, R. D., AEBI, M., PACKER, N. H., SEEBERGER, P. H., ESKO, J. D., STANLEY, P., HART, G., DARVILL, A., KINOSHITA, T., PRESTEGARD, J. J., SCHNAAR, R. L., FREEZE, H. H., MARTH, J. D., BERTOZZI, C. R., ETZLER, M. E., FRANK, M., Vliegenthart, J. F., LÜTTEKE, T., PEREZ, S., BOLTON, E., RUDD, P., PAULSON, J., KANEHISA,

- M., TOUKACH, P., AOKI-KINOSHITA, K. F., DELL, A., NARIMATSU, H., YORK, W., TANIGUCHI, N. & KORNFELD, S. 2015. Symbol Nomenclature for Graphical Representations of Glycans. *Glycobiology*, 25, 1323-4.
- VAUTIER, S., MACCALLUM, D. M. & BROWN, G. D. 2012. C-type lectin receptors and cytokines in fungal immunity. *Cytokine*, 58, 89-99.
- VIGERUST, D. J., VICK, S. & SHEPHERD, V. L. 2012. Characterization of functional mannose receptor in a continuous hybridoma cell line. *BMC Immunol*, 13, 51.
- VINUESA, E., HOTTER, G., JUNG, M., HERRERO-FRESNEDA, I., TORRAS, J. & SOLA, A. 2008. Macrophage involvement in the kidney repair phase after ischaemia/reperfusion injury. *J Pathol*, 214, 104-13.
- VOIT, B. & APPELHANS, D. 2010. Glycopolymers of Various Architectures — More than Mimicking Nature. *Trends in Polymer Science* [Online], 211.
- WANG, J.-S., MATYJASZEWSKI, K. 1995a. Controlled/"living" radical polymerization. atom transfer radical polymerization in the presence of transition-metal complexes. 117.
- WANG, J.-S. A. M. K. 1995b. Controlled Living Radical Polymerization. Atom Transfer Radical Polymerization in the Presence of Transition-Metal Complexes. 5614--5615.
- WANG, Y., WANG, Y. P., ZHENG, G., LEE, V. W., OUYANG, L., CHANG, D. H., MAHAJAN, D., COOMBS, J., WANG, Y. M., ALEXANDER, S. I. & HARRIS, D. C. 2007. Ex vivo programmed macrophages ameliorate experimental chronic inflammatory renal disease. *Kidney Int*, 72, 290-9.
- WEIS, W. I., DRICKAMER, K. & HENDRICKSON, W. A. 1992. Structure of a C-type mannose-binding protein complexed with an oligosaccharide. *Nature*, 360, 127-34.
- WEIS, W. I., TAYLOR, M. E. & DRICKAMER, K. 1998. The C-type lectin superfamily in the immune system. *Immunol Rev*, 163, 19-34.
- WIENKE, D., MACFADYEN, J. R. & ISACKE, C. M. 2003. Identification and characterization of the endocytic transmembrane glycoprotein Endo180 as a novel collagen receptor. *Mol Biol Cell*, 14, 3592-604.
- WILEMAN, T., BOSHANS, R. & STAHL, P. 1985. Uptake and transport of mannosylated ligands by alveolar macrophages. Studies on ATP-dependent receptor-ligand dissociation. *J Biol Chem*, 260, 7387-93.
- WILEMAN, T., BOSHANS, R. L., SCHLESINGER, P. & STAHL, P. 1984. Monensin inhibits recycling of macrophage mannose-glycoprotein receptors and ligand delivery to lysosomes. *Biochem J*, 220, 665-75.
- WILEMAN, T. E., LENNARTZ, M. R. & STAHL, P. D. 1986. Identification of the macrophage mannose receptor as a 175-kDa membrane protein. *Proc Natl Acad Sci U S A*, 83, 2501-5.
- WOJCIECH, J., NICOLAY, V. T., PATRICK, M. & KRZYSZTOF, M. 2012. Controlled Radical Polymerization Guide. Materials Science Aldrich.
- XU, H., ZHANG, G. X., CIRIC, B. & ROSTAMI, A. 2008. IDO: a double-edged sword for T(H)1/T(H)2 regulation. *Immunol Lett*, 121, 1-6.
- YILMAZ, G. & BECER, C. R. 2014. Glycopolymer code based on well-defined glycopolymers or glyconanomaterials and their biomolecular recognition. *Frontiers in bioengineering and biotechnology*, 2, 39-39.
- ZAMZE, S., MARTINEZ-POMARES, L., JONES, H., TAYLOR, P. R., STILLION, R. J., GORDON, S. & WONG, S. Y. 2002. Recognition of bacterial capsular polysaccharides and lipopolysaccharides by the macrophage mannose receptor. *J Biol Chem*, 277, 41613-23.
- ZELENSKY, A. N. & GREASY, J. E. 2005. The C-type lectin-like domain superfamily. *FEBS J*, 272, 6179-217.
- ZHANG, Q. W., LIU, L., GONG, C. Y., SHI, H. S., ZENG, Y. H., WANG, X. Z., ZHAO, Y. W. & WEI, Y. Q. 2012. Prognostic significance of tumor-

- associated macrophages in solid tumor: a meta-analysis of the literature. *PLoS One*, 7, e50946.
- ZHANG, Y., CHAN, J. W., MORETTI, A. & UHRICH, K. E. 2015. Designing polymers with sugar-based advantages for bioactive delivery applications. *J Control Release*, 219, 355-68.
- ZHAO, T. 2015. *Controlled/living radical polymerisation of multi-vinyl monomer towards hyperbranched polymers for biomedical applications*. University College Dublin.
- ZINCHUK, V., ZINCHUK, O. & OKADA, T. 2007. Quantitative colocalization analysis of multicolor confocal immunofluorescence microscopy images: pushing pixels to explore biological phenomena. *Acta Histochem Cytochem*, 40, 101-11.